[Pharmaceutical Sciences (PhD) Dissertations](#)   [Dissertations and Theses](#)

12-2021

KSHV Susceptibility and Transmission Within Tonsillar Specimens

Farizeh Aalam
Chapman University, aalam@chapman.edu

Follow this and additional works at: https://digitalcommons.chapman.edu/pharmaceutical_sciences_dissertations

Part of the [Immunology and Infectious Disease Commons](#), [Other Pharmacy and Pharmaceutical Sciences Commons](#), and the [Virology Commons](#)

Recommended Citation

KSHV SUSCEPTIBILITY AND TRANSMISSION WITHIN TONSILLAR SPECIMENS

A Dissertation by

Farizeh Aalam

Chapman University

Irvine, CA

School of Pharmacy

Submitted in partial fulfillment of the requirements for the degree of

Doctor of Philosophy in Pharmaceutical Sciences

December 2021

Committee in charge:

Jennifer E. Totonchy, Ph.D., Chair

Rennolds Ostrom, Ph.D.

Sun Yang, Ph.D.

Ajay Sharma, Ph.D.

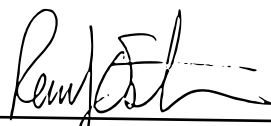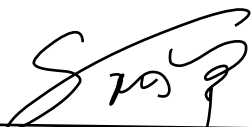The dissertation of Farizeh Aalam is approved.

_____

Jennifer E. Totonchy, Ph.D., Chair

_____

Rennolds Ostrom, Ph.D.

_____

Sun Yang, Ph.D.

_____

Ajay Sharma, Ph.D.

November 2021

KSHV Susceptibility and Transmission Within Tonsillar Specimens

III

ACKNOWLEDGEMENTS

The completion of this dissertation was made possible by the collective efforts, commitments, and compromises made by a group of individuals. This dissertation is dedicated to all those who challenged, supported, encouraged and believed in me during my successes and failures. I have been extremely fortunate to pursue my passion for science alongside the eminent scientist Dr. Jennifer E. Totonchy. There are no words that can fully convey my sincere gratitude for her invaluable mentorship. This amazing research work would not be possible without her expertise. I would also like to thank my committee members for their constructive feedbacks, which shaped my academic journey, and this dissertation as the final results.

I appreciate all of my friends at the Rinker Campus including current and past Totonchy lab members. Special thanks to my dear friends Nedaa Alomari, Emily Romano, as well as Dr. Farideh Amirad of the Dr. Nauli Lab who provided me with amazing personal and professional support throughout these years.

I am highly obliged to my extended family here in the US including my uncle and his wife, as well as my late grandfather for their lending hands and unfailing support. Even though being away from my parents over the last several years has been emotionally challenging, my family here in the US have been amazing in filling that void. They have always been there for me selflessly, and were crucial in making all of this possible.

I must express my heartfelt appreciation to my wonderful parents to whom I am greatly indebted for their unconditional love, support, and unremitting encouragement. They are my parents and my best friends. They have instilled in me the values and virtues which have made me who I am today, and I am forever grateful to them for their endless sacrifices in paving the way for my success. All that I am, and all that I will ever be, I owe to my parents.

Finally, I must explicitly dedicate this dissertation to the love of my life, Shehram Djafroodi. He is my rock, and I have always been able to lean on him in any circumstance. We have traveled through the ups and downs of this journey together as I worked my way towards the completion of my PhD. The love and stability he brings to my life day in and day out grounds me, and motivates me to pursue my dreams with even greater enthusiasm.

LIST OF PUBLICATIONS

Aalam, F., Nabiee, R., Romano, E., & Totonchy, J. (2021). Establishing the dynamics of cell-to-cell transmission of KSHV in human tonsil-derived cell types. Submitted to *Journal of Virology*

Alomari, N., **Aalam, F**., Nabiee, R., Castano, J. R., & Totonchy, J. (2021). IL-21 signaling promotes early dissemination of KSHV infection in B lymphocytes. Submitted to *PLoS pathogens*

Aalam, F., Alomari, N., Muniraju, M., Ogembo, J. G., & Totonchy, J. (2021). KSHV-gH EphA interactions dominate entry into B lymphocytes and mask gH-independent routes of infection. Manuscript under preparation for submission to *Viruses.*

Palmerin, N., **Aalam, F**., Nabiee, R., Muniraju, M., Ogembo, J. G., & Totonchy, J. (2021). Suppression of DC-SIGN and gH Reveals Complex, Subset-Specific Mechanisms for KSHV Entry in Primary B Lymphocytes. *Viruses,* 13(8), 1512.

Aalam, F., & Totonchy, J. (2020). Molecular Virology of KSHV in the Lymphocyte Compartment—Insights From Patient Samples and De Novo Infection Models. *Frontiers in Cellular and Infection Microbiology*, *10*, 765.

Aalam, F., Nabiee, R., Castano, J. R., & Totonchy, J. (2020). Analysis of KSHV B lymphocyte lineage tropism in human tonsil reveals efficient infection of CD138+ plasma cells. *PLoS pathogens*, *16*(10), e100896.

ABSTRACT

KSHV Susceptibility and Transmission Within Tonsillar Specimens

by Farizeh Aalam

Despite nearly three decades of research, not much is known regarding the early stages of development for KSHV lymphoproliferative disorders, hindering our ability to develop prophylactic measures or effective treatments. This dissertation will focus on the host and viral factors influencing the magnitude and dynamics of KSHV infection in the human tonsil to pave the way for future interventions directed at limiting person-to-person transmission of KSHV.

To understand the contribution of host factors to KSHV susceptibility in B lymphocytes, we generated a library of 40 tonsillar specimens. Our results indicate that the immunological composition of tonsillar lymphocytes varies across our donor samples, and KSHV possess a diverse B lymphocyte tropism. Furthermore, the highly specific targeting of plasma cells is not due to CD138 (Syndecan-1) being used as an attachment factor, and heparan sulfates, in general, do not play an important role in KSHV infection of B cells. Finally, the donor-dependent immunological factors and immune status of individual samples influences the overall susceptibility, as well as specific targeting of B cell lineages.

To understand the significance of viral gH/gL glycoprotein interaction with some of the key EphA family of receptors in the process of KSHV entry into B lymphocytes, we demonstrate that the expression of EphA2, EphA4, and EphA7 are donor and subset-specific and gH/gL-EphA interactions are important for KSHV-WT infection of primary tonsil lymphocytes. These

interactions are critical for establishing KSHV-WT infection of plasma cells and germinal center cells, and KSHV exploits alternative mechanism of entry in absence of gH.

Finally, we develop a model for cell-to-cell transmission of KSHV within human tonsils by examining KSHV spread within and between primary cell types derived from tonsil specimens, located at the proximity of the crypt lumen, which are in direct contact with external pathogens present in saliva. We show that a variety of primary tonsillar cells are susceptible to KSHV infection and can differentially transmit the infection into B cells. We demonstrate that KSHV spread between and within tonsil cell types is directed, suggesting, this tropism may be influenced by differential virion composition arising from each cell type.

TABLE OF CONTENTS

LIST OF TABLES

LIST OF FIGURES

XIII

LIST OF ABBREVIATIONS

Abbreviation	Meaning
CMV	Cytomegalovirus
HHV	Human Herpesvirus
VZV	Varicella-Zoster Virus
EBV	Epstein-Barr Virus
KSHV	Kaposi Sarcoma Herpes Virus
HCMV	Human Cytomegalovirus
DLBCL	Diffuse large B-cell lymphoma
LMP	Latent membrane protein
EBNA	EBV nuclear antigen
EBER	EBV- small nuclear RNAs
KS	Kaposi's sarcoma
PEL	primary effusion lymphoma
MCD	multicentric Castleman disease
KICS	KSHV inflammatory cytokine syndrome
RRV	Rhesus monkey rhadinovirus
HVS	herpesvirus saimiri
MHV68	Murine herpesvirus 68
HIV	human immunodeficiency virus
IL	Interleukin
VEGF	vascular endothelial growth factor

IgM	Immunoglobulin M
GC	Germinal center
DNA	Deoxyribonucleic acid
RNA	Ribonucleic acid
LANA	latency-associated nuclear antigen
v-FLIP	viral Fas like inhibitory protein
ORF	Open reading frame
CDK	Cyclin dependent kinase
NF-κB	Nuclear factor-κB
PI3-K	Phosphoinositide 3-kinase
DC-SIGN	Dendritic Cell-Specific Intercellular adhesion molecule-3-Grabbing Non-integrin
nAbs	Neutralizing antibody
HSPG	Heparan sulfate proteoglycans
xCT	cystine–glutamate antiporter
HSC	hematopoietic stem cells
BM	bone marrow
MZ	marginal zone
MHC	Histocompatibility Complex Class
PAMPs	Pathogen Associated Molecular Patterns
PS	Polysaccharides
TLR	Toll-like receptors
PBMC	Peripheral blood monocyte
RTA	Replication and transcription activator
NMD	Nonsense-mediated mRNA decay
IRF	interferon-regulatory factor

BCR	B cell receptor
Eph	Erythropoietin producing hepatocellular receptors
FBS	Fetal bovine serum
RPMI	Roswell Park Memorial Institute Medium
PBS	Phosphate-buffered saline
UV	Ultraviolet
DMEM	Dulbecco's Modified Eagle Medium
CD	Cluster of differentiation markers
CCS	Cosmic calf serum
BAC16	Bacterial artificial Chromosome 16 containing KSHV genome
AIDS	Acquired immunodeficiency syndrome

1 CHAPTER I: Introduction

1.1 Introduction

Herpesviridae are a family of over 200 types of herpesviruses known to infect vertebrates (Edelman 2005). Human herpesviruses (HHVs) are the most prevalent viral infections in humans (Lan and Luo 2017). The three subfamilies of *alphaherpesvirinae*, *betaherpesvirinae*, and *gammaherpesvirnae* encompass eight known members of HHVs that are distinctively divided biologically and phylogenetically. The eight human herpesviruses are: cytomegalovirus (CMV), herpes simplex virus 1 (HSV-1), herpes simplex virus 2 (HSV-2), human herpesvirus 6A (HHV-6A), human herpesvirus 6B (HHV-6B), human herpesvirus 7 (HHV-7), varicella-zoster virus (VZV), Epstein-Barr virus (EBV), and Kaposi's sarcoma herpesvirus (KSHV) (Minson et al. 2000; Lan and Luo 2017) (**Fig 1.1.1**). Although HHVs vary substantially in their biology, they share the characteristic of establishing infection that persists for the lifetime of the host. They accomplish this by exploiting two distinctive biological programs: latency, in which the viral DNA is maintained as an extrachromosomal episome, allowing the virus to hide from immunological surveillance and remain quiescent for years in the same host, and lytic reactivation which allows for the creation of viral progeny and person-to-person spread (Lan and Luo 2017).
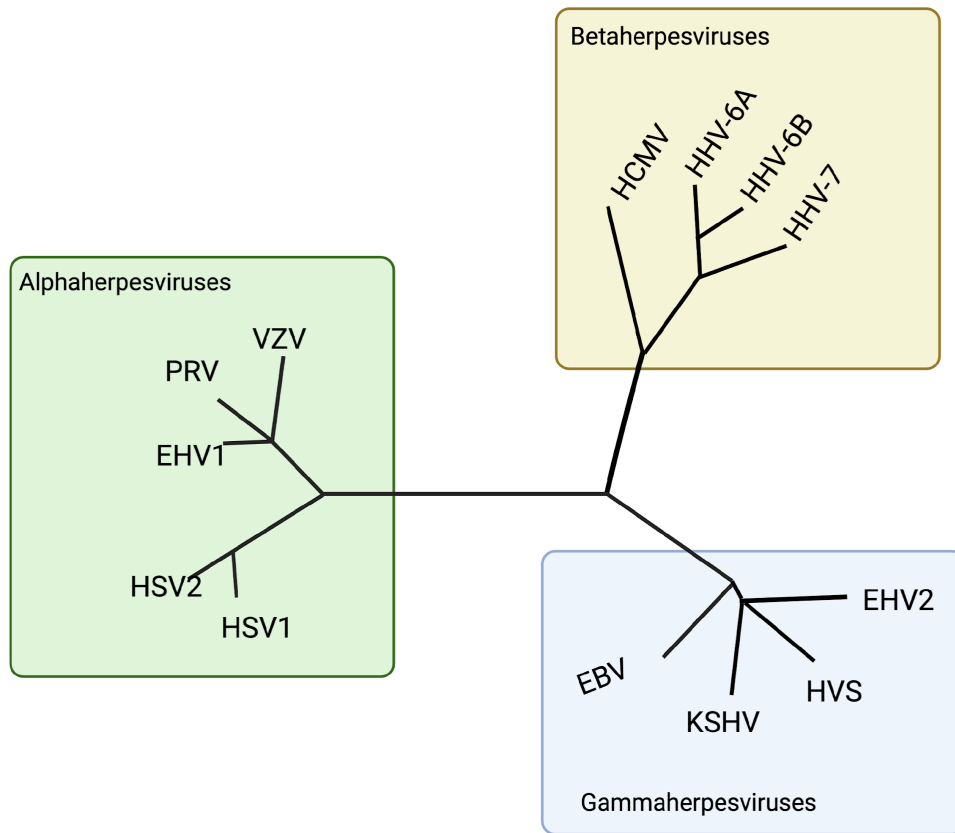
Figure 1.1-1 Phylogeny tree of herpesviruses based on amino acid sequence similarity.

Partially adapted from (Moore et al. 1996)

1.1.1 Alphaherpesvirinae

Among the *alphaherpesvirinae* subfamily, HSV-1and HSV-2 are the most prevalent pathogens causing simplex infections associated with encephalitis, conjunctivitis, oral and genital herpes in 90% of the people infected with either or both viruses (Boppana and Fowler 2007). *Alphaherpesvirinae* tend to have broad cellular tropism due to an abundance of entry receptors on the target cell types, but their persistent infection occurs in the nervous system (Margolis et al. 2007; Kramer and Enquist 2013; Oliver, Zhou, and Arvin 2020). Latency is the default pathway for HSVs, with some sporadic reactivations leading to viral shedding (Roizman and Whitley 2013). Alphaherpesviruses usually infect epithelial cells, and, following replication, they are transmitted into the peripheral nervous system and travel through axons of the neurons to establish lifelong latent infection. Reactivation of the virus may result in travel back to the epithelium resulting in lesions at the skin or mucous membranes, or, in rare cases, viral spread into the central nervous system and subsequently fatal encephalopathy (Steiner, Kennedy, and Pachner 2007; Antinone and Smith 2010).

Generally, HSVs are considered sexually transmitted diseases and their primary infections are mainly localized and asymptomatic. HSV-1 is a significant cause of viral encephalitis in adults in developed countries; the impact and the extent of this orofacial infection can be as simple as cold sores or as severe as herpes keratitis leading to blindness (Farooq and Shukla 2012; Kaye and Choudhary 2006). HSV-1 is chiefly associated with primary genital infection, and since HSV-2 is more frequently reactivated than HSV-1, it can be isolated and detected at any time during the course of infection. Hence, HSV-2 is associated with genital lesions as well as neonatal encephalitis (Pereira et al. 2012; Kaneko et al. 2008; Looker, Garnett, and Schmid 2008).

Another member of alphaherpesviruses subfamily is VZV that causes chickenpox (varicella) during the initial infection, and shingles (herpes zoster) during the viral reactivation (Oliver, Zhou, and Arvin 2020). The risk of viral reactivation increases with age and immunological status (P. O. Lang et al. 2013). VZV is transmitted via air droplets and direct contact with blisters from zoster rashes, and its primary infection is systemic and widespread (Kennedy et al. 2015). VZV is the only HHV for which vaccines have been successfully developed, with both the live attenuated and recombinant VZV vaccines significantly reducing the risk of primary infection and/or reactivation (P.-O. Lang and Aspinall 2021).

1.1.2 Betaherpesvirinae

The *betaherpesvirinae* subfamily includes HHV-6A, HHV-6B, HHV-7, and cytomegalovirus (HCMV) (Nishimura and Mori 2018). Co-infection of HHV-6A&B and HCMV with KSHV plays an essential role in KSHV tumorigenesis and reactivation (Thakker and Verma 2016). HHV-6 was initially labeled as a lymphotropic virus comprising two variants of HHV-6A and HHV-6B. It is now established that HHV-6 and HHV-7 replicate within CD4+ lymphocytes, and HHV-6A and HHV-6B are two distinct viruses (F.-Z. Wang and Pellett 2007; Ablashi et al. 2014). HHV-6B is the causative agent of *Roseola infantum* and is generally acquired during infancy or childhood and HHV-6A is generally contracted during adulthood through asymptomatic infection. Similarly, primary HHV-7 infections cause roseola, although to a lesser extent (King and Al Khalili 2021; de Andrade 1989). The HHV-6s and HHV-7 can infect monocytes, T cells, epithelial cells, and fibroblasts (Gugliesi et al. 2020). HHV-6A and HHV-6B infection of neuronal cells is associated with progressive multifocal leukoencephalopathy and multiple sclerosis (MS) (Tyler 2003; Caserta, Mock, and Dewhurst 2001). Although the current data regarding HHV-6 transmission are

limited, studies show that HHV-6 is transmitted through saliva or vertical transmission *in utero* (Joshi et al. 2000; Braun, Dominguez, and Pellett 1997).

HCMV (HHV-5) is capable of infecting a broad cell range, including epithelial cells, fibroblasts, vascular endothelial cells, smooth muscle cells, hepatocytes, macrophages, and dendritic cells (Gugliesi et al. 2020). Cellular enlargement and intracellular inclusion bodies due to formation of new virions and lysosomes are the typical characteristics of HCMV infected cells (Boppana and Fowler 2007). HCMV primary infection is usually asymptomatic but when symptomatic, it can cause rash, fatigue, fever, night sweats, hypertransaminasemia, joint and muscle pain that lasts for weeks (Horwitz et al. 1986). Severe HCMV infection can cause gastrointestinal tract and hematological abnormalities, central nervous system morbidities, blindness, hepatitis, pneumonitis of the lungs, and thrombosis of the vasculature (Rafailidis et al. 2008). HCMV is acquired during childhood through direct contact with bodily fluids or transmitted prenatally (Gugliesi et al. 2020). Prenatal transmission of HCMV during the first or second trimester can lead to significant impairments in development of the fetal nervous system, bone marrow, and internal organs resulting in birth defects, as well as mental and motor deficits (Buxmann et al. 2017).

1.1.3 Gammaherpesvirinae

Epstein-Barr virus (EBV) and Kaposi Sarcoma Herpes Virus (KSHV) are lymphotropic viruses, and their infection is associated with increased risk of viral tumorigenesis in HIV infected and immunocompromised individuals (Thakker and Verma 2016). It is thought that the combination of chronic antigenic activation and immunosuppression are the hallmarks of EBV infection in developing this neoplastic course (Shannon-Lowe, Rickinson, and Bell 2017). While these viruses belong to the same subfamily, they differ in tropism, oncogenicity, and prevalence (Thakker and

Verma 2016). EBV infection is detected in more than 90% of the adult population globally and KSHV seropositivity varies between 20 - 80% in Mediterranean and African regions and it is less than 10% in the USA and Europe (Shannon-Lowe, Rickinson, and Bell 2017; Minhas and Wood 2014). The focus of this section will be only on EBV as we have dedicated a separate part for KSHV.

EBV infection of lymphocytes and epithelial cells is associated with several cancers including Burkitt's lymphoma, Hodgkin's lymphoma, nasopharyngeal carcinoma, and gastric carcinoma (Shannon-Lowe, Rickinson, and Bell 2017; Kempkes and Robertson 2015). Diffuse large B-cell lymphoma (DLBCL) is the most aggressive form of B cell lymphoma that sometimes co-exists with EBV infection (Shannon-Lowe, Rickinson, and Bell 2017). Like other herpesviruses, EBV has two life cycles, lytic replication and latency. The lytic phase occurs at the beginning of the infection and is required for cell-to-cell transmission. The lytic phase takes place before activation of immune surveillance. After activation of cellular and humoral immunity, EBV resumes latency in memory B cells (its reservoir) to remain unrecognized by the immune system. EBV has three distinctive latency types characterized by different patterns of viral gene expression. The EBV latent phase in B cells proceeds from type III to II to I (Taylor et al. 2015). EBV encodes for latent membrane protein (LMP 1, 2A and 2B) and EBV nuclear antigen (EBNA 1, 2, 3A, 3B, 3C and – LP) proteins. Expression of these proteins in the pre-latent phase of infection begins the B lymphocyte reprogramming (Mrozek-Gorska et al. 2019). Initially, EBV infects resting naïve B cells and maximally expresses its viral genes at its latency stage III, leading to viral protein production to initiate the cytotoxic T-cell reaction. Subsequently, viral protein expression gets limited to fewer proteins such as latent membrane protein (LMP)-1, LMP-2, and Epstein-Barr nuclear antigen (EBNA)-1, marking the entrance into the type II latency. Latency II drives the

differentiation of naive to the memory B cells. EBNA2 expression is lost in B cells with type II latency and the only EBV's gene products expressed are EBNA1, LMP1, LMP2A, viral microRNAs, and small nuclear RNAs (EBERs). Ultimately, the type I latency is achieved by expressing EBV-encoded small RNA (EBER) and EBNA-1 to maintain and replicate the EBV episome. EBV-infected resting memory B cells can undergo long-term latency with maximal suppression of viral antigens (Kempkes and Robertson 2015; Taylor et al. 2015). There are two major serotypes of EBV found in humans: type 1 and type 2. Their genomes are closely identical except for some nuclear protein encoding genes that ultimately determines their oncogenesis and alters T cell responses (Kempkes and Robertson 2015; Moss et al. 1988).

1.2   Kaposi Sarcoma Herpes Virus

KSHV (HHV8) belongs to the gamma-herpesvirus family and is associated with both lymphoid and non-lymphoid cell tumors in humans (Y. Chang et al. 1994; Cesarman et al. 1995). KSHV-associated malignancies occur primarily in the context of immunodeficiency. KSHV is the etiologic agent of Kaposi's sarcoma (KS), as well as B cell lymphoproliferative disorders; primary effusion lymphoma (PEL) and multicentric Castleman disease (MCD) (Y. Chang et al. 1994; Cesarman et al. 1995) and the recently discovered KSHV inflammatory cytokine syndrome (KICS) (Uldrick et al. 2010).

While KSHV persistence in non-human primates has been reported (H. Chang et al. 2009), as a human virus, a true KSHV infection model system representing its biology does not exist. In the absence of such model systems, transgenic animals and homologous viruses have been investigated. Rhesus monkey rhadinovirus (RRV) and herpesvirus saimiri (HVS) are two lineages under the rhadinovirus subgroup that often serve as good model systems for KSHV (Dittmer,

Damania, and Sin 2015). RRV has two different strains that share high similarities to each other and the KSHV genome. HVS on the other hand shares some positional homology with KSHV genome, implements similar molecular mechanisms, and has similar tropism (Damania 2004; Guo et al. 2014). Murine herpesvirus 68 (MHV68) is the murine homolog of KSHV that replicates with high titer *in vitro* and *in vivo,* but does not cause lymphoma and skin lesions in non-transgenic mice (Liang et al. 2011). Each of these viruses can represent distinctive characteristics of KSHV in terms of pathogenesis and determining the function of specific viral gene products, which contributes to advances in KSHV research. In addition, some groups have recently had success with KSHV research in humanized mice (Münz 2020).

1.3   KSHV Pathology and Etiology

Primary infection of KSHV in immunocompetent individuals is associated with fever, maculopapular rash, and lymphadenopathy in adults (Yan et al. 2019; Q. J. Wang et al. 2001), and maculopapular rash and febrile illness in children (Andreoni et al. 2002).

KS is the most prevalent cancer in sub-Saharan Africa associated with HIV infection (Gbabe et al. 2014). KS lesions classically involve the mucosal surface or dermal area of the upper and lower extremities, it can also emerge from viscera of the spleen and lung as well as lymph nodes (Restrepo et al. 2006). KS lesions are heavily vascularized and are characterized by the presence of poorly differentiated spindle cells of endothelial cell origin and inflammatory cell infiltration. KS spindle cells are mostly latently infected with sporadic lytic infection (Yan et al. 2019). Whether these endothelial spindle cells are of vascular or lymphatic origin is still debated (Li et al. 1996; Hong et al. 2004; Morris, Punjabi, and Lagunoff 2008). Lymph node involvement and immune status of the host are the primary determinants of the severity and the stages of KS

progression (J. F. Taylor et al. 1971; Kyalwazi 1981). Among the four variants of KS, classical KS is the most benign form of KS, and primarily affects elderly men of eastern Europe and Mediterranean regions (DiGiovanna and Safai 1981). Epidemic KS is the most aggressive form of KS associated with HIV-infected individuals (Gbabe et al. 2014), and endemic KS is found in eastern and central African countries with the lymphadenopathic type occurring primarily in children and associated with high mortality rate (Stein et al. 1994; Dutz and Stout 1960; J. F. Taylor et al. 1971). The last type is iatrogenic KS, which occurs in patients receiving immunosuppressant after a transplant to prevent organ rejection (Siegel et al. 1969).

KSHV inflammatory cytokine syndrome is the newly characterized KSHV-associated disease that occurs in the patients with classical MCD with no pathological symptoms (Uldrick et al. 2010). It is typically characterized by elevated viral and human IL-6 and IL-10 cytokines, accompanied by high viral load in the bloodstream (Uldrick et al. 2010). In fact, KICS, MCD, and PEL share some common clinical manifestations of disease (Lurain et al. 2019).

MCD and PEL are two B cell proliferative disorders associated with KSHV infection (Cesarman et al. 1995; Chang et al. 1994). PEL, a non-Hodgkin lymphoma, was named as it was initially detected as an effusion lymphoma in HIV patients; the extracavitary manifestation of PEL was subsequently detected in other patients (Y. Chang et al. 1994; Soulier et al. 1995; Cesarman et al. 1995). Nearly 80% of PEL cases are coinfected with EBV, occasionally with the combined KS and MCD clinical manifestation (Ramaswami et al. 2016). Cytologically, PEL neoplastic cells are large with a noticeable nucleoli and round to irregular nuclei with immunoblastic, plasmablastic or anaplastic morphology (Calabrò and Sarid 2018). PEL cells secrete high levels of both the viral and cellular IL-6 and IL-10 and vascular endothelial growth factor (VEGF) (Foussat et al. 1999), while human and viral IL-6 stimulate B cell growth and angiogenesis, IL-10 is important for tumor

progression, and VEGF enhances vascular permeability (Foussat et al. 1999; Drexler et al. 1999; Calabrò et al. 2009; Aoki and Tosato 1999).

MCD is a rare polyclonal B cell proliferative cancer, affecting both HIV-negative and HIV-positive subjects (Castleman, Iverson, and Menendez 1956) and EBV co-infection is rarely detected in MCD cases (Barozzi et al. 1996). MCD is a benign mass of lymphoid tissue that can involve single or several lymph nodes (Chan et al. 2016). Histologically, there are three variations of MCD; the hyaline vascular type (representing 90% of unicentric cases), plasmablastic type, and the mixed variants of these two (Calabrò and Sarid 2018). Furthermore, the phenotypic characteristics of MCD are not necessarily plasmablastic, as cases have been identified that are CD20 positive and CD138 negative (Dupin et al. 1999, 2000). MCD plasmablasts are polyclonal but are of monotypic IgM-lambda type and the lack of somatic mutation in their Ig genes rearrangement may be indicative of their origin from naive pre-GC B cells (Du et al. 2001; Calabrò and Sarid 2018). Finally, the systemic illness including cell-free pleural effusion, thrombocytopenia, lymphadenopathy, edema, anemia, severe fatigue, fever, weight loss and splenomegaly are associated with high levels of human and viral IL-6 (Calabrò and Sarid 2018).

1.4 KSHV Life Cycle

KSHV has a double-stranded DNA genome of about 165 kb, encoding for nearly 100 proteins. The genomic DNA is enclosed in a nucleocapsid and covered with a lipid bilayer envelope. The space between the capsid and the envelope is known as the tegument, a loosely associated layer of capsid associated proteins and microRNAs (Yan et al. 2019). Like other herpesviruses, KSHV undergoes lytic or latent replication after entry into the host cells, characterized by unique patterns of gene expression (Barrett et al. 2020). The latent state allows for persistent infection; where

KSHV persist as extrachromosomal episome in its inert state, avoiding the lytic phase and immunosurveillance through manipulation of the immune system (Yan et al. 2019; Grinde 2013). Viral latency is marked by the expression of latency-associated nuclear antigen (LANA/ORF73), viral Fas like inhibitory protein (v-FLIP/ORF72), the viral cylin D homolog (vCyclin/ORF71), and viral microRNAs (Uppal et al. 2014).

LANA is a multifunctional protein capable of tethering the KSHV genome to the host chromosome to maintain its replication and segregation during cell division (Uppal et al. 2014). LANA is considered an oncoprotein, and its binding to various proteins such as p53, p73, and VHL promotes oncogenesis and represses apoptosis (Santag et al. 2013). v-Cyclin is viral mimicry of a human cyclin D that regulates cellular proliferation and cell cycle (Van Dross et al. 2005). It forms a complex with CDK6 to facilitate phosphorylation and inhibition of p7, pRb, CDK inhibitors, and histone H1 (Direkze and Laman 2004). v-Cyclin-CDK6 complex can bind to LANA and recruit epigenetic factors that control the latent-lytic switch (Sarek et al. 2010; Uppal et al. 2014).

v-FLIP is another viral mimicry of a human gene; homologous to cellular FLIP. It activates the NF-κB pathway through binding to IκB kinase γ (IKKγ) to promote cell survival signals (Field et al. 2003). It also inhibits KSHV lytic replication through NF-κB-mediated suppression of the AP-1 pathway (Guasparri, Keller, and Cesarman 2004). vFLIP-mediated activation of the NF-κB pathway leads to modulation of genes involved in cell proliferation, cytokine secretion, immune activation, acute phase responses, transformation, and protection against apoptosis (Rayet and Gélinas 1999).

Physiological and environmental stimuli such as hypoxia and oxidative stress act as effective triggers to lytic reactivation (Ye et al. 2011; Davis et al. 2001). The productive phase of viral

infection is lytic replication, when KSHV genome replication, infectious virion production, assembly, and release leads to cell lysis (Aneja and Yuan 2017). The reactivation state leads to transcription of the immediate early regulatory genes (regulators and transcription factors) and early genes (required for the production of viral protein and DNA replication), and finally late genes (viral structural components) (Yan et al. 2019).

Following the expression of lytic genes, the assembly of the virus commences in the nucleus by incorporation of replicated genome into the synthesized capsids and its association with tegument proteins, and lastly budding from the cell membrane resulting in cell lysis and release of the viral progeny (Gradoville et al. 2000). Although the latent infection is required for viral persistence (Giffin and Damania 2014), lytic reactivation plays an important role in pathogenesis of KSHV associated malignancies, particularly MCD and PEL (Uldrick and Whitby 2011).

1.5   KSHV Tropism and Entry

KSHV DNA has been detected in B cells of both the peripheral blood and secondary lymphoid organs as well as keratinocytes, monocytes, fibroblasts, epithelial cells, and endothelial cells (Chandran 2010). These cell types can all be infected *in vitro* (Muniraju et al. 2019; Cerimele et al. 2001). However, primary B cells and B lymphoma cell lines show poor susceptibility to KSHV infection *in vitro* compared to adherent cell lines (Bechtel et al. 2003). HHV-8 DNA is detectable in B cells from both HIV+ and HIV-PEL and MCD cases (Dupin et al. 1999). Interestingly, KSHV isolated from EBV+PEL cells is able to infect B cells from seronegative patients (Mesri et al. 1996). Phylogenetic analysis and the association of KSHV infection with pathological lymphoproliferations are sufficient to characterize KSHV as a lymphotropic gamma-herpesvirus. The extensive *in vitro* susceptibility of adherent cell lines can partly be explained by the presence

of various cellular receptors used by the viral glycoproteins for attachment and entry (Großkopf et al. 2019; S M Akula et al. 2001a; Chen et al. 2019; Hahn et al. 2009; Muniraju et al. 2019; S M Akula et al. 2001b; S M Akula et al. 2002; Rappocciolo et al. 2008)

The process of KSHV entry into cells is a multistep and sequential process that requires interaction of several host cell receptors with viral envelope glycoproteins. The first step of KSHV entry into target cells begins with binding of the KSHV's glycoproteins to host cell receptors (Chandran 2010). Among the herpesvirus conserved glycoproteins; gB (ORF8), gH (ORF22), gL (ORF47), gN (ORF53), gM (ORF39), and KSHV-specific glycoproteins proteins; K8.1A and B, KCP (ORF4), ORF45, ORF68, ORF27, ORF28, the canonical core entry machinery gB, gH/gL, K8.1, and KCP are thought to be essential in facilitating KSHV entry into a variety of cell lines (Wang et al. 2001; Akula, Wang, et al. 2001; Akula, Pramod, et al. 2001; Birkmann et al. 2001; Spiller et al. 2006; Chandran 2010; Kerur et al. 2010; Dollery et al. 2019; van der Meulen et al. 2021). Not all of the host cellular receptors used by these glycoproteins are entry receptors, some serve as binding receptors to concentrate KSHV on the cell surface (Connolly et al. 2011; van der Meulen et al. 2021). Once the interaction between the virion and the host cell membrane is established, the subsequent signal transduction involving tyrosine kinase activation leads to viral entry and trafficking (Veettil et al. 2014). As an example, KSHV binding to cellular integrins results in phosphorylation of focal adhesion kinase (FAK), leading to the activation of Src tyrosine kinases, Diaphanous 2, PI3-K, and Rho GTPases to control virion internalization (Chandran 2010). Viral entry into cells employs different endocytosis pathways such as caveolin or clathrin mediated endocytosis, and micropinocytosis, depending on the cell type (Veettil et al. 2014; Raghu et al. 2009).

Once KSHV is internalized, the capsid is released into the cytoplasm as a result of the fusion of viral envelope to the membrane of the endosome. Thereafter, the capsid transits to the nuclear membrane and the KSHV genome passes through nuclear pores and forms a circular episome in the nucleus (Chandran 2010; van der Meulen et al. 2021)

1.6 KSHV Entry into B cells

As mentioned earlier, the process of KSHV entry into the cells is a complex process that involves various cellular and viral proteins interaction. The remainder of this section discusses these cellular interactions, focusing on our current knowledge and the gaps in KSHV entry into B lymphocytes. KSHV virion attachment to adherent cells can be facilitated through heparan sulfate proteoglycans on the host cell surface (S M Akula et al. 2001a), and the low in vitro susceptibility of B cells has been attributed to a lack of HS expression. This theory is supported by the observation that restoration of cell surface HS in B cell lines results in increased susceptibility to infection (Jarousse, Chandran, and Coscoy 2008; Dollery et al. 2019; Jarousse et al. 2011). Whether heparan sulfate proteoglycans play a role in KSHV attachment to primary tonsillar B cells or any B cell subsets remains to be answered.

The lectin DC-SIGN has also been implicated as an attachment factor for KSHV entry into B cells. Approximately 8% of CD19+CD20+ peripheral blood B cells and 26% of tonsillar B cells are positive for DC-SIGN, and activation of peripheral blood B cells with IL-4 and CD40L results in 3 to 3.5 fold increase in DC-SIGN and CD23 expression (Rappocciolo et al. 2006). Activated B cells are more susceptible to KSHV infection and KSHV infected B cells show increased DC-SIGN levels compared to uninfected cells (Rappocciolo et al. 2008). Interestingly, B cells expressing DC-SIGN can bind and transfer HIV-1 virions to T cells (Rappocciolo et al. 2006).

Taken together, these observations suggest that KSHV and HIV infections act synergistically. KSHV infection of B cells can facilitate the dissemination of HIV-1 to CD4+ T cells via upregulation of B cell DC-SIGN expression, and HIV, in turn, depletes the CD4+ T cell pool creating an immunological milieu in which KSHV benefits from the lack of immune surveillance.

KSHV encodes a variety of glycoproteins which facilitate virion attachment, fusion, and viral entry into the host cell. Among the various KSHV glycoproteins, gH/gL complex is proved to be the major antigenic determinant of KSHV-specific nAbs in the plasma of KS patients regardless of their disease status (Mortazavi et al. 2020), suggesting that this complex is critical for virus entry. Binding of gH/gL glycoprotein complex to the surface is not well characterized, but it is not HSPG-dependent (Hahn et al. 2009). KSHV entry into the BJAB cell line has been linked to gH/gL binding to EphA7 (Großkopf et al. 2019). Eph4 also binds to gH/gL, and is expressed in B cells, endothelial, fibroblast, and epithelial cells (Chen et al. 2019). In HEK293T cells Eph4 binds more tightly with gH/gL than Eph2 (Chen et al. 2019). RNA sequencing data shows that B cells express Eph4 on their cell surface, albeit not as abundant as endothelial cells but higher than epithelial cells (Chen et al. 2019). Thus, it is possible that gH/gL complex can establish interaction with Eph4 in B cells, since B cells may have almost the same level of Eph4 as HEK293 (epithelial cells) on their surface. However, use of Eph4 as a KSHV entry receptor for B cells has not been studied specifically. Interestingly, the MC116 lymphoma cell line expresses both EphA7 and Eph4, and is susceptible to KSHV infection, but studies with a KSHV mutant lacking gH demonstrated that KSHV entry into MC116 cells is not dependent upon gH/gL (Muniraju et al. 2019). This study, in particular, highlights the significant gaps in our understanding of the molecular virology of KSHV entry into B cells (**Fig 1.6.1**).

Another study showed that K8.1A is required for KSHV infection of both MC116 and CD20+CD3- B cells from tonsil. The cellular receptor interacting with K8.1A in this context is not known, but it is independent of HS binding (Dollery et al. 2019). Finally, the KSHV glycoprotein gB, which is presumed to be the KSHV fusion protein, binds to DC-SIGN *in situ* in a dose dependent manner (Hensler et al. 2014), but whether this interaction is essential for KSHV entry into B cells has not been formally studied. xCT, the light chain has been shown to be involved in KSHV fusion and entry in several cell lines. Although, its mRNA expression is undetectable in CD19+ peripheral blood mononuclear cells (PBMCs) (Kaleeba and Berger 2006b, 2006a) xCT is highly expressed on the surface of PEL cell lines and targeting it by xCT selective inhibitor, induces apoptosis in a caspase dependent manner. Selective inhibition of xCT in an immune deficient mouse xenograft model proves that it plays a key role in tumor progression, survival, and growth of PEL cells (Dai et al. 2014). The expression of xCT can be induced by KSHV miRNAs conferring permissiveness to KSHV in murine microphages and HUVEC cells. Additionally, the expression of xCT within the KS lesion is correlated with the tumor stage (Qin et al. 2010). Whether KSHV miRNAs and change in redox balance contribute to upregulation of xCT in primary B cells to increase the KSHV permissiveness, remains to be answered.

To date, no comprehensive studies been done on primary human B cells samples to elucidate the cellular receptors involved in KSHV entry into B lymphocytes or the individual and collective contributions of KSHV glycoproteins to this process. Further studies are needed to determine these important interactions to facilitate the rational design of vaccine strategies that will effectively limit the establishment of infection in the lymphocyte compartment.
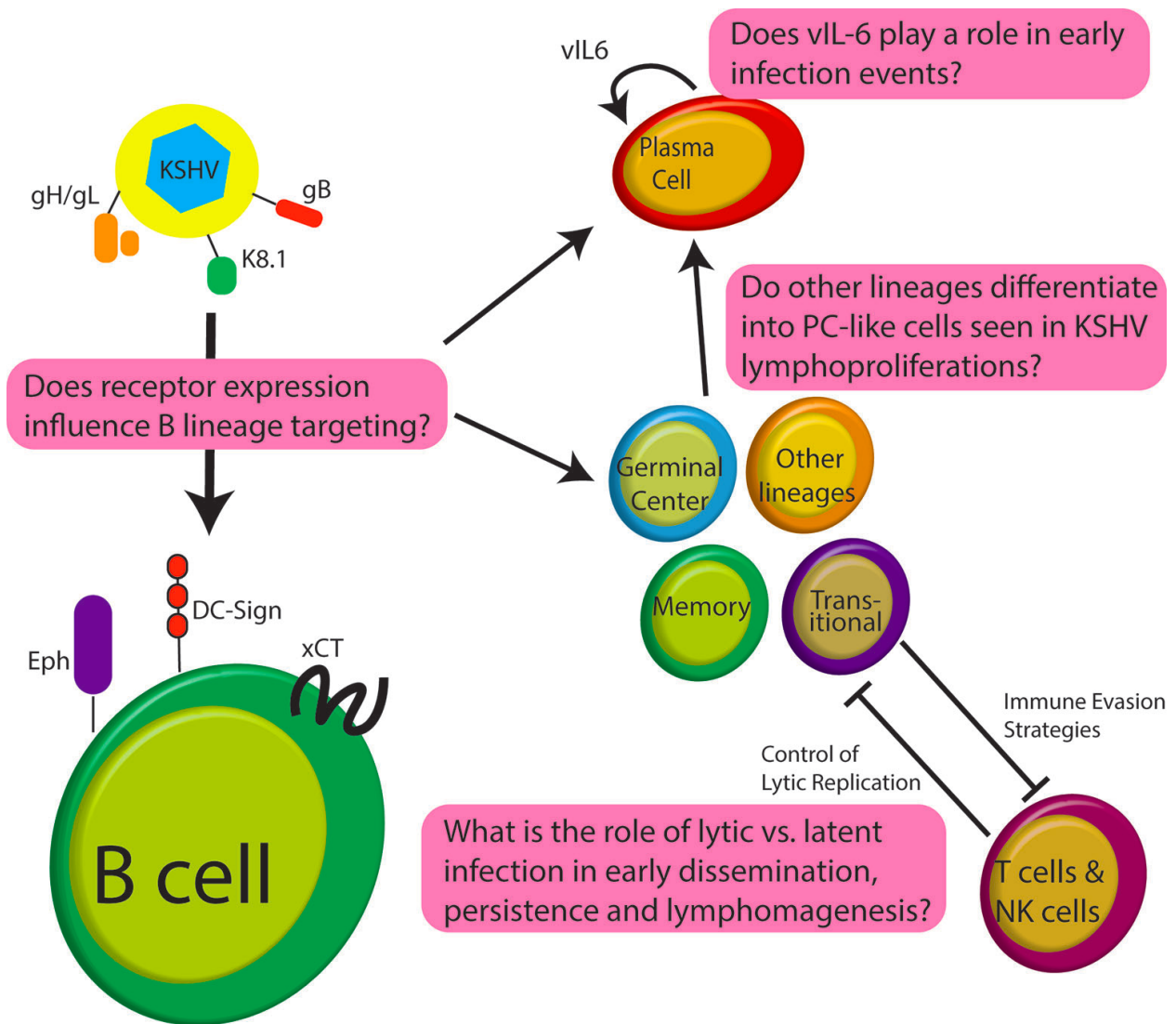
Figure 1.6-1 Schematic of early infection events for KSHV in B lymphocytes highlighting some of the significant questions that remain unanswered in the field.

1.7   B Lymphocyte Maturation

B cells and their antibodies are an integral part of both humoral and adaptive immunity. Any defect in the developmental stages of B cells can impact the maturation and the functionality of B cells, resulting in allergies, autoimmunity, immunodeficiencies, and malignancies (Pieper, Grimbacher, and Eibel 2013). There are significant gaps in our understanding of how KSHV targets B cells for infection, and how the virus manipulates B cell physiology in the development of PEL and MCD. Further studies of KSHV molecular virology of lymphocytes are needed to understand the pathogenesis of KSHV-associated lymphoproliferation, so that effective treatments can be developed. Therefore, this section is intended to provide a brief background on B cell development. In the next section, we explore our current understanding of KSHV biology in B cells by concentrating on studies which use *de novo* infection of human B cells, analysis of patient samples from KSHV lymphoproliferative disease, and relevant lymphoma cell lines.

Development of B lymphocytes begins in the fetal livers' hematopoietic stem cells (HSC) and continues in the bone marrow (BM) during the lifetime of an individual (Müller et al. 1994). Early B-cell development in BM is a series of functional genomic rearrangements of immunoglobin called V(D)J recombination. The functional V(D)J recombination of heavy chain and light chain results in expression of antibody repertoires to facilitate recognition of billions of antigens by B cells (Pieper, Grimbacher, and Eibel 2013). At the pre-B cell stage, the cell undergoes one to two divisions, along with rearrangement of the gene encoding either κ or λ light chain genes. Formation of the μ heavy chain combined with one of the light chains leads to expression of IgM molecules on the cell surface (van Zelm et al. 2007). These cells are immature B cells ready to depart BM and travel to the secondary lymphoid organs, where they can begin their early developmental stage by differentiation into naive, follicular, or marginal zone (MZ) B cells (Pieper, Grimbacher, and

Eibel 2013; Shahaf et al. 2016). Immature B cells arrive at the peripheral lymphoid tissues as transitional B cells (Shahaf et al. 2016) (**Fig.1.7.1**). Transitional B cells concentrate into different locations to mature into professional antibody secreting plasma cells via either T-cell dependent or T-cell independent pathways (Dunkelberger and Song 2010).

Germinal centers (GC) are the important sites of antibody maturation, where T-cell dependent B cell differentiation takes place (Stebegg et al. 2018). The germinal center is partitioned into two major compartments: dark zone and light zone. B cells within the dark zone undergo proliferation, somatic hypermutation, class-switch recombination and differentiate into centroblasts. Centroblasts exiting the cell cycle are entering into the light zone as centrocytes (Stebegg et al. 2018). Centrocytes within the light zone are the target of selection, and in order to survive, they should successfully process the internalized antigen and present it on their Major Histocompatibility Complex Class II (MHC II) to helper T cells via binding to CD4 and the T cell receptor (Adler et al. 2017). This binding results in upregulation of CD40L on the T cells that can subsequently bind to the CD40 receptor on the centrocytes and initiate secretion of cytokines. The cytokines further stimulate the proliferation of centrocytes, and their somatic hypermutation leads to the formation of memory cells, plasmablasts, and plasma cells as B cells depart GC zone (Adler et al. 2017).

T-cell-independent, GC independent, or extrafollicular pathway of B cell development requires no T cell interactions (Pieper, Grimbacher, and Eibel 2013). It takes place in the marginal zone, the region interfacing non-lymphoid and lymphoid pulp of the spleen (Palm and Kleinau 2021). This maturation pathway is triggered by Pathogen Associated Molecular Patterns (PAMPs) binding pattern recognition receptors on naïve B cells (Yam-Puc et al. 2018). PAMPs are polysaccharides (PS) or lipopolysaccharides having repetitive epitopes capable of activating toll-like receptors

(TLR) to initiate B cell proliferation and its differentiation into plasmablasts and plasma cells (Yam-Puc et al. 2018). Plasmablasts are short-lived B cell lineages awaiting maturation into the long-lived plasma cells that mainly reside in BM and secrete functional antibodies (Khodadadi et al. 2019). Memory B cells are incapable of differentiating into plasma cells without the interference of helper T cells (Yam-Puc et al. 2018). Whether follicular or extrafollicular, B cell development and maturation is required for the maintenance of the host defense against pathogens. Moving to the next section, readers will be introduced to the molecular mechanism implemented by KSHV to manipulate B cells to its own advantage. What B cell lineages are targeted by KSHV? And how does KSHV enter into primary human B lymphocytes? These are the rudimentary questions that haven't been answered thus far.
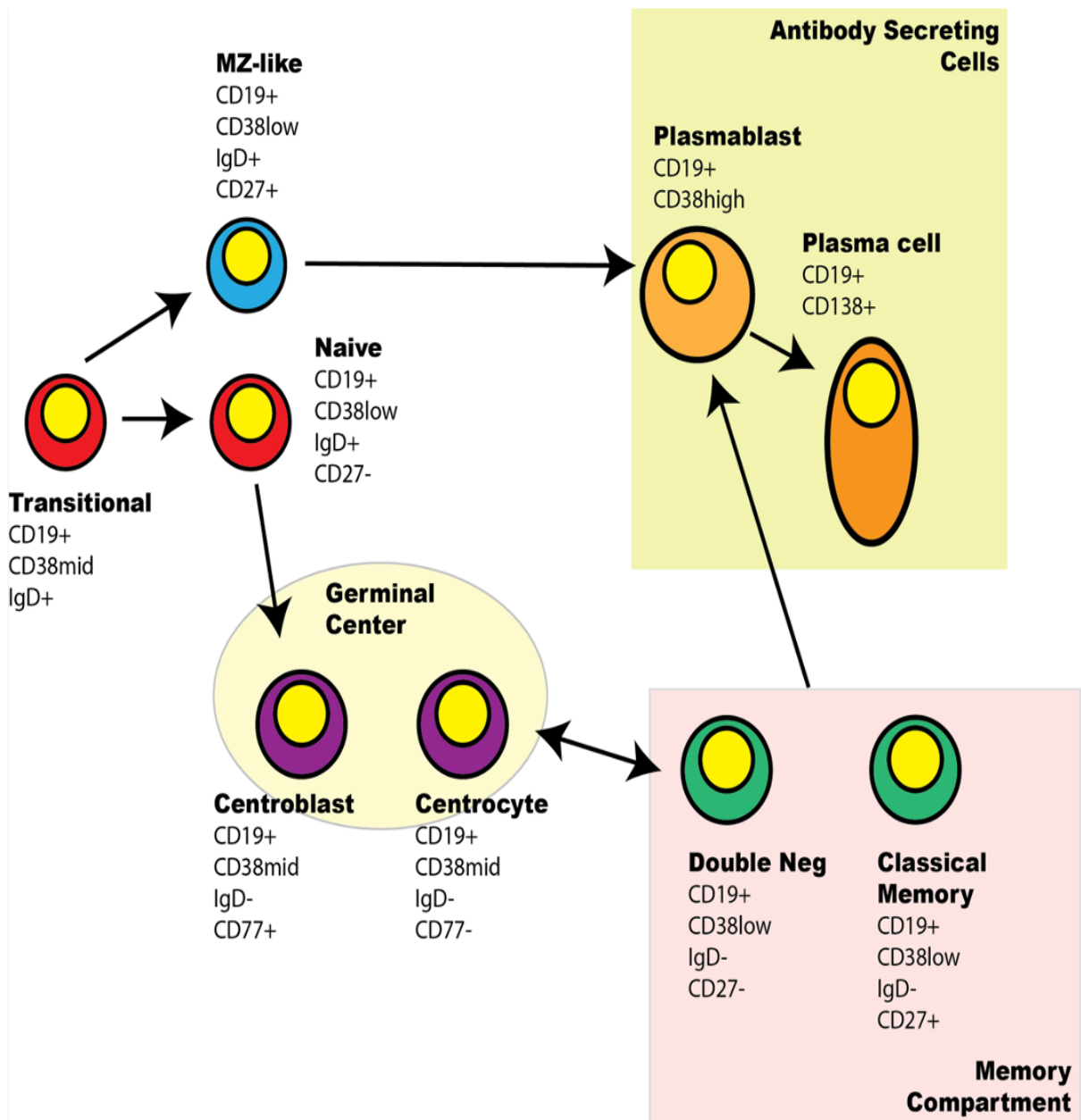
Figure 1.7-1 B lymphocyte maturation

1.8 KSHV in the Lymphocyte Compartment

1.8.1 KSHV manipulation of the cell cycle in B cells

KSHV can establish latent infection in many adherent cell lines, including human and non-human cells of epithelial, endothelial, and mesenchymal origin (Bechtel et al. 2003). Previous studies in primary human B cells report that infection is lytic, particularly in the absence of T cells, but what controls the lytic switch in these cells remains to be established (Myoung and Ganem, 2011a). In addition to T cell control of latency, B cell immunophenotype and activation state have been implicated as factors influencing the lytic/latent balance in B cells (Rappocciolo et al. 2008; Hassman et al. 2011; Myoung and Ganem, 2011a), as well as the immunological status of the individual and the presence of other pathogens (Gregory et al. 2009).

Although the latent phase of infection allows viral persistence and immune-evasion, the production of viral progeny and viral transmission and spread between the cells, depends on the lytic phase. De novo infected PBMCs exhibit simultaneous expression of numerous latent and lytic markers at the very beginning of the infection (Purushothaman et al. 2015). This short lytic replication seems to be a prerequisite for the establishment of the latent phase in PBMCs infected with EBV (Halder et al. 2009). Nevertheless, the lytic gene expression is not required for KSHV infection of PBMCs before or after EBV infection or mitogenic activation (Faure et al. 2019). Do B cells represent a significant source of KSHV virions during human infection? The early lytic gene K8 (K-bZIP), a cell cycle regulator showing homology to EBV' Zta, is required for viral lytic DNA replication and virion production in PEL cell lines (Wu et al. 2002; Lefort and Flamand, 2009). Its expression concurs with augmented C/EBPα, p21 and p27 in the nucleus, causing the cell arrest in G1 phase (Wu et al. 2002; Izumiya et al. 2003a). This prolonged G1 arrest is as a result of K8 binding to CKD2, interfering its kinase activity, giving ample time for viral early gene transcription and

translation (Izumiya et al. 2003a). K8 also interacts with p53 inhibiting its transcription, preventing apoptosis (Park et al. 2000). However, in another study by Hollingworth et al. lytic replication in PEL cells was shown to require S phase entry (Hollingworth et al. 2020). Replication and transcription activator (RTA) is a protein encoded by ORF8 has been shown to co-localize with K8 within the nucleus of the PEL cells, and its association with the K8 (Izumiya et al. 2003b) can initiate lytic reactivation from latency by binding to a particular sequence on the host and viral DNA further modulating the transcription of viral and host regulatory genes throughout KSHV lytic reactivation (Kaul et al. 2019). Viral DNA replication is controlled by both transcriptional coactivator p300 and CBP. P300 was shown to be involved in the oncogenesis of PEL by driving B cell proliferation and inhibiting KSHV lytic replication. Knockout of p300 in PEL cells decreased KSHV genome copy number and virion production by suppressing lytic gene expression, possibly maintaining the latency of KSHV via binding with ATF3 (Sun et al. 2020). Nonsense-mediated mRNA decay (NMD) is an RNA quality control implemented by the cells to restrict the action of the RNA viruses and serve cellular quality control. Interestingly, viral RTA' mRNA is targeted by NMD, impeding KSHV lytic reactivation in PEL cells (Zhao et al. 2020). However, KSHV has evolved to overcome some of these quality controls and exonuclease activities by circularizing its structural and regulatory RNAs incorporated into the virions (Abere et al. 2020). Taken together, the current literature demonstrates that multiple layers of both viral and cellular regulation influence KSHV latency and lytic reactivation in B cells. It is notable that most of this work has been done in PEL cells, and future studies investigating how KSHV manipulates the cell cycle and cell type specific control of latency and reactivation in primary B

lymphocytes will be critical for understanding early events in KSHV infection and pathogenesis of KSHV-associated lymphoproliferative diseases.

1.8.2 Immune evasion

KSHV infection persists for the lifetime of the host and, like all herpesviruses, KSHV must have an arsenal of mechanisms for evading host immunity in order to accomplish this. Lymphotropic gamma-herpesviruses are particularly interesting in this regard because they can manipulate and evade the host immune system via mechanisms that require direct infection of immune cells. Moreover, the inflammatory nature of KSHV-associated malignancies indicates that KSHV immune-evasion mechanisms may also directly contribute to pathogenesis in KSHV-associated diseases. Indeed, this immune-evasion is manifested at the transcriptional level within the first few hours of infection, by hampering the expression of immune response genes and inducing the proapoptotic regulators in BJAB cells (Naranatt et al. 2004). KSHV can infect both B and T cells in tonsil primary cell culture, however evidence suggests that infection of T cells is abortive (Myoung and Ganem, 2011b). Moreover, there is reciprocal activation of T cells by KSHV-infected B cells and contact-dependent control of KSHV lytic reactivation by T cells in ex vivo tonsil cultures, and in this system the activation of T cells is independent of both KSHV antigen and MHC restriction (Myoung and Ganem, 2011a).

Activated, KSHV infected B lymphocytes from PBMC and tonsils show downregulation of MHC class I (HLA-A, HLA-B, and HLA-C) within 24 h of infection as well as decreased expression of CD20 (Rappocciolo et al. 2008). Modulation of MHC class I expression is also observed in PEL derived B cell-lines and is thought to be partially due to reduced expression of the TAP-1 gene. Importantly, this MHC-I modulation can disrupt cytotoxic T lymphocyte surveillance of KSHV

infected cells (Brander et al. 2000), aiding in KSHV persistence and tumorigenesis in B cells. The CD20 low phenotype of KSHV infected cells is also present in MCD and may limit B cell-targeted treatment options for MCD patients. However, these patients still show clinical benefit from rituximab (an anti-CD20 monoclonal antibody) treatment (Naresh et al. 2009).

KSHV encodes four viral interferon regulatory factors (vIRFs). These proteins have minimal homology to human IRFs, but vIRF1, vIRF2, and vIRF3 are known to bind DNA elements similar to their human IRF counterparts (Lubyova and Pitha, 2000; Park et al. 2007; Hu et al. 2016) vIRFs exert their regulatory role at varying levels ranging from hampering the antiviral interferon response to inhibition of signaling pathways to control the function of cellular proteins, thereby interfering with the cellular processes such as apoptosis (Rivas et al. 2001; Nakamura et al. 2001; Lee et al. 2009) proliferation and angiogenesis (Wies et al. 2008; Li et al. 2019; Li et al. 2020) vIRF3 (LANA-2) expression is detected in nearly all virus infected cells in PEL and MCD tumors, and vIRF3 is a bona fide oncogene which can inhibit the function of p53. Moreover, among the KSHV vIRFs, the function of vIRF3 is thought to be B cell-specific. Interestingly, the expression level of vIRF3 does not fluctuate even after lytic reactivation (Rivas et al. 2001), suggesting that there is an alternative level of regulation driving vIRF3 expression in B cells. In latently infected PEL cell lines, vIRF3 is linked to decreased MHC-II expression, and vIRF3 also modulates both type II (Schmidt et al. 2011) and type I interferon responses (Lubyova et al. 2004). vIRF3-mediated inhibition of IFNγ results in inhibition of both PIII and PIV promoter of class II transactivator (CIITA) transcription (Schmidt et al. 2011). Importantly, vIRF3 is required for the survival of both EBV co-infected and EBV negative B cell lymphomas in vitro (Wies et al. 2008).

1.8.3 Proliferation and plasmablast differentiation

PEL is an immunoblastic tumor affecting the pericardial or pleural area of the body cavities. PEL tumor cells are negative for most B cell surface markers except CD138/syndecan, a marker of terminal plasma cell differentiation (Jenner et al. 2003). These terminally differentiated CD138+CD20+ and CD20− plasma cells are highly targeted by KSHV infection in primary B cells of tonsillar sample, gaining greater survival rate for CD20− cells over 3 days post infection. This indirect survival effect is as a result of differentiation of other B cell lineages into the CD138+ cells (Aalam et al. 2020). Interestingly, more than 60% of the KSHV infected B cells from PBMCs of KS positive patients are positive for CD138 (Bella et al. 2010). In MCD, the pathological cells are monotypic/polyclonal plasmablasts located in the mantle zone of spleen and lymph nodes (Du et al. 2001). These cells express PRDM1 / BLIMP1 marking them as pre-plasma or terminal plasma stage of B-cell differentiation (Chadburn et al. 2008). Most of KSHV infected B cells in MCD patients express IL-6 (Du et al. 2001), and the importance of IL-6 signaling in MCD is illustrated by the finding that tocilizumab (an IL-6R blocking monoclonal antibody) can ameliorate the symptoms or even lead to prolonged remission in some MCD cases (Song et al. 2010; Galeotti et al. 2012; Ramaswami et al. 2020). In ex vivo infection models, particularly those performed in tonsillar B lymphocytes, the immunophenotype of infected cells closely resembles the pathological cells present in MCD (Du et al. 2001; Chadburn et al. 2008; Totonchy et al. 2018). Latently KSHV infected B cells from the tonsil (characterized by LANA dots), proliferate, and express a high level of IL-6R and CD27 on their surface exhibiting plasma blast morphology at 72 h post-infection (Hassman et al. 2011). Similarly, KSHV infection of naïve B lymphocytes from human tonsil upregulates IL-6 secretion as well as CD27 expression (Totonchy et al. 2018). Ex vivo infection of activated peripheral blood B cells expressing DC-SIGN results in infection of primarily naive

and IgM memory B cells at early times post-infection (Rappocciolo et al. 2008). Remarkably, a similar expansion of MZ-like memory and naive B cells is seen in PBMC from HIV negative KS patients (Bella et al. 2010). Taken together, the concordance between pre-disease immunophenotypes, ex vivo infection immunophenotypes and the phenotypes seen in KSHV lymphoproliferative diseases suggests that KSHV infection manipulates B cell compartment toward particular immunophenotypes even in the absence of overt KSHV-associated lymphoproliferation.

1.8.4 Induction of immunoglobulin light chain revision

One of the more puzzling characteristics of MCD is the fact that KSHV infection is restricted to Igλ positive B lymphocytes in patient samples (Du et al. 2001). The same restriction is observed in KSHV infected B lymphocytes derived from tonsil samples (Hassman et al. 2011). Moreover, in PEL, most infected B cells are lg negative with occasional Igλ positive B cells (Matolcsy et al. 1998). Our group was able to show that KSHV infection in Igκ tonsil lymphocytes induces Igλ expression via re-induction of V(D)J recombination driving BCR revision. These cells express LANA, K8.1 and ORF59 markers, indicating a mixed population of lymphocytes in latent and lytic stages of infection (Totonchy et al. 2018). The same study also detects the Igλ+ KSHV infected cells in biopsies of HIV positive patients with AIDS-related lymphadenopathy (ARL) having no histologically similar characteristics of MCD, again supporting the conclusion that KSHV manipulates B cell physiology even in the absence of KSHV-associated lymphoproliferative disease and establishing that the Igλ+ phenotype in MCD is driven directly by KSHV infection. Further study is needed to characterize the intervening events that drive KSHV infected B cells from these early manipulations of B cell phenotype and physiology to overt pathological lymphoproliferation.

1.9 KSHV Transmission

Serological diagnosis is the standard method of KSHV detection and prevalence estimation, as KSHV DNA is not detectable in all infected individuals (Uldrick and Whitby 2011). Sadly, a majority of the conducted epidemiological studies suffer from implementation of unstandardized serological diagnostic techniques, underestimating the cases with low titers of anti-KSHV antibodies (Tedeschi, Dillner, and De Paoli 2002). As a result, not only are the epidemiological studies impacted, but the KSHV pathology is somewhat underrepresented as well.

Unlike other herpesviruses, the epidemiology of KSHV is not the same around the world, and its transmission is mainly affected by the sociodemographic background and endemicity (Iftode et al. 2020). KSHV was initially thought to be a sexually transmitted disease during the AIDS pandemic (Mesri, Cesarman, and Boshoff 2010). It is now believed that salivary transmission is the major route of KSHV transmission in endemic areas, while sexual risk factors dominate transmission in certain populations (Martin and Osmond 2000). The seroprevalence of KSHV is higher in men who have sex with men as compared to heterosexuals (Martin et al. 1998), which is most likely due to presence of other risk factors associated with homosexuality and sexual practices; such as number of sexual partners and co-infection with other pathogens, along with salivary exchange (Martin et al. 1998; Martin and Osmond 2000; Martró et al. 2007; Wakeham et al. 2013).

Primary KSHV infection usually occurs during childhood, and transmission may occur anytime in adulthood via both sexual and non-sexual routes (Minhas and Wood 2014). KSHV DNA has been detected in oropharyngeal mucosa, saliva, PBMCs, prostate glands, semen, and cervicovaginal secretions (T. Chen and Hudnall 2006; Kedes et al. 1996; Mantina et al. 2001; Mbulaiteye et al. 2003). KSHV infected solid organ transplants and blood transfusions are also routes of KSHV transmission that should not be neglected (Marcelin et al. 2004; Hladik et al. 2006).

KSHV is thought to be transmitted from mother to child, and seropositivity increases with age (Wakeham et al. 2013). In a study conducted on South African mothers, KSHV DNA was detected in breast milk of about 20% of the subjects, suggesting that KSHV may be transmitted from mother to child via breastfeeding (Dedicoat et al. 2004). However, this finding was not supported by another study, thus the transmission via this route is debatable (Brayfield et al. 2004). Another possible route of KSHV transmission from mother to child is during gestation, indicated by high KSHV DNA load in genital secretions (Lisco et al. 2006). The development of KS during infancy is further proof of this route of transmission at the prenatal stage (Gutierrez-Ortega et al. 1989). Nevertheless, in endemic and non-endemic areas, the prevalence of premastication of food for young children could account for salivary transmission as a prominent mode of horizontal transmission, if KSHV is not acquired prenatally (Cunha et al. 2005; Rohner et al. 2016; Cao et al. 2014).

1.10 Justification and Significance of Study

Saliva is widely accepted as the principal mode of KSHV transmission (Casper et al. 2004, 2007) and KSHV disease frequently manifests in the oral cavity (Pantanowitz et al. 2013; Feller et al. 2007). KSHV DNA is detectable in human saliva, and salivary transmission is thought to be the primary route of person-to-person transmission for KSHV (Quinlivan et al. 2001; Olp et al. 2016; Totonchy et al. 2018), making the oral lymphoid tissue a likely site for the initial infection of B lymphocytes in a naïve human host. Thus, the tonsil and other oral lymphoid tissues, which are in contact with transmitted saliva and are rich in KSHV target cell types, represent a critical niche for early infection events in the human host.

To date, several other groups, including our own, have been successful in infecting B lymphocytes derived from human tonsils (Hassman, Ellison, and Kedes 2011; Myoung and Ganem 2011b, 2011a; Bekerman et al. 2013; Nicol et al. 2016; Totonchy et al. 2018). *Ex vivo* infection of tonsil lymphocytes is emerging as a viable strategy for studying early infection events for KSHV infection in B lymphocytes. However, the existing literature on KSHV infection of tonsil lymphocytes is highly varied in both approach and outcome. The previous studies of B cell infection suffer from analyzing limited markers (Hassman, Ellison, and Kedes 2011; Totonchy et al. 2018; Nicol et al. 2016; Bekerman et al 2013) and use of co-culture method of B cell infection (Bekerman et al 2013). Thus, limiting our understanding of KSHV targets within B cell sub-populations. In these studies, we aim to characterize the frequency of lymphocyte populations in human tonsillar specimens using lineage-defining immunological markers by flow cytometry. We then attempt to infect naïve B cells with KSHV according to our unique in-house method to determine the host factor's contribution to KSHV susceptibility of B cells by correlating baseline frequencies of immunological subsets with susceptibility of tonsil specimens to KSHV infection.

An extensive body of literature has illustrated saliva, blood, and organ transplants as the main sources of horizontal KSHV transmission (Uldrick and Whitby 2011; Minhas and Wood 2014), indicative of KSHV transmission within and between different cell types. Although tonsillar primary cells can be successfully infected in tissue culture (M Duss et al. 2004; Muniraju et al. 2019) the dynamic of the transmission of KSHV infection within the tonsillar cell types has not been appropriately addressed. This represents a significant gap in our understanding, which specifically limits our ability to develop strategies to decrease KSHV transmission. Hence, limiting our understanding of how KSHV transmitted from these cells to target B cells or vice versa to manipulate B cell physiology in the development of PEL and MCD.

Many models predict that transfer of EBV infection from tonsillar B lymphocytes to epithelial cells contributes substantially to the release of EBV particles into saliva (Thorley-Lawson et al. 2013), but similar mechanisms have not been characterized for KSHV. A variety of the adherent cell lines including primary adherent cell lines from tonsils are susceptible to KSHV infection (Bechtel et al. 2003; Muniraju et al. 2019). Having access to patients' autologous cell types makes our experimental approach distinctly unique in that the viral transmission within these cell types can be demonstrated. Thus, analyzing the dynamics of infection, persistence and virus production in non-lymphocyte tonsil cell types may reveal novel but generalizable avenues for limiting initial infection and preventing the spread of infection to B lymphocytes, which has not been done in the past. Thus, we aim to develop a model for cell-to-cell transmission of KSHV within the human tonsil. For this approach, we extract and sort the tonsillar primary cells (epithelial, fibroblast, and B lymphocytes), and monitor the dynamic of KSHV infection via cell-to-cell and cell free virion transmission through implementation of co-culture and use of appropriate markers for analysis.

Another major gap in our understanding of KSHV transmission is KSHV's broad cellular tropism and the implementation of a distinctive collection of viral and cellular receptors for the entry process into each cell type (van der Meulen et al. 2021). The majority of the data on KSHV entry comes from studying adherent cells, while there is limited data regarding KSHV entry into B cells (van der Meulen et al. 2021).

Erythropoietin producing hepatocellular receptors (Eph) are tyrosine kinases, together with their corresponding ephrin ligands, they are fundamental regulators of a diversity of cellular processes, such as proliferation, differentiation, cell migration, angiogenesis, and tissue boundary formation (Haqshenas and Doerig 2019). Eph receptors are divided into A and B classes according to their sequence similarity and their binding affinity towards their ligands (de Boer, van Gils, and van

32

Gils 2020). Among the EphA class of receptors, EphA2 serves as an entry receptor for KSHV, Epstein–Barr virus (EBV) or HHV-4 (Chen et al. 2018; Zhang et al. 2018; Hahn et al. 2012). KSHV interaction with EphA2 results in the amplification of the signaling events required for efficient infection (Chakraborty et al. 2012). It has been demonstrated that gH/gL binding to EphA2 activates its phosphorylation, which leads to KSHV endocytosis (Hahn et al. 2012). The dynamic of EphA2 interaction with gH/gL has been established (Hahn and Desrosiers 2014; Light et al. 2021; Su et al. 2020), and its role in KSHV infectivity of epithelial, endothelial and fibroblast cells have been evaluated (Hahn et al. 2012; Chakraborty et al. 2012; Dutta et al. 2013). However, its role in entry into B cells has not been demonstrated. We have recently analyzed the role of gH glycoprotein and DC-SIGN cellular receptor in KSHV infection of B lymphocytes. We were able to demonstrate that KSHV entry into B cell subsets is subtype specific (Palmerin et al. 2021). Given the importance of EphA2 in KSHV entry (Hahn et al. 2012), it is distinctly possible that EphA2 serves as an entry receptor in some of our tonsillar B cell subtypes. KSHV gH/gL has binding affinity towards EphA4 and EphA7, albeit with lower avidity as compared to EphA2 (Hahn et al. 2012; Chen et al. 2019; Großkopf et al. 2019). Indeed, it has been demonstrated that EphA4 and EphA7 can serve as entry receptors for KSHV as well (J. Chen et al. 2019; Großkopf et al. 2019).

Glycoprotein gH is not dispensable for the infection of epithelial, endothelial, and fibroblast cells. Therefore, KSHV-ΔgH is incapable of infecting these cells (Muniraju et al. 2019b). Studies demonstrate that gH/gL binding to EphA2 complex is established by the contribution of both the gH and gL glycoproteins (Light et al. 2021; Su et al. 2020). Absence of gH results in retention of gL within the cell (A. Hahn et al. 2009), thus KSHV-ΔgH virions lack the gH/gL complex. Therefore, to analyze the role of EphA2, A4, and A7 as the entry receptors for KSHV in tonsillar

B cells, we will use a strain of KSHV in which gH has been functionally removed via insertion of sequential stop codons into the open reading frame (KSHV-ΔgH) to infect total B lymphocytes and determine whether EphA-gH interactions are important for KSHV entry. We first aim to determine the distribution of EphA receptors on tonsillar B lymphocyte subtypes, we then assess their biological role in the infection process by neutralization strategies. Comparing the neutralization conditions of both WT and ΔgH with the baseline level of EphA2, A4, and A7 allows us to discover the importance of gH/gL complex interaction with these Eph receptors in the infection process in lymphocyte subtypes that have not been investigated before.

2 CHAPTER II: Analysis of KSHV B lymphocyte lineage tropism in human tonsil reveals efficient infection of CD138+ plasma cells

Farizeh Aalam and Romina Nabiee were co-first authors on this manuscript. Ms. Aalam performed the extensive baseline analysis of tonsil lymphocyte T and B cells subsets that is used to determine whether immunological baseline factors correlate to susceptibility on a per-sample basis (Figure 2.3-1, Figure 2.3-3F, Figure 2.3-5, Figure 2.3-6). In addition, Ms. Aalam performed the experiments testing the contribution of HSPG and CD138 to KSHV infection in tonsil lymphocytes (Figure 2.3-4).

Abstract

Despite 25 years of research, the basic virology of Kaposi Sarcoma Herpesviruses (KSHV) in B lymphocytes remains poorly understood. This study seeks to fill critical gaps in our understanding by characterizing the B lymphocyte lineage specific tropism of KSHV. Here, we use lymphocytes derived from 40 human tonsil specimens to determine the B lymphocyte lineages targeted by KSHV early during de novo infection in our ex vivo model system. We characterize the immunological diversity of our tonsil specimens and determine that overall susceptibility of tonsil lymphocytes to KSHV infection varies substantially between donors. We demonstrate that a variety of B lymphocyte subtypes are susceptible to KSHV infection and identify CD138+ plasma cells as a highly targeted cell type for de novo KSHV infection. We determine that infection of tonsil B cell lineages is primarily latent with few lineages contributing to lytic replication. We explore the use of CD138 and heparin sulfate proteoglycans as attachment factors for the infection of B lymphocytes and conclude that they do not play a substantial role. Finally, we determine that the host T cell microenvironment influences the course of de novo infection in B lymphocytes. These results improve our understanding of KSHV transmission and the biology of early KSHV infection in a naïve human host and lay a foundation for further characterization of KSHV molecular virology in B lymphocyte lineages.

Author summary

KSHV infection is associated with cancer in B cells and endothelial cells, particularly in the context of immune suppression. Very little is known about how KSHV is transmitted and how it initially establishes infection in a new host. Saliva is thought to be the primary route of person-to-person transmission for KSHV, making the tonsil a likely first site for KSHV replication in a new human host. Our study examines KSHV infection in B cells extracted from the tonsils of 40 human donors in order to determine what types of B cells are initially targeted for infection and examine how the presence (or absence) of other immune cells influence the initial stages of KSHV infection. We found that a variety of B cell subtypes derived from tonsils can be infected with KSHV. Interestingly, plasma cells (mature antibody-secreting B cells) were a highly targeted cell type. These results lay the foundation for further studies into the specific biology of KSHV in different types of B cells, an effort that may help us ultimately discover how to prevent the establishment of infection in these cells or reveal new ways to halt the progression of B cell cancers associated with KSHV infection.

2.1 **Introduction**

Kaposi Sarcoma-associated Herpesvirus (KSHV/HHV-8) is a lymphotropic gammaherpesvirus. In addition to its role in the pathogenesis of Kaposi Sarcoma (KS) (Chang, et al. 1994), KSHV infection is associated with two lymphoproliferative disorders, multicentric Castleman disease (MCD) and primary effusion lymphoma (PEL) (Cesarman E, 1995; Soulier J, 1995), as well as a recently characterized inflammatory disorder KSHV inflammatory cytokine syndrome (KICS) (Uldrick TS, 2010). Although KSHV-associated lymphoproliferative disorders are rare, their incidence has not declined as HIV treatment has improved (Powles T, 2009; Bhutani M, 2015) suggesting that, in contrast to KS, immune reconstitution is not sufficient to prevent KSHV associated lymphoproliferative disease in people living with HIV/AIDS. Moreover, the KSHV-associated lymphoproliferative diseases are uniformly fatal with few effective treatment options (Carbone A V. E. 2014). Despite the fact that KSHV is lymphotropic and causes pathological lymphoproliferation in vivo, study of de novo KSHV infection in B lymphocytes has historically been difficult (Kang S, 2017). Resting peripheral B cells and many established B cell-derived cell lines are refractory to KSHV infection but unstimulated tonsil-derived lymphocytes are susceptible to infection (Rappocciolo et al. 2008). To date, several other groups, including our own, have been successful in infecting B lymphocytes derived from human tonsils (Hassman LM, 2011; Myoung J, 2011; Myoung J, 2011; Bekerman E, 2013; Totonchy et al 2018; Nicol SM, 2016). KSHV DNA is detectable in human saliva and salivary transmission is thought to be the primary route of person-to-person transmission for KSHV (Casper C K. E.-L. 2007; Pauk J, 2000; Casper C R. M.-L. 2004; Vieira J, 1997) making the oral lymphoid tissues a likely site for the initial infection of B lymphocytes in a naïve human host. Thus, in addition to being susceptible to ex vivo infection, tonsil lymphocytes represent a highly relevant model for understanding early infection events in

KSHV transmission. The existing studies of KSHV infection in tonsil-derived B cells have explored a limited number of cell surface markers including IgM, immunoglobulin light chains and activation markers on infected cells (Hassman LM, 2011; Totonchy J, 2018; Nicol SM, 2016). One study using PBMC-derived B lymphocytes identified naïve, memory and plasma cell-like lineages as infection targets in both in vitro infection experiments and blood samples from KS patients (Knowlton ER, 2014). However, no studies to date have comprehensively explored the specific B lymphocyte lineages targeted by KSHV infection in human tonsil specimens.

In this study, we performed KSHV infection of 40 human tonsil specimens from diverse donors and utilized lineage-defining immunological markers by flow cytometry to establish the primary B cell lineage tropism of KSHV. Our results demonstrate that the susceptibility of tonsil-derived B lymphocytes to ex vivo KHSV infection varies substantially from donor-to-donor, and that a variety of B cell lineages are susceptible to KSHV infection and that, at least at early stages post infection KSHV is primarily latent in most cell types. In particular, CD138+ plasma cells are highly targeted by KSHV infection despite the fact that they are present at low frequencies in tonsil tissue. We demonstrate that high susceptibility of plasma cells to KSHV infection is not due to the presence of CD138 heparin sulfate proteoglycan as an attachment factor. Moreover, HSPG are not generally important for infection of primary B lymphocytes. Finally, we demonstrate that although the baseline T cell microenvironment does not seem to influence overall susceptibility of tonsil specimens to KSHV infection, the specific lineage distribution of KSHV infection is affected by the T cell microenvironment and manipulation of CD4/CD8 T cell ratios can alter the targeting of specific B cell lineages by KSHV. These results provide new insights into early events driving the

establishment of KSHV infection in the human immune system and demonstrate that alterations in immunological status can affect the dynamics of KSHV infection in B lymphocytes.

2.2   Materials and Methods

2.2.1   Ethics statement

Human specimens used in this research were de-identified prior to receipt from NDRI and thus were not subject to IRB review as human subjects research.

2.2.2   Reagents and cell lines

CDw32 L cells (CRL-10680) were obtained from ATCC and were cultured in DMEM supplemented with 20% FBS (Sigma Aldrich) and Penicililin/Streptomycin/L-glutamine (PSG/Corning). For preparation of feeder cells CDw32 L cells were trypsinized and resuspended in 15 ml of media in a petri dish and irradiated with 45 Gy of X-ray radiation using a Rad-Source (RS200) irradiator. Irradiated cells were then counted and cyropreserved until needed for experiments. Cell-free KSHV.219 virus derived from iSLK cells (Myoung & Ganem, 2011)was a gift from Javier G. Ogembo (City of Hope). Human tonsil specimens were obtained from NDRI. Human fibroblasts were derived from primary human tonsil tissue and immortalized using HPV E6/E7 lentivirus derived from PA317 LXSN 16E6E7 cells (ATCC CRL-2203). Antibodies for flow cytometry were from BD Biosciences and Biolegend and are detailed below.

2.2.3   Isolation of primary lymphocytes from human tonsils

De-identified human tonsil specimens were obtained after routine tonsillectomy by NDRI and shipped overnight on wet ice in DMEM+PSG. All specimens were received in the laboratory lessthan24hourspost-surgeryandwerekeptat4℃ throughout the collection and transportation

process. Lymphocytes were extracted by dissection and maceration of the tissue in RPMI media. Lymphocyte-containing media was passed through a 40µm filter and pelleted at 1500rpm for 5 minutes. RBC were lysed for 5 minutes in sterile RBC lysing solution (0.15M ammonium chloride, 10mM potassium bicarbonate, 0.1M EDTA). After dilution to 50ml with PBS, lymphocytes were counted, and pelleted. Aliquots of $5(10)7$ to $1(10)8$ cells were resuspended in 1ml of freezing media containing 90% FBS and 10% DMSO and cryopreserved until needed for experiments.

2.2.4 **Infection of primary lymphocytes with KSHV**

Lymphocytes were thawed rapidly at 37˚C, diluted dropwise to 5ml with RPMI and pelleted. Pellets were resuspended in 1ml RPMI+20%FBS+100µg/ml DNase I+ Primocin 100µg/ml and allowed to recover in a low-binding 24 well plate for 2 hours at 37˚C, 5% CO2. After recovery, total lymphocytes were counted, and Naïve B cells were isolated using Mojosort Naïve B cell isolation beads (Biolegend 480068) or Naïve B cell Isolation Kit II (Miltenyi 130-091-150) according to manufacturer instructions. Bound cells (non-naïve B and other lymphocytes) were retained and kept at 37˚C in RPMI+20% FBS+ Primocin 100µg/ml during the initial infection process. $1(10)6$ Isolated naïve B cells were infected with iSLK-derived KSHV.219 (dose equivalent to the ID20 at 3dpi on human fibroblasts) or Mock infected in 400ul of total of virus + serum free RPMI in 12x75mm round bottom tubes via spinoculation at 1000rpm for 30 minutes at 4˚C followed by incubation at 37˚C for an additional 30 minutes. Following infection, cells were plated on irradiated CDW32 feeder cells in a 48 well plate, reserved bound cell fractions were added back to the infected cell cultures, and FBS and Primocin (Invivogen) were added to final concentrations of 20% and 100µg/ml, respectively. Cultures were incubated at 37˚C, 5% CO2 for the duration of the experiment. At 3 days post-infection, cells were harvested for analysis by flow cytometry.

2.2.5 Flow cytometry staining and analysis of KSHV infected tonsil lymphocytes

A proportion of lymphocyte cultures at baseline or 3dpi representing ~500,000 cells were pelleted at 1400 rpm for 3 minutes into 96-well round bottom plates. Cells were resuspended in 100µl PBS containing (0.4ng/ml) fixable viability stain (BD 564406) and incubated on ice for 15 minutes. Cells were pelleted and resuspended in 100µl cold PBS without calcium and magnesium containing 2% FBS,0.5% BSA (FACS Block) and incubated on ice for 10 minutes after which 100µl cold PBS containing 0.5% BSA and 0.1% Sodium Azide (FACS Wash) was added. Cells were pelleted and resuspended in FACS Wash containing B cell phenotype panel as follows for 15 minutes on ice: (volumes indicated were routinely used for up to $0.5(10)^{\wedge}6$ cells and were based on titration of the individual antibodies on primary tonsil lymphocyte specimens) CD19-PerCPCy5.5 (2.5µl, BD 561295), CD20-PE-Cy7 (2.5ul, BD 560735), CD38-APC (10µl, BD 555462), IgD-APC-H7 (2.5µl, BD 561305), CD138-v450 (2.5µl, BD 562098), CD27-PE (10µl BD 555441). After incubation, 150µl FACS Wash was added and pelleted lymphocytes were washed with a further 200µl of FACS Wash prior to being resuspended in 200µl FACS Wash for analysis. Data was acquired on a BD FACS VERSE Flow Cytometer and analyzed using FlowJo software. Readers should note that the BD FACS VERSE analysis instrument lacks a 561nm laser so RFP lytic reporter expression from the KSHV.219 genome is not detectable in the PE channel. For baseline T cell frequencies 0.5e6 cells from baseline uninfected total lymphocyte samples were stained and analyzed as above with phenotype antibody panel as follows: CD95-APC (2µl, Biolegend 305611), CCR7-PE (2µl, BD 566742), CD28-PE Cy7 (2µl, Biolegend 302925), CD45RO-FITC (3µl, Biolegend 304204), CD45RAPerCP Cy5.5 (2µl, 304121), CD4-APC H7 (2µl, BD 560158), CD19-V510 (3µl, BD 562953), CD8-V450 (2.5µl, BD 561426).

2.2.6 B lymphocyte lineage isolation by cell sorting

At 3 days post-infection cells were collected and pelleted at 1400 rpm for 3 minutes into 12x75mm round bottom tubes. Cells were resuspended in 200μl PBS containing (0.4ng/ml) fixable viability stain (BD 565388) and incubated on ice for 15 minutes. Cells were pelleted and resuspended in 200μl cold MACS buffer containing 5% FBS (Sort Block) and incubated on ice for 10 minutes after which 200μl cold MACS buffer was added. Cells were pelleted and resuspended in MACS buffer containing B cell phenotype panel as follows for 15 minutes on ice: (volumes indicated are for each $1(10)^6$ cells and were scaled depending upon the number of cells being stained for sorting). For single cell sorting of plasma cells the panel was follows: CD19-PerCPCy5.5 (5μl, BD 561295), CD20-PE-Cy7 (5ul, BD 560735), and CD138-APC (5μl, Biolegend 352307). For other lineages the panel was as follows: CD19-PerCPCy5.5 (5μl, BD 561295), CD38-APC (20μl, BD 555462), IgD-PE-Cy7 (5, BD 561314), CD27-PE-Cy5 (5μl eBioscience 15-0279-42). After incubation, 500μl MACS buffer was added and pelleted lymphocytes were washed with a further 500μl of MACS buffer prior to being resuspended in 200μl MACS buffer and put through a cell strainer before sorting using the 70-micron nozzle on a BD FACSAria Fusion Cell Sorter.

2.2.7 RT-PCR

At 3 days post infection, lymphocytes were harvested into Trizol or sorted into Trizol LS reagent 300μl Trizol was used for >1e5 cells and 100μl Trizol was used for <1e5 cells. An equal volume of DNA/RNA shield (Zymo Research R110- 250) was added after collection and RNA extraction was performed using Zymo Directzol Microprep (Zymo Research R2060) according to manufacturer instructions. RNA was eluted in 10μl H2O containing 2U RNase inhibitors and a second DNase step was performed for 30 minutes using the Turbo DNA-Free kit (Invitrogen AM1907M) according to manufacturer instructions. One step RT-PCR cDNA synthesis and

preamplification of GAPDH, LANA and K8.1transcripts was performed on 5µl of RNA using the Superscript III One-step RT-PCR kit (ThermoFisher 12574026) and 2µM outer primers for each target gene as follows: GAPDH outer forward (5'-TCGGAGTCAACGGATTTGGT-3'), GAPDH outer reverse (5'- GGGTCTTACTCCTTGGAGGC-3'), LANA outer forward (5'-AATGGGAGCCACCGGTAAAG-3'), LANA outer reverse (5'-CGCCCTTAACGAGAGGAAGT-3'), K8.1 outer forward (5'-ACCGTCGGTGTGTAGGGATA-3'), K8.1 outer reverse (5'-TCGTGGAACGCACAGGTAAA-3'). Duplicate no RT (NRT) control reactions were assembled for each lineage/sample containing only Platinum Taq DNA polymerase (Thermofisher 15966005) instead of the Superscript III RT/Taq DNA polymerase mix. After cDNA synthesis and 40 cycles of target pre-amplification, 0.002µl of pre-amplified cDNA or NRT control reaction was used as template for multiplexed real-time PCR reactions using TaqProbe 5x qPCR MasterMix - Multiplex (ABM MasterMix-5PM), 5% DMSO, primers at 900nM and probes at 250nM against target genes as follows: GAPDH forward (5'- TCGGAGTCAACGGATTTGGT-3'), GAPDH reverse (5'-GGGTCTTACTCCTTGGAGGC-3'), GAPDH probe (5'[HEX]-ACGCCACAGTTTCCCGGAGG-[BHQ1]3') LANA forward (5'-AATGGGAGCCACCGGTAAAG-3'), LANA reverse (5'-CGCCCTTAACGAGAGGAAGT-3'), LANA probe (5' [6FAM]- ACACAAATGCTGGCAGCCCG-[BHQ1]3'), K8.1 forward (5'-ACCGTCGGTGTGTAGGGATA-3'), K8.1 reverse (5'- TCGTGGAACGCACAGGTAAA-3'), K8.1 probe (5'[FAM]-TGCGCGTCTCTTCCTCTAGTCGTTG-[TAMRA]3') and analyzed using a 40 cycle program on a ThermoFisher QuantStudio 3 real time thermocycler. Data is represented as quantitation cycle (Cq) and assays in which there was no detectable Cq value were set numerically as Cq=41 for analysis and data visualization..

2.2.8 Single cell RT-PCR

Single cells meeting lineage sort criteria were sorted into each well of a 0.2ml 96-well PCR plate containing 4μl of 0.5x PBS, 10mM DTT (Pierce no-weigh A39255), 1.2U RNase inhibitor (Lucigen 30281-2). After sorting, plates were sealed, centrifuged briefly to collect all material in the bottom of the well and stored at -80˚C prior to analysis. Plates were thawed on ice and 2μl of DNase buffer (Invitrogen 18068-015) containing 0.5μl 10x buffer, 0.1U DNase, 0.4μl H2O) were added to each well. After incubation at room temperature for 15 minutes, EDTA (Thermofisher AM9260G) was added to a final concentration of 2mM and DNase was inactivated by incubation for 10 minutes at 65˚C. One-Step RT-PCR reactions and no RT (NRT) controls were assembled using outer primers to GAPDH, LANA, and K8.1 as described above. 2μl of pre-amplified cDNA was used in the real time PCR reactions for GAPDH, K8.1, LANA as described above with the exception that the assay was multiplexed with all three targets using the same K8.1 probe sequence labeled with 5'Cy5 and 3'BHQ-2 quencher and analyzed on a BioRad CFX96 real time PCR thermocycler. KSHV neutralization via soluble CD138 Syndecan-1. Infections were performed as described above except KSHV.219 virus was pre-incubated for 30 minutes on ice with serum free RPMI only or serum free RPMI containing recombinant human syndecan-1 protein (srCD138, Bio Vision, 7879-10) prior to being added to Naïve B lymphocytes. srCD138 concentrations noted in the text indicate the final concentration of recombinant syndecan-1 in the reconstituted total lymphocyte culture. Infection was analyzed at 3 days post-infection by flow cytometry for B cell lineages and KSHV infection as detailed above. For experiments involving human fibroblasts virus was added to cells in serum free media, cells were spinoculated for 30 minutes at 1000rpm, incubated at 37˚C for 1 hour, then infection media was removed and replaced with complete media. At 3dpi cells were harvested via trypsinization and analyzed for infection by flow cytometry.

2.2.9 Heparinase treatment of human fibroblasts and lymphocytes

Total lymphocytes were thawed and recovered as described above and treated with Heparinase I and III Blend from Flavobacterium heparinum (Sigma-Aldrich # H3917) at 9U/25e6 of lymphocytes and incubated over irradiated CDW32 feeder cells at 37˚C, 5% CO_2 for 24 hours in complete media. E6/E7 transformed fibroblasts from human tonsil were treated at 4.5U/1e6 for 24hrs at 37˚C, 5% CO_2. To evaluate the effectiveness of the Heparinase treatment the samples were stained for flow cytometry, as described above, with Heparan Sulfate (10E4 epitope) (FITC) (United States Biological # H1890) at 2 μl/5e5 of the lymphocytes or E6/E7 transformed fibroblasts and analyzed with flow cytometry for loss of HSPG signal. Control untreated or Heparinase-treated samples were either Mock infected or infected with KSHV as described above. At 3 days post infection, fibroblasts were trypsinized and analyzed for GFP expression by flow cytometry and lymphocytes were harvested, stained for B cell lineages, and analyzed by flow cytometry as described above.

2.2.10 T cell depletion studies

Infections were performed as described above except a sub-population of total lymphocytes were depleted of either CD4 or CD8 T cells using positive selection magnetic beads (Biolegend MojoSort Human CD4 T Cell Isolation Kit 480009, MojoSort Human CD8 T Cell Isolation Kit 480011). The resulting depleted fractions or unmanipulated total lymphocytes were used to reconstitute naïve B lymphocytes following infection rather than bound lymphocyte fractions as described above.

2.2.11 Statistical Analysis

Statistical Analysis. Data plots and statistical analysis were performed in R software[40] using ggplot2, ggcorrplot{ggcorrplot:2018tg} and RColorBrewer packages. Specific methods of statistical analysis and resulting values for significance and correlation are detailed in the corresponding figure legends.

2.3 Results

2.3.1 Variable immunological composition of human tonsil specimens

In order to explore the B cell lineages targeted by KSHV infection in human tonsils, we procured a cohort of 40 de-identified human tonsil specimens from donors of diverse age, sex, and self-reported race (Figure 2.3-1A and Table 2.3 1). Analysis of the baseline frequencies of B and T cell lineages by multi-color flow cytometry (Appendix A.1, Appendix A.2 and Table 2.3 2) revealed that the composition of individual human tonsil specimens is highly variable (Fig 2.3-1B&D). This variation was independent of donor age for many lineages. However, overall B cell frequencies declined with age as did germinal center, plasmablast and transitional B cell populations while memory and naïve populations increased in frequency with donor age (Fig 2.3-1C). Similarly, most T cell lineages were not significantly correlated with donor age except for CD4+ transitional memory and CD8+ terminal effector lineages which were both moderately, but significantly, negatively correlated with donor age (Fig 2.3-1E).

Table 2.3-1. Donor demographics for the tonsil specimens used in the study (n=40)

Sex, n (%)	
Male	19 (47.5)
Female	21 (52.5)
Race, n (%)	
ND	6 (15)
White	17 (42.5)
Black	13 (32.5)
Hispanic	1 (2.5)
Asian	1 (2.5)
Other	2 (5)
Age, (years)	
(mean ± S.D.)	26.2 ± 16.47
Range	2-65
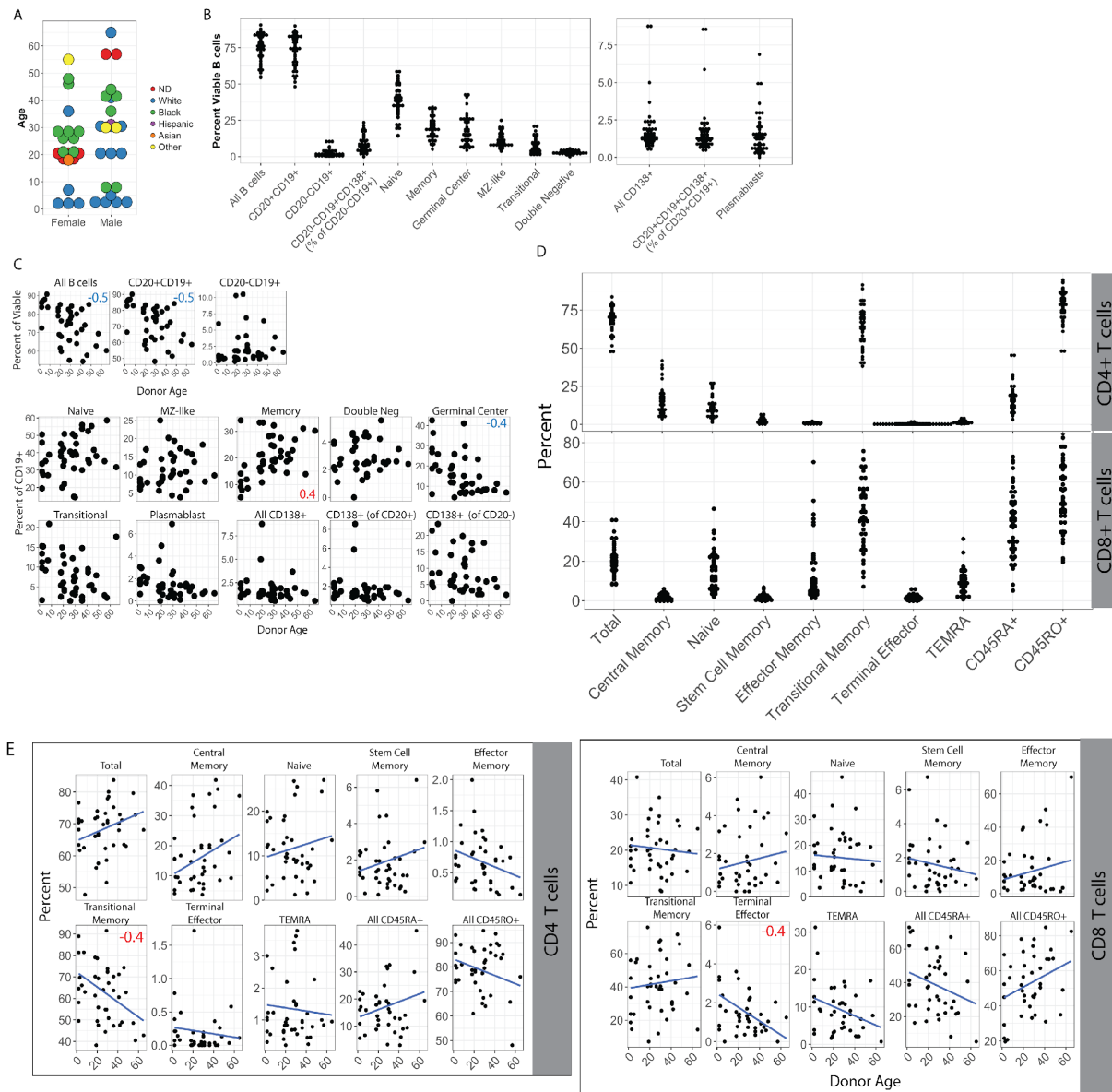
Figure 2.3-1. Variability and age-dependence of B lymphocyte lineage distribution in human tonsils.

(A) Donor demographics for human tonsil specimens used in this study. Plotted by age (y-axis), sex (x-axis) and self-reported race (color) ND = not determined. **(B)** Frequency distributions of B cell lineages in tonsil specimens (see S1A Fig and Table 2.3-2 for lineage definitions). All B cells are shown as frequency of viable lymphocytes, other B cell subsets are shown as frequency of viable, CD19+ B cells unless otherwise specified in parenthesis. **(C)** Frequency of B cell lineages based on donor age. Pearson correlation coefficients (r) with an absolute value greater than or equal to 0.4 are shown as red or blue inset text in the subset panels. **(D)** Frequency distributions of T cell lineages in tonsil specimens (see S1B Fig and

49

Table 2.3-2 for lineage definitions). All T cells are shown as frequency of viable CD4+ (top) or CD8+ (bottom) T cell except total CD4+ and total CD8+ (far left) which are shown as frequency of viable lymphocytes. **(E)** Frequency of CD4+ (left) and CD8+ (right) T cell lineages based on donor age. Pearson correlation coefficients (r) with an absolute value greater than or equal to 0.4 are shown as red or blue inset text in the subset panels

Table 2.3-2. Lineage definitions for lymphocyte subsets used in the study

B Lymphocytes

Subset	Molecular Markers
Plasma	CD19$^+$, CD20$^{+/-}$, CD138$^{+(Mid\ to\ High)}$, CD38$^-$
Transitional	CD19$^+$, CD138$^-$, CD38^{Mid}, IgD$^{+\ (Mid\ to\ High)}$
Plasmablast	CD19$^+$, CD138$^-$, CD38^{High}, IgD$^{+\ /-\ (mostly\ -)}$
Germinal Center	CD19$^+$, CD138$^-$, CD38^{Mid}, IgD$^-$
Naïve	CD19$^+$, CD138$^-$, CD38^{Low}, CD27$^-$, IgD$^{+\ (Mid\ to\ High)}$
Marginal Zone Like (MZ-Like)	CD19$^+$, CD138$^-$, CD38^{Low}, CD27$^{+\ (Mid\ to\ High)}$, IgD$^{+\ (Mid\ to\ High)}$
Memory	CD19$^+$, CD138$^-$, CD38^{Low}, CD27$^{+\ (Mid\ to\ High)}$, IgD$^-$
Double Negative	CD19$^+$, CD138$^-$, CD38^{Low}, CD27$^-$, IgD$^-$

T lymphocytes

Subset	Molecular Markers
CD4+	CD19$^-$, CD4$^{+(Mid\ to\ High)}$, CD8$^-$
CD8+	CD19$^-$, CD4$^-$, CD8$^{+\ (Mid\ to\ High)}$
Naïve	CD19$^-$, CD4+ or CD8+, CCR7$^{+(High)}$, CD45RA$^{+(Mid\ to\ High)}$, CD45RO$^-$, CD28$^+$, CD95$^-$
Stem Cell Memory	CD19$^-$, CD4+ or CD8+, CCR7$^{+(High)}$, CD45RA$^{+(Mid\ to\ High)}$, CD45RO$^-$, CD28$^+$, CD95$^{+\ (Low\ to\ Mid)}$
Central Memory	CD19$^-$, CD4+ or CD8+, CCR7$^+$, CD45RA$^-$ CD45RO$^{+(Mid\ to\ High)}$, CD28$^{+\ (Mid\ to\ High)}$
Transitional Memory	CD19$^-$, CD4+ or CD8+, CCR7$^-$, CD45RA$^-$ CD45RO$^{+(Mid)}$, CD28$^{+\ (Mid\ to\ High)}$
Effector Memory	CD19$^-$, CD4+ or CD8+, CCR7$^-$, CD45RA$^-$ CD45RO$^{+(Mid)}$, CD28$^-$
Terminal Effector Memory	CD19$^-$, CD4+ or CD8+, CCR7$^-$, CD45RA$^-$ CD45RO$^-$, CD28$^-$
TEMRA CD4+ Cells	CD19$^-$, CD4+ or CD8+, CCR7$^-$, CD45RA$^{+(High)}$, CD45RO$^-$, CD28$^-$

2.3.2 **Variable susceptibility of tonsil-derived B cells to *ex vivo* KSHV infection**

Because of the heterogeneous nature of the tonsil samples, we predicted that each sample would also have variable levels of susceptible B cell subtypes. Therefore, we employed a method for normalizing infectious dose from donor-to-donor in order to obtain cross-sectional data that was directly comparable (**Fig 2.3 2A**). For each sample we used magnetic sorting to isolate untouched naïve B cells, which are a known susceptible cell type (Totonchy J, 2018), and infected 1 million naïve B cells with equivalent doses of cell-free KSHV.219 virus. After infection, bound lymphocytes from the magnetic separation were added back to each sample to reconstitute the total lymphocyte environment. Infected cultures were incubated for three days and analyzed for both B cell lineage markers and the GFP reporter present in the KSHV.219 genome to identify infected cells. We restricted our analysis to a single timepoint at 3 days post-infection in order to observe the establishment of infection in different lineages with minimal contribution of virus mediated shifting of cellular immunophenotypes, which we observed in our previous study (Totonchy J, 2018), We first compared the overall lymphocyte populations between baseline (day 0 uninfected), Mock, and KSHV infected conditions to determine whether our infection and culture system and/or KSHV infection itself was causing significant shifts in the B lymphocyte composition of the samples. These results demonstrate that most lineages were not substantially altered by our culture system or KSHV infection compared to the baseline samples (**Fig 2.3 2B, Appendix A.2, Appendix A.3**). However, naïve B cells were significantly reduced compared to baseline levels in both Mock and KSHV infected samples at 3 dpi, suggesting that the infection method may reduce naïve cell survival in this mixed model or that the culture model drives differentiation of naïve cells into a different immunophenotype. Interestingly, B cells with a transitional phenotype are significantly increased compared to baseline in both Mock and KSHV-infected cultures. Given

that there is a relationship between transitional (IgD+, CD38mid) and naïve (IgD+, CD38low, CD27-) it is possible that naïve B cells are acquiring increased CD38 expression as a result of the infection and culture process and are thus falling into the transitional lineage gate at 3 dpi. Finally, this analysis shows that our culture system does not favor the survival of CD138+ plasma cells indicated by a significant decrease comparing baseline and Mock at 3dpi. However, this effect was lower in the KSHV-infected cultures. This result suggests that KSHV infection is either providing a survival advantage for CD138+ cells in the culture system or driving the differentiation of new CD138+ cells during infection.

Overall, susceptibility of B cells to KSHV infection varied substantially within the cohort with the majority of samples showing between 1 and 2% GFP+ B cells at 3dpi and an overall range of 0.76-3.27% (**Fig 2.3 2C, Appendix A.2**). Analysis by point-biserial correlation revealed that susceptibility was not significantly correlated with sex (rpb=0.17). Kruskal-Wallis rank sum test showed no significant association of race and susceptibility (p=0.6) and both Pearson (r=0.09) and Spearman (r=0.01) correlation tests indicated no linear or monotonic relationship between donor age and susceptibility in our data set. Thus, we can conclude that donor demographics do not substantially contribute to the variable susceptibility we observe in our tonsil lymphocyte samples.
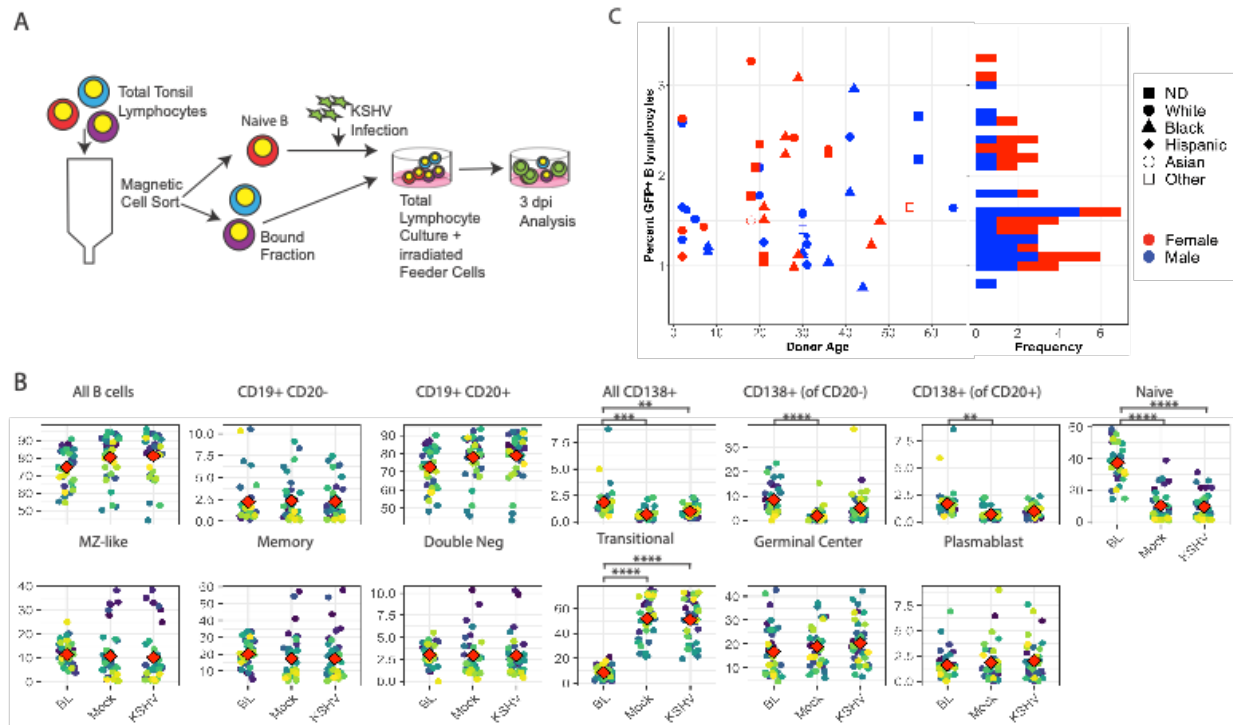
Figure 2.3-2. Tonsil-derived B lymphocytes from diverse donors display variable susceptibility to KSHV infection.

(A) Schematic of lymphocyte infection procedure. Untouched naive B cells are magnetically separated from total lymphocytes and 1e6 naive B cells are infected per condition. Following infection, bound fractions are added back to reconstitute a total lymphocyte environment and cells are plated on X-ray irradiated CDw32 feeder cells. Analysis is performed by flow cytometry at 3 days post-infection for B cell lineage markers as shown in S1 Fig and Table 2.3-2 and GFP reporter expression for KSHV infection. **(B)** The effect of KSHV infection and the culture system on overall B cell lineage frequency was examined by comparing the frequency of B cell lineages at baseline (BL, unmanipulated samples) and 3 days post infection in Mock infected and KSHV infected cultures. Student's T test was used to determine statistical significance for all comparisons **p<0.004, ***p<0.0002, ****p<1e-6 **(C)** Infection frequency data for viable, CD19+GFP+ lymphocytes at 3 dpi n = 50 from 40 tonsil specimens with biological replicates for 10 specimens displayed with respect to donor age (xaxis, left panel), sex (color), and self-reported race (shape, left panel). The histogram in the right panel is included to show the distribution of infection frequencies with the majority of infections resulting in 1–2% GFP+ B lymphocytes at 3 dpi.

2.3.3 **Specific targeting of individual B cell lineages by KSHV infection**

We next sought to establish the B lymphocyte tropism of KSHV in human tonsil lymphocytes by determining which B cell lineages are targeted for KSHV infection at early timepoints. Because levels of individual B cell lineages are highly variable between samples (**Fig 2.3-1B**), we have generally represented lineage-specific susceptibility data as the percentage of GFP+ cells within each lineage so that data could be directly compared cross-sectionally within the sample cohort. Our analysis of specific B cell lineages targeted for infection by KSHV revealed that, although they represent a small proportion of the B cells within human tonsils (**Fig 2.3-1B**), CD138+ plasma cells are infected at high frequencies at this early timepoint. Indeed, CD19+ CD20- plasma cells displayed the highest within-lineage susceptibility of any cell type with several replicates showing 100% infection of this lineage at 3 dpi (**Fig 2.3-3A**). Other B cell lineages were susceptible to infection but were infected at relatively low within-population frequencies compared to plasma cells (**Fig 2.3-1A&B, Appendix A.2**). Most B cell lineages showed linear correlation between within-lineage infection and overall infection, while others like Plasmablast, double negative, and CD20- plasma cells showed no significant correlation between within-subset infection frequency and overall infection (**Fig 2.3-3B**).

The observation that plasma cells are highly targeted for infection is interesting given that we observed a decrease in overall plasma cell numbers in our cultures system that was somewhat abrogated in the KSHV-infected conditions (**Fig 2.2-3B**). Thus, we wanted to determine whether the apparent survival advantage for plasma cells in the KSHV-infected cultures was a direct result of infection. Interestingly, subset analysis for the plasma cells into total, CD20+ and CD20- plasma cells showed that the greatest survival effect (KSHV-Mock for the lineage) was within the CD20- population (**Fig 2.3-3C**, left panel), which was also the population with the highest level of

infection among B lymphocytes (**Fig 2.3-3A**) When we plotted survival of each plasma cell sub-population against the percent of infection for that population, there was no significant correlation observed (**Fig 2.3-3C**, right panels).

This data supports a conclusion of an indirect effect of KSHV infection on survival or differentiation of a different B cell lineage into CD138+ cells in our KSHV infected tonsil lymphocyte cultures rather than KSHV conferring a survival advantage only to infected cells. We next calculated within-subset frequency of infection for each lineage as a proportion of the total B lymphocytes (i.e. within-lineage % GFP x frequency of lineage within B lymphocytes) for each sample in order to determine the contribution of each lineage to the overall infection (**Fig 2.3-3D & E**). When shown on a per-sample basis, the data reveals high variability between donors with no discernable contribution of the overall susceptibility (shown by the order of the samples on the x-axis) (**Fig 2.3-3D**). When shown on a per-lineage basis, the data reveals that germinal center, transitional and memory cells make the largest contributions to overall infection, plasma cells and MZ-like cells are intermediate contributors and double negative, naïve and plasmablast lineages make up a minor proportion of the infected cells (**Fig 2.3-3E**).
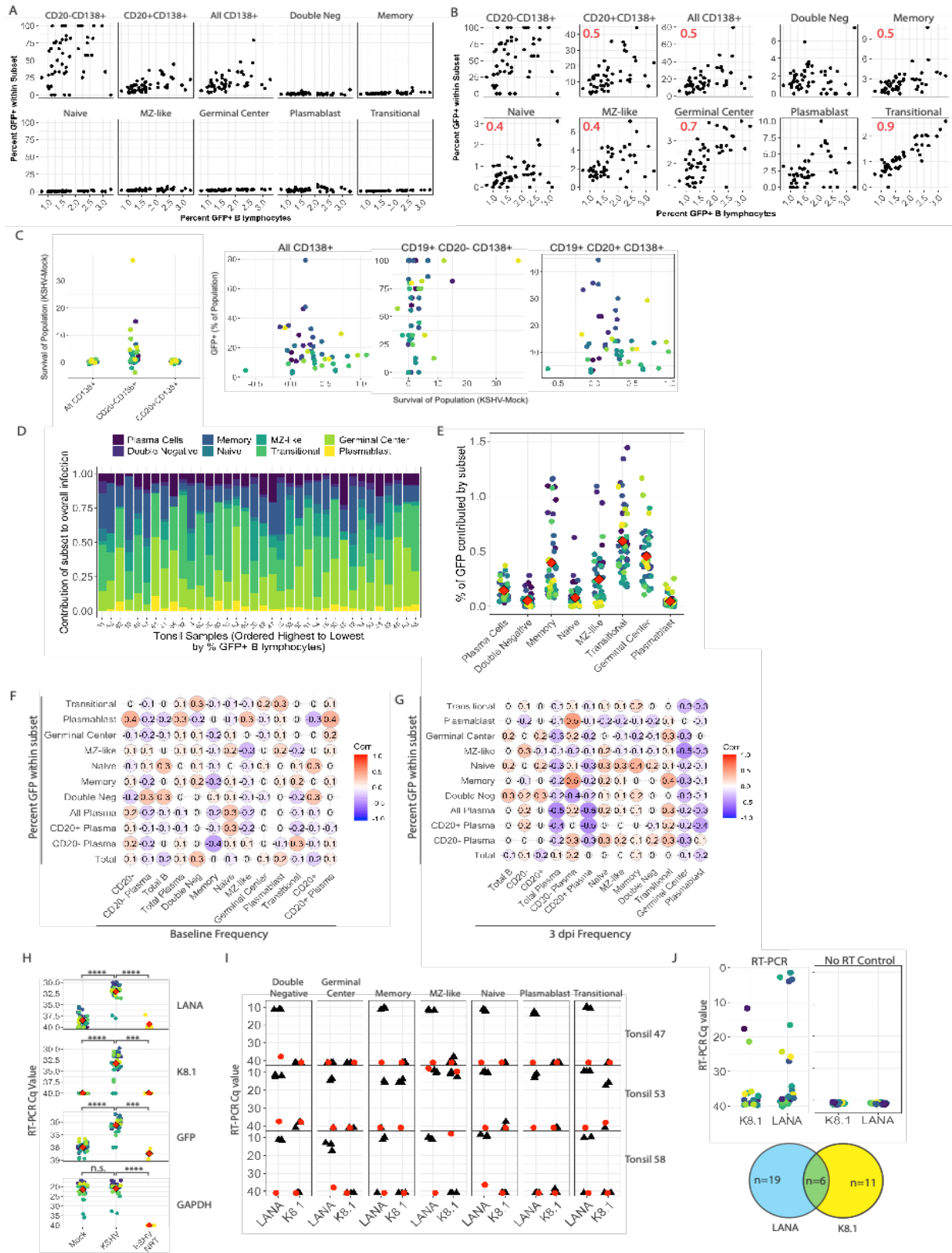
Figure 2.3-3. B lymphocyte lineage tropism of KSHV

Naïve B lymphocytes from 40 individual human tonsil specimens (n = 50) were infected with KSHV.219 as in Fig 2.3-2A. Cells were collected at 3dpi, stained for B cell lineages as shown in Appendix A1and Table 2.3-2 and analyzed flow cytometry for B cell lineages and KSHV infection based on GFP reporter expression. The within-lineage infection frequency (y-axis) as a function of overall B cell infection frequency (x-axis) at 3dpi in for n = 50 infections from 40 individual tonsil specimens shown **(A)** normalized to 100% or **(B)** scaled to each individual lineage population. Pearson correlation coefficients (r) with an absolute value greater than or equal to 0.4 are shown in (B) as red inset text in the subset panels. **(C)** The survival of plasma cell lineages (frequency of viable B lymphocytes in KSHV-Mock samples at 3 dpi) was plotted for all CD138+, CD20-CD138+ and CD20+CD138+ lineages (left panel) and each lineage's frequency of KSHV infection was plotted against its survival (right three panels) with individual tonsil samples designated by color. Statistical analysis was performed for both linear (Pearson) and monotonic (Spearman) correlations. For all plasma cells r = 0.15, ρ = 0.2; for CD20- plasma cells r = 0.3, ρ = 0.32, for CD20+ plasma cells r = 0.15, ρ = 0.13. The contribution of specific B cell lineages to overall infection in each sample was calculated as % GFP within lineage * % of lineage within viable B cells in each sample, and results are shown in **(D)** for each tonsil sample ordered from highest to lowest (right to left) based on overall GFP+ B lymphocytes (overall susceptibility) and **(E)** by lineage with individual samples designated by color and the mean infection frequency of each lineage shown as a red diamond. Correlation matrix analysis showing linear relationships (Pearson's correlation coefficient) between within-lineage infection frequency and **(F)** baseline (pre-infection) overall frequency or **(G)** 3 dpi overall frequency in KSHV-infected cultures for B lymphocytes and their subsets. Statistical power analysis indicates that this dataset can predict correlations at the level of r > |0.4| with alpha = 0.05 and power = 0.8. Thus, r values $\geq$ 0.4 can be considered a statistically significant correlation for this data. **(H)** KSHV transcripts LANA and K8.1 as well as GFP and GAPDH transcripts analyzed for n = 20 tonsil specimens by RT-PCR in bulk lymphocyte cultures at 3 dpi. Left panels show Ct values with individual samples designated by color and the mean Ct values for each condition shown as a red diamond. Student's T-test was used to determine statistical significance for all comparisons ***p<1e-7, ****p<2e-10. **(I)** At 3 dpi, 10 million KSHV-infected lymphocytes from three tonsil specimens were stained for B lymphocyte surface markers and lineages were sorted into Trizol LS. RNA was extracted, reverse transcribed (black triangles) or amplified without reverse transcriptase (NRT, red circles) and analyzed by nested RT-PCR for viral transcripts in sorted B lymphocyte lineages. **(J)** At 3 days post-infection, 1 million KSHV-infected B cells from three tonsil specimens were stained for viability, CD19 and CD138. 187 single cells that were viable, CD19+, CD138+ were sorted into 96- well plates and analyzed by nested RT-PCR for viral transcripts. Colors indicate single plasma cells analyzed with RT-PCR (left) or control reactions including no reverse transcriptase (right) The bottom panel is a venn diagram quantitating the number of plasma cells in RT-PCR reactions which amplified for each and both viral transcripts.

Next, we wanted to determine whether the targeting of individual B cell lineages by KSHV infection is merely a function of the frequency of that lineage within the sample or dictated by the virus biology. Pairwise correlations between KSHV infection of specific lineages and the baseline (pre-infection) frequency of that lineage within the sample revealed no significant effect of the baseline frequency of any B cell lineage on the susceptibility of that lineage to KSHV infection, (**Fig 2.3-3F**). Interestingly, there were some significant correlations between baseline frequencies of specific lineages and infection of other lineages. Infection of plasmablasts was positively correlated with the baseline number of both CD20 negative B cells in the culture and the number of CD20+ plasma cells, and infection of CD20+ plasma cells was negatively correlated with the baseline frequency of memory B cells in the sample. Similarly, given that some populations shift in their frequency during the infection time course (**Fig 2.3-2B**), we wanted to determine whether KSHV infection of specific lineages was a result of the frequency of that population within the sample at 3 dpi. Pairwise correlations between KSHV infection of specific lineages and the frequency of that lineage at 3 dpi similarly revealed no direct correlations between lineage frequencies and infection frequencies (**Fig 2.3-3G**). These comparisons revealed more strong relationships between lineage frequencies and infection frequencies. Infection of CD138+ plasma cells and CD20+ plasma cells (which are the more numerous of the two-plasma cell sub-populations as shown in **Fig 2.3-1B** was negatively correlated with the total population of plasma cells and the CD20+ sub-population of plasma cells. This result may indicate that infection of CD20+ plasma cells results in significant toxicity for that lineage. Moreover, infection of many B cell lineages was negatively correlated with germinal center B cells at 3 dpi with MZ like B cell infection being significantly associated. This observation could indicate that lymphocyte cultures with a microenvironment that favors the survival of germinal center cells establish a different

subset distribution of B lymphocyte infection. Finally, the 3dpi level of CD20- plasma cells were positively correlated with infection of both Plasmablast and memory B cell lineages. This data could indicate that these lineages are differentiating into plasma cells upon infection.

Taken together, these data indicate that the B lymphocyte tropism of KSHV is broad and highly variable from donor to donor. Plasma cells are highly targeted as a lineage, but transitional, memory and germinal center lineages make up the bulk of the viral load in tonsil specimens. The distribution of KSHV infection among lineages is not simply a function of lineage population frequency within the sample and is likely dictated by cell-intrinsic factors as well as complex immunological interplay within the sample that remains to be fully characterized.

2.3.4 **Viral gene expression in KSHV infected B lymphocytes**

Our observation that KSHV targets diverse B cell lineages for infection is based on expression of the GFP reporter in the KSHV.219 genome, which is controlled by a non-viral EF1-alpha promoter. We wanted to validate that the GFP signal we observed by flow cytometry represents bona fide infection and not simply virus entry. In order to do this, we first examined total RNA extracted from mock or KSHV-infected lymphocyte cultures at 3 dpi and analyzed these samples by RTPCR for viral transcripts (LANA and K8.1) as well as GFP as a marker for virus entry and GAPDH as a housekeeping gene for the efficacy of RNA extraction (**Fig 2.3-3H**). The data show that viral transcripts and GFP are absent in Mock samples but present in KSHV-infected samples with an average -ΔCt of 6.1 cycles for LANA, 6.6 cycles for K8.1 and 4 cycles for GFP. NRT controls were consistently negative, confirming that viral DNA was not the source of genetic material for these results.

Both LANA and K8.1 were detected in the majority of samples, suggesting a mix of lytic and latent infection programs in B lymphocytes. This data demonstrates bona fide infection, with the production of viral transcripts, is present in tonsil lymphocyte samples at 3 dpi. Given that the bulk RT-PCR data showed mixed lytic and latent transcripts present in our tonsil lymphocyte cultures, we wanted to determine whether B lymphocyte lineages preferentially undergo a particular viral replication program. To accomplish this, we performed large-scale lymphocyte infections, as above, for three unique tonsil specimens, stained for B cell lineage markers, and sorted individual lineages using our FACSAria Fusion cell sorter. We were able to obtain between 10,000 and 200,000 cells for each lineage from the cell sorting. Total RNA was extracted from sorted samples and subjected to nested RT-PCR analysis for GAPDH, LANA and K8.1. These results show that LANA transcripts are present in all lineages for at least 2/3 tonsil samples analyzed. Transcription of the K8.1 late lytic gene was observed in memory cells and transitional cells for 1/3 tonsil samples along with LANA transcripts indicating that in this sample there was a mixture of lytic and latent cells within the lineage populations. NRT negative controls (red circles) for most lineages were negative or amplified >10 cycles later than the matched RT positive samples indicating that viral DNA was not the source of genetic material for these results. However, the MZ-like lineage had positive amplifications in NRT controls for 2/3 tonsil samples. This result may indicate that in some samples there is a high load of KSHV DNA present in this lineage so that even the extensive DNase digestion used in our protocol failed to remove it sufficiently (**Fig 2.3-3I**). Because plasma cells are a low abundance cell type in our tonsil samples, we were uncertain whether bulk sorting would result in sufficient cells to successfully extract RNA for RT-PCR analysis. Thus, in order to determine the viral transcription program in plasma cells we gated viable/CD19+/CD138+ cells and sorted single cells directly into 96-well plates containing a

hypotonic lysis buffer. We performed single cell nested RT-PCR analysis without RNA extraction for LANA, K8.1 and GAPDH on 187 plasma cells from three unique tonsil samples (**Fig 2.3-3J**, left panel). NRT controls were consistently negative confirming that viral DNA was not the source of genetic material for these results (**Fig 2.3-3J**, right panel). We observed 19 plasma cells expressing LANA transcripts only, 11 plasma cells expressing K8.1 only and 6 plasma cells expressing both viral transcripts (**Fig 2.3-3J**, bottom).

Our gene expression data validates the lineage-specific tropism observed in our flow cytometry data, showing that each lineage identified as susceptible by GFP expression also contains viral transcripts, indicating bona fide KSHV infection. Moreover, these results demonstrate that most B cell lineages express latent transcripts only, with few lineages including plasma cell, memory, transitional and possibly MZ-like lineages contributing to lytic replication. Given that transitional and memory cells represent a high proportion of the per-sample viral load in our analysis (**Fig 2.3-3D & E**) it is not surprising to find that they are competent for lytic replication. However, germinal center cells are uniformly latent in this data, but were a highly represented cell type in our analysis of lineage contributions to overall infection. This may indicate that germinal center B cells are another highly targeted cell type. Finally, differences in this data between tonsil samples indicates that lytic replication in our system may be more dependent upon host factors than lineage-specific factors.

2.3.5 KSHV infection of B lymphocytes does not rely on heparin sulfate proteoglycans

Previous studies have shown that heparin sulfate proteoglycans (HSPG) of the syndecan family can serve as an attachment factor facilitating KSHV entry via interaction with the gH/gL glycoprotein complex (Hahn A, 2009). In order to test whether the high susceptibility of tonsil-derived plasma cells was due to increased attachment via CD138 (syndecan-1), we attempted to selectively neutralize KSHV entry by pre-treating cell-free virus particles with soluble recombinant CD138 (srCD138) protein prior to infection. We utilized recombinant CD138 for these experiments rather than a neutralizing antibody against CD138 because the biochemistry of the putative interaction between CD138 and gH has not been established. Thus, the soluble protein will contain all of the protein sequences that might be bound by gH while an antibody blocks only specific epitopes which may or may not be part of the interaction domain. Pre-treating KSHV virions with 12.5μg/ml of srCD138 showed a small decrease in overall KSHV infection of B lymphocytes in 6 of 7 tonsil samples tested (**Fig 2.3-4A**). However, the inhibition was not dose-dependent for any sample. B cell lineage analysis revealed decreased infection of plasma cell lineages in 3 of 7 samples, but again the effect was inconsistent within the data set and was not dose-dependent for any sample. KSHV infection of other B cell lineages was similarly inconsistently affected by srCD138 treatment of virus particles (**Fig 2.3-4B**). Next, we used srCD138 pre-treated virions to infect human fibroblasts to determine whether srCD138 was able to neutralize gH on another cell type. In these experiments we observed a slight decrease in infection in 4 of 6 replicates (**Fig 2.3-4C**). Taken together, these results suggest that, although srCD138 treatment seems to weakly neutralize KSHV viral particles, the effect is not B cell specific. As a way of confirming these results with a cell-directed method as opposed to a virus neutralization approach, we used heparinase treatment to remove all HSPG prior to KSHV

infection. Treatment of human fibroblasts with a heparinase I/III blend resulted in decreased cell surface heparin sulfate by flow cytometry analysis (**Fig 2.3-4D**) and, as demonstrated previously in human fibroblasts (Akula SM, 2001), consistently reduced KSHV infection of treated target cells compared to untreated controls (**Fig 2.3-4E**). Lymphocytes had lower steady-state HSPG levels compared to fibroblasts, which was further reduced by heparinase treatment (**Fig 2.3-4F**). Interestingly, heparinase treatment of lymphocytes did not result in a reproducible decrease in KSHV infection (**Fig 2.3-4G**). We next wanted to determine whether there was any effect of heparinase treatment on KSHV infection of particular B cell lineages. Because the most reliable cell surface marker for plasma cells is the CD138 HSPG, which would be removed by heparinase treatment, we first confirmed that plasma cells recovered CD138 expression before our 3 dpi analysis timepoint (**Fig 2.3-4H**). Subset analysis revealed no significant differences in KSHV infection between control and heparinase treated populations for any B lymphocyte lineage (**Fig 2.3-4I**). Taken together these data do not support the conclusion that plasma cell expressed CD138 is used as an attachment factor for KSHV entry and, indeed, indicates that HSPG are not a significant factor in KSHV attachment to B primary lymphocytes.
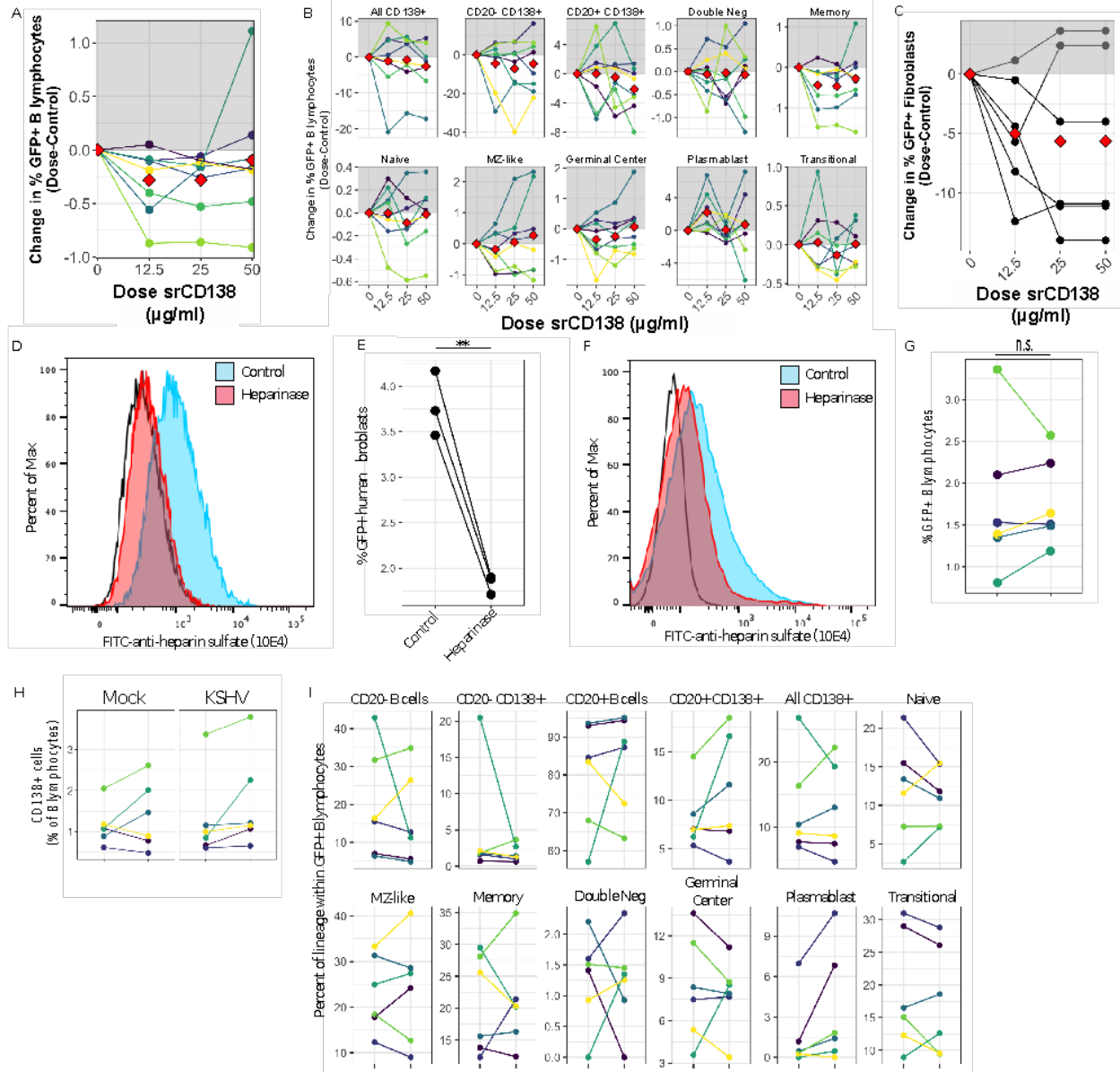
Figure 2.3-4. CD138 and heparin sulfate proteoglycans as attachment factors for KSHV in B lymphocytes

(A) Purified KSHV virions were pre-treated with srCD138 protein at indicated concentrations (x-axis) and used for infection of B lymphocytes. Cells were collected at 3dpi, stained for B cell lineages as shown in S1A Fig and Table 2.3-2 and analyzed by flow cytometry for lineage frequencies and KSHV infection by GFP reporter expression. 8 experimental replicates of 5 unique tonsil specimens are shown where the average infection rate was 1.8±0.5% in untreated controls. Data is represented as change in GFP+ cells at each dose of srCD138 compared to untreated control. Colors denote individual experimental replicates and red diamonds are the

65

mean change at each dose for all replicates. **(B)** Data as in (A) for within-subset GFP quantitation. **(C)** Similar experiments were performed in E6/E7 transformed fibroblasts derived from human tonsils. 6 experimental replicates are shown where the average infection rate was 25.5±16% in untreated controls. Data is represented as change in GFP+ cells as in (A). **(D)** 1 million E6/E7 transformed human tonsil fibroblasts were treated with 4.5 units of heparinase I/III blend for 24 hours and removal of heparin sulfate proteoglycans was verified by flow cytometry using a heparin sulfate-FITC antibody. Black line indicates no antibody control. **(E)** Control (untreated) or heparinase-treated fibroblasts were infected with KSHV.219 and analyzed for infection by GFP reporter expression at 3 dpi. Student's T-test was used to compare control and heparinase-treated cultures for n = 3 experimental replicates p = 0.007. **(F)** 25 million human tonsil lymphocytes were treated with 9U of heparinase I/III blend and plated on X-ray irradiated CDW32 feeder cells for 24 hours. After incubation removal of heparin sulfate proteoglycans was verified by flow cytometry as in (D). **(G)** After heparinase treatment lymphocytes were fractionated and infected as shown in Fig 2A and viable, GFP+ B lymphocytes were quantitated by flow cytometry at 3 days post-infection. 6 experimental replicates with 6 tonsil specimens were performed and colors designate unique samples and can be compared between this panel, panel H and panel I. Student's t-test was performed to compare infection of control and heparinase treated lymphocytes p = 0.969. **(H)** the recovery of cell surface CD138 HSPG after 3 days of culture was examined by comparing CD138+ cells as a percent of viable B cells in control and heparinase treated samples for both mock and KSHV-infected conditions. Colors indicate unique tonsil specimens. Student's T-test was performed to compare control vs. heparinase conditions for mock p = 0.57, for KSHV p = 0.52 **(I)** Data for KSHV-infected cultures at 3dpi with or without heparinase pre-treatment as in (G) showing the level of KSHV infection for specific B cell lineages. Student's T-test indicates no significant difference comparing control and heparinase treated samples for any lineage.

2.3.6 **Immune status alters KSHV infection of B lymphocytes**

KSHV lymphoproliferative disorders occur primarily in the context of immunosuppression, and other studies have shown interactions between T cells and KSHV infected B cells in tonsil lymphocyte cultures affecting the frequency of lytic reactivation (Myoung J, 2011). Therefore, we wanted to determine whether the immunological composition of the tonsil lymphocyte environment would affect the establishment of KSHV infection in B lymphocytes and specifically whether overall susceptibility or targeting of particular B cell lineages is influenced by the presence or absence of T cells. Like B cell lineages, levels of CD4+ and CD8+ T cell lineages vary considerably between tonsil donors (**Fig 2.3-1D**). However, unlike B lymphocyte subsets, the distribution of T cell subsets are not generally correlated with donor age (**Fig 2.3-1E**). Examination of whether the ratio of CD4/CD8 T cells in individual tonsil specimens was correlated with the susceptibility of B lymphocytes to KSHV infection revealed no significant correlation (**Fig 2.3-5A**).

Next, we examined correlations between B cell infections and baseline levels of various CD4 and CD8+ T cell subsets to determine whether any T cell lineages affected the tropism of KSHV for particular B cell lineages (**Fig 2.3-5B**). Interestingly, levels of naïve and stem cell memory CD4+ T cells was positively correlated with infection of plasma cells (**Fig 2.3-5B and Fig 2.3-5C, left panels**) with a greater effect on CD20+ plasma cells than CD20- plasma cells, while overall levels of CD45RO+ activated memory T cells were negatively correlated with KSHV infection of plasma cells (**Fig 2.3-5C**, right panel). In addition, although the correlations were too weak to be significant in this data set, nearly every B cell lineage and overall KSHV infection was negatively correlated with the presence of CD4+ T cells expressing a TEMRA phenotype (**Fig 2.3-5B**). Baseline levels of CD8+ T cells had less effect on KSHV infection with only one significant

positive correlation observed in our dataset between CD8+ terminal effector cells and KSHV

infection of naïve B cells (**Fig 2.3-5B**).
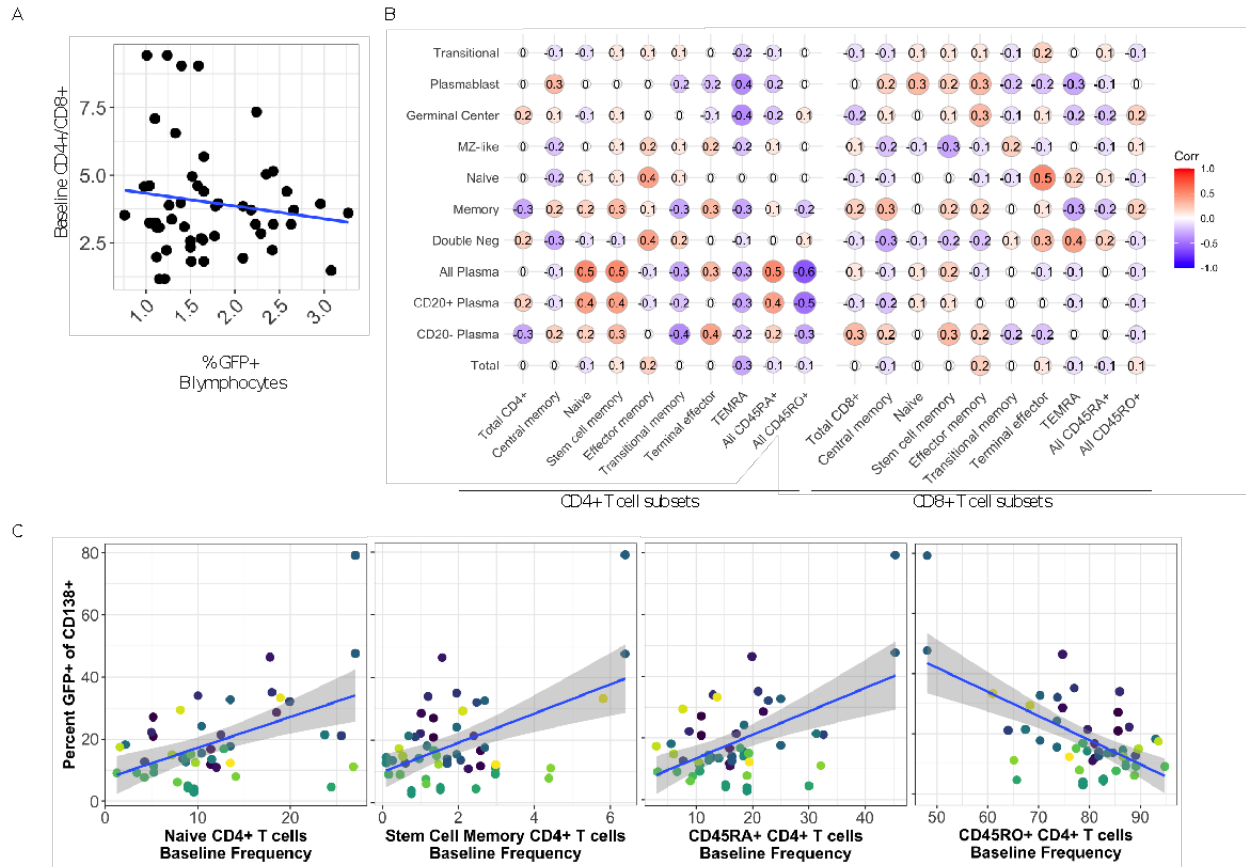
Figure 2.3-5. The donor specific CD4+ T cell microenvironment influences infection of CD138+ plasma cells.

(A) For each donor, baseline levels of CD4+ T cells/CD8+ T cells is plotted against the overall susceptibility of the specimen based on the percent of GFP+ B lymphocytes at 3 dpi. Blue line indicates least means linear regression. Correlation analysis reveals no significant linear or monotonic relationship between the variables. **(B)** Pairwise linear correlations (Pearson method) were performed for overall (Total) and lineage specific KSHV infection at 3 dpi (vertical axis) and baseline T cell subsets as defined in S1 Fig and Table 2.3-2. Power analysis reveals that the data set can predict significant correlations at the level of p>|0.4| with alpha = 0.05 and power = 0.8. **(C)** Scatter plots of significant correlations from (B) between the baseline frequency of CD4+ T cell subsets (x axis) and KSHV infection of CD138+ plasma cells (y-axis). Blue lines indicate least means linear regression and grey shading is standard error. Colors indicate unique tonsil specimens and can be compared across panels within the figure.

To determine whether manipulating the T cell environment would affect KSHV infection in individual tonsil samples, we performed T cell depletion experiments. Based on the correlation data shown in **Figure 2.3-5B**, we hypothesized that depletion CD4+ T cells would have a greater effect on KSHV infection. We performed KSHV infections in which total lymphocytes, CD4-depleted total lymphocytes or CD8-depleted total lymphocytes were added back following infection of sorted naïve B cells. At 3dpi, we validated T cell depletions (**Fig 2.3-6A**) and analyzed KSHV infection of B lymphocytes. The effect of T cell depletion varied substantially from sample to sample and neither CD4 nor CD8 depletion significantly altered overall KSHV infection in tonsil-derived B cells when data from 11 tonsil samples were aggregated (**Fig 2.3-6 B**). However, due to the heterogeneous nature of our tonsil samples (**Fig 2.3-1B & D**), we hypothesized that the baseline T cell composition of each sample might influence the effect of T cell depletion on KSHV infection. Indeed, when the change in KSHV infection in depleted fractions is plotted against the baseline CD4/CD8 T cell ratio, we observe that KSHV infection increased when depletions were performed in samples with high baseline levels of CD4+ T cells (**Fig 2.3-6 C**). We next analyzed the effect of T cell depletion on KSHV infection of specific B cell lineages (**Fig 2.3-6 D**). These data reveal that depletion of CD4+ T cells increases infection of plasma cells as well as MZ-like and Transitional B cell lineages and that the effect is dependent upon the baseline CD4/CD8 T cell ratio in the sample with CD4+ T cell-rich samples showing the greatest effect. Interestingly, CD8 depletions altered infection of different lineages compared to CD4 depletions but showed a similar dependence on the baseline level of CD4+ T cells. Power analysis indicates that only the effect on CD138+ cells and MZ-like lineages in the CD4-depleted condition and plasmablast lineage in the CD8-depleted condition can be considered statistically significant based on the sample size. Taken

70

together, these data support the conclusion that the T cell microenvironment influences the lineages targeted by KSHV infection in the B lymphocyte compartment.
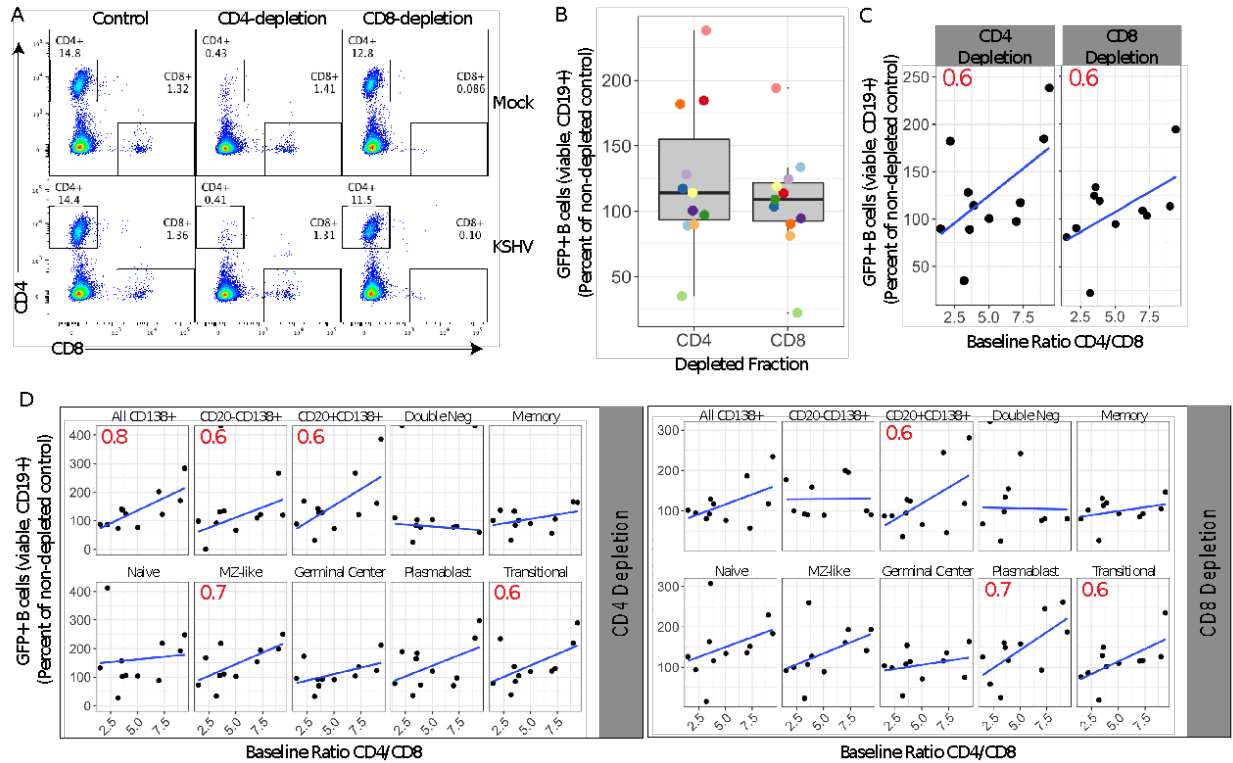
Figure 2.3-6. Manipulation of T cell microenvironment alters KSHV tropism for B cell lineages.

Naïve B lymphocytes from 11 human tonsil specimens were infected with KSHV.219 as in Fig 2.3-2A, total lymphocytes added back following infection were either untreated or depleted of CD4+ or CD8+ T cells. At 3 days post-infection cells were collected. (**A**) T cell depletions were validated by flow cytometry and (**B**) Cells were stained for B cell lineages as shown in S1A Fig and Table 2.3-2 and analyzed flow cytometry for lineage frequencies and KSHV infection by GFP reporter expression to determine the change in GFP+ B lymphocytes (viable, CD19+) in CD4 or CD8 depleted samples compared to non-depleted controls. Colors indicate individual tonsil specimens (n = 11). Student's T test reveals no statistically significant change in GFP+ B cell frequency between either CD4-depleted or CD8-depleted and non-depleted controls. (**C**) Infection data for T cell depletion studies as in (A) plotted against the baseline (pre-infection) CD4/CD8 T cell ratio in the sample. (**D**) Within-lineage infection frequency plotted against baseline (pre-infection) CD4/CD8 T cell ratio. For B and C linear regression of the data is shown as a blue line and Pearson correlation coefficients (r) are shown as red text within panels only for r with an absolute value ≥ 0.6. Statistical power analysis indicates that this dataset can predict correlations at the level of r > |0.7| with alpha = 0.05 and power = 0.8. Thus, r values ≥ 0.7 can be considered a statistically significant correlation for this data.

2.4   Discission

Ex vivo infection of tonsil lymphocytes is emerging as a viable strategy for studying early infection events for KSHV infection in B lymphocytes. However, the existing literature on KSHV infection of tonsil lymphocytes is highly varied in both approach and outcome. Hassman et. al. used cell free wild-type BCBL-1 derived KSHV virions to infect total CD19+ B lymphocytes from tonsil specimens and used staining for LANA as the only marker for infection, thus limiting their analysis to latently infected cells (Hassman LM, 2011). Bekerman et. al. also used isolated CD19+ B cells as infection targets but employed a co-culture infection procedure using iSLK cells infected with the recombinant KSHV.219 strain employing the GFP reporter as a marker for infection. Nicol et. al. also employed a co-culture method to infect tonsil lymphocytes with KSHV.219 but used Vero cells as producers and did not isolate CD19+ B cells prior to infection. In two studies, Myoung et. al. used cell free KSHV.219 produced from Vero cells to infect mixed lymphocyte cultures. With the exception of Bekerman et. al, all of the abovementioned studies employed some kind of activating agent (PHA stimulation or CD40L stimulation) to manipulate the activation and/or proliferation of cells in vitro. For our studies, we used cell-free, iSLK-derived KSHV.219 to infect naïve B lymphocytes followed by reconstitution of the total lymphocyte environment. We also avoided activation of lymphocytes in both the isolation and culture procedures using our previously characterized CDw32 feeder cell system (Totonchy J, 2018). To date, no consensus has yet emerged on how to perform tonsil lymphocyte infection studies with KSHV, and how differences in infection and culture procedure influences the resulting data remains to be established.

Although previous studies in mixed lymphocyte cultures have explored limited surface markers including immunoglobulins and activation markers (Hassman LM, 2011; Nicol SM, 2016) and

NK cell ligands (Bekerman E, 2013), these studies essentially treated all B cells as one population. Targeting of specific lineages including naïve, memory and CD138+ plasma cell-like B lymphocytes was explored by Knowlton et. al. using B cells derived from peripheral blood, but their detection method for infected cells was immunostaining for ORF59 protein and thus their enumeration of infection was biased towards cells undergoing lytic replication (Knowlton ER, 2014). Our current study is the first to use a comprehensive panel of lineage-defining cell surface markers to carefully explore the lineage-specificity of KSHV infection in B lymphocytes.

Although previous studies of KSHV infection in tonsil-derived B lymphocytes have shown the acquisition of plasmablast-like features at later timepoints post-infection (Hassman LM, 2011; Kang S, 2017), the CD38 high plasmablast lineage is a minor proportion of our infected cultures at 3 dpi. Based upon these studies, we might expect to see the emergence of more plasmablast-like cells over time and it will be interesting to determine whether this is a result of infected plasmablasts expanding or trans-differentiation from other lineages. Our observation that KSHV-infected B cells are primarily latent in our mixed tonsil lymphocyte cultures is consistent with previous observations that T lymphocytes control lytic reactivation of KSHV in tonsil-derived B cells (Myoung J, 2011). For the gamma-herpesviruses EBV and MHV68, the current consensus is that naïve B cells are the primary infection target and infected cells transit the germinal center as a way of increasing viral load without resorting to lytic replication and lifelong latent infection is established in memory B cells while plasma cells are a source of lytic replication constantly replenishing the viral reservoir by producing virus which infects more naïve B cells (Johnson KE, 2020). Here, we show that multiple lineages from human tonsils, including terminally differentiated CD138+ plasma cells, can be targeted by KSHV for de novo infection. In our data, plasma cells are not primarily lytic as in EBV models, but instead are a mix of lytic and latent

74

transcription programs with latency slightly predominating (**Fig. 2.3-3J**). This result is not surprising given that KSHV-associated lymphoproliferative diseases are characterized by primarily latent infection in cells with plasma-like features but PEL derived cell lines are competent for KSHV replication given the proper stimulus. In future studies, it will be interesting to examine what factors influence the lytic/latent balance for KSHV in primary plasma cells. Additionally, our data indicate that memory cells are competent for lytic replication (**Fig 2.3-3I**), which is also different from the current model for EBV. However, the studies upon which the EBV models are based are primarily examination of cells from previously infected human hosts, representing EBV distribution in an established infection. We are unaware of any study of EBV infection in human tonsil that recapitulates the early infection timepoint and the level of detail in characterizing B cell lineages that is used here, thus it is difficult to place our data in the context of EBV infection. Given that recombinant EBV molecular genetics systems and ex vivo tonsil lymphocyte culture systems are now well established, perhaps a second look at the early-stage B lymphocyte tropism of EBV is warranted.

Our finding that KSHV efficiently targets CD138+ plasma cells early in infection of tonsil B lymphocytes is particularly intriguing and relevant in the context of KSHV mediated lymphoproliferative diseases, which often have a plasma cell or plasmablast-like phenotype (Chadburn A, 2008; Carbone A V. E., 2014). Particularly for PEL, which uniformly presents as a clonal CD138+ neoplasm, these results suggest that the pathological cells may not be derived from KSHV-driven differentiation from less mature lineages, but instead could be the result of modifications of differentiated plasma cells by direct infection. Recent studies have revealed that XBP-1, a critical cellular mediator of the unfolded protein response (UPR) which is essential for the differentiation of plasma cells (Iwakoshi NN, 2003), can activate expression of KSHV vIL-6

without inducing ORF45 or other lytic genes (Hu D, 2016). The fact that the UPR and XBP-1 are uniformly active in immunoglobulin-producing cells, like plasma cells, suggests that these cells may provide a unique niche for KSHV persistence where vIL-6 can be produced to support infected plasma cell survival in the absence of KSHV lytic replication. Future studies will examine whether vIL-6 is responsible for the survival advantage we observed for plasma cells in the KSHV-infected conditions in this study (**Fig 2.3-2B**).

Current models of human plasma cell maturation suggest that CD20 expression is lost on plasma cells as they mature and migrate from peripheral lymphoid organs (such as the tonsil) to the blood and finally the bone marrow (Medina F, 2002). Thus, CD138+CD20- plasma cells in tonsil that are highly targeted by KSHV in our analysis may represent a population of cells that is ready to leave the tonsil and migrate to the bone marrow. A few studies have shown KSHV infection in bone marrow from patients with MCD (Bacon CM, 2004; Ibrahim HAH, 2016) and HIV positive patients without MCD (Meggetto F, 2001), and it would be interesting to pursue the idea that KSHV uses plasma cells to disseminate to the bone marrow early in infection. Certainly, our results highlight the virology of KSHV in primary plasma cells as an area urgently requiring further study.

 In this study, we were unable to establish that targeting of plasma cells was due to enhanced virion binding via gH/gL interaction with the CD138 HSPG molecule, as was suggested by a previous study (Hahn A, 2009). However, we acknowledge that selectively blocking virion binding to a specific HSPG in a primary cell system is technically difficult, and we have no way to directly verify that our neutralization of gH/gL binding sites using soluble CD138 was effective. Our data using heparinase treatment to remove HSPG from B lymphocytes prior to infection supports the conclusion that CD138 is not used as an attachment factor for plasma cells, and indeed, HSPG are generally dispensable for infection of B cells in our system (**Fig. 2.3-4G-I**). These results are

consistent with a previous study that shows low HSPG levels on the KSHV-susceptible MC116 lymphoma cell line (Dollery SJ, 2018) and another study showing that ectopic HS expression enhanced binding but was not sufficient to allow efficient KSHV infection of the BJAB lymphoma cell line (Jarousse N, 2011). Thus, the mechanisms underlying KSHV targeting of plasma cells and other B lymphocyte lineages for infection remains to be established. Additional studies in lymphoma cell lines have identified Ephrin receptors as critical factors in KSHV entry (Großkopf AK, 2019; Muniraju M, 2019). Thus, our future studies in this area will examine Ephrin family receptors in KSHV infection of tonsillar B lymphocyte lineages.

Our characterization of immunological diversity of a large cohort of human tonsil specimens will be of interest to the general immunology community. Although a few studies have examined T cell (Petra D, 2015) or B cell (Varon LS, 2017) subsets in tonsils associated with particular disease states. To our knowledge, only one other study has used multicolor flow cytometry to examine the immunological composition of both B cells and T cells in a large cohort of human tonsil samples (Stanisce L, 2018), and this study was focused on comparing the microenvironments present in matched tonsils and adenoids rather than comparison between donors based upon demographic data as we have done here.

In this study, we make the observation that manipulating the T cell composition has a more profound effect on KSHV infection in tonsil specimens that were CD4+ T cell rich at baseline. Moreover, although the specific B cell lineages affected by depletion was different depending on whether CD4+ or CD8+ T cells were experimentally depleted, the greater effect in CD4+ T cell rich samples was consistent. This data in combination with the viral transcript data shown in **Figure 2.3-3H-J** reveals that KSHV infection of B cells and the lytic/latent balance is sensitive to the host-specific overall immunological microenvironment and highlight that there is complexity

to this relationship that cannot be adequately understood in the context of the current study. It will be interesting in future studies to explore the contribution of donor-specific and context-specific immunology to KSHV lytic reactivation in tonsillar B lymphocyte lineages.

3 CHAPTER III: KSHV-gH EphA interactions dominate entry into B lymphocytes and mask gH-independent routes of infection

Associated Publications and Author Contributions:

Authors: Farizeh Aalam[1], Murali Muniraju[2], Javier Gordon Ogembo[2] and Jennifer

Totonchy[1]‡

[1]School of Pharmacy, Chapman University, Irvine, California, USA

[2] Department of Immuno-Oncology, Beckman Research Institute of City of Hope, Duarte, CA 91010, USA

Abstract

KSHV entry into cell is an intricated process, requiring engagement of multiple viral and cellular receptors. In this study, we assess the importance of KSHV glycoprotein H (gH) and gL complex and EphA family of cellular receptors in KSHV infection of tonsil-derived B lymphocytes. We characterize EphA2, A4, and A7 distribution at baseline in tonsil lymphocytes and relate EphA levels to KSHV susceptibility. We then directly assess the importance of EphA receptors in KSHV entry by blocking either EphA receptors on target cells or using soluble EphA receptors to neutralize virus particles. We use both KSHV-WT and a gH mutant virus (KSHV-ΔgH) in these experiments to assess the contribution of gH/gL to these interactions. Our results indicate that although KSHV-gH interaction for entry into B cells appears to be indispensable, (1) gH/gL and EphA interactions are important for the establishment of infection in tonsil-derived B cells; (2) gH/gL and EphA interactions are important for entry into plasma cells and germinal center cells, and in the absence of gH/gL, KSHV exploits alternative mechanisms to enter B lymphocytes.

3.1 **Introduction**

Kaposi sarcoma associated herpesvirus (KSHV) is associated with both lymphoid and non-lymphoid cell tumors in humans (Chang et al. 1994; Cesarman et al. 1995), primarily in the context of immunosuppression. The two lymphoproliferative disorders, primary effusion lymphoma (PEL), and multicentric Castleman disease (MCD) are associated with KSHV infection of B cells (Cesarman et al. 1995; Soulier et al. 1995). One strategy for prevention of these diseases is the design and implementation of a preventative vaccination. However, rational design of such a vaccine is limited by our understanding of the mechanisms of KSHV entry into target cells, particularly cells of the immune system, which are thought to be the major reservoir of long-term KSHV infection (Flaño et al. 2000).

The process of KSHV entry into cells is a multistep and sequential process that requires interactions between several host cell receptors and viral envelope glycoproteins; as a result, KSHV has tropism for a variety of adherent cell types (Bechtel et al. 2003; Muniraju et al. 2019) and also targets a wide variety of B cell subsets (Aalam et al. 2020). To infect different cell types, KSHV employs a repertoire of glycoproteins; some are specific to KSHV (i.e. K8.1A and B, ORF4), and others are structurally conserved across herpesvirus families (i.e. gB, gH/gL, gN, and gM) (van der Meulen et al. 2021). Functional binding of glycoproteins to entry receptors induces fusion of the viral membrane with the host membrane, and there is often a non-essential, secondary tethering interaction that improves infection efficiency by concentrating virions on the host cell surface, and in some cases facilitating endocytosis of virions, prior to entry receptor binding and fusion (Connolly et al. 2011). Among the ten known KSHV glycoproteins, only a few of them are characterized to bind to the cellular targets. For instance, glycoprotein machinery gB, gH/gL complex, K8.1, and KCP are implicated for interaction with heparan sulfate (HS) in epithelial

cells, endothelial , and fibroblast cells, and monocytes (F. Z. Wang et al. 2001; Akula, Wang, et al. 2001; Akula, Pramod, et al. 2001; Birkmann et al. 2001; Spiller et al. 2006; Chandran 2010; Kerur et al. 2010). In addition to HS interaction, there are some orphan host-cell receptors for KSHV whose binding partners are unidentified, for example the combination of αvβ1, αvβ5, and α3β1 integrins in monocytes and fibroblast cells (Kerur et al. 2010; Veettil et al. 2008) and αvβ1, αvβ5,α3β1, xCT, and CD98 cellular receptors in endothelial cells (Veettil et al. 2008).

Much less is known about KSHV entry for B cells, and most studies have been performed in transformed B cell lines and not in primary human B lymphocytes. In the BJAB lymphoma cell line, HSPG binding is important for entry (Jarousse, Chandran, and Coscoy 2008) as well as DC-SIGN-gB interactions (Akula, Pramod, et al. 2001). Previous studies in primary human B cells (Rappocciolo et al. 2008) also indicated that DC-SIGN is critical for B cell entry, but we recently published data that contradicts this claim (Palmerin et al. 2021). Moreover, our recent work demonstrated that HSPG are dispensable for infection of tonsil-derived B cells (Aalam et al. 2020). Finally, our recent work has shown that gH/gL is dispensable for KSHV entry into B cells (Muniraju et al. 2019), but there are subset-specific mechanisms of KSHV entry that depend upon gH/gL (Palmerin et al. 2021). Thus, the current literature shows that KSHV entry into B cells employs distinct mechanisms that differ from those used for entry into other cell types, but our understanding of these mechanisms is currently very limited.

Erythropoietin producing hepatocellular receptors (Eph) are tyrosine kinases, that together with their corresponding ephrin ligands, are fundamental regulators of a diversity of cellular processes such as proliferation, differentiation, cell migration, angiogenesis, and tissue boundary formation (Haqshenas and Doerig 2019). Eph receptors are divided into A and B classes according to their sequence similarity and their binding affinity towards their ligands (de Boer, van Gils, and van

Gils 2020). Among the EphA class of receptors, EphA2 serves as an entry receptor for both KSHV and Epstein–Barr virus (EBV) (Chen et al. 2018; H. Zhang et al. 2018; Hahn et al. 2012). KSHV interaction with EphA2 results in amplification of the signaling events required for efficient infection (Chakraborty et al. 2012). It has been demonstrated that gH/gL binding to EphA2 activates its phosphorylation, leading to KSHV endocytosis (Hahn et al. 2012). Indeed, gH/gL binding to EphA2 receptor is a mimicry of the natural Ephrin ligand (Light et al. 2021; Hahn and Desrosiers 2014). The dynamic of EphA2 interaction with gH/gL has been established by several studies (Hahn et al. 2012; Chen et al. 2019; Großkopf et al. 2019) and its role in KSHV infectivity of epithelial, endothelial and fibroblast cells have been evaluated (Hahn et al. 2012; Chakraborty et al. 2012; Dutta et al. 2013). KSHV gH/gL has binding affinity towards EphA4 and EphA7, albeit with lower avidity as compared with EphA2 (Chen et al. 2019; Großkopf et al. 2019). EphA4 was shown to participate in KSHV infection of epithelial cells, and EphA7 facilitates cell-to-cell transmission of KSHV in BJAB lymphoma cell lines (Chen et al. 2019; Großkopf et al. 2019). While, primary B cells express appreciable amount of these EphA receptors (Großkopf et al. 2019; Huang et al. 2016; Alonso-C et al. 2009) no study has directly characterized their contribution to KSHV infection of primary human B cells.

In this study, we utilize our established tonsil lymphocyte culture model to characterize the expression and distribution of EphA2, A4 and A7 receptors in tonsil-derived B lymphocytes. We utilize different strategies for blocking the interaction of KSHV virions with EphA receptors in the context of both KSHV-WT and KSHV-ΔgH infections. Our results demonstrate that EphA expression is broad within B cell subtypes and highly variable between donors in tonsil lymphocyte samples. We show that gH/gL-EphA interactions are important for KSHV-WT infection of primary tonsil lymphocytes, but that KSHV-ΔgH has a separable entry mechanism

that is EphA independent. The gH/EphA-dependent entry mechanism seems to be critical for establishing KSHV-WT infection particularly in plasma cells and germinal center cells. Finally, our data supports the conclusion that gH-independent entry mechanisms exist for KSHV, but that their use is masked by the presence of gH/gL in KSHV-WT particles and, therefore, many not be particularly physiologically relevant for infection and dissemination of KSHV within the human immune system.

3.2   Materials and Methods

3.2.1   Cell-free KSHV Virion Preparation

Stably infected iSLK cell lines with recombinant BAC16, KSHV-WT (Myoung and Ganem 2011) and KSHV-ΔgH (Muniraju et al. 2019) were cultured in DMEM supplemented with 10% CCS, G418 (250 µg/mL), hygromycin (1.2 mg/mL), puromycin (1 µM), and 1% PSG at 37ºC in 5% CO_2. The cell lines were expanded to 12 × T185 flasks and upon 70–80% confluency, they were induced with 2 µM doxycycline hyclate and 3 mM sodium butyrate. At 72 hours post induction, supernatants were collected and centrifuged at 1700 rpm for 10 min at 4ºC and passed through 0.45µm vacuum filter. To pellet the virions, clarified supernatant was overlayed on a 25% sucrose cushion prepared in TNE buffer [pH 7.4] (50 mM Tris, 0.1 mM EDTA, 100 mM NaCl) and centrifuged at 22,000 rpm for 2 hours. The pelleted virions were the resuspended in 2mL TNE and stored in smaller aliquots at −80ºC. Doses for B cell infection with KSHV-WT were calculated by titration on human fibroblast cells and quantified at 3 days post infection with flow cytometry detecting the GFP reporter present in the BAC16 genome and calculation, via linear regression, of the dose needed to achieve 20% infection (ID20) in microliters per cell. KSHV-ΔgH was titered by quantitative real-time PCR using the GFP cassette in the BAC16 backbone as a target and

infections were performed using equivalent genome copy numbers compared to KSHV-WT at its ID20.

3.2.2 Isolation of Primary Tonsillar Lymphocytes

Informed consent exempted (de-identified) human tonsil specimens were provided by National Disease Research Interchange (NDRI). The specimens were maintained in DMEM+ 1%PSG, at 4 ºC, and shipped to the laboratory within 24h following the routine tonsillectomy. To extract the lymphocytes, tonsillar tissue was dissected and macerated in RPMI media. The media was then passed through a 40 μm filter and the lymphocytes were pelleted at 1500 rpm for 5 min. The lymphocyte pellet was resuspended in red blood cell lysing solution (10 mM potassium bicarbonate, 0.15 M ammonium chloride, 0.1 M EDTA), after incubation for 3 min, cells were diluted to 50ml with PBS-/-, counted, pelleted, and resuspended in freezing media (90% FBS, 10% DMSO) in aliquots of 1e8 cells/vial and cryopreserved.

3.2.3 Total B cell Isolation and Infection Procedure

Cryopreserved aliquots of tonsillar lymphocytes were thawed rapidly at 37ºC, and gradually diluted with RPMI, and pelleted at 1400 rpm for 5 min. Lymphocytes were resuspended in 1 mL 20% FBS, RPMI, 100 μg/mL Primocin, with addition of 100 μg/mL DNase I, maintained for two hours of recovery in a well of low-binding plate at 37 ºC and 5% CO2 incubator. After recovery, Mojosort™ Human Pan B cell isolation kit (Biolegend 480082) was used to isolate total B lymphocytes following manufacturer's instructions. The bound fraction of magnetic sorting were retained in complete media at 37 ºC and 5% CO2. The sorted fraction containing total B lymphocytes were resuspended in serum free RPMI at 400μl/1e6 cells per experimental condition and total B lymphocytes were infected through spinoculation at 1000 rpm for 30 min at 4º C.

Thereafter, the cells were incubated at 37 ºC and 5% CO2 for 30 min. After incubation, the cells were reconstituted with the equal proportion of the bound fraction and supplemented with 20% fetal bovine serum, and 100 µg/mL of Primocin and cultured over x-ray irradiated feeder cells (CDW32 L cells) for 3 days.

3.2.4 EphrinA2-Fc Cell Neutralization Experiments

B lymphocytes were isolated as described above, resuspended in serum-free RPMI and incubated with Recombinant Human Ephrin-A2 Fc Chimera Protein (7856-A2, R&D systems) at varying concentrations (0 µg/ml, 20 µg/ml, 40 µg/ml, 60 µg/ml) for 45 min on ice. Cells were then washed twice with serum free RPMI prior to infection as described above.

3.2.5 Soluble EphA Receptor Virus Neutralization Experiments

Purified virions for KSHV-WT and KSHV-ΔgH were incubated with Recombinant Human Eph-A2 (3035-A2, R&D systems), Eph-A4 (6827-A4, R&D systems), Eph-A4(6756-A7, R&D systems) at varying concentrations (0 µg/ml, 0.25 µg/ml, 1 µg/ml, 2 µg/ml) for 30 min on ice and subsequently used to infect B lymphocytes as described above.

3.2.6 Flow cytometry staining and analysis of baseline EphA receptor expression

Following thawing and recovery, 0.5 $(10)^6$ total lymphocytes at day zero (baseline) were collected into 96-well round bottom plates and pelleted at 1400 for 4 min. The cells were resuspended in 100 µl of PBS containing fixable viability dye (BD 565388) and were incubated on ice for 15 min. The cells were pelleted and incubated with 100 µl FACS Block (PBS, 0.5% BSA, and 2% FBS) for 10 min on ice, followed by addition of 100 µl FACS Wash (PBS, 0.5% BSA, and 0.1% Sodium Azide) and pelleting the cells. The baseline staining of lymphocytes were done using 10 µl BD

Brilliant Stain Buffer Plus (BD 566385) and antibodies as follows: CD19-PerCPCy5.5 (2.0 µl/test, BD 561295), CD20-PECy7 (2.5 µl/test, BD 560735), IgD-BUV395 (2.5 µl/test BD 563823), CD38-V450 (3 µl/test BD 561378), CD138-BUV737 (2 µl/test BD 612834), CD27-BV750 (2 µl/test BD 563328) in 50 µl of FACS Wash for 15 min. The lymphocytes were permeabilized and fixed by resuspension in 100 µl of BD Cytofix/Cytoperm™ (BD554722) for 15 min at room temperature followed by 2X washes of BD Perm/Wash™ (BD554723). Thereafter, 50µl Perm/Wash containing EphA2-PE(2.5 µl/test, BioLegend 356803), EphA4-AF647 (2.5 µl/test, Santa Cruz Biotech. sc-365503), andEphA7-AF680 (2.5 µl/test, Santa Cruz Biotech. sc-393973) antibodies was added to the cells and incubated at room temperature for 20 min, followed by two washes and resuspension in FACS Wash followed by data acquisition on BD Fortessa X20 flow cytometer and analysis of the data using FlowJo software. The concentration of antibodies for intracellular EphA staining were determined by titration on lymphocytes and fluorescent minus one (FMO) controls were used to establish the gating for the intracellular EphA stains.

3.2.7 Flow cytometry staining and analysis of KSHV infection

At 3 days post infection, a half of the cultures were collected into 96-well round bottom plates and pelleted at 1400 for 4 min. The cells were resuspended in 100 µl of PBS containing zombie violet fixable viability dye (423113, BioLegend) and were incubated on ice for 15 min. The cells were pelleted and incubated with 100 µl FACS Block (PBS, 0.5% BSA, and 2% FBS) for 10 min on ice, followed by addition of 100 µl FACS Wash (PBS, 0.5% BSA, and 0.1% Sodium Azide) and pelleting the cells. Thereafter, the cells were resuspended in 50 µl FACS Wash containing 10 µl BD Brilliant Stain Buffer Plus (BD 566385) and antibodies as follows: CD19-PerCPCy5.5 (2.0 µl/test, BD 561295) CD20-APCH7 (2 µl/test BL 302313), IgD-BUV395 (2.5 µl/test BD 563823), CD38-APC (10 µl/test BD 560158), CD138- BUV737 (2 µl/test BD 612834), CD27-BV750 (2

μl/test BD 563328), CD77-BV510 (2.0 μl/test BD 563630) for 15 min on ice. The staining was followed by 2X FACS Wash and resuspension of lymphocytes in FACS Wash for data acquisition on BD Fortessa X20 flow cytometer and data was analyzed using FlowJo software.

3.2.8 Statistical Analysis

Data plots and statistical analysis were performed in Rstudio software (version 7.0) using reshape2 (Z. Zhang 2016), and tidyverse (Wickham et al. 2019) packages. Statistical analysis was performed using R package: rstatix (Kassambara 2020). Specific statistical tests and the resulting values are described in detail in the corresponding figure legends.

3.3 Results

3.3.1 EphA receptor distribution on tonsil-derived B cells

In order to determine the importance of gH/gL interaction with EphA family of receptors, we included EphA2, A4, and A7 in our study. EphA2 and EphA4 are involved in KSHV entry into various adherent cells (Hahn et al. 2012; Chakraborty et al. 2012; Dutta et al. 2013; Chen et al. 2019) and EphA7 was demonstrated to be critical for cell-to-cell transmission of KSHV in B cells (Großkopf et al. 2019). We first wanted to establish the distribution of these EphA family receptors in tonsil lymphocytes. To do this, we used a surface immunophenotyping panel to quantitate the baseline level of B cell subsets within 27 unique tonsil specimens followed by fixation and intracellular stain for EphA2, EphA4 and EphA7. B cell subset definitions are listed in Table 1 and a representative gating scheme for B cell subsets can be found in our previous study (Palmerin et al. 2021). The intracellular staining approach for EphA receptors was necessary due to a lack of commercially-available antibodies binding the extracellular domains of these proteins. However, we acknowledge it is not ideal given that it does not specifically quantitate cell surface EphA

receptor expression, which might be most relevant for understanding binding and entry of KSHV. This analysis reveals that EphA2 has the highest mean expression in tonsil B lymphocytes while EphA7 is least abundant (**Fig 3.3-1A**). Our analysis clearly shows that EphA receptor expression varies substantially based on tonsil donor (**Fig 3.3-1B-D**). In most samples, within-subsets expression of EphA2 and EphA4 were fairly consistent between subsets, while EphA7 shows the most variable, subset-specific expression (**Fig 3.3-1B**). Moreover, many tonsil samples show high levels of EphA2 in all B cell sub-populations, while other samples show uniformly low EphA2 expression except for plasma cell and plasmablast lineages which were enriched for EphA2 expression even in samples with low EphA2 in other lineages. Similarly, EphA7 expression is low in most tonsil samples, but there is an enrichment of EphA7 expression in the plasmablast lineage. EphA4 levels were generally consistent across all B cell subsets within tonsil donors, but donor-specific levels of EphA4 were highly variable with the majority of samples showing less than 25% EphA4 expression across all lineages. However, we observe that EphA4 is particularly enriched in germinal center cells (**Fig 3.3-1C**). When we examined co-expression of EphA receptors on tonsil-derived B cells in a subset of our tonsil samples, we observed similarly variable results based on tonsil donor. However, even within these variable data, we observed that EphA2 and EphA4 are more likely to be co-expressed, while EphA2/EphA7 double positive cells and cells expressing all three EphA receptors are rare (**Fig 3.3-1D**). Taken together, these results suggest that EphA expression in tonsil B lymphocytes is most heavily influenced by donor-specific factors but some subset-specific influences exist.

Table 3.3-1. B lymphocytes subtype definitions used in this study.

Subset	Molecular Markers
Plasma	CD19$^+$, CD20$^{+/-}$, CD138$^{+(Mid\ to\ High)}$, CD38$^-$
Transitional	CD19$^+$, CD138$^-$, CD38^{Mid}, IgD$^{+\ (Mid\ to\ High)}$
Plasmablast	CD19$^+$, CD138$^-$, CD38^{High}, IgD$^{+\ /-\ (mostly\ -)}$
Germinal Center	CD19$^+$, CD138$^-$, CD38^{Mid}, IgD$^-$
Naïve	CD19$^+$, CD138$^-$, CD38^{Low}, CD27$^-$, IgD$^{+\ (Mid\ to\ High)}$
Marginal Zone Like (MZ-Like)	CD19$^+$, CD138$^-$, CD38^{Low}, CD27$^{+\ (Mid\ to\ High)}$, IgD$^{+\ (Mid\ to\ High)}$
Memory	CD19$^+$, CD138$^-$, CD38^{Low}, CD27$^{+\ (Mid\ to\ High)}$, IgD$^-$
Double Negative	CD19$^+$, CD138$^-$, CD38^{Low}, CD27$^-$, IgD$^-$

Figure 3.3-1. Distribution of EphA receptors in tonsil lymphocytes is donor-dependent.

Thawed and recovered tonsil lymphocytes from 27 unique tonsil specimens were stained for surface markers to identify B cell subsets followed by fixation, permeabilization and intracellular staining for EphA2, EphA4 and EphA7 and analyzed by flow cytometry. **(A)** Percent of viable, CD19+ cells positive for each EphA receptor. **(B)** distribution of B cell subsets (see Table 3.3-1) within EphA positive cells in each sample. Samples are ordered on the X-axis based on their overall percent positivity for the corresponding EphA with higher positivity sam-ples to the left. **(C)** Percent of each B lymphocyte subset that was positive for each EphA receptor. Colors in Figures A and C represent individual tonsil specimens and are comparable between the panels. **(D)** cell-level co-expression data for EphA2 (red), EphA4 (blue) and EphA7 (yellow), in 5 representative tonsil specimens. n represents the total number of viable B lymphocytes included in the analysis and sample designations are preceded by "ND".

3.3.2 Baseline expression of EphA receptors is not positively correlated with susceptibility to KSHV infection

We next wanted to determine whether the baseline level of EphA receptor expression within B cell subsets is correlated with overall infection or subset-specific infection for KSHV-WT or KSHV-ΔgH at 3dpi. Interestingly, there were no positive correlations between EphA receptor expression and overall susceptibility of tonsil samples to KSHV infection in this dataset (**Fig 3.3-2A**). Similarly, subset-specific expression of EphA receptors was not positively correlated with overall susceptibility to infection (**Fig 3.3-2B**). EphA4 expression had the strongest negative correlation with KSHV-WT infection while infection with KSHV-ΔgH was not correlated with the baseline expression of EphA2, EphA4 or EphA7 (**Fig 3.3-2A&B**).
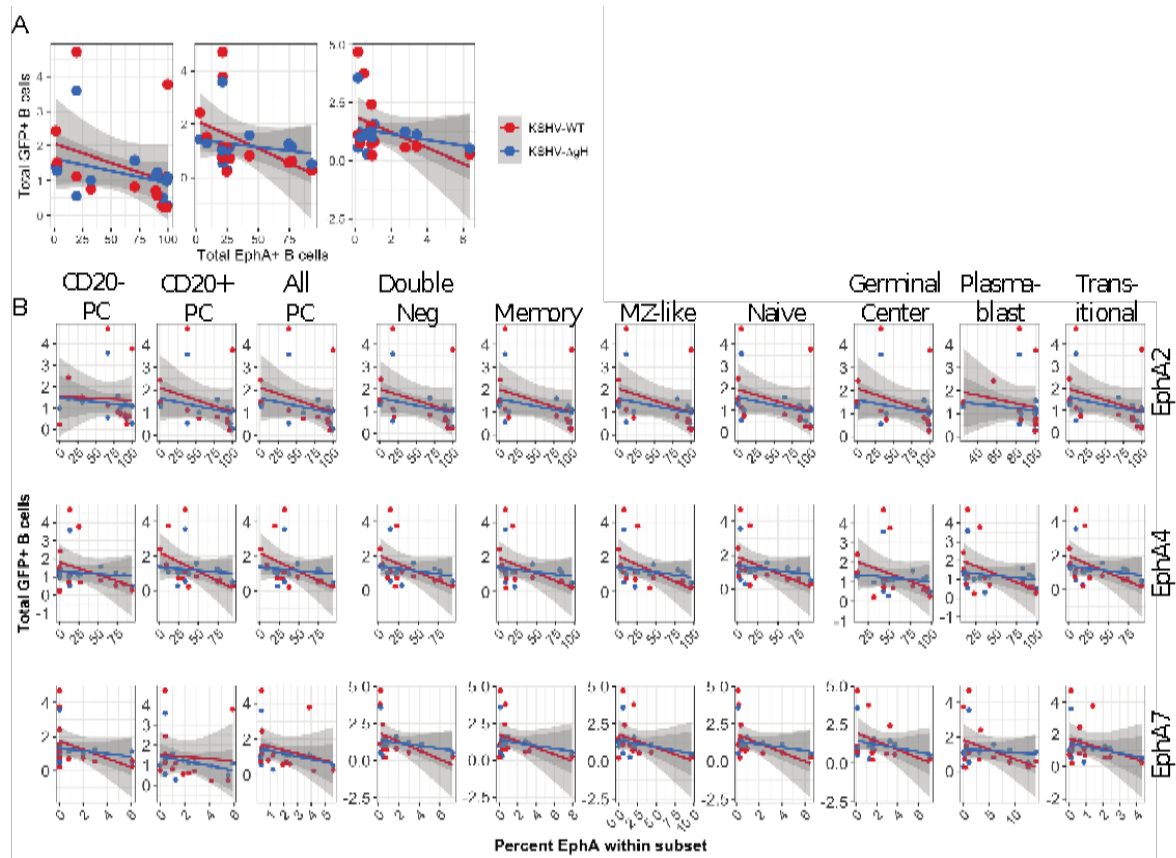
Figure 3.3-2. Baseline expression of EphA receptors is not positively correlated with susceptibility to KSHV infection.

Tonsil lymphocyte samples were infected with KSHV-WT or KSHV-ΔgH and analyzed by flow cytometry at 3 dpi for B cell immunophenotypes and the frequency and subset-specific distribution of GFP+ cells to assess KSHV infection. Total viable, CD19+GFP+ cells at 3dpi were correlated with baseline frequencies of EphA receptors in the same samples and linear regressions were performed using linear model fit with 95% confidence intervals represented by grey shading for **(A)** total EphA expression and **(B)** within subsets EphA expression. No correlations in this analysis were statistically significant using Pearson's method.

3.3.3 Treatment of target cells with an EphA ligand inhibits B lymphocyte infection by KSHV-WT but not KSHV-ΔgH

In order to more directly determine whether EphA receptors are participating in KSHV entry into B lymphocytes, we treated lymphocytes from 12 unique tonsil donors with a recombinant ephrin-A2-Fc fusion protein prior to infection with either KSHV-WT or KSHV-ΔgH. The ephrin-A2 ligand binds all EphA family receptors with varying affinities (Darling and Lamb 2019) and has been used as a broadly-acting EphA blocking reagent in previous studies (Hahn and Desrosiers 2013). We analyzed these data at 3 days post-infection (dpi) for KSHV infection (using the constitutive GFP reporter contained in the BAC16 genome) and B lymphocyte immunophenotypes by flow cytometry analysis. We previously showed that KSHV-WT and KSHV-ΔgH target tonsil-derived B lymphocytes at similar rates and with similar subset distributions, and demonstrated that gH is not required for entry into any lymphocyte subsets (Palmerin et al. 2021). The data sets in this study are consistent with our previous work, showing similar levels of total GFP and similar subset distributions for KSHV-WT and KSHV-ΔgH in untreated cultures (**Fig 3.3-3A&B**) with the exception of a significant increase in targeting of memory B cells with KSHV-ΔgH (**Fig 3.3-3B**). This difference was also present in our previous study but was not statistically significant, likely because of the smaller sample number. Analysis of KSHV infection as GFP+ cells within the viable CD19+ B cell population shows that treatment of lymphocytes with ephrin-A2-Fc inhibits infection of B cells with KSHV-WT in a dose-dependent manner, but has no effect on infection with KSHV-ΔgH (**Fig 3.3-3A**). Two-way repeated measures ANOVA analysis reveals that the main effect of WT vs. ΔgH in this context is significant ($p=0.04$, $F=5.6$) and there is a significant interaction of virus strain and dose in the data ($p=0.04$, $F=3.1$). Post-hoc paired T tests revealed that total infection is significantly different between the two viruses at the 40 ($p=0.001$) and 60μg/ml ($p=0.04$) doses of ephrin-A2-Fc.

We then examined the within subsets distribution of infection to determine whether ephrin-A2-Fc was altering the ability of KSHV-WT to target specific B cell sub-populations. The effect of ephrin-A2-Fc treatment on targeting of specific B cell subsets by KSHV-WT and KSHV-ΔgH is shown in **Figure 3.3-3C**. **Figure 3.3-3D** shows the same data normalized to the untreated control for each sample within each subset and virus strain so that the effect of ephrin-A2-Fc treatment can be more easily visually interpreted. We performed two-way repeated measures ANOVA analysis on the raw data (**Fig 3.3-3C**) to determine the main effects of ephrin-A2-Fc treatment and virus strain as well as interactions between these factors for each B cell subset. The results of the ANOVA analysis are shown in Table 3.3-2. Significant main effects of KSHV-WT vs. KSHV-ΔgH are indicated by blue boxes on Figure 3C and significant interaction effects of virus strain and ephrin-A2-Fc treatment are indicated by red boxes on Figure 3D. These results reveal that the decrease in overall infection in KSHV-WT infected, ephrin-A2-Fc treated cultures is associated with a decrease in CD20+ plasma cell and germinal center cell infection in most samples. For KSHV-ΔgH under the same conditions, infection of CD20+ plasma cells increased and germinal center cell infection was unchanged. Taken together, these results show that binding of KSHV-gH to EphA receptors is important for KSHV-WT entry, but in the absence of gH alternative entry strategies are exploited. Moreover, blocking EphA receptors limits the establishment of KSHV-WT infection in CD20+ plasma cells and germinal center cells, specifically, suggesting that gH-EphA interactions are particularly important for entry into these B cell subsets.
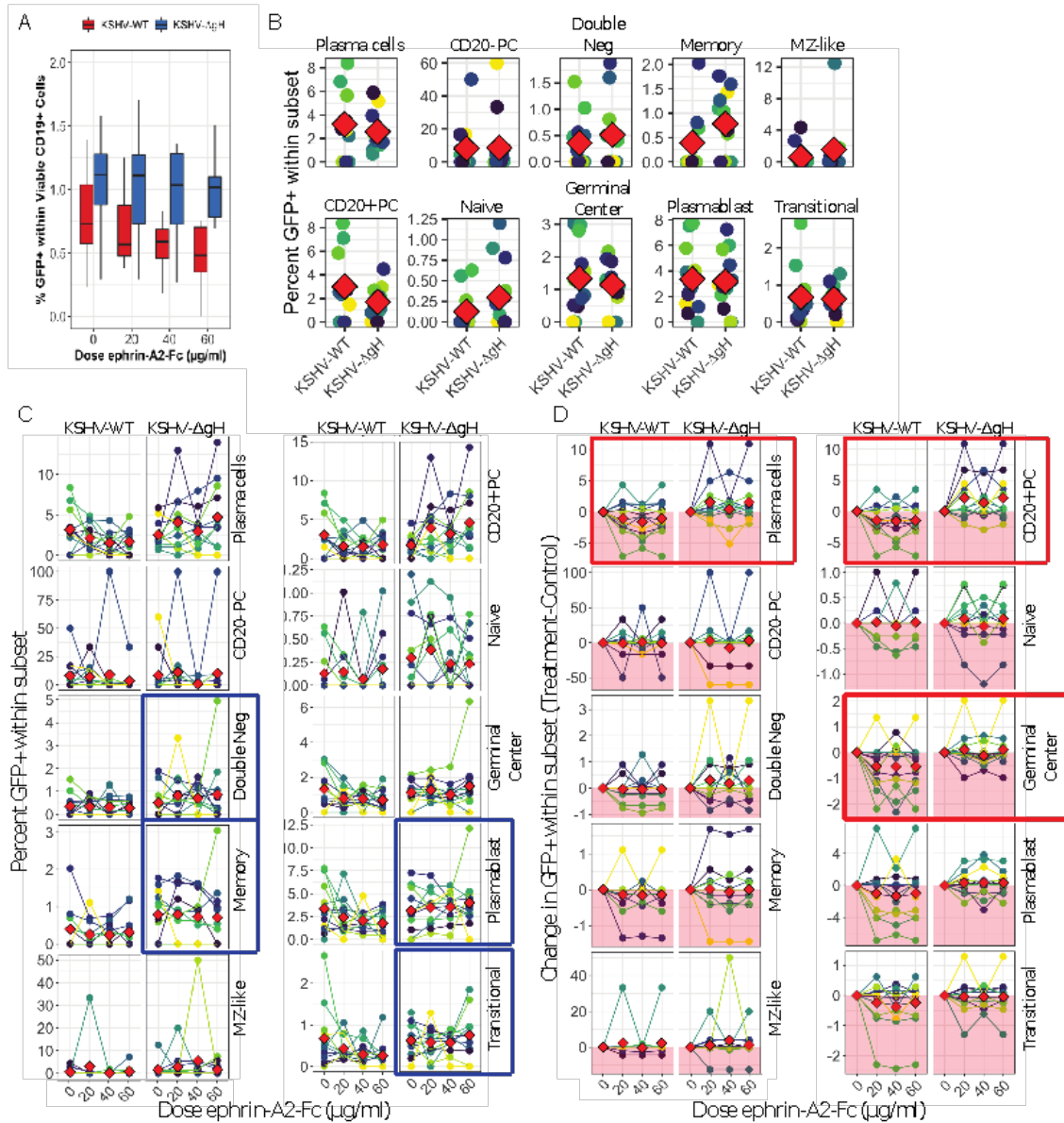
Figure 3.3-3. Treatment of target cells with an EphA ligand inhibits B lymphocyte infection by KSHV-WT but not KSHV-ΔgH.

Tonsil lymphocytes from 12 unique tonsil donors were pre-treated with indicated concentrations (in µg/ml) of recombinant ephrin-A2-Fc protein and subsequently infected with KSHV-WT or KSHV-ΔgH. B cell immunophenotyping and assessment of the frequency and distribution of KSHV infection was analyzed by flow cytometry at 3 dpi. **(A)** total percent of viable, CD19+ B lymphocytes that were GFP+ in each condition. **p=0.001, *p=0.04 **(B)** Subset-specific targeting of KSHV-WT vs. KSHV-ΔgH in untreated controls. *p=0.03 **(C)** GFP+ cells within each B cell subset for each condition. Blue boxes indicate subsets with significant main effects of virus strain via two-way repeated measures ANOVA. **(D)** data as in

(C) normalized to the sample, subset and virus-specific GFP value in untreated control cultures. Red boxes indicate subsets with significant interaction effects of virus strain and ephrin-A2-Fc treatment via two-way repeated measures ANOVA. ANOVA statistics can be found in Table 3.3-2. For panels B-D red diamonds indicate the mean of all values in the condition and colors indicate specific tonsil specimens and can be compared between panels in the figure.

Table 3.3-2. Statistical analysis of the data shown in Figure 3.3-3D

Subset	Effect	DFn	DFd	F	*p*	*p*<.05	ges
Plasma cell	Dose	3	33	1.006	0.402		0.021
Plasma cell	Cond	1	11	3.747	0.079		0.076
Plasma cell	Dose:Cond	3	33	3.599	0.024	*	0.065
CD20- PC	Dose	1.25	13.77	0.619	0.48		0.007
CD20- PC	Cond	1	11	0.782	0.396		0.000507
CD20- PC	Dose:Cond	1.2	13.16	0.556	0.499		0.021
Double Neg	Dose	3	33	0.212	0.888		0.006
Double Neg	Cond	1	11	14.523	0.003	*	0.076
Double Neg	Dose:Cond	3	33	0.38	0.768		0.012
Memory	Dose	1.97	21.72	0.274	0.76		0.005
Memory	Cond	1	11	13.846	0.003	*	0.134
Memory	Dose:Cond	2.13	23.42	0.174	0.854		0.003
MZ-like	Dose	1.88	20.73	0.361	0.689		0.017
MZ-like	Cond	1	11	2.227	0.164		0.017
MZ-like	Dose:Cond	1.41	15.55	1.116	0.331		0.027
CD20+ PC	Dose	3	33	0.855	0.474		0.017
CD20+ PC	Cond	1	11	3.353	0.094		0.071
CD20+ PC	Dose:Cond	3	33	5.079	0.005	*	0.094
Naïve	Dose	3	33	0.566	0.642		0.017
Naïve	Cond	1	11	4.68	0.053		0.062
Naïve	Dose:Cond	3	33	0.442	0.725		0.011
Germinal Center	Dose	1.93	21.23	0.829	0.446		0.02
Germinal Center	Cond	1	11	1.839	0.202		0.038
Germinal Center	Dose:Cond	3	33	3.003	0.044	*	0.043
Plasmablast	Dose	3	33	0.257	0.856		0.008
Plasmablast	Cond	1	11	8.812	0.013	*	0.082
Plasmablast	Dose:Cond	3	33	2.61	0.068		0.047
Transitional	Dose	3	33	1.123	0.354		0.034
Transitional	Cond	1	11	8.674	0.013	*	0.064
Transitional	Dose:Cond	3	33	1.815	0.164		0.051

3.3.4 Neutralization of KSHV virions with soluble EphA receptors reveals that EphA binding is essential for KSHV entry into CD20- plasma cells

Because of the broad binding of ephrin-A2 to multiple EphA receptors, treating target lymphocytes with the recombinant ephrin-A2-Fc ligand putatively blocks multiple EphA receptors with varying efficacy depending on their affinities for the ligand. In order to more specifically examine which EphA receptors might be participating in entry for KSHV-WT and KSHV-ΔgH, we performed a second set of experiments in which we treated KSHV virions with different doses of soluble recombinant EphA receptors prior to infection of lymphocytes. In this scenario, the recombinant EphA receptors should compete with cell-associated EphA receptors for binding of KSHV glycoproteins. In this data, we observed no significant impact of neutralization via soluble recombinant EphA ligands on overall infection with either virus (**Fig 3.3-4A**). When we normalized the data to the untreated control within each KSHV strain, we observed that neutralization had a highly variable effect on KSHV-ΔgH, but the effect was consistent within tonsil samples and across EphA proteins. In contrast, neutralization had minimal to effect on KSHV-WT except for one tonsil sample where infection was reduced via treatment with any soluble EphA receptor (**Fig 3.3-4B & C**). These data are consistent with the conclusion that the effectiveness of soluble EphA proteins in neutralizing KSHV virions is highly donor-dependent, which is consistent with our previous data showing the levels and distribution of EphA2, A4 and A7 on tonsil-derived B lymphocytes also vary substantially based on donor.

When we examined the subset-specific response to EphA-mediated neutralization via three-way repeated measures ANOVA, results showed that KSHV targeting of most subsets was not affected by the treatment (Supplemental Figure in Appendix B1 and Supplemental Table in Appendix B2). The only significant effect in this analysis was that of EphA neutralization dose on infection of

CD20- plasma cells (p=0.03, F=6.6). We can observe that any EphA ligand was able to reduce infection of CD20- plasma cells by both KSHV-WT and KSHV-ΔgH (**Fig 3.3-4D&E**). Indeed, in several samples, GFP+ CD20- plasma cells were not observed in any neutralized conditions. This observation is notable because, although they are a rare cell type in tonsil, CD20- plasma cells have one of the highest within-subsets targeting during early KSHV infection (Aalam et al. 2020). These data indicate that KSHV requires EphA receptor binding to enter CD20- plasma cells, but that gH is not involved in this interaction. Finally, we wanted to determine whether the effect of EphA-mediated neutralization on infection was related to the baseline levels of EphA receptor expression in the tonsil samples. Interestingly, we observed significant correlations between response of infection to EphA2 treatment and baseline EphA2 expression. However, the effects were opposite for the two virus strains with EphA2-mediated neutralization having a greater inhibitory effect on KSHV-WT infection in samples with higher baseline EphA2 expression (r=0.7, *p*=0.006), and EphA2-mediated neutralization having an enhancing effect on KSHV-ΔgH infection in samples with high baseline EphA2 expression and an inhibitory effect in samples with low EphA2 expression (r=-0.8, *p*=0.0001) (**Fig 3.3-4F**). For KSHV-WT, the negative correlation between total EphA2 expression and response to virion neutralization with soluble EphA2 may indicate that this EphA receptor, in particular, is critical for gH-dependent KSHV entry into B cells. The positive correlation seen in the same data with KSHV-ΔgH is more difficult to interpret, but may indicate that gH-independent entry mechanism(s) are influenced by EphA signaling and adding soluble EphA receptors in the context of low baseline EphA expression deprives cells of ephrin signals which facilitate entry specifically for KSHV-ΔgH.
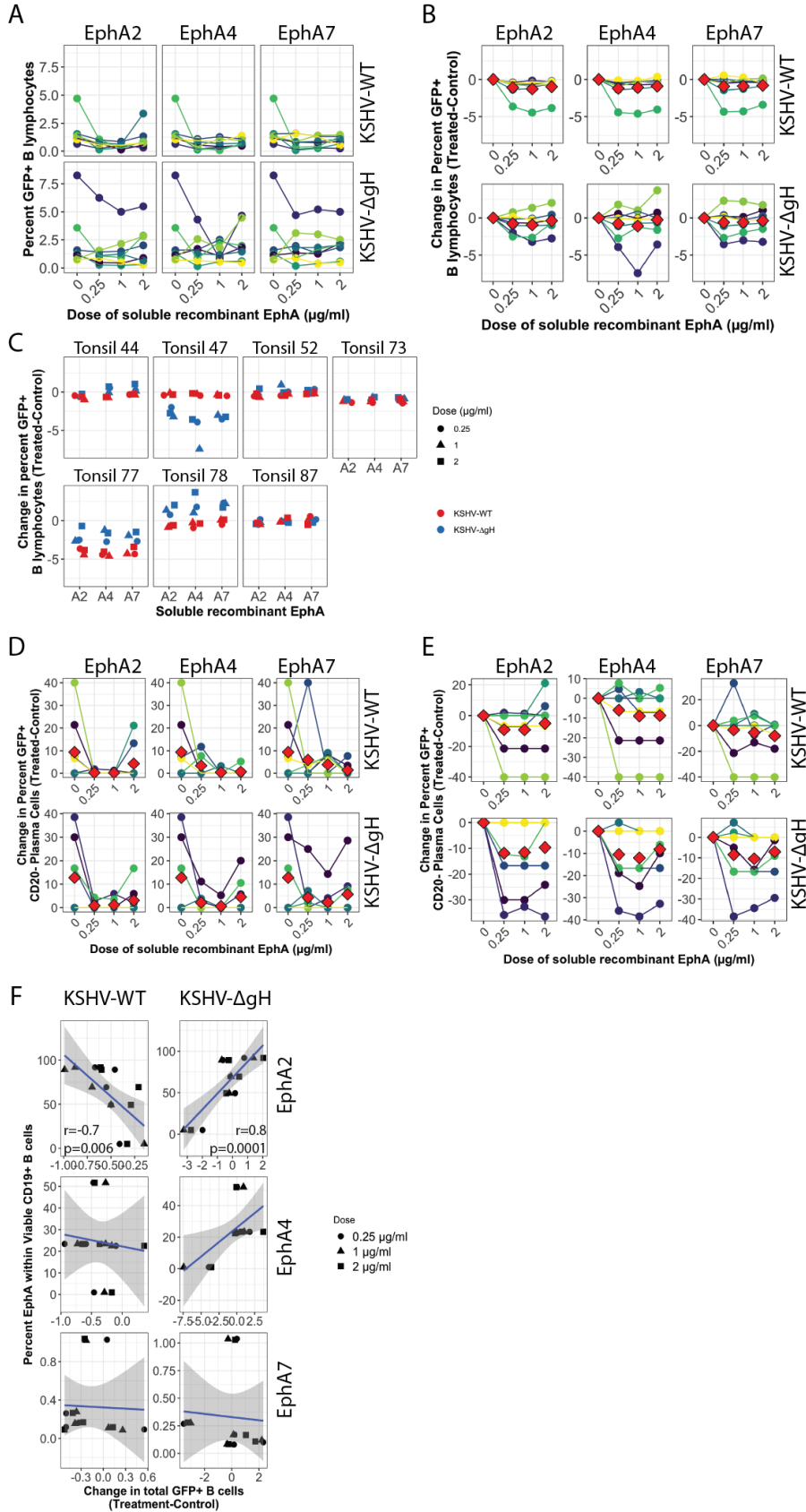
Figure 3.3-4. Neutralization of KSHV virions with soluble EphA receptors reveals that EphA binding is essential for KSHV entry into CD20- plasma cells.

Purified virions for KSHV-WT and KSHV-ΔgH were treated with indicated doses (in µg/ml) of soluble recombinant EphA2, EphA4 or EphA7 protein. Virions were then used to infect tonsil lymphocytes from 7 unique tonsil donors. B cell immunophenotyping and assessment of the frequency and distribution of KSHV infection was analyzed by flow cytometry at 3 dpi. **(A)** total percent of viable, CD19+ B lymphocytes that were GFP+ in each condition. **(B)** data as in (A) normalized to the sample and virus-specific GFP value in untreated control cultures. **(C)** data as in (B) separated by sample with colors indicating virus strain and shapes indicating treatment dose for each EphA protein. **(D)** Percent of GFP+ cells within the CD20- plasma cell subset for each condition. **(E)** Data as in (D) normalized to the sample and virus specific GFP value. This data for all subsets can be found in Supplemental Figure (Appendix B1). For panels A, B, D and E red diamonds indicate the mean of all values in the condition and colors indicate specific tonsil specimens and can be compared between panels in the figure. **(F)** Correlation of the frequency of EphA expression within viable CD19+ B cells at baseline (day 0) with the ability of soluble recombinant EphA receptors to neutralize KSHV infection at 3 dpi. Linear regressions were performed using linear mode fit and grey shading indicates 95% confidence intervals. Correlation coefficients and p-values calculated using Pearson's method are shown on panels with significant correlations.

3.4 Discussion

The success of immunization in reducing rates of human papilloma virus-associated cancers provides a strong rationale driving efforts to limit virus-associated cancers by the simple, but often difficult, strategy of limiting the spread of the pathogen within the human population. The oncogenic lymphotropic herpesviruses pose a particular challenge for this strategy given that they are generally acquired early in life and the human immune system is uniformly unable to clear the infection, which remains for the lifetime of the host. Moreover, these viruses cause lymphoproliferation, so infection of even a single B cell can serve as an expansion point that will greatly limit the effectiveness of a vaccination strategy that is designed to block the establishment of infection. Thus, the rational design of a vaccine to prevent primary KSHV infection requires much more complete knowledge of how KSHV infects B cells than is currently available, and our group has begun a series of studies aimed at filling this critical knowledge gap.

We previously showed that KSHV entry in primary tonsil-derived B cells is not dependent on DC-SIGN, and that KSHV can still enter tonsillar B cells when the gH/gL complex is removed from the virion by directed mutagenesis of the gH gene (Palmerin et al. 2021). Importantly, results from that previous study indicated that gH/gL does have a role in B cell tropism, but that, in all B cell subsets, alternative mechanisms are employed when gH/gL is absent. Here, we extend these findings using the same virus strains and tonsil lymphocyte infection system, but aim to determine whether EphA receptor-gH interactions play a role in KSHV infection of B cells. We employ two complementary strategies to block KSHV-EphA interactions: (1) broadly binding EphA receptors on target cells using a recombinant ephrin-A2 protein, and (2) neutralizing EphA-gp interactions by treating virion preparations with soluble EphA receptors.

We propose a model unifying our interpretation of the data in **Figure 3.4-1**. In the first set of experiments with ephrin-A2 occupying cell surface EphA receptors, we observe that KSHV-WT infection is inhibited but infection with KSHV-ΔgH is unaffected by treatment. These results imply that EphA-gH interactions are important for entry of KSHV-WT but that in the absence of gH/gL KSHV is able to enter B cells via an alternative route. Importantly, the inhibition we see for KSHV-WT implies that these alternative entry strategies are unavailable when gH/gL is incorporated into the virion, but a lack of inhibition in the corresponding experiments in which we treated KSHV virions with soluble EphA receptors may indicate that binding of soluble EphA to gH unmasks gH-independent entry mechanisms that can be exploited for entry.
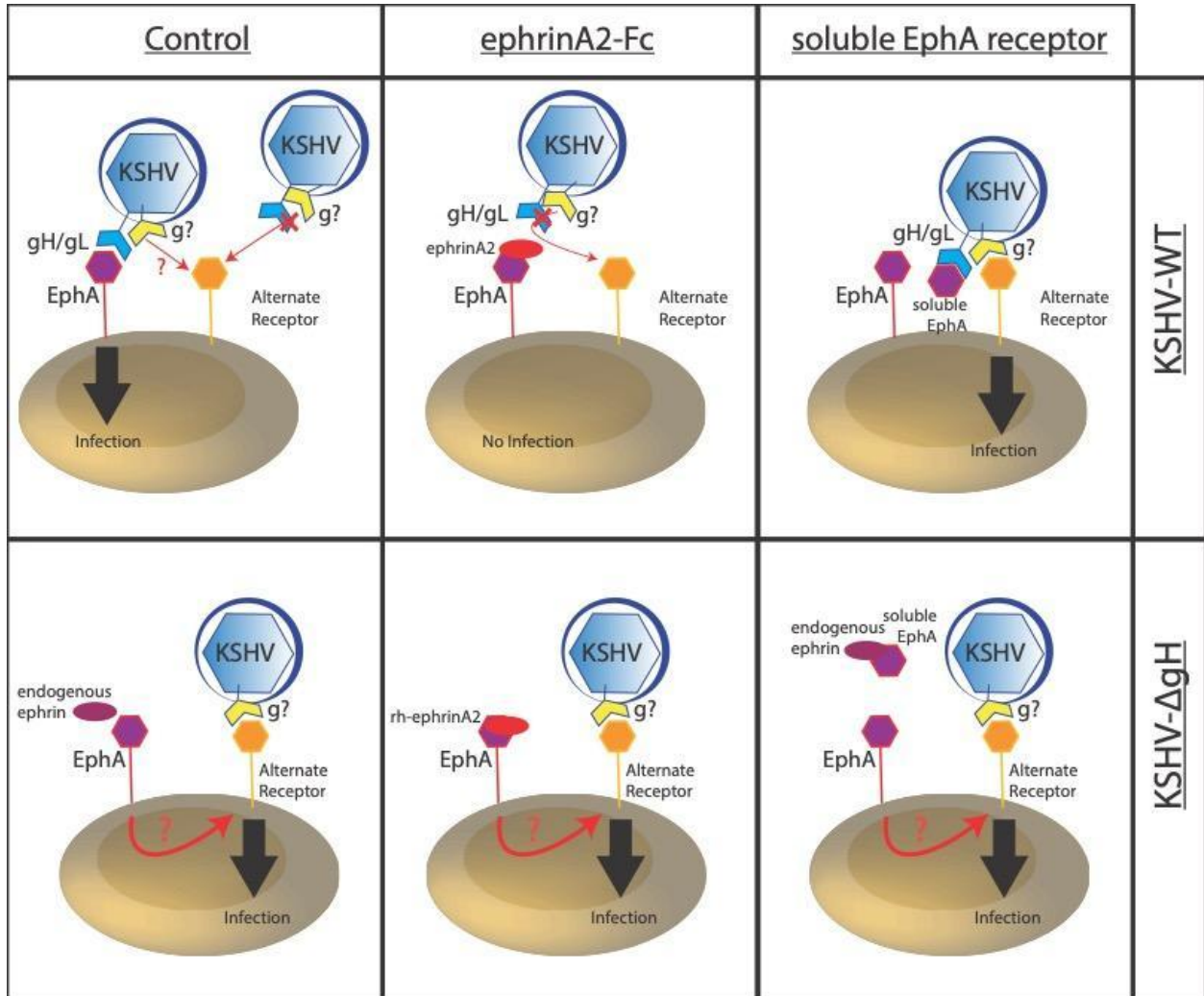
Figure 3.4-1. A theoretical model, supported by the data, of interactions in the different experimental conditions in the study.

Our experiments using soluble EphA receptors to neutralize KSHV virions revealed that all three EphA types tested (EphA2, EphA4, and EphA7) behaved similarly and generally failed to significantly inhibit KSHV entry (**Fig 3.3-4**). Indeed, the effect of these treatments was more dependent upon the particular tonsil sample than the virus strain, EphA type or dose of treatment. Previous studies have shown that EphA2, in particular, is an important receptor for KSHV entry into endothelial cells, epithelial cells and fibroblasts (Hahn et al. 2012; Chakraborty et al. 2012; Dutta et al. 2013) and that EphA4 can mediate KSHV entry in HEK-293 cells (Chen et al. 2019) while EphA7 seems to be important for direct cell-cell transmission of KSHV in the BJAB lymphoma cell line (Großkopf et al. 2019). Our data neither supports nor refutes these observations for B cells given that virion neutralization with soluble EphA2, EphA4 and EphA7 had similar, non-significant effects on infection in our system with both KSHV-WT and KSHV-ΔgH virus strains. We did observe significant, but opposite, correlations with the two virus strains when we compared the response to soluble EphA treatment and baseline EphA2 expression (**Fig 3.3-4F**). Although these results are difficult to interpret, the fact that they are sample specific and correlated to the baseline levels of EphA2 specifically indicates that the effect may due to soluble EphA receptors depriving EphA2 of ephrin ligands. In this context, the data support a contribution of EphA2 signaling to KSHV entry or early dissemination of infection in B cells that is independent of actual interactions between EphA2 and virion glycoproteins. Indeed, the effect of EphA2 signaling on early events in KSHV infection has been previously reported for endothelial cells (Chakraborty et al. 2012). In particular, our data with KSHV-ΔgH in the context of soluble EphA neutralization leads us to speculate that EphA signaling might regulate the expression of the receptor(s) mediating gH-independent binding and entry. Additionally, EphA signaling may

facilitate the early proliferation or differentiation of infected cells as has been shown previous with EphA4 in EBV-infected lymphocytes (Huang et al. 2016).

Although other studies have examined transcripts for EphA receptors and ephrin-A ligands in B lymphocytes (Alonso-C et al. 2009; Chen et al. 2019), we believe that the data presented in Figure 1 of this study is the first detailed examination of EphA receptor distribution and co-expression in tonsil-derived B cell subsets. We demonstrate that, although there are some subsets that are enriched for expression of particular EphA proteins, distribution of these receptors is much more dependent upon host factors vs. subset-specific factors. This is interesting in light of our previous work showing highly variable targeting of tonsil-derived lymphocytes based on unknown host-level factors that are independent of age, sex or racial demographics (Aalam et al. 2020). Although we did not find any significant correlation between baseline EphA receptor expression and overall susceptibility of tonsil lymphocytes to KSHV infection in this study (**Fig. 3.3-2**), these new results provide evidence that receptors important for KSHV infection are one factor that can vary substantially from host-to-host, and may be partially responsible for the variable susceptibility we observe. Thus, a broader survey of putative entry receptors and their distribution within B cell subsets and between tonsil lymphocyte samples is warranted.

The very different responses of KSHV-ΔgH vs. KSHV-WT in our studies underscore the longstanding issue of using glycoprotein knockout mutants to study herpesvirus entry. The complexity and interactions of herpesvirus gps with cellular receptors can make interpretation of results difficult, and glycoprotein mutant virions may utilize entry mechanisms that are not available in a wild-type context and therefore are not necessarily physiologically relevant. Thus, in future studies we would propose to combine glycoprotein mutants with experiments employing specific anti-gp neutralizing antibodies in the context of KSHV-WT in order to dissect the

functional interactions more carefully and obtain a clearer picture of how KSHV entry might be targeted immunologically. Moreover, future studies examining the role of additional putative receptors and KSHV-glycoproteins are needed to support and extend these studies to develop a more complete picture of KSHV entry into the human immune system.

4 CHAPTER IV: Establishing the dynamics of cell-to-cell transmission of KSHV in human tonsil-derived cell types

Associated Publications and Author Contributions:

Authors: Farizeh Aalam, Romina Nabiee, Emily Romano and JenniferTotonchy‡

This chapter is a manuscript submitted to *Journal of Virology*

Farizeh Aalam performed the experiments presented in Figure 3.4-1B, Figure 3.4-2, Figure 3.4-3, Figure 3.4-4, and Figure 4.4-1.

Abstract

Saliva is widely accepted as the primary route of person-to-person transmission for KSHV, making the oral cavity a likely site for the establishment of KSHV infection in a new human host. However, it is yet to be determined how KSHV infects the oral mucosa and what cell types play a role in establishing KSHV infection in disease-relevant cell types like B cells. Here, we take advantage of our library of primary tonsillar lymphocytes and donor-matched adherent cell lines to explore KSHV transmission between tonsil-derived cell types. We show that a variety of primary tonsillar cells are susceptible to KSHV infection and can differentially transmit the infection into B cells. We demonstrate that KSHV spread between and within tonsil cell types is directed, suggesting that, as has been demonstrated for EBV, tropism may be influenced by differential virion composition arising from each cell type. Our results represent a first step toward establishing the mechanisms of KSHV spread within this physiologically important tissue and may have significant implications for the prevention of person-to-person transmission of KSHV and the establishment of infection in disease-relevant cell types in humans.

Importance

Kaposi Sarcoma Herpesvirus (KSHV) is associated with several cancers in humans including immunological cancers in B cells. Despite many years of research, how KSHV establishes infection in a new human host is poorly understood. Because KSHV is present in saliva, and infects B cells and cells of the lymph vessels in tumors, the tonsil is a likely site for the initial establishment of KSHV infection in humans. This study examines the transfer of KSHV infection

between cell types extracted from human tonsils as a first step to understanding how the virus might invade this tissue and establish infection in the human immune system.

4.1 Introduction

An extensive body of literature has established saliva, blood, and organ transplant as the main sources of horizontal KSHV transmission (Uldrick and Whitby 2011; Minhas and Wood 2014). KSHV DNA is readily detected in human saliva and epidemiological data suggest that salivary transmission is the primary route of person-to-person transmission for KSHV in endemic areas (Pica and Volpi 2007; Quinlivan et al. 2001; Olp et al. 2016) Moreover, the oral cavity is a major site for viral replication, indicated by readily detectable infectious virus in saliva and viral transcripts in oral tissues (Vieira et al. 1997; Pauk et al. 2000; Gasperini et al. 2005; Chagas et al. 2006; Webster-Cyriaque et al. 2006). These observations, taken together with the broad tropism of KSHV for cell types present in tonsil (Bechtel et al. 2003; Muniraju et al. 2019; Totonchy et al. 2018) and the presence of disease-relevant cell types like B cells and lymphatic endothelial cells, makes the oral lymphoid tissues a likely site for initial infection events during KSHV transmission into a naïve human host. Moreover, the oral lymphoid tissues are particularly likely to be the site at which KSHV initially invades the immune system. Importantly, the dynamics of KSHV infection within and transmission between tonsillar cell types has not been addressed. This represents a significant gap in our understanding of the early events that occur during KSHV transmission into a new human host. Furthermore, this knowledge gap specifically limits our ability to develop strategies to prevent both person-to-person transmission of KSHV and the establishment of infection in disease-relevant cell types.

Many models predict that transfer of EBV infection from tonsillar B lymphocytes to epithelial cells contributes substantially to the release of EBV particles into saliva (Thorley-Lawson et al. 2013), but similar mechanisms have not been characterized for KSHV. The presence of KSHV latent and lytic transcripts in epithelial cells found in saliva samples (Vieira et al. 1997) prompted many investigations regarding KSHV transmission within oral epithelial cells (Cerimele et al. 2001; Bechtel et al. 2003; Duus et al. 2004; Johnson, Maronian, and Vieira 2005; Seifi et al. 2011; Gong et al. 2014; Muniraju et al. 2019) and the current *in vitro* models of KSHV transmission suggest that viral replication and shedding is due to differentiation of epithelial cells (Johnson, Maronian, and Vieira 2005; Seifi et al. 2011). However, these studies do not address whether epithelial derived virions are responsible for early infection and dissemination of KSHV during primary infection.

In this study, we leverage our unique library of donor-matched tonsil lymphocyte and adherent cell cultures to examine how KSHV is transmitted within and between cell types as a first attempt at developing a model for cell-to-cell transmission of KSHV within the human tonsil during the early stages of primary infection. We successfully isolate and culture epithelial cells and fibroblasts from human tonsil specimens and demonstrate that they are susceptible to KSHV infection *in vitro*. Subsequently we perform both co-culture and supernatant transfer experiments to determine whether KSHV is efficiently transmitted within and between these cell types as well as whether there is spread to/from these cell types to donor-matched B cells. We demonstrate that KSHV transmission between tonsil-derived cell types is specific and directed, and that B cells can receive infection efficiently from both epithelial and fibroblast cell types via direct contact. These results establish a foundation for understanding KSHV transmission and the establishment of

KSHV infection in B cells, and strongly suggest that KSHV employs mechanisms for directed transmission between cell types during early infection which requires further study.

4.2   Material and Methods

4.2.1   Preparation of CDw cells

CDw32 L cells (CRL-10680) were obtained from ATCC and were cultured in DMEM supplemented with 20% FBS (Sigma Aldrich) and Penicililin/Streptomycin/L-glutamine (PSG/ Corning). For preparation of feeder cells CDw32 L cells were trypsinized and resuspended in 15 ml of media in a petri dish and irradiated with 45 Gy of X-ray radiation using a Rad-Source (RS200) irradiator. Irradiated cells were then counted and cryopreserved until needed as feeder cells for lymphocyte and epithelial cell cultures

4.2.2   Isolation of tonsillar primary cells

De-identified human tonsils removed by routine tonsillectomies were provided by the National Disease Research Interchange (NDRI). The tonsil specimens were maintained on ice and in DMEM and 1%PSG until delivery to the laboratory for processing within 24 hours post-surgery. The epithelial layer of the tonsillar surface was carefully excised and transferred to a gentleMACS™ C Tubes (Miltenyi Biotech) containing 2 ml of DMEM/PSG, 100μg/ml of DNaseI, 62.5μg/ml of Liberase™ DH (05401054001, Roche Applied Science). The remaining tissue was dissected and macerated in RPMI media to release lymphocytes. The media was passed through a 40μm filter and pelleted at 1500rpm for 5 minutes for collection of lymphocytes. The lymphocytes were further resuspended in RBC lysing solution (0.15M ammonium chloride, 10mM potassium bicarbonate, 0.1M EDTA) for 5 minutes and diluted with 50ml of PBS. Lymphocyte

aliquots of 5(10)7 to 1(10)8 cells were cryopreserved in 90% FBS and 10% DMSO for later experiments.

The remaining tonsillar tissue was transferred to another gentleMACS™ C tube containing 125μg of Liberase and 100μg of DnaseI. Both the epithelial layer and residual tissue were dissociated via two rounds of incubation at 37 °C with 600rpm shaking for 15 minutes followed by processing on a gentleMACS™ Dissociator (Miltenyi Biotec) using "Multi-a-c-tube " program. After the last dissociation step, the cells were resuspended in RPMI and passed through a 40μm cell strainer and pelleted at 1500rpm for 5 minutes followed by RBC lysis step as described above. Cells from the dissociated epithelial fraction were subjected to CD45 depletion using magnetic CD45 microbeads (480029, BioLegend) according to manufacturer instructions and plated on collagen I treated plates (354456, Corning) in epithelial media (NC0117184, Sciencell Research Laboratories) with the addition of 1e5 CDW32 feeder cells, 20% FBS, 100μg/ml primocin, and 10μM of ROCK inhibitor (Y27632, Hello Bio). The remaining dissociated cells were supplemented with Endothelial media (CC-4147, Lonza) and primocin and plated on collagen I treated plates. At 24 h post plating, the plates were gently washed with PBS++ and supplemented with the media without FBS until confluent and ready for sorting.

4.2.3 Cell sorting

The cells were gently lifted with Accutase ® (A6964, Sigma-Aldrich) and pelleted in FBS containing media at 1500 rpm. The pellet was resuspended in MACS Buffer (PBS + 2% FBS + 1mM EDTA) + 5% FBS and then incubated on ice for10 minutes for blocking. After incubation, the cells were pelleted and resuspended in MACS Buffer containing the following antibodies; CD44-PerCPCy5.5 (338819, BioLegend), CD90-PE-Cy7 (328123, BioLegend), NGFR-PE

(345106, BioLegend) and incubated on ice for 15 minutes. After incubation the cells were washed two times with MACS buffer, passed through 35μm cell strainer, and resuspended in MACS Buffer + 25% Accumax (A7089, Sigma-Aldrich). The stained cells were sorted with BD FACSAria™ Fusion cell sorter, using a 100μm nozzle and purity sort mode. The sorted cells were collected in PBS containing 20% FBS and plated in appropriate media (see above) for further experiments.

4.2.4 Preparation and titration of cell free KSHV

iSLK stably infected with recombinant KSHV BAC16 (Myoung and Ganem 2011a) were cultured in DMEM supplemented with 10% Cosmic Calf Serum (CCS), 1% PSG, 250μg/ml G418, 50μg/ml gentamicin, 1.2mg/ml Hygromycin, 1μM Puromycin. The cells were expanded to twelve confluent T185 flasks at 37 ºC in 5% CO2. Upon reaching 70-80% confluency, the cells were induced with 2μM Doxycycline and 3mM Sodium Butyrate for 72 hours. Supernatants from induced cultures were collected and clarified by centrifugation at 1500rpm for 12 minutes at 4ºC and passed through a 0.45um filter. The virions were pelleted by ultracentrifugation over a 25% sucrose/TNE cushion (100 mM NaCl, 50 mM Tris [pH 7.4], 0.1 mM EDTA, pH 7.4) at 22,000 rpm for 120 minutes. Virus pellets were resuspended in 2ml TNE buffer and aliquots were stored at -80˚C. Virus stocks were titrated on immortalized human fibroblasts and analyzed for expression of the GFP reporter at 3 dpi by flow cytometry. Linear regression was used to calculate the virus dose (in microliters per cell) needed to infect 20% of fibroblasts at 3 dpi and this dose is used to normalize infection on all cell types for each virus preparation.

4.2.5 Primary cell infection with concentrated, iSLK-derived KSHV

All the experiments using adherent cells were performed on passage-matched autologous cells with passage numbers ranging between 3 to 6, to avoid phenotypic changes due to culture conditions. Primary lymphocytes were used directly after thawing together with autologous adherent cells from the same tonsil specimen to avoid artifacts due to allogenic reactions. Primary cells (total B cells, epithelial, and fibroblast cells) were infected with BAC16 WT KSHV based on cell-number adjusted ID20 from fibroblast titers (see above). Infection of fibroblast and epithelial cells were performed in 1ml of serum free RPMI at 37 ∘C and 5% CO_2 for 90 minutes followed by cell surface washes and addition of complete growth media.

Lymphocytes were thawed rapidly and gradually diluted with 5 to 6 ml of RPMI and pelleted at 1400 rpm for 5 minutes. The lymphocyte pellet was resuspended in 1 ml RPMI containing 20% FBS, 1% PSG, 100μg/ml of DNaseI, and 100μg/ml of Primocin and plated on a low-binding 24 well plate and kept at 37º C and 5% CO_2 for two hours. Naïve B cells were isolated by subjecting lymphocytes to magnetic separation using Mojosort™ Naïve B cell isolation kit (480068, BioLegend) according to manufacturer's instructions. The bound fraction of the lymphocytes was maintained at 37 ºC and 5% CO_2 incubator in complete media during the infection procedure. For the infection, naïve B cells were resuspended in serum free RPMI media at 400μl/1e6 cells per experimental condition and the infection was performed through spinoculation at 1000 rpm for 30 min at 4º C followed by incubation at 37º C and 5% CO_2 for 30 min. After incubation, the infected naïve B cells were cultured in 48-well plates containing a confluent layer of CDW32 feeder cells and reconstituted with the same proportion of the bound fraction, 20% fetal bovine serum, and 100 μg/mL of Primocin. All the primary cells were incubated at 37º C, 5% CO_2 for 3 days

4.2.6 **Transfer of infection to lymphocytes**

At 3 dpi, a fresh aliquot of donor-matched tonsil lymphocytes was thawed and magnetically separated as described above. A total of 1e6 naïve B cells per transfer experiment were resuspended and reconstituted with the same proportion of the bound fraction in 400µl of epithelial media and incubated over the infected confluent layer of adherent cells in a 24 well plate for 1 hour at 37 ºC and 5% CO2 incubator. After the incubation, the lymphocytes were supplemented with CDw32 cells and 100µg/ml of Primocin in 100µl of FBS with the addition of ROCK inhibitor in case of epithelial cell co-culture. The primary cell co-cultures were further incubated at 37º C, 5% CO2 for 3 days. At 3 days post co-culture, the lymphocytes were resuspended in the media and pelleted at 1500 rpm for antibody staining and FACs analysis. For the experiments involving supernatant transfer to lymphocytes, the collected supernatants at 3dpi were clarified of cellular debris by centrifugation, added to the freshly sorted naive B lymphocytes and incubated for 1 hour at 37 ºC and 5% CO2 incubator. After incubation, the naive B lymphocytes were reconstituted with bound fraction in fresh epithelial media containing a total of 20% FBS and cultured over a well of CDw32 plate cells for 3 days.

4.2.7 **Transfer of infection to adherent cells**

At 3 days post infection, infected B lymphocytes and uninfected and infected primary fibroblasts and epithelial cells were gently lifted with Accutase and pelleted in FBS containing media at 1500 rpm. The cells were further washed and resuspended in epithelial media containing CDw32 cells, 100µg/ml of Primocin, 20% FBS (for the lymphocyte co-culture) and ROCK inhibitor (for the epithelial cell co-culture), counted and seeded at appropriate densities to cover the surface of collagen coated 24 well plate and allowed to recover at 37º C, 5% CO2 for 3 hours before co-culturing with lymphocytes.

4.2.8 Genome titer (qPCR)

To evaluate the viral copy number in the supernatants, qPCR was performed. DNA was extracted from donor cell's supernatant using Quick-DNA/RNA Viral kit (D7020, Zymo Research) according to the manufacturer's instruction. Extracted genome was quantified using TaqMan™ Fast Advanced Master Mix (4444557, Applied Biosystems™), along with 1μM primers targeting the BAC16 eGFP cassette (Fwd: 5' -TGACCCTGAAGTTCATCTGC-3', Rev: 5'-GAAGTCGTGCTGCTTCATGT-3', and 250nM of Probe:5'-[6FAM]-CCCACCCTCGTGACCACCCT-3'. The samples were analyzed in duplicate reactions. Standard curves for absolute quantification of viral genome copies were assembled using linearized pCR2.1 plasmid containing a cloned fragment of the GFP gene covering the qPCR amplicon sequence, diluted in 10ng/μl salmon sperm DNA. The samples were run and analyzed a standard 40 cycle program on a Thermofisher QuantStudio™ 3 real time PCR instrument.

4.2.9 Flow cytometry analysis

At 3 days post co-culture, a portion of cells were harvested for staining and flow cytometry analysis. The staining procedures were performed on ice using cold buffers and the centrifugation steps were done at 1500 rpm for 5 minutes. The adherent cells of about ~500,000 cells were gently lifted using Accutase ® (A6964, Sigma-Aldrich) and diluted with 10% FBS in PBS and pelleted at 1500 rpm. The cell were stained with 500μl PBS containing viability dye (see below) and incubated for 15 minutes. Cells were further washed with FACS Block (PBS, 0.5% BSA, and 2% FBS), pelleted, resuspended and incubated in FACS Block for 10 minutes. After the incubation, equal volume of FACS Wash (PBS, 0.5% BSA, and 0.1% Sodium Azide) was added to the cells for pelleting. The cells were resuspended in 500μl of FACS Wash containing antibodies (see below) and incubated for 15 minutes. After incubation, the cells were washed two times with

FACS Wash, and resuspended in FACS Wash. Data was acquired on a BD Fortessa X20 flow cytometer and analyzed using FlowJo software. Co-cultures of adherent cells were stained with viability dye (423113, BioLegend), CD44-PerCPCy5.5 (338819, BioLegend), CD90-PE-Cy7 (328123, BioLegend), and NGFR-PE (345106, BioLegend). Lymphocytes samples were stained with fixable viability dye (BD 565388) and CD19-PerCPCy5.5 (BD 561295).

4.3 Results

4.3.1 Isolation and infection of non-lymphocyte tonsil cell lines

We have previously showed that a variety of tonsillar B lymphocyte subsets are susceptible to KSHV infection via direct inoculation with iSLK-derived BAC16 KSHV virions (Aalam et al. 2020). In this study, we wanted to characterize whether other non-lymphocyte cell types could infect tonsil-derived B cells and examine whether adherent cell types have directed methods of transfer within and between them. Thus, we developed a method for isolating non-lymphocyte cell types during our tonsil extractions. In early experiments, mixed tonsil epithelial cell cultures were prone to differentiation and loss of adherence, making longitudinal experiments difficult. However, when we isolated CD44+/CD90+/NGFR+ epithelial cells via cell sorting (**Figure 4.3-1A**), which are found in the relatively thin crypt epithelium and the lower layers of surface epithelium (S. Y. C. Kang et al. 2015) and cultured them in the absence of FBS and the presence of the ROCK inhibitor Y-27632, we were able to obtain stable epithelial cell cultures for experiments (**Figure 4.3-1B**). CD44+/CD90+/NGFR- fibroblasts were readily cultured from both residual tissue following tonsil lymphocyte extraction as well as the NGFR- fractions from epithelial cell sorting (**Figure 4.3-1A**). Unfortunately, despite multiple attempts using various isolation and culture conditions as well as markers and methods for cell sorting, we were unable

to obtain cultures of endothelial cells that were free of fibroblast contamination. Thus, we have

excluded endothelial cells from this manuscript as the experiments performed herein would be

uninterpretable without a pure endothelial cell culture.
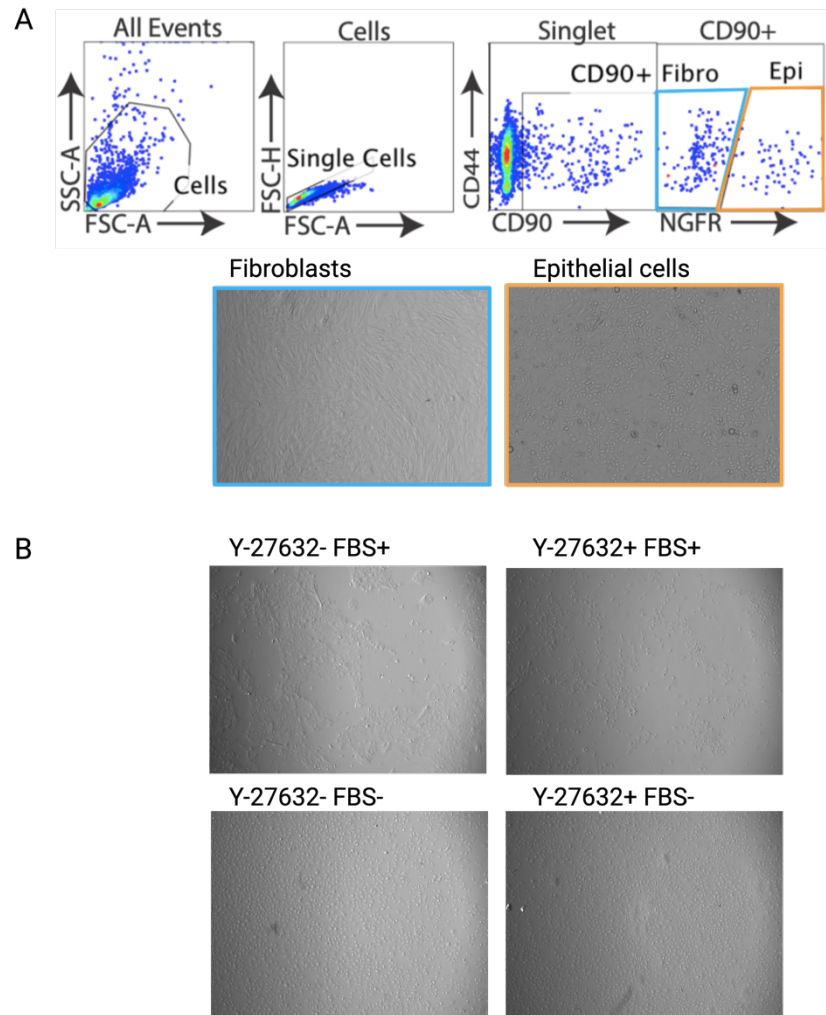
Figure 4.3-1. Phenotypic characterization of non-lymphocyte primary cells.

A) Gating strategy for cell sorting and morphology at 4X magnification of resulting primary fibroblasts and epithelial cells**. B)** Optimization of the culture conditions for primary epithelial cells. 5e5 sorted epithelial cell cultures were sub-cultured in 35mm collagen coated plates in epithelial cell basal media containing the indicated additives for 24hrs prior to analysis via microscopy at 4X magnification

4.3.2 Tonsillar Tonsil-derived primary fibroblasts and epithelial cells are susceptible to KSHV infection

With tonsil epithelial and fibroblast cultures in hand from 10 human tonsil specimens, we first wanted to validate that these cells are susceptible to KSHV infection. For these experiments, we seeded equal numbers of epithelial cells and fibroblasts in 24-well plates and infected them with equivalent doses of purified, iSLK-derived BAC16 KSHV-WT virions. After 3 days of infection, we examined the cultures for GFP+ cells as an indicator of infection. These experiments revealed that, in all specimens GFP+ cells can be detected at 3 dpi for both fibroblast (**Figure 4.3-2A**) and epithelial cell (**Figure 4.3-2B**) cultures. White light microscopy reveals that, despite plating at a specific cell density the day before infection, samples from different tonsil donors have variable growth rates in culture. When we quantitated the sample-specific infection efficiency from these images (GFP+ cells/total cells), the data show that fibroblasts are generally much less susceptible to infection compared to epithelial cells and that susceptibility of both cell types varies substantially based on tonsil donor (**Figure 4.3-2C**). These data suggest that, like our previous lymphocyte data (Aalam et al. 2020), donor-specific factors can influence KSHV infection in tonsil-derived primary cell lines.

In order to compare the production of KSHV from these cultures, we performed DNA isolation and qPCR analysis for KSHV genomes on clarified supernatants from infected cell cultures at 3 dpi. KSHV genomes per ml of culture supernatant were much higher for B cells compared to epithelial cells and fibroblasts (**Figure 4.3-2D**). When we corrected for the differing densities of cells at day 0, a very different picture emerges with fibroblasts displaying significantly higher and B cell significantly lower per-cell levels of KSHV DNA in culture supernatants (**Figure 4.3-2E**).
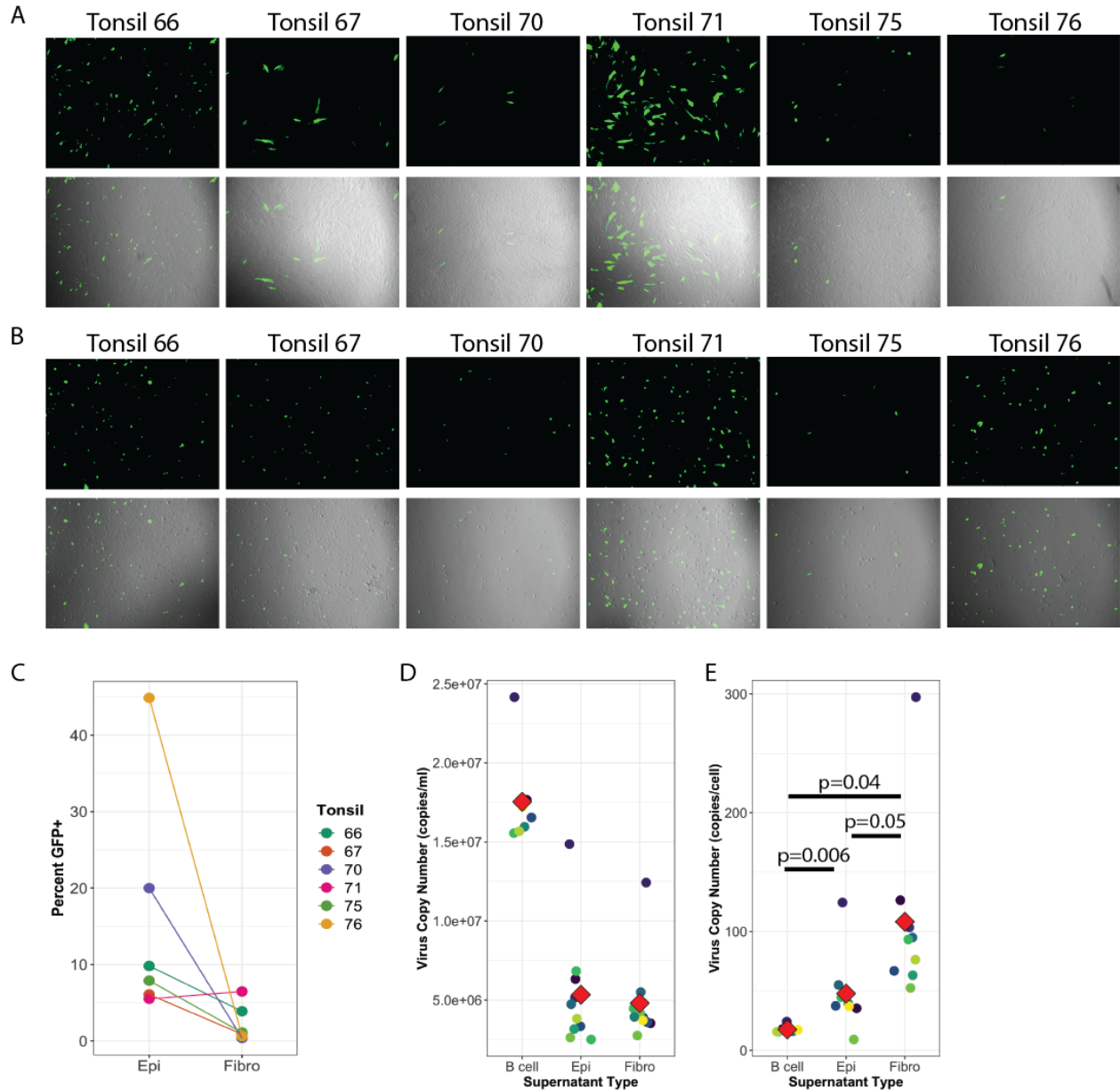
Figure 4.3-2. Susceptibility of tonsil-derived cell cultures to KSHV infection and estimation of productive infection.

Microscopy images taken at 4X magnification at 3 dpi for GFP (top panels) or merged GFP and white light images (bottom panels) of matched donor A) fibroblasts and B) epithelial cells infected with ID20 of BAC16 KSHV-WT. C) GFP quantification via cell counting from images in (A) and (B) D) Quantitation of genome copy number per ml of culture supernatant by qPCR for the GFP reporter cassette in the BAC16 genome E) Data as in (D) normalized to the starting cell number for each cell type. P-values for significance were derived using Student's T test. For panels D and E colors indicate unique tonsil specimens and can be compared between the panels.

122

4.3.3 **Transmission studies reveal B lymphocyte-derived virus has broad tropism**

We next performed a detailed set of experiments to examine the transmission of KSHV within and between cell types using epithelial cells, fibroblasts and B cells from the same tonsil donor. For these experiments, we had matched sets of all three cell types from 15 unique tonsil donors. An example of the experimental setup for epithelial cells is summarized in **Figure 4.3-3A** and analogous procedures were performed starting with fibroblasts and B cells for each tonsil specimen in the study. Briefly, donor cells were infected at the per cell ID20 dose from titration on fibroblasts and cultured for 3 days to establish infection. Recipient cultures were thawed (for lymphocytes) or trypsinized (for epithelial and fibroblast) at 3 dpi, and directly mixed with donor cells for epithelial and fibroblast co-culture experiments or were allowed to adhere to dishes for three hours prior to the addition of lymphocytes or clarified supernatants from infected cultures. After a further three days of culture, recipient cultures/co-cultures were analyzed by flow cytometry to determine the transfer of infection. For epithelial/fibroblast co-cultures we utilized cell surface immunophenotyping to distinguish donor cells from recipient cells (**Figure 4.3-3B, right panels**). Interestingly, despite being CD44+ at the time of cell sorting, after culture, tonsil epithelial cells become CD44 low. Thus, in co-cultures epithelial cells are CD44-CD90- and fibroblasts are CD44+CD90+. The same immunophenotyping was used on cultures where supernatant was transferred to validate that results were not due to unintentional transfer of infected cells (**Figure 4.3-3B**, center panels). Within cell-type studies were performed only using transfer of clarified supernatants as donor/recipient cells would not be distinguishable in co-cultures for the same cell type. For B cell recipient cultures, adherent donor cells were left on the plate at analysis and surface staining for CD19 was used to identify only recipient B cells. In all cases, viability dyes were used to exclude dead cells from the analysis.
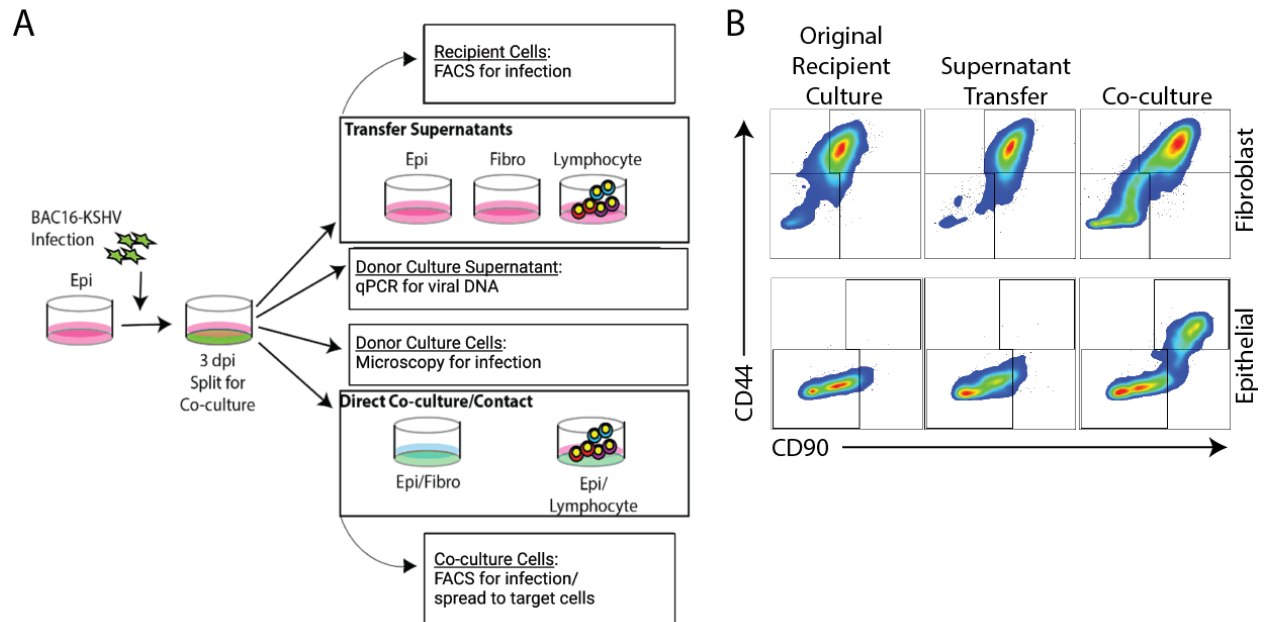
Figure 4.3-3. Experimental procedure for examining KSHV transfer between tonsil-derived cell types.

A) Schematic overview of experimental procedure. Epithelial cells (Epi) are used as donor cells in this example, but analogous experiments were performed with fibroblasts (Fibro) and lymphocytes as infected donors. **B)** Representative immunophenotypic analysis of fibroblast and epithelial cells before (left panels) and after co-culture (right panels) or supernatant transfer (center panels).

When we examined B cells as the recipient cell type for co-culture and supernatant transfer experiments, the data showed that both epithelial and fibroblast cultures can efficiently transfer infection to B cells in direct co-culture. Indeed, these infections were generally higher than what we observe using purified iSLK-derived virions at the same time point (Aalam et al. 2020). In contrast, supernatants were less effective at transferring infection to B cells. Indeed, only a few epithelial cell supernatants showed detectable B cell infection at 3 days post-transfer and fibroblast supernatants were uniformly unable to infect B cells (**Figure 4.3-4A**). These data indicate that efficient infection of B cells is possible from both epithelial and fibroblast cells but that cell-cell contact is needed for efficient transfer. Conversely, B cell-derived virus is able to infect both epithelial and fibroblast cells efficiently by both direct contact and supernatant transfer with epithelial cells notably more susceptible to infection from B cells compared to fibroblasts for both transfer methods. These results indicate that B cells produce cell-free virus that is able to efficiently infect both adherent cell types (**Figure 4.3-4 B&C**, left columns in panels).

4.3.4 **Fibroblast-derived KSHV is non-infectious to autologous fibroblasts**

When we examined fibroblasts as acceptor cells (**Figure 4.3-4B**), we observed that they are relatively refractory to infection by other tonsil cell types. We observed more frequent, but lower-level transfer from B cells and epithelial cells via supernatant transfer. The highest levels of infection in fibroblasts were obtained via direct co-culture with infected B cells. However, only a few samples displayed this behavior with the remaining samples remaining uninfected. These data further support our observation that, even in adherent cell types, donor-specific factors have some impact on susceptibility to KSHV infection. Interestingly, supernatant transfer from infected fibroblasts cultures was completely unable to infect both new fibroblast cultures and B cell cultures despite detectable KSHV DNA in these supernatants (**Figure 4.3-2D&E**) and the same

supernatants causing detectable infection in a subset of epithelial cell cultures (**Figure 4.3-4C**). This lack of spread within fibroblast cultures may also explain the overall low level of fibroblast infection we observed at 3dpi during de novo infection with iSLK-derived virions (**Figure 4.3-2C**), These data are consistent with the conclusion that tonsil fibroblasts produce KSHV virions that are selectively non-infectious to fibroblasts and B cells while being competent to infect epithelial cells.

4.3.5 **Fibroblast-epithelial transmission is unidirectional via cell-cell contact**

When we examined epithelial cells as acceptors in these experiments (**Figure 4.3-4C**), there was high transmission to epithelial cells from B cells and this high rate of transfer was consistent between both co-culture and supernatant transfer conditions. Interestingly, co-culture of epithelial cells with KSHV-infected fibroblasts resulted in high rates of transfer while fibroblast supernatants were much less efficient at infecting epithelial cells. It should be noted that recovery of viable epithelial cells was relatively poor after co-culture with fibroblasts, limiting the number of samples where we were able to obtain interpretable data. Finally, epithelial-derived supernatants reliably infected autologous epithelial cell cultures, although at relatively low rates compared to B cell supernatants.
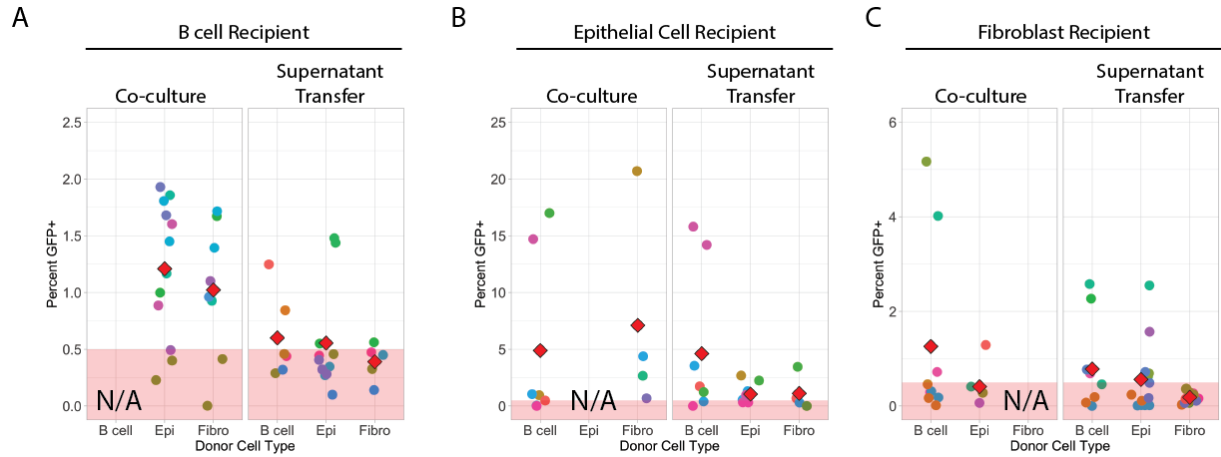
Figure 4.3-4. Transfer of KSHV between tonsil-derived cell types by direct contact or supernatant transfer.

Left panels are data from transfer via direct contact and right panels are data from transfer via clarified supernatant. Different data point colors represent the primary cell samples from each of 15 unique tonsil specimens and can be compared between panels in the figure and the red diamonds indicate mean value for each sample group. In all cases, the indicated donor cell types (x-axis) were from autologous tonsil specimens to **A)** recipient B cells**, B)** recipient epithelial cells and **C)** recipient fibroblasts. Red shading is set at 0.5% which is the limit of detection for this analysis. N/A indicates same cell-type co-culture which was not performed for this set of experiments.

4.4 **Discussion**

Despite KSHV being lymphotropic, KSHV infection of B cells has been generally inefficient without activation of B cells (S. Kang and Myoung 2017). While KSHV seems to replicate poorly in B cells and *de novo* infection of B lymphocytes results in predominantly latent infection of B cells (Hassman, Ellison, and Kedes 2011; Myoung and Ganem 2011b; Aalam et al. 2020), our previous work has shown that some B cell subsets can undergo lytic replication and that donor-dependent factors exert a strong influence on lytic replication in our tonsil lymphocyte culture system (Aalam et al. 2020). We generally obtain less than 2% infection at 3 dpi in tonsil specimens, and on a per-cell basis in this study B cell supernatants contain much less KSHV DNA compared to fibroblast and epithelial cell cultures. Despite this, B cell-derived supernatants can effectively infect epithelial cells and they produce a higher level of infection of autologous B cells compared to *de novo* infection with purified, iSLK-derived virions (**Figure 4.3-4A&B**). These results may indicate that B cell-derived virus is either more infectious to B cells based on a unique virion composition or that KSHV infection of B cells is associated with the secretion of soluble factors which increase the efficiency of KSHV transmission within and between B cells. Further studies are needed to determine if this second hypothesis is true and whether soluble factors play a substantial role in the initial spread of KSHV within the lymphocyte compartment.

Our results are contrary to the directed transmission of EBV that epithelial-derived virions more efficiently infect B cells than B cell derived-virions (Borza and Hutt-Fletcher 2002). A combination of gH/gL and gp42 in virion formation is required for EBV entry into B lymphocytes and the interaction of gp42 and HLA II is necessary for this entry process. While HLA II processing in B lymphocytes affects the integration of gp42 into the nascent virions, these virions are ineffective in infection of B cells as opposed to the epithelial-derived virions (Borza and Hutt-

Fletcher 2002). By contrast, KSHV infection of B cells results in down regulation of MHC I (Rappocciolo et al. 2008) and MHC II (Schmidt, Wies, and Neipel 2011). It remains to be determined whether the differences we observe are a result of differential virion composition or other factors, but our data indicate that KSHV differs substantially compared to EBV in this regard.

On the other hand, KSHV gH/gL is indispensable for the infection of epithelial and fibroblast cells, but it is not necessary for the infection of B cells (Muniraju et al. 2019), as alternative entry mechanisms exist (Palmerin et al. 2021). Furthermore, KSHV glycoproteins K8.1A, which is thought to be a B cell tropism determinant, is dispensable for the infection of other cell types (Dollery et al. 2019). K8.1 shares no homology with gp42 of EBV and it is transcribed from the gene positionally homologous to BLLF1 gene of EBV encoding for gp350/220 and positional homologs of BLLF1 gene of EBV in some human and non-human herpesviruses encode for glycoproteins resulted from alternative splicing and implicated in the tropism switch between different cell types (Stewart et al. 1996; Hutt-Fletcher 2007; Machiels et al. 2011, 2013). Therefore, the fact that fibroblast-derived virions were not infectious and direct contact is the only efficient mode of transmission from fibroblasts to the other cells could imply that fibroblasts may tamper with the processing and splicing of some glycoproteins.

Our observation that the effectiveness of KSHV transmission from epithelial cells to B lymphocytes increases with the direct contact (**Figure 4.3-4A**) is not surprising. Our infection methodology uses iSLK derived cell free virions that generally results in less than 2% infection at 3dpi in tonsil-derived B cells (Aalam et al. 2020). However, it has previously been shown that co-culturing B cells with iSLK, which are an epithelial carcinoma cell line, yields better infection efficiency than cell-free virions (Großkopf et al. 2019; Bekerman et al. 2013)

Mature surface epithelial cells of the oral cavity are difficult to infect and it has been hypothesized that efficient entry for EBV and HPV may require access to deeper layers of epithelium via wounding (Temple et al. 2014; Temple, Meyers, and Sample 2017; Roberts et al. 2007; S. Y. C. Kang et al. 2015). However, the tonsillar crypts represent a unique niche where the epithelial layers are thin and interspersed with B cells that may be able to directly interact with external antigens (S. Y. C. Kang et al. 2015; Perry and Whyte 1998). Given that CD44+NGFR+ epithelial progenitors are located at the crypt lumen of tonsil (Kang et al. 2015), and our data presented in this study show that these cells are highly susceptible to infection without need for any activation or other aid to viral entry. Thus, we speculate that crypt epithelium, along with the resident B lymphocytes, can be directly infected by KSHV present in oropharyngeal secretions. It has been demonstrated that KSHV lytic activation resulting from epithelial cell differentiation into keratinocytes contributes to viral production (Johnson, Maronian, and Vieira 2005) while, our culturing system avoided the differentiation of epithelial cells by addition of ROCK inhibitor, it is possible that differentiation of infected epithelial cells located at the basal layer and their transmission to the outer layers of epithelial cells sheds virus into saliva (Seifi et al. 2011). However, we showed that these epithelial cell derived virions are not as effective as B cell derived virions in infection of the epithelial cells residing at the crypt lumen (**Figure 4.3-4C**), indicating that differentiation of infected cells likely plays a larger role than spread of infection within the epithelial cell layers of the tissue.

We have previously shown that KSHV targets a variety of the tonsillar B cells, whether mature or immature; but plasma cells are a rare but highly targeted population and that infected plasma cells show a mixture of lytic and latent infection based on viral transcript analysis (Aalam et al. 2020). Moreover, KSHV infection of B cells derives their proliferation and differentiation (Hassman,

130

Ellison, and Kedes 2011) into plasma cell-like phenotypes. Our current results show that B cell-derived KSHV is highly infectious to both B cells and other cell types. Co-culture experiments demonstrate that B cells are a likely amplification point for KSHV. Moreover, we would speculate from the infectivity of B cell supernatants that B cell derived virions produced at the tonsil crypt, where epithelial cells do not form a significant barrier, may contribute to KSHV viral shedding into saliva.

Fibroblasts play a major role in enhancement of tumor progression, angiogenesis and tumor invasiveness (Crawford et al. 2009; Mueller et al. 2007). KSHV infected fibroblasts are also known to contribute to KS pathogenesis (Akula et al. 2003; Qin et al. 2011; Dai et al. 2012). However, their role in KSHV transmission and propagation within tonsillar cells have not been characterized. Our data indicates that fibroblast-derived cell-free virus is poorly infectious to B cells and epithelial cells, making it unlikely that fibroblasts play a large role in the release of KSHV virions into saliva. However, fibroblasts can efficiently infect both B cells and epithelial cells via direct contact. These results imply that there is an uncharacterized mechanism of KSHV spread that requires direct contact. This will be an important mechanism to unravel in future studies. Previous studies have shown that KSHV establishes latent infection in oral fibroblast cells and confers the tumor-associated fibroblast phenotype to these cells, enhancing the KS microenvironment (Dai et al. 2012). Interestingly, tonsillar progenitor mesenchymal cells (TMPC), have spindle fibroblast-like morphology and express CD44 and CD90 surface markers and are immunosuppressive by inhibition of T cell proliferation (Janjanin et al. 2008). Thus, although fibroblasts may play a minor role in KSHV dissemination, their targeting may have a role to play in KSHV persistence and pathogenesis.

We believe these data are among the first evidence that KSHV utilizes directed mechanisms for cell-to-cell spread within tissues, and we have developed a working model from these results as a starting place for understanding how KSHV may invade tonsil tissues and gain access to the lymphocyte compartment (**Figure 4.4-1**). Future studies that include both blood vascular and lymphatic endothelial cells derived from tonsil are important and will certainly add critical information about how KSHV accesses the vasculature to this model. Based on the extensive literature for EBV and other herpesviruses, we hypothesize that, at least for cell-free virions, this directed spread is accomplished by differential glycoprotein compositions in virions derived from different cell types. Our group has recently updated the KSHV virion proteome from iSLK cells, and we detected some additional proteins incorporated into KSHV virions (Nabiee et al. 2020) that were not detected by previous studies using PEL-derived virions (Bechtel, Winant, and Ganem 2005; Zhu et al. 2005). This raises the question of whether these differences are as a result of producer cell line variations, implementation of different methodologies, or both. Indeed, KSHV induction of cellular transcription profile is unique and cell line specific, affecting many cellular processes ranging from immune modulation, cell cycle regulation and angiogenesis (Naranatt et al. 2004). Future studies examining the protein composition of virions from different producer cell types are certainly warranted by our results. However, feasibility will be an issue with these studies as obtaining sufficient purified virions from primary cell cultures for proteomic analysis will be challenging.
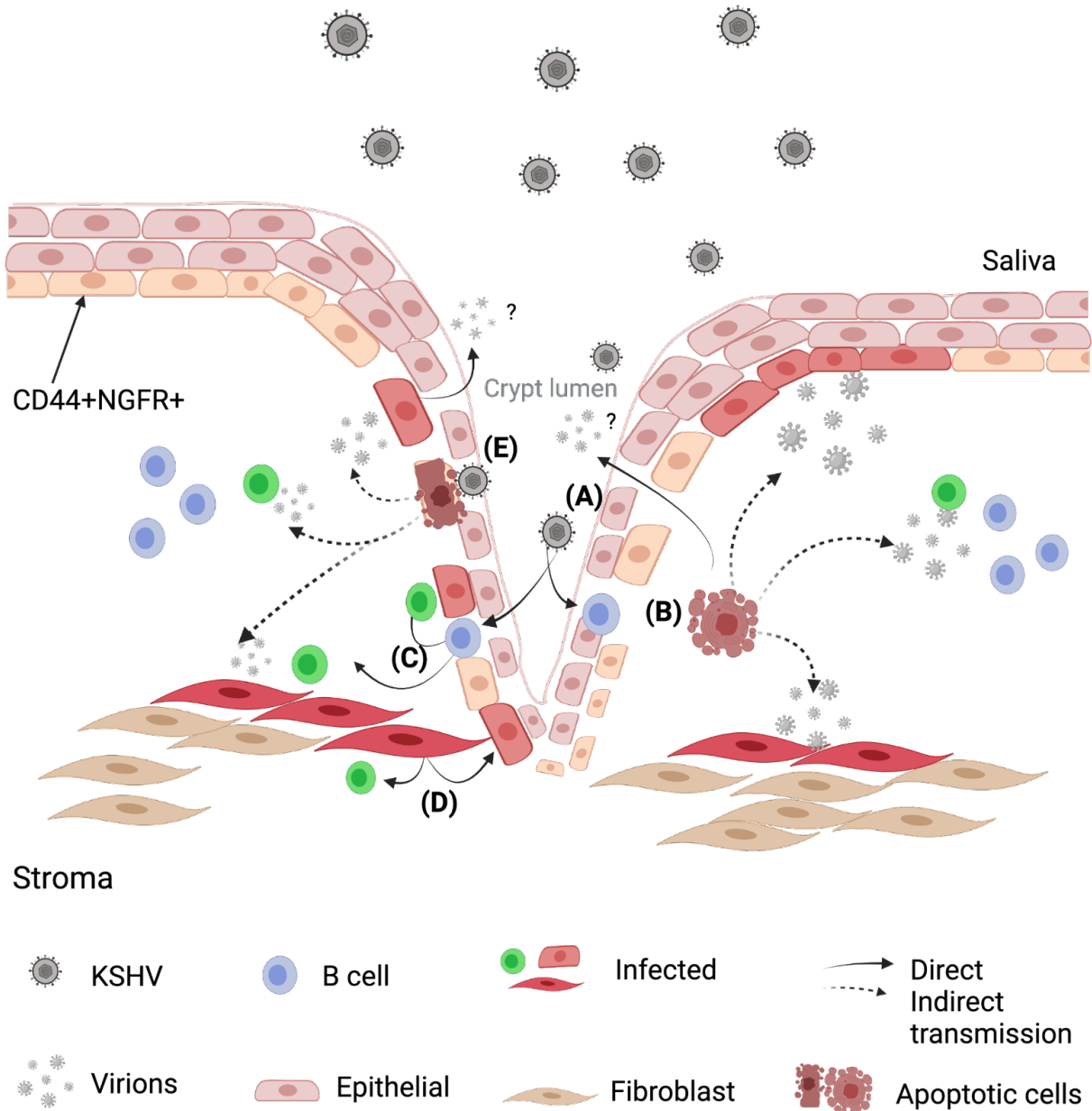
Figure 4.4-1. Schematic overview of KSHV entrance, egress, and transmission via cryptic lumen of tonsil

At the crypt lumen, where the reticulated epithelium is interspersed with the lymphocytes, B cells can readily interact with the external antigens. When KSHV enters the crypt lumen; It directly infects B cells **(A)** and epithelial cells **(E).** The infected B cells transmit KSHV to epithelial, fibroblast and other B cells by cell-free virions **(B)** and direct contact with the epithelial and fibroblast cells **(C).** The infected fibroblasts can transmit KSHV to the neighboring B cells and epithelial cells by direct contact only **(D)** Directly infected epithelial cells infect B cells, fibroblasts and other epithelial cells by cell-free virions **(E).**

5 CHAPTER V: Conclusions and Future Directions

Despite nearly three decades of research, many fundamental questions remain about KSHV biology. In this dissertation, we explored the early dynamics and B cell subset-specific tropism of KSHV infection in tonsil specimens, examined KSHV entry mechanisms in B lymphocytes, and evaluated the dynamics of transmission within and between some primary tonsillar cells. We have developed a robust model for KSHV infection in human tonsil lymphocytes that recapitulates the total lymphocyte environment and used it to uncover biologically relevant mechanisms that inform our understanding of KSHV transmission and the initial establishment of KSHV infection in a new human host. Moreover, we have developed novel tonsil-derived primary cell cultures that can be used for studying KSHV infection of other primary cells to monitor the behavior of KSHV as it enters the tonsil tissue. It should be noted that the tonsil specimens used in these studies were removed due to either sleep apnea or tonsillitis conditions. Consequently, the immunological composition and T cell activation of these samples could be perturbed due to inflammation (Geißler et al. 2020). Studies have shown that acute tonsillitis induces a weaker T cell receptor stimulation response (Boomer et al. 2012; Geißler et al. 2017) and this T cell response has a distinctive signature in local vs. chronic tonsillitis cases (Geißler et al. 2017). While we did not include any self-reported viral infection or pathological conditions, KSHV susceptibility of our samples could be affected by viral and/or bacterial co-pathogens, and commensal microbe populations. Recent studies propose that the oral microbiome can strongly influence KSHV biology and virulence (Yu et al. 2014; Dai et al. 2014). Importantly, household transmission studies in Africa strongly indicate that establishment of KSHV infection may require an inflamed microenvironment as KSHV seroconversion young children often happens immediately following

exposure to a different pathogen (Gantt et al. 2016). If this is the case, the baseline inflammatory state of tonsil lymphocytes may be one reason the mode is so successful compared to peripheral blood B cells, which are generally refractory. Furthermore, KSHV pathogenesis is frequently associated with co-infection with EBV and HIV (da Siva and de Oliveira, 2011), considering the high prevalence of herpes virus infections within human population (Boppana and Fowler 2007), it is highly likely that most of our samples were infected with at least one of these micro-organisms. Thus, in future, our lab plans to perform metagenomic sequencing of the samples to correlate microbial taxa and other viral infections that may influence susceptibility to KSHV infection. Hence, our results lay a foundation for future investigation of KSHV pathology within lymphocyte compartment. The significant findings of our studies and conclusions of each chapter with suggested future directions are presented below.

5.1 KSHV tropism in B lymphocyte compartment

Although KSHV is a lymphotropic herpesvirus, there is sparse data regarding KSHV infection of primary B lymphocytes. Only a small number of previous studies analyzed primary B lymphocyte targets of KSHV and these used limited markers to identify specific B cell subtypes (Rappocciolo et al. 2008; Hassman, Ellison, and Kedes 2011; Totonchy et al. 2018; Nicol et al. 2016; Knowlton et al. 2014). Therefore, to fill this gap, we aimed to establish KSHV B lymphocyte tropism by analyzing the B lymphocyte lineages targeted by KSHV early during *de novo* infection.

Using a comprehensive panel of antibodies, we first generated a library of lymphocyte specimens from 40 human tonsils and evaluated the level of B and T lymphocyte lineages at the baseline. We demonstrated that tonsillar lymphocytes varied in composition among donors and overall B cell frequencies declined with age as did germinal center, plasmablast and transitional B cell lineages.

However, memory and naïve populations increased in frequency as the age increased. Similarly, among T cell lineages, the level of CD4+ transitional memory and CD8+ terminal effector lineages declined with age.

In order to determine which B cell lineages were targeted by KSHV infection at early timepoints, we analyzed our data at 3 dpi and implemented a methodology for normalizing infectious dose from donor-to-donor. Our analysis showed that a variety of B lymphocyte subtypes are susceptible to KSHV infection and this susceptibility was independent of donors' demographic backgrounds. However, the donor-dependent immunological factors could be correlated with overall susceptibility. The ratio of CD4/CD8 T cells with the susceptibility of B lymphocytes to KSHV infection revealed no significant correlation, however, the levels of naïve and stem cell memory CD4+ T cells was positively correlated with infection of plasma cells with a larger effect on CD20+ plasma cells than CD20- plasma cells. We observed that the overall levels of CD45RO+ activated memory T cells were negatively correlated with KSHV infection of plasma cells and although not significantly, nearly every B cell lineage and KSHV infection in general was negatively correlated with the presence of CD4+ T cells expressing a TEMRA phenotype. Baseline levels of CD8+ T cells in turn, had less pronounced effect on overall KSHV infection but the level of CD8+ terminal effector cells was positively correlated with KSHV infection of naïve B cells.

Additionally, we have demonstrated that a variety of tonsillar B lymphocyte subsets are targeted at different frequencies, and CD138+ plasma cells are a highly targeted cell type in our *de novo* infection model. Indeed, plasma cells are terminally differentiated B cells and this phenotype is the characteristic of PEL and MCD cells (Chadburn et al. 2008; Carbone et al. 2010). Our results may suggest that KSHV has a particular tropism towards this population rather than KSHV driving differentiation of less mature B subtypes to plasma population, as was expected from the related

gammaherpesvirus EBV (Johnson and Tarakanova, 2020). We further showed that KSHV infection of CD138+ plasma cells and overall B cell infection is HSPGindependent and that the particular susceptibility of plasma cells is not due to KSHV using the CD138 HSPG as an attachment or entry factor.

Overall, our study generated a library of tonsil lymphocytes and data relevant to the B lymphocyte tropism of KSHV that can benefit both immunology and the KSHV research community. We have used our unique methodology for the extraction and infection of B lymphocytes that avoids B cell activation and our culture condition system did not significantly affect B cell population. Hence, further studies implementing our model system can be used to explore whether KSHV preferential targeting of plasma cells is due to abundance of any particular cellular KSHV entry receptor or as a result of rapid differentiation of other KSHV infected B cell lineages into plasma cells early in infection. To explore whether differentiation of less mature B lineages to plasma cells resulted in our finding, one approach could be the infection of each B cell lineage and then constituting it with total uninfected lymphocytes. Application of tracking dye on infected lineage before reconstitution allows for detection of differentiated lineage that may fall into the plasma gate at 3 days post infection.

Studies have shown that both the viral and human cytokines have a pronounced impact on the control and development of PEL and MCD (Foussat et al. 1999; Drexler et al. 1999; Calabrò et al. 2009; Aoki and Tosato 1999; Calabrò and Sarid 2018). Our observation that the immune status of individuals affects the course of infection can be further explored by analyzing the role of secreted cytokines in this microenvironment. Indeed, in our preliminary studies, we were able to show that the elevated level of some cellular interleukins are the major determinant of the refractory status of samples (data not shown). Interested readers are further encouraged to refer Alomari et al. 2021

(Appendix C) to explore our findings in this regard. Hence, studies can be conducted on determining the role of individual cytokines in promotion/prevention of KSHV transmission and infection in B lymphocytes and the influence of cytokines on the early targeting of plasma cells and other B cell subsets.

5.2 KSHV entry into B cells

KSHV entry into cells is a sequential process accomplished by the engagement of a variety of viral and cellular receptors (Connolly et al. 2011). As with all herpesviruses, entry mechanisms are highly complex and they are particularly poorly characterized for KSHV. In particular, the viral glycoproteins and cellular receptors utilized for KSHV entry into B cells have not been rigorously characterized, and, thus, the rudimentary question of how KSHV enters B cells remains to be answered. In the third chapter of this dissertation we investigated whether EphA2, A4 and A7 receptors in tonsil-derived B lymphocytes are used as entry receptors by KSHV, and whether this interaction is gH/gL complex-dependent. We showed that the distribution of tonsillar EphA receptors varies within B cell lineages and between donors. Indeed, the different results in neutralization of the cellular EphA receptors and the virion glycoproteins using soluble EphA mimics support the conclusion that gH/gL/EphA interactions are important for KSHV entry into B cells. In the cell neutralization scenario, when the EphA receptor is engaged with the ephrin-A2 ligand, the gH/gL interaction with EphA receptor is prevented in KSHV-WT and in the case of virus neutralization with the soluble EphA receptors, the engagement of the gH/gL in WT leaves the other WT-gps available to engage alternate mechanisms for entry into B cells. Our neutralization experiments indicated that gH/gL-EphA interactions are important for KSHV-WT infection of primary tonsil lymphocytes, but that KSHV-ΔgH implements different entry mechanisms, independent of EphA receptors. Our results further indicated that KSHV entry into

plasma cells and germinal center cells is strictly gH/gL/EphA-dependent. However, we were unable to specifically distinguish which EphA receptors used by the gH/gL complex in our cell neutralization experiments, as ephrin-A2 binds to multiple EphA receptors. Nevertheless, previous studies indicated that gH/gL complex binds to EphA2, A4, and A7 with the different affinities. However, our virion neutralization experiments detected no difference in the manner of neutralization across all three (EphA2, EphA4, and EphA7), with no significant effect on inhibition of KSHV entry. Therefore, based on the neutralization experiment results, there could be some other EphA receptors involved in KSHV entry that were not specifically addressed in our study. Remarkably, the EphA family of receptors exploit a variety of ephrin-ligand interactions with different avidities and sometimes one type ephrinA ligand is able to inhibit various EphA receptors with the same affinity (Darling and Lamb 2019). Therefore, distinction of the type of EphA receptor involved in the context of KSHV infection of B lymphocytes is impossible with our current knowledge. For future studies, use of selective inhibitors of each of the EphA receptors would be a suitable strategy, if there are any.

The different response in KSHV-ΔgH vs. KSHV-WT neutralization experiment shows that in the absence of gH/gL complex, KSHV can exploit different mechanisms of entry. Thus, for future studies, we propose to combine glycoprotein mutants with experiments employing specific anti-gp neutralizing antibodies in the context of KSHV-WT in order to dissect the functional interactions more carefully and obtain a clearer picture of how KSHV entry might be targeted immunologically.

5.3 KSHV transmission within tonsillar compartment

In the previous chapters, we had characterized B cell tropism of KSHV and the primary cellular interactions involved in entry into B cells. We were interested to study KSHV transmission within primary cells of the tonsil (epithelial cell, fibroblast cells), and into B cells. To accomplish this, we took advantage of our library of matched adherent cell lines that are extracted together with lymphocytes from tonsil specimens in our laboratory.

We used CD44+NGFR+ epithelial progenitor cells that are present at higher density at the basal layer and in the crypt area of the tonsil (Kang et al. 2015) and the fibroblast cells with progenitor mesenchymal cells (TMPC) characteristic phenotype (Janjanin et al. 2008). We demonstrated that primary epithelial and fibroblast cells display variable susceptibilities towards KSHV infection when infected with the same dose of a KSHV-BAC16 stock.

We observed that tonsil fibroblast-derived virions were ineffective in dissemination of KSHV between other cell types, but fibroblasts could efficiently transmit the virus via direct contact to both B lymphocytes and epithelial cells. Considering the important role of fibroblasts in enhancement of tumor progression, angiogenesis and tumor invasiveness (Crawford et al. 2009; Mueller et al. 2007) and in KS pathogenesis (Shaw M Akula et al. 2003; Qin et al. 2011; Dai et al. 2012), their targeting may have a role to play in KSHV persistence and pathogenesis in oral cavity. Nevertheless, presence of other biological factors in the supernatants may have interfered with the infectivity of our virions. Fibroblasts actively participate in cytokine production and extracellular vesicles secretion to control a variety of normal and pathological conditions (Bartekova et al. 2018; Oh et al. 2021; Kadota et al. 2020). Therefore, future studies can focus on the putative role of fibroblast-secreted cytokines and extracellular vesicles on prevention/promotion of KSHV spread in the oral cavity.

Our results indicated that epithelial-derived virions are infectious to other epithelial cells and B cells, however unlike what is reported for EBV (Borza and Hutt-Fletcher 2002), B cell-derived virions efficiently infect epithelial cells and, surprisingly, they infect B cells more strongly than purified virions. Indeed, our data indicate that B cells are universal donors for infection and they can be efficiently infected via direct contact. The mechanism of directed transmission for EBV is differential virion composition arising from different cell types, as a result of glycoprotein processing of HLA II (Borza and Hutt-Fletcher 2002). However, the current knowledge of KSHV implies that MHCI and II are downregulated in B cells (Rappocciolo et al. 2008; Schmidt, Wies, and Neipel 2011); therefore, it is unlikely that KSHV employs similar mechanisms for production of virions with unique glycoprotein configurations. However, our data indicate that KSHV may employ alternative, as yet uncharacterized mechanisms to accomplish the same goal. For example, differential protein expression affecting the virion composition may arise due to incorporation of different splice variants of the glycoproteins such as K8.1 into the virions. Hence, further studies are encouraged exploring the proteomics of virions prepared from different producer cell lines. Finally, here we propose that the inefficiency of B cell infection could be as a result of virions derived from epithelial producer cell-lines. Therefore, it would be interesting to compare the efficiency of different producer cell-line derived virions in infection of B lymphocytes and their effect on targeting specific B cell lineages.

Lastly, although they are a disease-relevant cell type important for KSHV biology, we failed to include endothelial cells in this data due to ongoing issues with fibroblast contamination in primary endothelial cell cultures which would have invalidated our conclusions from transmission studies. Hence, future studies with the inclusion of pure vascular and lymphatic endothelial cells into our

tonsillar transmission model system, will be needed to uncover how KSHV is transmitted into the lymphatic vasculature.

References

Aalam, Farizeh, Romina Nabiee, Jesus Ramirez Castano, and Jennifer Totonchy. 2020. "Analysis of KSHV B Lymphocyte Lineage Tropism in Human Tonsil Reveals Efficient Infection of CD138+ Plasma Cells." *PLoS Pathogens* 16 (10): e1008968. https://doi.org/10.1371/journal.ppat.1008968.

Abere, Bizunesh, Jinghui Li, Hongzhao Zhou, Tuna Toptan, Patrick S Moore, and Yuan Chang. 2020. "Kaposi's Sarcoma-Associated Herpesvirus-Encoded CircRNAs Are Expressed in Infected Tumor Tissues and Are Incorporated into Virions." MBio 11 (1). https://doi.org/10.1128/mBio.03027-19.

Ablashi, Dharam, Henri Agut, Roberto Alvarez-Lafuente, Duncan A Clark, Stephen Dewhurst, Dario DiLuca, Louis Flamand, et al. 2014. "Classification of HHV-6A and HHV-6B as Distinct Viruses." *Archives of Virology* 159 (5): 863–70. https://doi.org/10.1007/s00705-013-1902-5.

Adler, Lital N, Wei Jiang, Kartik Bhamidipati, Matthew Millican, Claudia Macaubas, Shu-Chen Hung, and Elizabeth D Mellins. 2017. "The Other Function: Class II-Restricted Antigen Presentation by B Cells." *Frontiers in Immunology* 8: 319. https://doi.org/10.3389/fimmu.2017.00319.

Akula, S M, F Z Wang, J Vieira, and B Chandran. 2001. "Human Herpesvirus 8 Interaction with Target Cells Involves Heparan Sulfate." Virology 282 (2): 245–55. https://doi.org/10.1006/viro.2000.0851.

Akula, S M, N P Pramod, F Z Wang, and B Chandran. 2001. "Human Herpesvirus 8 Envelope-Associated Glycoprotein B Interacts with Heparan Sulfate-like Moieties." Virology 284 (2): 235–49. https://doi.org/10.1006/viro.2001.0921.

Akula, Shaw M, Naranatt P Pramod, Fu Zhang Wang, and Bala Chandran. 2002. "Integrin Alpha3beta1 (CD 49c/29) Is a Cellular Receptor for Kaposi's Sarcoma-Associated Herpesvirus (KSHV/HHV-8) Entry into the Target Cells." Cell 108 (3): 407–19. https://doi.org/10.1016/s0092-8674(02)00628-1.

Akula, Shaw M, Pramod P Naranatt, Neelam-Sharma Walia, Fu-Zhang Wang, Barbara Fegley, and Bala Chandran. 2003. "Kaposi's Sarcoma-Associated Herpesvirus (Human Herpesvirus 8) Infection of Human Fibroblast Cells Occurs through Endocytosis." *Journal of Virology* 77 (14): 7978–90. https://doi.org/10.1128/jvi.77.14.7978-7990.2003.

Alomari, Nedaa, and Jennifer Totonchy. 2020. "Cytokine-Targeted Therapeutics for KSHV-Associated Disease." Viruses 12 (10). https://doi.org/10.3390/v12101097.

Alonso-C, Luis M, Eva M A Trinidad, Beatriz de Garcillan, Monica Ballesteros, Milagros Castellanos, Ignacio Cotillo, Juan J Muñoz, and Agustin G Zapata. 2009. "Expression Profile of Eph Receptors and Ephrin Ligands in Healthy Human B Lymphocytes and Chronic Lymphocytic Leukemia B-Cells." *Leukemia Research* 33 (3): 395–406. https://doi.org/10.1016/j.leukres.2008.08.010.

Andrade, R P de. 1989. "A Multicenter Clinical Evaluation of a New Monophasic Combination: Minulet (Gestodene and Ethinyl Estradiol)." *International Journal of Fertility* 34 Suppl (September): 22–30.

Andreoni, Massimo, Loredana Sarmati, Emanuele Nicastri, Gamal El Sawaf, Mahmoud El Zalabani, Ilaria Uccella, Roberto Bugarini, Saverio G Parisi, and Giovanni Rezza. 2002. "Primary Human Herpesvirus 8 Infection in Immunocompetent Children." *JAMA* 287 (10): 1295–1300. https://doi.org/10.1001/jama.287.10.1295.

Aneja, Kawalpreet K, and Yan Yuan. 2017. "Reactivation and Lytic Replication of Kaposi's Sarcoma-Associated Herpesvirus: An Update." *Frontiers in Microbiology* 8: 613. https://doi.org/10.3389/fmicb.2017.00613.

Antinone, Sarah Elizabeth, and Gregory Allan Smith. 2010. "Retrograde Axon Transport of Herpes Simplex Virus and Pseudorabies Virus: A Live-Cell Comparative Analysis." *Journal of Virology* 84 (3): 1504–12. https://doi.org/10.1128/JVI.02029-09.

Aoki, Y, and G Tosato. 1999. "Role of Vascular Endothelial Growth Factor/Vascular Permeability Factor in the Pathogenesis of Kaposi's Sarcoma-Associated Herpesvirus-Infected Primary Effusion Lymphomas." *Blood* 94 (12): 4247–54.

Bacon, Chris M, Robert F Miller, Mahdad Noursadeghi, Christopher McNamara, Ming-Qing Du, and Ahmet Dogan. 2004. "Pathology of Bone Marrow in Human Herpes Virus-8 (HHV8)-Associated Multicentric Castleman Disease." British Journal of Haematology 127 (5): 585–91. https://doi.org/10.1111/j.1365-2141.2004.05230.x.

Barozzi, P, M Luppi, L Masini, R Marasca, M Savarino, M Morselli, M G Ferrari, M Bevini, G Bonacorsi, and G Torelli. 1996. "Lymphotropic Herpes Virus (EBV, HHV-6, HHV-8) DNA Sequences in HIV Negative Castleman's Disease." *Clinical Molecular Pathology* 49 (4): M232-5. https://doi.org/10.1136/mp.49.4.m232.

Barrett, Lindsey, Jungang Chen, Lu Dai, Karlie Plaisance-Bonstaff, Luis Del Valle, and Zhiqiang Qin. 2020. "Role of Interleukin-1 Family Members and Signaling Pathways in KSHV Pathogenesis." *Frontiers in Cellular and Infection Microbiology* 10: 587929. https://doi.org/10.3389/fcimb.2020.587929.

Bartekova, Monika, Jana Radosinska, Marek Jelemensky, and Naranjan S Dhalla. 2018. "Role of Cytokines and Inflammation in Heart Function during Health and Disease." *Heart Failure Reviews* 23 (5): 733–58. https://doi.org/10.1007/s10741-018-9716-x.

Bechtel, Jill T, Richard C Winant, and Don Ganem. 2005. "Host and Viral Proteins in the Virion of Kaposi's Sarcoma-Associated Herpesvirus." *Journal of Virology* 79 (8): 4952–64. https://doi.org/10.1128/JVI.79.8.4952-4964.2005.

Bechtel, Jill T, Yuying Liang, Joshua Hvidding, and Don Ganem. 2003. "Host Range of Kaposi's Sarcoma-Associated Herpesvirus in Cultured Cells." Journal of Virology 77 (11): 6474–81. https://doi.org/10.1128/jvi.77.11.6474-6481.2003.

Bekerman, Elena, Diana Jeon, Michele Ardolino, and Laurent Coscoy. 2013. "A Role for Host Activation-Induced Cytidine Deaminase in Innate Immune Defense against KSHV." *PLoS Pathogens* 9 (11): e1003748. https://doi.org/10.1371/journal.ppat.1003748.

Bella, Silvia Della, Adriano Taddeo, Elena Colombo, Lucia Brambilla, Monica Bellinvia, Fabrizio Pregliasco, Monica Cappelletti, Maria Luisa Calabrò, and Maria Luisa Villa. 2010. "Human Herpesvirus-8 Infection Leads to Expansion of the Preimmune/Natural Effector B Cell Compartment." PloS One 5 (11): e15029. https://doi.org/10.1371/journal.pone.0015029.

Bhutani, Manisha, Mark N Polizzotto, Thomas S Uldrick, and Robert Yarchoan. 2015. "Kaposi Sarcoma-Associated Herpesvirus-Associated Malignancies: Epidemiology, Pathogenesis, and Advances in Treatment." Seminars in Oncology 42 (2): 223–46. https://doi.org/10.1053/j.seminoncol.2014.12.027.

Birkmann, A, K Mahr, A Ensser, S Yağuboğlu, F Titgemeyer, B Fleckenstein, and F Neipel. 2001. "Cell Surface Heparan Sulfate Is a Receptor for Human Herpesvirus 8 and Interacts with Envelope Glycoprotein K8.1." Journal of Virology 75 (23): 11583–93. https://doi.org/10.1128/JVI.75.23.11583-11593.2001.

Blackbourn, D J, E Lennette, B Klencke, A Moses, B Chandran, M Weinstein, R G Glogau, et al. 2000. "The Restricted Cellular Host Range of Human Herpesvirus 8." AIDS (London, England) 14 (9): 1123–33. https://doi.org/10.1097/00002030-200006160-00009.

Boer, Esther C W de, Janine M van Gils, and Marit J van Gils. 2020. "Ephrin-Eph Signaling Usage by a Variety of Viruses." *Pharmacological Research* 159 (September): 105038. https://doi.org/10.1016/j.phrs.2020.105038.

Boppana, Suresh B, and Karen B Fowler. 2007. "Persistence in the Population: Epidemiology and Transmisson." In , edited by Ann Arvin, Gabriella Campadelli-Fiume, Edward Mocarski, Patrick S Moore, Bernard Roizman, Richard Whitley, and Koichi Yamanishi. Cambridge.

Boppana, Suresh B, and Karen B Fowler. 2007. "Persistence in the Population: Epidemiology and Transmisson." In , edited by Ann Arvin, Gabriella Campadelli-Fiume, Edward Mocarski, Patrick S Moore, Bernard Roizman, Richard Whitley, and Koichi Yamanishi. Cambridge.

Borza, Corina M, and Lindsey M Hutt-Fletcher. 2002. "Alternate Replication in B Cells and Epithelial Cells Switches Tropism of Epstein-Barr Virus." *Nature Medicine* 8 (6): 594–99. https://doi.org/10.1038/nm0602-594.

145

Brander, C, T Suscovich, Y Lee, P T Nguyen, P O'Connor, J Seebach, N G Jones, M van Gorder, B D Walker, and D T Scadden. 2000. "Impaired CTL Recognition of Cells Latently Infected with Kaposi's Sarcoma-Associated Herpes Virus." Journal of Immunology (Baltimore, Md. : 1950) 165 (4): 2077–83. https://doi.org/10.4049/jimmunol.165.4.2077.

Brandtzaeg, Per. 2015. "Immunobiology of the Tonsils and Adenoids." In *Mucosal Immunology*, 1985–2016. Elsevier.

Braun, D K, G Dominguez, and P E Pellett. 1997. "Human Herpesvirus 6." *Clinical Microbiology Reviews* 10 (3): 521–67. https://doi.org/10.1128/CMR.10.3.521.

Brayfield, Brad P, Chipepo Kankasa, John T West, Jubra Muyanga, Ganapati Bhat, Winslow Klaskala, Charles D Mitchell, and Charles Wood. 2004. "Distribution of Kaposi Sarcoma-Associated Herpesvirus/Human Herpesvirus 8 in Maternal Saliva and Breast Milk in Zambia: Implications for Transmission." *The Journal of Infectious Diseases* 189 (12): 2260–70. https://doi.org/10.1086/421119.

Buxmann, Horst, Klaus Hamprecht, Matthias Meyer-Wittkopf, and Klaus Friese. 2017. "Primary Human Cytomegalovirus (HCMV) Infection in Pregnancy." *Deutsches Arzteblatt International* 114 (4): 45–52. https://doi.org/10.3238/arztebl.2017.0045.

Calabrò, Maria Luisa, and Ronit Sarid. 2018. "Human Herpesvirus 8 and Lymphoproliferative Disorders." *Mediterranean Journal of Hematology and Infectious Diseases* 10 (1): e2018061. https://doi.org/10.4084/MJHID.2018.061.

Calabrò, Maria Luisa, Paola Gasperini, Iole Maria Di Gangi, Stefano Indraccolo, Massimo Barbierato, Alberto Amadori, and Luigi Chieco-Bianchi. 2009. "Antineoplastic Activity of Lentiviral Vectors Expressing Interferon-Alpha in a Preclinical Model of Primary Effusion Lymphoma." *Blood* 113 (19): 4525–33. https://doi.org/10.1182/blood-2008-09-180307.

Carbone, Antonino, Emanuela Vaccher, Annunziata Gloghini, Liron Pantanowitz, Akin Abayomi, Paolo de Paoli, and Silvia Franceschi. 2014. "Diagnosis and Management of Lymphomas and Other Cancers in HIV-Infected Patients." Nature Reviews. Clinical Oncology 11 (4): 223–38. https://doi.org/10.1038/nrclinonc.2014.31.

Carbone, Antonino, Ethel Cesarman, Annunziata Gloghini, and Hans G Drexler. 2010. "Understanding Pathogenetic Aspects and Clinical Presentation of Primary Effusion Lymphoma through Its Derived Cell Lines." *AIDS (London, England)*. https://doi.org/10.1097/QAD.0b013e3283365395.

Caserta, M T, D J Mock, and S Dewhurst. 2001. "Human Herpesvirus 6." *Clinical Infectious Diseases : An Official Publication of the Infectious Diseases Society of America* 33 (6): 829–33. https://doi.org/10.1086/322691.

Casper, Corey, Elizabeth Krantz, Stacy Selke, Steven R Kuntz, Jie Wang, Meei-Li Huang, John S Pauk, Lawrence Corey, and Anna Wald. 2007. "Frequent and Asymptomatic Oropharyngeal Shedding of Human Herpesvirus 8 among Immunocompetent Men." *The Journal of Infectious Diseases* 195 (1): 30–36. https://doi.org/10.1086/509621.

Casper, Corey, Mary Redman, Meei-Li Huang, John Pauk, Thomas M Lampinen, Stephen E Hawes, Cathy W Critchlow, et al. 2004. "HIV Infection and Human Herpesvirus-8 Oral Shedding among Men Who Have Sex with Men." *Journal of Acquired Immune Deficiency Syndromes (1999)* 35 (3): 233–38. https://doi.org/10.1097/00126334-200403010-00003.

Castillo, Jorge J, Brady E Beltran, Roberto N Miranda, Semra Paydas, Eric S Winer, and James N Butera. 2011. "Epstein-Barr Virus-Positive Diffuse Large B-Cell Lymphoma of the Elderly: What We Know so Far." *The Oncologist* 16 (1): 87–96. https://doi.org/10.1634/theoncologist.2010-0213.

Castleman, B, L Iverson, and V P Menendez. 1956. "Localized Mediastinal Lymphnode Hyperplasia Resembling Thymoma." *Cancer* 9 (4): 822–30. https://doi.org/10.1002/1097-0142(195607/08)9:4<822::aid-cncr2820090430>3.0.co;2-4.

Cerimele, F, F Curreli, S Ely, A E Friedman-Kien, E Cesarman, and O Flore. 2001. "Kaposi's Sarcoma-Associated Herpesvirus Can Productively Infect Primary Human Keratinocytes and Alter Their Growth Properties." *Journal of Virology* 75 (5): 2435–43. https://doi.org/10.1128/JVI.75.5.2435-2443.2001.

Cesarman, E, Y Chang, P S Moore, J W Said, and D M Knowles. 1995. "Kaposi's Sarcoma-Associated Herpesvirus-like DNA Sequences in AIDS-Related Body-Cavity-Based Lymphomas." *The New England Journal of Medicine* 332 (18): 1186–91. https://doi.org/10.1056/NEJM199505043321802.

Chadburn, A, E M Hyjek, W Tam, Y Liu, T Rengifo, E Cesarman, and D M Knowles. 2008. "Immunophenotypic Analysis of the Kaposi Sarcoma Herpesvirus (KSHV; HHV-8)-Infected B Cells in HIV+ Multicentric Castleman Disease (MCD)." Histopathology 53 (5): 513–24. https://doi.org/10.1111/j.1365-2559.2008.03144.x.

Chagas, Cristiano Aparecido, Luiza Hayashi Endo, Eulália Sakano, Glauce Aparecida Pinto, Pierre Brousset, and José Vassallo. 2006. "Detection of Herpesvirus Type 8 (HHV8) in Children's Tonsils and Adenoids by Immunohistochemistry and in Situ Hybridization." International Journal of Pediatric Otorhinolaryngology 70 (1): 65–72. https://doi.org/10.1016/j.ijporl.2005.04.030.

Chakraborty, Sayan, Mohanan Valiya Veettil, Virginie Bottero, and Bala Chandran. 2012. "Kaposi's Sarcoma-Associated Herpesvirus Interacts with EphrinA2 Receptor to Amplify Signaling Essential for Productive Infection." *Proceedings of the National Academy of Sciences of the United States of America* 109 (19): E1163-72. https://doi.org/10.1073/pnas.1119592109.

Chan, Kah-Lok, Stephen Lade, H Miles Prince, and Simon J Harrison. 2016. "Update and New Approaches in the Treatment of Castleman Disease." *Journal of Blood Medicine* 7: 145–58. https://doi.org/10.2147/JBM.S60514.

Chandran, Bala. 2010. "Early Events in Kaposi's Sarcoma-Associated Herpesvirus Infection of Target Cells." *Journal of Virology* 84 (5): 2188–99. https://doi.org/10.1128/JVI.01334-09.

Chang, Heesoon, Lynn M Wachtman, Christine B Pearson, Jong-Soo Lee, Hye-Ra Lee, Steven H Lee, Jeffrey Vieira, Keith G Mansfield, and Jae U Jung. 2009. "Non-Human Primate Model of Kaposi's Sarcoma-Associated Herpesvirus Infection." *PLoS Pathogens* 5 (10): e1000606. https://doi.org/10.1371/journal.ppat.1000606.

Chang, Y, E Cesarman, M S Pessin, F Lee, J Culpepper, D M Knowles, and P S Moore. 1994. "Identification of Herpesvirus-like DNA Sequences in AIDS-Associated Kaposi's Sarcoma." *Science (New York, N.Y.)* 266 (5192): 1865–69. https://doi.org/10.1126/science.7997879.

Chen, Jia, Karthik Sathiyamoorthy, Xianming Zhang, Samantha Schaller, Bethany E Perez White, Theodore S Jardetzky, and Richard Longnecker. 2018. "Ephrin Receptor A2 Is a Functional Entry Receptor for Epstein-Barr Virus." *Nature Microbiology* 3 (2): 172–80. https://doi.org/10.1038/s41564-017-0081-7.

Chen, Jia, Xianming Zhang, Samantha Schaller, Theodore S Jardetzky, and Richard Longnecker. 2019. "Ephrin Receptor A4 Is a New Kaposi's Sarcoma-Associated Herpesvirus Virus Entry Receptor." *MBio* 10 (1). https://doi.org/10.1128/mBio.02892-18.

Chen, Tiansheng, and S David Hudnall. 2006. "Anatomical Mapping of Human Herpesvirus Reservoirs of Infection." *Modern Pathology : An Official Journal of the United States and Canadian Academy of Pathology, Inc* 19 (5): 726–37. https://doi.org/10.1038/modpathol.3800584.

Connolly, Sarah A, Julia O Jackson, Theodore S Jardetzky, and Richard Longnecker. 2011. "Fusing Structure and Function: A Structural View of the Herpesvirus Entry Machinery." *Nature Reviews. Microbiology* 9 (5): 369–81. https://doi.org/10.1038/nrmicro2548.

Crawford, Yongping, Ian Kasman, Lanlan Yu, Cuiling Zhong, Xiumin Wu, Zora Modrusan, Josh Kaminker, and Napoleone Ferrara. 2009. "PDGF-C Mediates the Angiogenic and Tumorigenic Properties of Fibroblasts Associated with Tumors Refractory to Anti-VEGF Treatment." *Cancer Cell* 15 (1): 21–34. https://doi.org/10.1016/j.ccr.2008.12.004.

Cunha, A M G, A Caterino-de-Araujo, S C B Costa, E Santos-Fortuna, N C A Boa-Sorte, M S Gonçalves, F F Costa, and B Galvão-Castro. 2005. "Increasing Seroprevalence of Human Herpesvirus 8 (HHV-8) with Age Confirms HHV-8 Endemicity in Amazon Amerindians from Brazil." *The Journal of General Virology* 86 (Pt 9): 2433–37. https://doi.org/10.1099/vir.0.81087-0.

Dai, Lu, Michael R DeFee, Yueyu Cao, Jiling Wen, Xiaofei Wen, Mairi C Noverr, and Zhiqiang Qin. 2014. "Lipoteichoic Acid (LTA) and Lipopolysaccharides (LPS) from Periodontal Pathogenic Bacteria Facilitate Oncogenic Herpesvirus Infection within Primary Oral Cells." *PloS One* 9 (6): e101326. https://doi.org/10.1371/journal.pone.0101326.

Dai, Lu, Yueyu Cao, Yihan Chen, Chris Parsons, and Zhiqiang Qin. 2014. "Targeting XCT, a Cystine-Glutamate Transporter Induces Apoptosis and Tumor Regression for KSHV/HIV-

Associated Lymphoma." Journal of Hematology & Oncology 7 (April): 30. https://doi.org/10.1186/1756-8722-7-30.

Dai, Lu, Zhiqiang Qin, Michael Defee, Bryan P Toole, Keith L Kirkwood, and Chris Parsons. 2012. "Kaposi Sarcoma-Associated Herpesvirus (KSHV) Induces a Functional Tumor-Associated Phenotype for Oral Fibroblasts." *Cancer Letters* 318 (2): 214–20. https://doi.org/10.1016/j.canlet.2011.12.019.

Damania, Blossom. 2004. "Oncogenic Gamma-Herpesviruses: Comparison of Viral Proteins Involved in Tumorigenesis." *Nature Reviews. Microbiology* 2 (8): 656–68. https://doi.org/10.1038/nrmicro958.

Darling, Thayer K, and Tracey J Lamb. 2019. "Emerging Roles for Eph Receptors and Ephrin Ligands in Immunity." *Frontiers in Immunology* 10: 1473. https://doi.org/10.3389/fimmu.2019.01473.

Davis, D A, A S Rinderknecht, J P Zoeteweij, Y Aoki, E L Read-Connole, G Tosato, A Blauvelt, and R Yarchoan. 2001. "Hypoxia Induces Lytic Replication of Kaposi Sarcoma-Associated Herpesvirus." *Blood* 97 (10): 3244–50. https://doi.org/10.1182/blood.v97.10.3244.

Dedicoat, Martin, Robert Newton, Khaled R Alkharsah, Julie Sheldon, Ildiko Szabados, Bukekile Ndlovu, Taryn Page, et al. 2004. "Mother-to-Child Transmission of Human Herpesvirus-8 in South Africa." *The Journal of Infectious Diseases* 190 (6): 1068–75. https://doi.org/10.1086/423326.

DiGiovanna, J J, and B Safai. 1981. "Kaposi's Sarcoma. Retrospective Study of 90 Cases with Particular Emphasis on the Familial Occurrence, Ethnic Background and Prevalence of Other Diseases." *The American Journal of Medicine* 71 (5): 779–83. https://doi.org/10.1016/0002-9343(81)90364-8.

Direkze, Shamindra, and Heike Laman. 2004. "Regulation of Growth Signalling and Cell Cycle by Kaposi's Sarcoma-Associated Herpesvirus Genes." *International Journal of Experimental Pathology* 85 (6): 305–19. https://doi.org/10.1111/j.0959-9673.2004.00407.x.

Dittmer, Dirk P, Blossom Damania, and Sang-Hoon Sin. 2015. "Animal Models of Tumorigenic Herpesviruses--an Update." *Current Opinion in Virology* 14 (October): 145–50. https://doi.org/10.1016/j.coviro.2015.09.006.

Dollery, Stephen J, Rey J Santiago-Crespo, Deboeeta Chatterjee, and Edward A Berger. 2019. "Glycoprotein K8.1A of Kaposi's Sarcoma-Associated Herpesvirus Is a Critical B Cell Tropism Determinant Independent of Its Heparan Sulfate Binding Activity." *Journal of Virology* 93 (6). https://doi.org/10.1128/JVI.01876-18.

Drexler, H G, C Meyer, G Gaidano, and A Carbone. 1999. "Constitutive Cytokine Production by Primary Effusion (Body Cavity-Based) Lymphoma-Derived Cell Lines." *Leukemia* 13 (4): 634–40. https://doi.org/10.1038/sj.leu.2401371.

Dross, Rukiyah Van, Shan Yao, Shaheena Asad, Grant Westlake, Deborah J Mays, Laura Barquero, Stephanie Duell, Jennifer A Pietenpol, and Philip J Browning. 2005. "Constitutively Active K-Cyclin/Cdk6 Kinase in Kaposi Sarcoma-Associated Herpesvirus-Infected Cells." *Journal of the National Cancer Institute* 97 (9): 656–66. https://doi.org/10.1093/jnci/dji113.

Du, M Q, H Liu, T C Diss, H Ye, R A Hamoudi, N Dupin, V Meignin, E Oksenhendler, C Boshoff, and P G Isaacson. 2001. "Kaposi Sarcoma-Associated Herpesvirus Infects Monotypic (IgM Lambda) but Polyclonal Naive B Cells in Castleman Disease and Associated Lymphoproliferative Disorders." *Blood* 97 (7): 2130–36. https://doi.org/10.1182/blood.v97.7.2130.

Dunkelberger, Jason R, and Wen-Chao Song. 2010. "Complement and Its Role in Innate and Adaptive Immune Responses." *Cell Research* 20 (1): 34–50. https://doi.org/10.1038/cr.2009.139.

Dupin, N, C Fisher, P Kellam, S Ariad, M Tulliez, N Franck, E van Marck, et al. 1999. "Distribution of Human Herpesvirus-8 Latently Infected Cells in Kaposi's Sarcoma, Multicentric Castleman's Disease, and Primary Effusion Lymphoma." *Proceedings of the National Academy of Sciences of the United States of America* 96 (8): 4546–51. https://doi.org/10.1073/pnas.96.8.4546.

Dupin, N, T L Diss, P Kellam, M Tulliez, M Q Du, D Sicard, R A Weiss, P G Isaacson, and C Boshoff. 2000. "HHV-8 Is Associated with a Plasmablastic Variant of Castleman Disease That Is Linked to HHV-8-Positive Plasmablastic Lymphoma." *Blood* 95 (4): 1406–12.

Dutta, Dipanjan, Sayan Chakraborty, Chirosree Bandyopadhyay, Mohanan Valiya Veettil, Mairaj Ahmed Ansari, Vivek Vikram Singh, and Bala Chandran. 2013. "EphrinA2 Regulates Clathrin Mediated KSHV Endocytosis in Fibroblast Cells by Coordinating Integrin-Associated Signaling and c-Cbl Directed Polyubiquitination." *PLoS Pathogens* 9 (7): e1003510. https://doi.org/10.1371/journal.ppat.1003510.

DUTZ, W, and A P STOUT. 1960. "Kaposi's Sarcoma in Infants and Children." *Cancer* 13: 684–94. https://doi.org/10.1002/1097-0142(196007/08)13:4<684::aid-cncr2820130408>3.0.co;2-g.

Duus, Karen M, Vivian Lentchitsky, Timothy Wagenaar, Charles Grose, and Jennifer Webster-Cyriaque. 2004. "Wild-Type Kaposi's Sarcoma-Associated Herpesvirus Isolated from the Oropharynx of Immune-Competent Individuals Has Tropism for Cultured Oral Epithelial Cells." Journal of Virology 78 (8): 4074–84. https://doi.org/10.1128/jvi.78.8.4074-4084.2004.

Dytrych, Petra, Petra Krol, Michaela Kotrova, Daniela Kuzilkova, Petr Hubacek, Ladislav Krol, Rami Katra, et al. 2015. "Polyclonal, Newly Derived T Cells with Low Expression of Inhibitory Molecule PD-1 in Tonsils Define the Phenotype of Lymphocytes in Children with Periodic Fever, Aphtous Stomatitis, Pharyngitis and Adenitis (PFAPA) Syndrome." Molecular Immunology 65 (1): 139–47. https://doi.org/10.1016/j.molimm.2015.01.004.

Edelman, Daniel C. 2005. "Human Herpesvirus 8--a Novel Human Pathogen." *Virology Journal* 2 (September): 78. https://doi.org/10.1186/1743-422X-2-78.

Farooq, Asim V, and Deepak Shukla. 2012. "Herpes Simplex Epithelial and Stromal Keratitis: An Epidemiologic Update." *Survey of Ophthalmology* 57 (5): 448–62. https://doi.org/10.1016/j.survophthal.2012.01.005.

Faure, Aurélia, Mitch Hayes, and Bill Sugden. 2019. "How Kaposi's Sarcoma-Associated Herpesvirus Stably Transforms Peripheral B Cells towards Lymphomagenesis." Proceedings of the National Academy of Sciences of the United States of America 116 (33): 16519–28. https://doi.org/10.1073/pnas.1905025116.

Feller, Liviu, Johan Lemmer, Neil H Wood, Yusuf Jadwat, and Erich J Raubenheimer. 2007. "HIV-Associated Oral Kaposi Sarcoma and HHV-8: A Review." *Journal of the International Academy of Periodontology* 9 (4): 129–36.

Field, Nigel, Walter Low, Mark Daniels, Steven Howell, Laurent Daviet, Chris Boshoff, and Mary Collins. 2003. "KSHV VFLIP Binds to IKK-Gamma to Activate IKK." *Journal of Cell Science* 116 (Pt 18): 3721–28. https://doi.org/10.1242/jcs.00691.

Flaño, E, S M Husain, J T Sample, D L Woodland, and M A Blackman. 2000. "Latent Murine Gamma-Herpesvirus Infection Is Established in Activated B Cells, Dendritic Cells, and Macrophages." Journal of Immunology (Baltimore, Md.: 1950) 165 (2): 1074–81. https://doi.org/10.4049/jimmunol.165.2.1074.

Foussat, A, J Wijdenes, L Bouchet, G Gaidano, F Neipel, K Balabanian, P Galanaud, J Couderc, and D Emilie. 1999. "Human Interleukin-6 Is in Vivo an Autocrine Growth Factor for Human Herpesvirus-8-Infected Malignant B Lymphocytes." *European Cytokine Network* 10 (4): 501–8.

Galeotti, Caroline, Adeline Boucheron, Séverine Guillaume, and Isabelle Koné-Paut. 2012. "Sustained Remission of Multicentric Castleman Disease in Children Treated with Tocilizumab, an Anti-Interleukin-6 Receptor Antibody." Molecular Cancer Therapeutics 11 (8): 1623–26. https://doi.org/10.1158/1535-7163.MCT-11-0972.

Gantt, Soren, Jackson Orem, Elizabeth M Krantz, Rhoda Ashley Morrow, Stacy Selke, Meei-Li Huang, Joshua T Schiffer, et al. 2016. "Prospective Characterization of the Risk Factors for Transmission and Symptoms of Primary Human Herpesvirus Infections Among Ugandan Infants." *The Journal of Infectious Diseases* 214 (1): 36–44. https://doi.org/10.1093/infdis/jiw076.

Gasperini, Paola, Massimo Barbierato, Canio Martinelli, Paolo Rigotti, Francesco Marchini, Giulia Masserizzi, Francesco Leoncini, Luigi Chieco-Bianchi, Thomas F Schulz, and Maria Luisa Calabrò. 2005. "Use of a BJAB-Derived Cell Line for Isolation of Human Herpesvirus 8." Journal of Clinical Microbiology 43 (6): 2866–75. https://doi.org/10.1128/JCM.43.6.2866-2875.2005.

Gbabe, Oluwatoyin F, Charles I Okwundu, Martin Dedicoat, and Esther E Freeman. 2014. "Treatment of Severe or Progressive Kaposi's Sarcoma in HIV-Infected Adults." *The Cochrane Database of Systematic Reviews* 8 (8): CD003256. https://doi.org/10.1002/14651858.CD003256.pub2.

Giffin, Louise, and Blossom Damania. 2014. "KSHV: Pathways to Tumorigenesis and Persistent Infection." *Advances in Virus Research* 88: 111–59. https://doi.org/10.1016/B978-0-12-800098-4.00002-7.

Gong, Danyang, Nicholas C Wu, Yafang Xie, Jun Feng, Leming Tong, Kevin F Brulois, Harding Luan, et al. 2014. "Kaposi's Sarcoma-Associated Herpesvirus ORF18 and ORF30 Are Essential for Late Gene Expression during Lytic Replication." Journal of Virology 88 (19): 11369–82. https://doi.org/10.1128/JVI.00793-14.

Gradoville, L, J Gerlach, E Grogan, D Shedd, S Nikiforow, C Metroka, and G Miller. 2000. "Kaposi's Sarcoma-Associated Herpesvirus Open Reading Frame 50/Rta Protein Activates the Entire Viral Lytic Cycle in the HH-B2 Primary Effusion Lymphoma Cell Line." *Journal of Virology* 74 (13): 6207–12. https://doi.org/10.1128/jvi.74.13.6207-6212.2000.

Gregory, Sean M, John A West, Patrick J Dillon, Chelsey Hilscher, Dirk P Dittmer, and Blossom Damania. 2009. "Toll-like Receptor Signaling Controls Reactivation of KSHV from Latency." Proceedings of the National Academy of Sciences of the United States of America 106 (28): 11725–30. https://doi.org/10.1073/pnas.0905316106.

Grinde, Bjørn. 2013. "Herpesviruses: Latency and Reactivation - Viral Strategies and Host Response." *Journal of Oral Microbiology* 5 (October). https://doi.org/10.3402/jom.v5i0.22766.

Großkopf, Anna K, Sarah Schlagowski, Bojan F Hörnich, Thomas Fricke, Ronald C Desrosiers, and Alexander S Hahn. 2019. "EphA7 Functions as Receptor on BJAB Cells for Cell-to-Cell Transmission of the Kaposi's Sarcoma-Associated Herpesvirus and for Cell-Free Infection by the Related Rhesus Monkey Rhadinovirus." *Journal of Virology* 93 (15). https://doi.org/10.1128/JVI.00064-19.

Grundhoff, Adam, and Don Ganem. 2004. "Inefficient Establishment of KSHV Latency Suggests an Additional Role for Continued Lytic Replication in Kaposi Sarcoma Pathogenesis." The Journal of Clinical Investigation 113 (1): 124–36. https://doi.org/10.1172/JCI17803.

Guasparri, Ilaria, Shannon A Keller, and Ethel Cesarman. 2004. "KSHV VFLIP Is Essential for the Survival of Infected Lymphoma Cells." *The Journal of Experimental Medicine* 199 (7): 993–1003. https://doi.org/10.1084/jem.20031467.

Gugliesi, Francesca, Alessandra Coscia, Gloria Griffante, Ganna Galitska, Selina Pasquero, Camilla Albano, and Matteo Biolatti. 2020. "Where Do We Stand after Decades of Studying Human Cytomegalovirus?" *Microorganisms* 8 (5). https://doi.org/10.3390/microorganisms8050685.

Guo, Yang Eric, Kasandra J Riley, Akiko Iwasaki, and Joan A Steitz. 2014. "Alternative Capture of Noncoding RNAs or Protein-Coding Genes by Herpesviruses to Alter Host T Cell Function." *Molecular Cell* 54 (1): 67–79. https://doi.org/10.1016/j.molcel.2014.03.025.

Hahn, Alexander S, and Ronald C Desrosiers. 2013. "Rhesus Monkey Rhadinovirus Uses Eph Family Receptors for Entry into B Cells and Endothelial Cells but Not Fibroblasts." *PLoS Pathogens* 9 (5): e1003360. https://doi.org/10.1371/journal.ppat.1003360.

Hahn, Alexander S, and Ronald C Desrosiers. 2014. "Binding of the Kaposi's Sarcoma-Associated Herpesvirus to the Ephrin Binding Surface of the EphA2 Receptor and Its Inhibition by a Small Molecule." *Journal of Virology* 88 (16): 8724–34. https://doi.org/10.1128/JVI.01392-14.

Hahn, Alexander S, Johanna K Kaufmann, Effi Wies, Elisabeth Naschberger, Julia Panteleev-Ivlev, Katharina Schmidt, Angela Holzer, et al. 2012. "The Ephrin Receptor Tyrosine Kinase A2 Is a Cellular Receptor for Kaposi's Sarcoma–Associated Herpesvirus." *Nature Medicine* 18 (6): 961–66. https://doi.org/10.1038/nm.2805

Hahn, Alexander, Alexander Birkmann, Effi Wies, Dominik Dorer, Kerstin Mahr, Michael Stürzl, Fritz Titgemeyer, and Frank Neipel. 2009. "Kaposi's Sarcoma-Associated Herpesvirus GH/GL: Glycoprotein Export and Interaction with Cellular Receptors." Journal of Virology 83 (1): 396–407. https://doi.org/10.1128/JVI.01170-08.

Halder, Sabyasachi, Masanao Murakami, Subhash C Verma, Pankaj Kumar, Fuming Yi, and Erle S Robertson. 2009. "Early Events Associated with Infection of Epstein-Barr Virus Infection of Primary B-Cells." PloS One 4 (9): e7214. https://doi.org/10.1371/journal.pone.0007214.

Haqshenas, Gholamreza, and Christian Doerig. 2019. "Targeting of Host Cell Receptor Tyrosine Kinases by Intracellular Pathogens." *Science Signaling* 12 (599). https://doi.org/10.1126/scisignal.aau9894.

Hassman, Lynn M, Thomas J Ellison, and Dean H Kedes. 2011. "KSHV Infects a Subset of Human Tonsillar B Cells, Driving Proliferation and Plasmablast Differentiation." *The Journal of Clinical Investigation* 121 (2): 752–68. https://doi.org/10.1172/JCI44185.

Hensler, Heather R, Monica J Tomaszewski, Giovanna Rappocciolo, Charles R Rinaldo, and Frank J Jenkins. 2014. "Human Herpesvirus 8 Glycoprotein B Binds the Entry Receptor DC-SIGN." Virus Research 190 (September): 97–103. https://doi.org/10.1016/j.virusres.2014.07.003.

Hladik, Wolfgang, Sheila C Dollard, Jonathan Mermin, Ashley L Fowlkes, Robert Downing, Minal M Amin, Flora Banage, et al. 2006. "Transmission of Human Herpesvirus 8 by Blood Transfusion." *The New England Journal of Medicine* 355 (13): 1331–38. https://doi.org/10.1056/NEJMoa055009.

Hollingworth, Robert, Grant S Stewart, and Roger J Grand. 2020. "Productive Herpesvirus Lytic Replication in Primary Effusion Lymphoma Cells Requires S-Phase Entry." The Journal of General Virology 101 (8): 873–83. https://doi.org/10.1099/jgv.0.001444.

Hong, Young-Kwon, Kimberly Foreman, Jay W Shin, Satoshi Hirakawa, Christine L Curry, David R Sage, Towia Libermann, Bruce J Dezube, Joyce D Fingeroth, and Michael Detmar. 2004. "Lymphatic Reprogramming of Blood Vascular Endothelium by Kaposi Sarcoma-Associated Herpesvirus." *Nature Genetics* 36 (7): 683–85. https://doi.org/10.1038/ng1383.

Horwitz, C A, W Henle, G Henle, D Snover, H Rudnick, H H Jr Balfour, M H Mazur, R Watson, B Schwartz, and N Muller. 1986. "Clinical and Laboratory Evaluation of Cytomegalovirus-Induced Mononucleosis in Previously Healthy Individuals. Report of 82 Cases." *Medicine* 65 (2): 124–34. https://doi.org/10.1097/00005792-198603000-00005.

Hu, Duosha, Victoria Wang, Min Yang, Shahed Abdullah, David A Davis, Thomas S Uldrick, Mark N Polizzotto, et al. 2016. "Induction of Kaposi's Sarcoma-Associated Herpesvirus-Encoded Viral Interleukin-6 by X-Box Binding Protein 1." Journal of Virology 90 (1): 368–78. https://doi.org/10.1128/JVI.01192-15.

Hu, Haidai, Jiazhen Dong, Deguang Liang, Zengqiang Gao, Lei Bai, Rui Sun, Hao Hu, Heng Zhang, Yuhui Dong, and Ke Lan. 2016. "Genome-Wide Mapping of the Binding Sites and Structural Analysis of Kaposi's Sarcoma-Associated Herpesvirus Viral Interferon Regulatory Factor 2 Reveal That It Is a DNA-Binding Transcription Factor." Journal of Virology 90 (3): 1158–68. https://doi.org/10.1128/JVI.01392-15.

Huang, Ya-Chi, Sue-Jane Lin, Kai-Min Lin, Ya-Ching Chou, Chung-Wu Lin, Shan-Chi Yu, Chi-Long Chen, et al. 2016. "Regulation of EBV LMP1-Triggered EphA4 Downregulation in EBV-Associated B Lymphoma and Its Impact on Patients' Survival." *Blood* 128 (12): 1578–89. https://doi.org/10.1182/blood-2016-02-702530.

Hutt-Fletcher, Lindsey M. 2007. "Epstein-Barr Virus Entry." *Journal of Virology* 81 (15): 7825–32. https://doi.org/10.1128/JVI.00445-07.

Ibrahim, Hazem A H, Kirsty Balachandran, Mark Bower, and Kikkeri N Naresh. 2016. "Bone Marrow Manifestations in Multicentric Castleman Disease." British Journal of Haematology 172 (6): 923–29. https://doi.org/10.1111/bjh.13919.

Iftode, Nicoleta, Mihaela Andreea Rădulescu, Ștefan Sorin Aramă, and Victoria Aramă. 2020. "Update on Kaposi Sarcoma-Associated Herpesvirus (KSHV or HHV8) - Review." *Romanian Journal of Internal Medicine = Revue Roumaine de Medecine Interne* 58 (4): 199–208. https://doi.org/10.2478/rjim-2020-0017.

Iwakoshi, Neal N, Ann-Hwee Lee, Prasanth Vallabhajosyula, Kevin L Otipoby, Klaus Rajewsky, and Laurie H Glimcher. 2003. "Plasma Cell Differentiation and the Unfolded Protein Response Intersect at the Transcription Factor XBP-1." Nature Immunology 4 (4): 321–29. https://doi.org/10.1038/ni907.

Izumiya, Yoshihiro, Su-Fang Lin, Thomas Ellison, Ling-Yu Chen, Chie Izumiya, Paul Luciw, and Hsing-Jien Kung. 2003. "Kaposi's Sarcoma-Associated Herpesvirus K-BZIP Is a Coregulator of K-Rta: Physical Association and Promoter-Dependent Transcriptional Repression." *Journal of Virology* 77 (2): 1441–51. https://doi.org/10.1128/jvi.77.2.1441-1451.2003.

Izumiya, Yoshihiro, Su-Fang Lin, Thomas J Ellison, Alon M Levy, Greg L Mayeur, Chie Izumiya, and Hsing-Jien Kung. 2003. "Cell Cycle Regulation by Kaposi's Sarcoma-Associated Herpesvirus K-BZIP: Direct Interaction with Cyclin-CDK2 and Induction of G1 Growth Arrest." *Journal of Virology* 77 (17): 9652–61. https://doi.org/10.1128/jvi.77.17.9652-9661.2003.

Janjanin, Sasa, Farida Djouad, Rabie M Shanti, Dolores Baksh, Kiran Gollapudi, Drago Prgomet, Lars Rackwitz, Arjun S Joshi, and Rocky S Tuan. 2008. "Human Palatine Tonsil: A New Potential Tissue Source of Multipotent Mesenchymal Progenitor Cells." *Arthritis Research & Therapy* 10 (4): R83. https://doi.org/10.1186/ar2459.

Jarousse, Nadine, Bala Chandran, and Laurent Coscoy. 2008. "Lack of Heparan Sulfate Expression in B-Cell Lines: Implications for Kaposi's Sarcoma-Associated Herpesvirus and Murine Gammaherpesvirus 68 Infections." Journal of Virology 82 (24): 12591–97. https://doi.org/10.1128/JVI.01167-08.

Jarousse, Nadine, Damian L Trujillo, Sarah Wilcox-Adelman, and Laurent Coscoy. 2011. "Virally-Induced Upregulation of Heparan Sulfate on B Cells via the Action of Type I IFN." Journal of Immunology (Baltimore, Md.: 1950) 187 (11): 5540–47. https://doi.org/10.4049/jimmunol.1003495.

Jenner, Richard G, Karine Maillard, Nicola Cattini, Robin A Weiss, Chris Boshoff, Richard Wooster, and Paul Kellam. 2003. "Kaposi's Sarcoma-Associated Herpesvirus-Infected Primary Effusion Lymphoma Has a Plasma Cell Gene Expression Profile." Proceedings of the National Academy of Sciences of the United States of America 100 (18): 10399–404. https://doi.org/10.1073/pnas.1630810100.

Johnson, Andrew S, Nicole Maronian, and Jeffrey Vieira. 2005. "Activation of Kaposi's Sarcoma-Associated Herpesvirus Lytic Gene Expression during Epithelial Differentiation." *Journal of Virology* 79 (21): 13769–77. https://doi.org/10.1128/JVI.79.21.13769-13777.2005.

Johnson, Kaitlin E, and Vera L Tarakanova. 2020. "Gammaherpesviruses and B Cells: A Relationship That Lasts a Lifetime." Viral Immunology 33 (4): 316–26. https://doi.org/10.1089/vim.2019.0126.

Johnston, Benjamin P, Eric S Pringle, and Craig McCormick. 2019. "KSHV Activates Unfolded Protein Response Sensors but Suppresses Downstream Transcriptional Responses to Support Lytic Replication." PLoS Pathogens 15 (12): e1008185. https://doi.org/10.1371/journal.ppat.1008185.

Joshi, P J, R H Merchant, S L Pokharankar, K S Damania, I S Gilada, and R Mukhopadhyaya. 2000. "Perinatally Cotransmitted Human Herpesvirus 6 Is Activated in Children Born with Human Immunodeficiency Virus Infection." *Journal of Human Virology* 3 (6): 317–23.

Kaleeba, Johnan A R, and Edward A Berger. 2006b. "Broad Target Cell Selectivity of Kaposi's Sarcoma-Associated Herpesvirus Glycoprotein-Mediated Cell Fusion and Virion Entry." *Virology* 354 (1): 7–14. https://doi.org/10.1016/j.virol.2006.06.009.

Kaleeba, Johnan A R, and Edward A Berger. 2006a. "Kaposi's Sarcoma-Associated Herpesvirus Fusion-Entry Receptor: Cystine Transporter XCT." *Science (New York, N.Y.)* 311 (5769): 1921–24. https://doi.org/10.1126/science.1120878.

Kaneko, Hisatoshi, Takashi Kawana, Ken Ishioka, Shigeaki Ohno, Koki Aoki, and Tatsuo Suzutani. 2008. "Evaluation of Mixed Infection Cases with Both Herpes Simplex Virus Types 1 and 2." *Journal of Medical Virology* 80 (5): 883–87. https://doi.org/10.1002/jmv.21154.

Kang, Sangmin, and Jinjong Myoung. 2017. "Primary Lymphocyte Infection Models for KSHV and Its Putative Tumorigenesis Mechanisms in B Cell Lymphomas." Journal of Microbiology (Seoul, Korea) 55 (5): 319–29. https://doi.org/10.1007/s12275-017-7075-2.

Kang, Sung Yoon Catherine, Nagarajan Kannan, Lewei Zhang, Victor Martinez, Miriam P Rosin, and Connie J Eaves. 2015. "Characterization of Epithelial Progenitors in Normal Human Palatine Tonsils and Their HPV16 E6/E7-Induced Perturbation." *Stem Cell Reports* 5 (6): 1210–25. https://doi.org/10.1016/j.stemcr.2015.09.020.

Kassambara, Alboukadel. 2020. "Pipe-Friendly Framework for Basic Statistical Tests."

Kaul, Rajeev, Pravinkumar Purushothaman, Timsy Uppal, and Subhash C Verma. 2019. "KSHV Lytic Proteins K-RTA and K8 Bind to Cellular and Viral Chromatin to Modulate Gene Expression." PloS One 14 (4): e0215394. https://doi.org/10.1371/journal.pone.0215394.

Kaye, Stephen, and Anshoo Choudhary. 2006. "Herpes Simplex Keratitis." *Progress in Retinal and Eye Research* 25 (4): 355–80. https://doi.org/10.1016/j.preteyeres.2006.05.001.

Kedes, D H, E Operskalski, M Busch, R Kohn, J Flood, and D Ganem. 1996. "The Seroepidemiology of Human Herpesvirus 8 (Kaposi's Sarcoma-Associated Herpesvirus): Distribution of Infection in KS Risk Groups and Evidence for Sexual Transmission." *Nature Medicine* 2 (8): 918–24. https://doi.org/10.1038/nm0896-918.

Kempkes, Bettina, and Erle S Robertson. 2015. "Epstein-Barr Virus Latency: Current and Future Perspectives." *Current Opinion in Virology* 14 (October): 138–44. https://doi.org/10.1016/j.coviro.2015.09.007.

Kennedy, Peter G E, Joel Rovnak, Hussain Badani, and Randall J Cohrs. 2015. "A Comparison of Herpes Simplex Virus Type 1 and Varicella-Zoster Virus Latency and Reactivation." *The Journal of General Virology* 96 (Pt 7): 1581–1602. https://doi.org/10.1099/vir.0.000128.

Kerur, Nagaraj, Mohanan Valiya Veettil, Neelam Sharma-Walia, Sathish Sadagopan, Virginie Bottero, Arun George Paul, and Bala Chandran. 2010. "Characterization of Entry and Infection of Monocytic THP-1 Cells by Kaposi's Sarcoma Associated Herpesvirus (KSHV): Role of Heparan Sulfate, DC-SIGN, Integrins and Signaling." *Virology* 406 (1): 103–16. https://doi.org/10.1016/j.virol.2010.07.012.

Khodadadi, Laleh, Qingyu Cheng, Andreas Radbruch, and Falk Hiepe. 2019. "The Maintenance of Memory Plasma Cells." *Frontiers in Immunology* 10: 721. https://doi.org/10.3389/fimmu.2019.00721.

Knowlton, Emilee R, Giovanna Rappocciolo, Paolo Piazza, Lauren M Lepone, Sagar V Nadgir, Arlene Bullotta, Stella J Berendam, et al. 2014. "Human Herpesvirus 8 Induces Polyfunctional B Lymphocytes That Drive Kaposi's Sarcoma." MBio 5 (5): e01277-14. https://doi.org/10.1128/mBio.01277-14.

Koch, Sandra, Modester Damas, Anika Freise, Elias Hage, Akshay Dhingra, Jessica Rückert, Antonio Gallo, et al. 2019. "Kaposi's Sarcoma-Associated Herpesvirus VIRF2 Protein Utilizes an IFN-Dependent Pathway to Regulate Viral Early Gene Expression." PLoS Pathogens 15 (5): e1007743. https://doi.org/10.1371/journal.ppat.1007743.

Kramer, Tal, and Lynn W Enquist. 2013. "Directional Spread of Alphaherpesviruses in the Nervous System." *Viruses* 5 (2): 678–707. https://doi.org/10.3390/v5020678.

Kyalwazi, S K. 1981. "Kaposi's Sarcoma: Clinical Features, Experience in Uganda." *Antibiotics and Chemotherapy* 29: 59–67. https://doi.org/10.1159/000397440.

Lan, Ke, and Min Hua Luo. 2017. "Herpesviruses: Epidemiology, Pathogenesis, and Interventions." *Virologica Sinica* 32 (5): 347–48. https://doi.org/10.1007/s12250-017-4108-2.

Lang, Pierre Olivier, Sheila Govind, Annemieke Ten Bokum, Natalie Kenny, Emmanuel Matas, David Pitts, and Richard Aspinall. 2013. "Immune Senescence and Vaccination in the Elderly." *Current Topics in Medicinal Chemistry* 13 (20): 2541–50. https://doi.org/10.2174/15680266113136660181.

Lang, Pierre-Olivier, and Richard Aspinall. 2021. "Vaccination for Quality of Life: Herpes-Zoster Vaccines." *Aging Clinical and Experimental Research* 33 (4): 1113–22. https://doi.org/10.1007/s40520-019-01374-5.

Lee, Hye-Ra, Zsolt Toth, Young C Shin, Jong-Soo Lee, Heesoon Chang, Wei Gu, Tae-Kwang Oh, Myung Hee Kim, and Jae U Jung. 2009. "Kaposi's Sarcoma-Associated Herpesvirus Viral Interferon Regulatory Factor 4 Targets MDM2 to Deregulate the P53 Tumor Suppressor Pathway." Journal of Virology 83 (13): 6739–47. https://doi.org/10.1128/JVI.02353-08.

Lefort, Sylvain, and Louis Flamand. 2009. "Kaposi's Sarcoma-Associated Herpesvirus K-BZIP Protein Is Necessary for Lytic Viral Gene Expression, DNA Replication, and Virion Production in Primary Effusion Lymphoma Cell Lines." Journal of Virology 83 (11): 5869–80. https://doi.org/10.1128/JVI.01821-08.

Li, Da-Jiang, Dinesh Verma, Tim Mosbruger, and Sankar Swaminathan. 2014. "CTCF and Rad21 Act as Host Cell Restriction Factors for Kaposi's Sarcoma-Associated Herpesvirus (KSHV) Lytic Replication by Modulating Viral Gene Transcription." PLoS Pathogens 10 (1): e1003880. https://doi.org/10.1371/journal.ppat.1003880.

Li, J J, Y Q Huang, C J Cockerell, and A E Friedman-Kien. 1996. "Localization of Human Herpes-like Virus Type 8 in Vascular Endothelial Cells and Perivascular Spindle-Shaped Cells of Kaposi's Sarcoma Lesions by in Situ Hybridization." *The American Journal of Pathology* 148 (6): 1741–48.

Li, Wan, Fei Wang, Jiale Shi, Qi Feng, Yuheng Chen, Xiaoyu Qi, Cong Wang, et al. 2020. "Sperm Associated Antigen 9 Promotes Oncogenic KSHV-Encoded Interferon Regulatory Factor-Induced Cellular Transformation and Angiogenesis by Activating the JNK/VEGFA Pathway." PLoS Pathogens 16 (8): e1008730. https://doi.org/10.1371/journal.ppat.1008730.

Li, Wan, Qingxia Wang, Qi Feng, Fei Wang, Qin Yan, Shou-Jiang Gao, and Chun Lu. 2019. "Oncogenic KSHV-Encoded Interferon Regulatory Factor Upregulates HMGB2 and CMPK1 Expression to Promote Cell Invasion by Disrupting a Complex LncRNA-OIP5-AS1/MiR-218-5p Network." PLoS Pathogens 15 (1): e1007578. https://doi.org/10.1371/journal.ppat.1007578.

Liang, Xiaozhen, Clinton R Paden, Francine M Morales, Ryan P Powers, Joshy Jacob, and Samuel H Speck. 2011. "Murine Gamma-Herpesvirus Immortalization of Fetal Liver-Derived B Cells Requires Both the Viral Cyclin D Homolog and Latency-Associated Nuclear Antigen." *PLoS Pathogens* 7 (9): e1002220. https://doi.org/10.1371/journal.ppat.1002220.

Light, Taylor P, Delphine Brun, Pablo Guardado-Calvo, Riccardo Pederzoli, Ahmed Haouz, Frank Neipel, Félix A Rey, Kalina Hristova, and Marija Backovic. 2021. "Human Herpesvirus 8 Molecular Mimicry of Ephrin Ligands Facilitates Cell Entry and Triggers EphA2 Signaling." *PLoS Biology* 19 (9): e3001392. https://doi.org/10.1371/journal.pbio.3001392.

Lisco, Andrea, Massimo Barbierato, Josè R Fiore, Paola Gasperini, Anna Favia, Anna Volpe, Maria Chironna, Giuseppe Pastore, Luigi Chieco-Bianchi, and Maria Luisa Calabrò. 2006. "Pregnancy and Human Herpesvirus 8 Reactivation in Human Immunodeficiency Virus Type 1-Infected Women." *Journal of Clinical Microbiology* 44 (11): 3863–71. https://doi.org/10.1128/JCM.00791-06.

Looker, Katharine J, Geoffrey P Garnett, and George P Schmid. 2008. "An Estimate of the Global Prevalence and Incidence of Herpes Simplex Virus Type 2 Infection." *Bulletin of the World Health Organization* 86 (10): 805–12, A. https://doi.org/10.2471/blt.07.046128.

Lubyova, B, and P M Pitha. 2000. "Characterization of a Novel Human Herpesvirus 8-Encoded Protein, VIRF-3, That Shows Homology to Viral and Cellular Interferon Regulatory Factors." Journal of Virology 74 (17): 8194–8201. https://doi.org/10.1128/jvi.74.17.8194-8201.2000.

Lubyova, Barbora, Merrill J Kellum, Augusto J Frisancho, and Paula M Pitha. 2004. "Kaposi's Sarcoma-Associated Herpesvirus-Encoded VIRF-3 Stimulates the Transcriptional Activity of Cellular IRF-3 and IRF-7." The Journal of Biological Chemistry 279 (9): 7643–54. https://doi.org/10.1074/jbc.M309485200.

Lurain, Kathryn, Mark N Polizzotto, Karen Aleman, Manisha Bhutani, Kathleen M Wyvill, Priscila H Gonçalves, Ramya Ramaswami, et al. 2019. "Viral, Immunologic, and Clinical

Features of Primary Effusion Lymphoma." *Blood* 133 (16): 1753–61. https://doi.org/10.1182/blood-2019-01-893339.

Machiels, Bénédicte, Céline Lété, Katalin de Fays, Jan Mast, Benjamin Dewals, Philip G Stevenson, Alain Vanderplasschen, and Laurent Gillet. 2011. "The Bovine Herpesvirus 4 Bo10 Gene Encodes a Nonessential Viral Envelope Protein That Regulates Viral Tropism through Both Positive and Negative Effects." *Journal of Virology* 85 (2): 1011–24. https://doi.org/10.1128/JVI.01092-10.

Machiels, Bénédicte, Philip G Stevenson, Alain Vanderplasschen, and Laurent Gillet. 2013. "A Gammaherpesvirus Uses Alternative Splicing to Regulate Its Tropism and Its Sensitivity to Neutralization." *PLoS Pathogens* 9 (10): e1003753. https://doi.org/10.1371/journal.ppat.1003753.

Mahnke, Yolanda D, Tess M Brodie, Federica Sallusto, Mario Roederer, and Enrico Lugli. 2013. "The Who's Who of T-Cell Differentiation: Human Memory T-Cell Subsets." European Journal of Immunology 43 (11): 2797–2809. https://doi.org/10.1002/eji.201343751.

Mantina, H, C Kankasa, W Klaskala, B Brayfield, J Campbell, Q Du, G Bhat, F Kasolo, C Mitchell, and C Wood. 2001. "Vertical Transmission of Kaposi's Sarcoma-Associated Herpesvirus." *International Journal of Cancer* 94 (5): 749–52. https://doi.org/10.1002/ijc.1529.

Marcelin, Anne-Geneviève, Anne-Marie Roque-Afonso, Monika Hurtova, Nicolas Dupin, Micheline Tulliez, Mylène Sebagh, Zaïna Ait Arkoub, et al. 2004. "Fatal Disseminated Kaposi's Sarcoma Following Human Herpesvirus 8 Primary Infections in Liver-Transplant Recipients." *Liver Transplantation : Official Publication of the American Association for the Study of Liver Diseases and the International Liver Transplantation Society* 10 (2): 295–300. https://doi.org/10.1002/lt.20058.

Margolis, Todd P, Yumi Imai, Li Yang, Vicky Vallas, and Philip R Krause. 2007. "Herpes Simplex Virus Type 2 (HSV-2) Establishes Latent Infection in a Different Population of Ganglionic Neurons than HSV-1: Role of Latency-Associated Transcripts." *Journal of Virology* 81 (4): 1872–78. https://doi.org/10.1128/JVI.02110-06.

Martin, J N, and D H Osmond. 2000. "Invited Commentary: Determining Specific Sexual Practices Associated with Human Herpesvirus 8 Transmission." *American Journal of Epidemiology* 151 (3): 225–29; discussion 230. https://doi.org/10.1093/oxfordjournals.aje.a010196.

Martin, J N, D E Ganem, D H Osmond, K A Page-Shafer, D Macrae, and D H Kedes. 1998. "Sexual Transmission and the Natural History of Human Herpesvirus 8 Infection." *The New England Journal of Medicine* 338 (14): 948–54. https://doi.org/10.1056/NEJM199804023381403.

Martró, Elisa, Anna Esteve, Thomas F Schulz, Julie Sheldon, Gemma Gambús, Rafael Muñoz, Denise Whitby, and Jordi Casabona. 2007. "Risk Factors for Human Herpesvirus 8 Infection and AIDS-Associated Kaposi's Sarcoma among Men Who Have Sex with Men in a

European Multicentre Study." *International Journal of Cancer* 120 (5): 1129–35. https://doi.org/10.1002/ijc.22281.

Matolcsy, A, R G Nádor, E Cesarman, and D M Knowles. 1998. "Immunoglobulin VH Gene Mutational Analysis Suggests That Primary Effusion Lymphomas Derive from Different Stages of B Cell Maturation." The American Journal of Pathology 153 (5): 1609–14. https://doi.org/10.1016/S0002-9440(10)65749-5.

Mbulaiteye, Sam M, Ruth M Pfeiffer, Denise Whitby, Glen R Brubaker, John Shao, and Robert J Biggar. 2003. "Human Herpesvirus 8 Infection within Families in Rural Tanzania." *The Journal of Infectious Diseases* 187 (11): 1780–85. https://doi.org/10.1086/374973.

Medina, Francisco, Carmen Segundo, Antonio Campos-Caro, Inés González-García, and José A Brieva. 2002. "The Heterogeneity Shown by Human Plasma Cells from Tonsil, Blood, and Bone Marrow Reveals Graded Stages of Increasing Maturity, but Local Profiles of Adhesion Molecule Expression." Blood 99 (6): 2154–61. https://doi.org/10.1182/blood.v99.6.2154.

Meggetto, F, E Cesarman, L Mourey, P Massip, G Delsol, and P Brousset. 2001. "Detection and Characterization of Human Herpesvirus-8-Infected Cells in Bone Marrow Biopsies of Human Immunodeficiency Virus-Positive Patients." Human Pathology 32 (3): 288–91. https://doi.org/10.1053/hupa.2001.22749.

Mesri, E A, E Cesarman, L Arvanitakis, S Rafii, M A Moore, D N Posnett, D M Knowles, and A S Asch. 1996. "Human Herpesvirus-8/Kaposi's Sarcoma-Associated Herpesvirus Is a New Transmissible Virus That Infects B Cells." The Journal of Experimental Medicine 183 (5): 2385–90. https://doi.org/10.1084/jem.183.5.2385.

Mesri, Enrique A, Ethel Cesarman, and Chris Boshoff. 2010. "Kaposi's Sarcoma and Its Associated Herpesvirus." *Nature Reviews. Cancer* 10 (10): 707–19. https://doi.org/10.1038/nrc2888.

Meulen, Emma van der, Meg Anderton, Melissa J Blumenthal, and Georgia Schäfer. 2021. "Cellular Receptors Involved in KSHV Infection." *Viruses* 13 (1). https://doi.org/10.3390/v13010118.

Meulen, Emma van der, Meg Anderton, Melissa J Blumenthal, and Georgia Schäfer. 2021. "Cellular Receptors Involved in KSHV Infection." Viruses 13 (1). https://doi.org/10.3390/v13010118.

Minhas, Veenu, and Charles Wood. 2014. "Epidemiology and Transmission of Kaposi's Sarcoma-Associated Herpesvirus." *Viruses* 6 (11): 4178–94. https://doi.org/10.3390/v6114178.

Moore, P S, S J Gao, G Dominguez, E Cesarman, O Lungu, D M Knowles, R Garber, P E Pellett, D J McGeoch, and Y Chang. 1996. "Primary Characterization of a Herpesvirus Agent Associated with Kaposi's Sarcomae." *Journal of Virology* 70 (1): 549–58. https://doi.org/10.1128/JVI.70.1.549-558.1996.

Morris, Valerie A, Almira S Punjabi, and Michael Lagunoff. 2008. "Activation of Akt through Gp130 Receptor Signaling Is Required for Kaposi's Sarcoma-Associated Herpesvirus-Induced Lymphatic Reprogramming of Endothelial Cells." *Journal of Virology* 82 (17): 8771–79. https://doi.org/10.1128/JVI.00766-08.

Mortazavi, Yasaman, Salum J Lidenge, Tara Tran, John T West, Charles Wood, and For Yue Tso. 2020. "The Kaposi's Sarcoma-Associated Herpesvirus (KSHV) GH/GL Complex Is the Predominant Neutralizing Antigenic Determinant in KSHV-Infected Individuals." Viruses 12 (3). https://doi.org/10.3390/v12030256.

Moss, D J, I S Misko, S R Burrows, K Burman, R McCarthy, and T B Sculley. 1988. "Cytotoxic T-Cell Clones Discriminate between A- and B-Type Epstein-Barr Virus Transformants." *Nature* 331 (6158): 719–21. https://doi.org/10.1038/331719a0.

Mrozek-Gorska, Paulina, Alexander Buschle, Dagmar Pich, Thomas Schwarzmayr, Ron Fechtner, Antonio Scialdone, and Wolfgang Hammerschmidt. 2019. "Epstein-Barr Virus Reprograms Human B Lymphocytes Immediately in the Prelatent Phase of Infection." *Proceedings of the National Academy of Sciences of the United States of America* 116 (32): 16046–55. https://doi.org/10.1073/pnas.1901314116.

Mueller, Lars, Freya A Goumas, Marianne Affeldt, Susanne Sandtner, Ursula M Gehling, Silke Brilloff, Jessica Walter, et al. 2007. "Stromal Fibroblasts in Colorectal Liver Metastases Originate from Resident Fibroblasts and Generate an Inflammatory Microenvironment." *The American Journal of Pathology* 171 (5): 1608–18. https://doi.org/10.2353/ajpath.2007.060661.

Müller, A M, A Medvinsky, J Strouboulis, F Grosveld, and E Dzierzak. 1994. "Development of Hematopoietic Stem Cell Activity in the Mouse Embryo." *Immunity* 1 (4): 291–301. https://doi.org/10.1016/1074-7613(94)90081-7.

Muniraju, Murali, Lorraine Z Mutsvunguma, Joslyn Foley, Gabriela M Escalante, Esther Rodriguez, Romina Nabiee, Jennifer Totonchy, et al. 2019. "Kaposi Sarcoma-Associated Herpesvirus Glycoprotein H Is Indispensable for Infection of Epithelial, Endothelial, and Fibroblast Cell Types." Journal of Virology 93 (16). https://doi.org/10.1128/JVI.00630-19.

Münz, Christian. 2020. "Probing Reconstituted Human Immune Systems in Mice With Oncogenic γ-Herpesvirus Infections." Frontiers in Immunology 11: 581419. https://doi.org/10.3389/fimmu.2020.581419.

Myoung, Jinjong, and Don Ganem 2011b. "Infection of Primary Human Tonsillar Lymphoid Cells by KSHV Reveals Frequent but Abortive Infection of T Cells." *Virology* 413 (1): 1–11. https://doi.org/10.1016/j.virol.2010.12.036.

Myoung, Jinjong, and Don Ganem. 2011a. "Active Lytic Infection of Human Primary Tonsillar B Cells by KSHV and Its Noncytolytic Control by Activated CD4+ T Cells." *The Journal of Clinical Investigation* 121 (3): 1130–40. https://doi.org/10.1172/JCI43755.

Myoung, Jinjong, and Don Ganem. 2011b. "Generation of a Doxycycline-Inducible KSHV Producer Cell Line of Endothelial Origin: Maintenance of Tight Latency with Efficient Reactivation upon Induction." *Journal of Virological Methods* 174 (1–2): 12–21. https://doi.org/10.1016/j.jviromet.2011.03.012.

Nabiee, Ramina, Basir Syed, Jesus Ramirez Castano, Rukhsana Lalani, and Jennifer E Totonchy. 2020. "An Update of the Virion Proteome of Kaposi Sarcoma-Associated Herpesvirus." *Viruses* 12 (12). https://doi.org/10.3390/v12121382.

Nakamura, H, M Li, J Zarycki, and J U Jung. 2001. "Inhibition of P53 Tumor Suppressor by Viral Interferon Regulatory Factor." Journal of Virology 75 (16): 7572–82. https://doi.org/10.1128/JVI.75.16.7572-7582.2001.

Naranatt, Pramod P, Harinivas H Krishnan, Stan R Svojanovsky, Clark Bloomer, Sachin Mathur, and Bala Chandran. 2004. "Host Gene Induction and Transcriptional Reprogramming in Kaposi's Sarcoma-Associated Herpesvirus (KSHV/HHV-8)-Infected Endothelial, Fibroblast, and B Cells: Insights into Modulation Events Early during Infection." *Cancer Research* 64 (1): 72–84. https://doi.org/10.1158/0008-5472.can-03-2767.

Naresh, Kikkeri N, Pritesh Trivedi, Donna Horncastle, and Mark Bower. 2009. "CD20 Expression in the HHV-8-Infected Lymphoid Cells in Multicentric Castleman Disease." Histopathology. England. https://doi.org/10.1111/j.1365-2559.2009.03344.x.

Nicol, Samantha M, Shereen Sabbah, Kevin F Brulois, Jae U Jung, Andrew I Bell, and Andrew D Hislop. 2016. "Primary B Lymphocytes Infected with Kaposi's Sarcoma-Associated Herpesvirus Can Be Expanded In Vitro and Are Recognized by LANA-Specific CD4+ T Cells." *Journal of Virology* 90 (8): 3849–59. https://doi.org/10.1128/JVI.02377-15.

Nishimura, Mitsuhiro, and Yasuko Mori. 2018. "Structural Aspects of Betaherpesvirus-Encoded Proteins." *Advances in Experimental Medicine and Biology* 1045: 227–49. https://doi.org/10.1007/978-981-10-7230-7_11.

Nishita, Michiru, Seung-Yeol Park, Tadashi Nishio, Koki Kamizaki, ZhiChao Wang, Kota Tamada, Toru Takumi, et al. 2017. "Ror2 Signaling Regulates Golgi Structure and Transport through IFT20 for Tumor Invasiveness." Scientific Reports 7 (1): 1. https://doi.org/10.1038/s41598-016-0028-x.

Oliver, Stefan L, Momei Zhou, and Ann M Arvin. 2020. "Varicella-Zoster Virus: Molecular Controls of Cell Fusion-Dependent Pathogenesis." *Biochemical Society Transactions* 48 (6): 2415–35. https://doi.org/10.1042/BST20190511.

Olp, Landon N, Veenu Minhas, Clement Gondwe, Lisa K Poppe, A Michelle Rogers, Chipepo Kankasa, John T West, and Charles Wood. 2016. "Longitudinal Analysis of the Humoral Response to Kaposi's Sarcoma-Associated Herpesvirus after Primary Infection in Children." *Journal of Medical Virology* 88 (11): 1973–81. https://doi.org/10.1002/jmv.24546.

Palm, Anna-Karin E, and Sandra Kleinau. 2021. "Marginal Zone B Cells: From Housekeeping Function to Autoimmunity?" *Journal of Autoimmunity* 119 (May): 102627. https://doi.org/10.1016/j.jaut.2021.102627.

Palmerin, Nancy, Farizeh Aalam, Romina Nabiee, Murali Muniraju, Javier Gordon Ogembo, and Jennifer Totonchy. 2021. "Suppression of DC-SIGN and GH Reveals Complex, Subset-Specific Mechanisms for KSHV Entry in Primary B Lymphocytes." *Viruses* 13 (8). https://doi.org/10.3390/v13081512.

Pantanowitz, L, R A G Khammissa, J Lemmer, and L Feller. 2013. "Oral HIV-Associated Kaposi Sarcoma." *Journal of Oral Pathology & Medicine : Official Publication of the International Association of Oral Pathologists and the American Academy of Oral Pathology* 42 (3): 201–7. https://doi.org/10.1111/j.1600-0714.2012.01180.x.

Park, J, T Seo, S Hwang, D Lee, Y Gwack, and J Choe. 2000. "The K-BZIP Protein from Kaposi's Sarcoma-Associated Herpesvirus Interacts with P53 and Represses Its Transcriptional Activity." Journal of Virology 74 (24): 11977–82. https://doi.org/10.1128/jvi.74.24.11977-11982.2000.

Park, Junsoo, Myung-Shin Lee, Seung-Min Yoo, Kwi Wan Jeong, Daeyoup Lee, Joonho Choe, and Taegun Seo. 2007. "Identification of the DNA Sequence Interacting with Kaposi's Sarcoma-Associated Herpesvirus Viral Interferon Regulatory Factor 1." Journal of Virology 81 (22): 12680–84. https://doi.org/10.1128/JVI.00556-07.

Pauk, J, M L Huang, S J Brodie, A Wald, D M Koelle, T Schacker, C Celum, S Selke, and L Corey. 2000. "Mucosal Shedding of Human Herpesvirus 8 in Men." The New England Journal of Medicine 343 (19): 1369–77. https://doi.org/10.1056/NEJM200011093431904.

Pereira, Valeska S S, Raíza N C Moizeis, Thales A A M Fernandes, Josélio M G Araújo, Rosely V Meissner, and José V Fernandes. 2012. "Herpes Simplex Virus Type 1 Is the Main Cause of Genital Herpes in Women of Natal, Brazil." *European Journal of Obstetrics, Gynecology, and Reproductive Biology* 161 (2): 190–93. https://doi.org/10.1016/j.ejogrb.2011.12.006.

Perry, M, and A Whyte. 1998. "Immunology of the Tonsils." *Immunology Today* 19 (9): 414–21. https://doi.org/10.1016/s0167-5699(98)01307-3.

Pica, Francesca, and Antonio Volpi. 2007. "Transmission of Human Herpesvirus 8: An Update." Current Opinion in Infectious Diseases 20 (2): 152–56. https://doi.org/10.1097/QCO.0b013e3280143919.

Pieper, Kathrin, Bodo Grimbacher, and Hermann Eibel. 2013. "B-Cell Biology and Development." *The Journal of Allergy and Clinical Immunology* 131 (4): 959–71. https://doi.org/10.1016/j.jaci.2013.01.046.

Powles, Thomas, David Robinson, Justin Stebbing, Jonathan Shamash, Mark Nelson, Brian Gazzard, Sundhiya Mandelia, Henrik Møller, and Mark Bower. 2009. "Highly Active Antiretroviral Therapy and the Incidence of Non-AIDS-Defining Cancers in People with

HIV Infection." Journal of Clinical Oncology : Official Journal of the American Society of Clinical Oncology 27 (6): 884–90. https://doi.org/10.1200/JCO.2008.19.6626.

Purushothaman, Pravinkumar, Suhani Thakker, and Subhash C Verma. 2015. "Transcriptome Analysis of Kaposi's Sarcoma-Associated Herpesvirus during de Novo Primary Infection of Human B and Endothelial Cells." Journal of Virology 89 (6): 3093–3111. https://doi.org/10.1128/JVI.02507-14.

Qin, Zhiqiang, Eduardo Freitas, Roger Sullivan, Sarumathi Mohan, Rocky Bacelieri, Drake Branch, Margaret Romano, et al. 2010. "Upregulation of XCT by KSHV-Encoded MicroRNAs Facilitates KSHV Dissemination and Persistence in an Environment of Oxidative Stress." PLoS Pathogens 6 (1): e1000742. https://doi.org/10.1371/journal.ppat.1000742.

Qin, Zhiqiang, Lu Dai, Bryan Toole, Erle Robertson, and Chris Parsons. 2011. "Regulation of Nm23-H1 and Cell Invasiveness by Kaposi's Sarcoma-Associated Herpesvirus." *Journal of Virology* 85 (7): 3596–3606. https://doi.org/10.1128/JVI.01596-10.

Quinlivan, E B, R X Wang, P W Stewart, C Kolmoltri, N Regamey, P Erb, and P L Vernazza. 2001. "Longitudinal Sero-Reactivity to Human Herpesvirus 8 (KSHV) in the Swiss HIV Cohort 4.7 Years before KS." *Journal of Medical Virology* 64 (2): 157–66. https://doi.org/10.1002/jmv.1031.

Rafailidis, Petros I, Eleni G Mourtzoukou, Ioannis C Varbobitis, and Matthew E Falagas. 2008. "Severe Cytomegalovirus Infection in Apparently Immunocompetent Patients: A Systematic Review." *Virology Journal* 5 (March): 47. https://doi.org/10.1186/1743-422X-5-47.

Raghu, Hari, Neelam Sharma-Walia, Mohanan Valiya Veettil, Sathish Sadagopan, and Bala Chandran. 2009. "Kaposi's Sarcoma-Associated Herpesvirus Utilizes an Actin Polymerization-Dependent Macropinocytic Pathway to Enter Human Dermal Microvascular Endothelial and Human Umbilical Vein Endothelial Cells." *Journal of Virology* 83 (10): 4895–4911. https://doi.org/10.1128/JVI.02498-08.

Ramaswami, Ramya, Germaine Chia, Alessia Dalla Pria, David J Pinato, Kizzy Parker, Mark Nelson, and Mark Bower. 2016. "Evolution of HIV-Associated Lymphoma Over 3 Decades." *Journal of Acquired Immune Deficiency Syndromes (1999)* 72 (2): 177–83. https://doi.org/10.1097/QAI.0000000000000946.

Rappocciolo, Giovanna, Heather R Hensler, Mariel Jais, Todd A Reinhart, Amarendra Pegu, Frank J Jenkins, and Charles R Rinaldo. 2008. "Human Herpesvirus 8 Infects and Replicates in Primary Cultures of Activated B Lymphocytes through DC-SIGN." *Journal of Virology* 82 (10): 4793–4806. https://doi.org/10.1128/JVI.01587-07.

Rappocciolo, Giovanna, Paolo Piazza, Craig L Fuller, Todd A Reinhart, Simon C Watkins, David T Rowe, Mariel Jais, Phalguni Gupta, and Charles R Rinaldo. 2006. "DC-SIGN on B Lymphocytes Is Required for Transmission of HIV-1 to T Lymphocytes." PLoS Pathogens 2 (7): e70. https://doi.org/10.1371/journal.ppat.0020070.

Rayet, B, and C Gélinas. 1999. "Aberrant Rel/Nfkb Genes and Activity in Human Cancer." *Oncogene* 18 (49): 6938–47. https://doi.org/10.1038/sj.onc.1203221.

Restrepo, Carlos S, Santiago Martínez, Julio A Lemos, Jorge A Carrillo, Diego F Lemos, Paulina Ojeda, and Prakash Koshy. 2006. "Imaging Manifestations of Kaposi Sarcoma." *Radiographics : A Review Publication of the Radiological Society of North America, Inc* 26 (4): 1169–85. https://doi.org/10.1148/rg.264055129.

Rivas, C, A E Thlick, C Parravicini, P S Moore, and Y Chang. 2001. "Kaposi's Sarcoma-Associated Herpesvirus LANA2 Is a B-Cell-Specific Latent Viral Protein That Inhibits P53." Journal of Virology 75 (1): 429–38. https://doi.org/10.1128/JVI.75.1.429-438.2001.

Roberts, Jeffrey N, Christopher B Buck, Cynthia D Thompson, Rhonda Kines, Marcelino Bernardo, Peter L Choyke, Douglas R Lowy, and John T Schiller. 2007. "Genital Transmission of HPV in a Mouse Model Is Potentiated by Nonoxynol-9 and Inhibited by Carrageenan." Nature Medicine 13 (7): 857–61. https://doi.org/10.1038/nm1598.

Rohner, Eliane, Natascha Wyss, Zina Heg, Zully Faralli, Sam M Mbulaiteye, Urban Novak, Marcel Zwahlen, Matthias Egger, and Julia Bohlius. 2016. "HIV and Human Herpesvirus 8 Co-Infection across the Globe: Systematic Review and Meta-Analysis." *International Journal of Cancer* 138 (1): 45–54. https://doi.org/10.1002/ijc.29687.

Roizman, Bernard, and Richard J Whitley. 2013. "An Inquiry into the Molecular Basis of HSV Latency and Reactivation." *Annual Review of Microbiology* 67: 355–74. https://doi.org/10.1146/annurev-micro-092412-155654.

Santag, S, W Jäger, C B Karsten, S Kati, M Pietrek, D Steinemann, G Sarek, P M Ojala, and T F Schulz. 2013. "Recruitment of the Tumour Suppressor Protein P73 by Kaposi's Sarcoma Herpesvirus Latent Nuclear Antigen Contributes to the Survival of Primary Effusion Lymphoma Cells." *Oncogene* 32 (32): 3676–85. https://doi.org/10.1038/onc.2012.385.

Sarek, Grzegorz, Annika Järviluoma, Henna M Moore, Sari Tojkander, Salla Vartia, Peter Biberfeld, Marikki Laiho, and Päivi M Ojala. 2010. "Nucleophosmin Phosphorylation by V-Cyclin-CDK6 Controls KSHV Latency." *PLoS Pathogens* 6 (3): e1000818. https://doi.org/10.1371/journal.ppat.1000818.

Schmidt, Katharina, Effi Wies, and Frank Neipel. 2011. "Kaposi's Sarcoma-Associated Herpesvirus Viral Interferon Regulatory Factor 3 Inhibits Gamma Interferon and Major Histocompatibility Complex Class II Expression." *Journal of Virology* 85 (9): 4530–37. https://doi.org/10.1128/JVI.02123-10.

Seifi, Amir, Edward M Weaver, Mark E Whipple, Minako Ikoma, James Farrenberg, Meei-Li Huang, and Jeffery Vieira. 2011. "The Lytic Activation of KSHV during Keratinocyte Differentiation Is Dependent upon a Suprabasal Position, the Loss of Integrin Engagement, and Calcium, but Not the Interaction of Cadherins." *Virology* 410 (1): 17–29. https://doi.org/10.1016/j.virol.2010.10.023.

Shahaf, Gitit, Simona Zisman-Rozen, David Benhamou, Doron Melamed, and Ramit Mehr. 2016. "B Cell Development in the Bone Marrow Is Regulated by Homeostatic Feedback Exerted by Mature B Cells." *Frontiers in Immunology* 7: 77. https://doi.org/10.3389/fimmu.2016.00077.

Shannon-Lowe, Claire, Alan B Rickinson, and Andrew I Bell. 2017. "Epstein-Barr Virus-Associated Lymphomas." *Philosophical Transactions of the Royal Society of London. Series B, Biological Sciences* 372 (1732). https://doi.org/10.1098/rstb.2016.0271.

Siegel, J H, R Janis, J C Alper, H Schutte, L Robbins, and M D Blaufox. 1969. "Disseminated Visceral Kaposi's Sarcoma. Appearance after Human Renal Homograft Operation." *JAMA* 207 (8): 1493–96.

Silva, Suzane Ramos da, and Deilson Elgui de Oliveira. 2011. "HIV, EBV and KSHV: Viral Cooperation in the Pathogenesis of Human Malignancies." *Cancer Letters* 305 (2): 175–85. https://doi.org/10.1016/j.canlet.2011.02.007.

Song, Soken-Nakazawa J, Naohisa Tomosugi, Hiroshi Kawabata, Takayuki Ishikawa, Teppei Nishikawa, and Kazuyuki Yoshizaki. 2010. "Down-Regulation of Hepcidin Resulting from Long-Term Treatment with an Anti-IL-6 Receptor Antibody (Tocilizumab) Improves Anemia of Inflammation in Multicentric Castleman Disease." Blood 116 (18): 3627–34. https://doi.org/10.1182/blood-2010-03-271791.

Soulier, J, L Grollet, E Oksenhendler, P Cacoub, D Cazals-Hatem, P Babinet, M F d'Agay, J P Clauvel, M Raphael, and L Degos. 1995. "Kaposi's Sarcoma-Associated Herpesvirus-like DNA Sequences in Multicentric Castleman's Disease." *Blood* 86 (4): 1276–80.

Spiller, O B, L Mark, C E Blue, D G Proctor, J A Aitken, A M Blom, and D J Blackbourn. 2006. "Dissecting the Regions of Virion-Associated Kaposi's Sarcoma-Associated Herpesvirus Complement Control Protein Required for Complement Regulation and Cell Binding." *Journal of Virology* 80 (8): 4068–78. https://doi.org/10.1128/JVI.80.8.4068-4078.2006.

Spiller, O B, L Mark, C E Blue, D G Proctor, J A Aitken, A M Blom, and D J Blackbourn. 2006. "Dissecting the Regions of Virion-Associated Kaposi's Sarcoma-Associated Herpesvirus Complement Control Protein Required for Complement Regulation and Cell Binding." Journal of Virology 80 (8): 4068–78. https://doi.org/10.1128/JVI.80.8.4068-4078.2006.

Stanisce, Luke, Etty Sims, Cheryl Hou, Yekaterina Koshkareva, John P Gaughan, Igor Kuzin, and Andrea Bottaro. 2018. "Differential Cellular Composition of Human Palatine and Pharyngeal Tonsils." Archives of Oral Biology 96 (December): 80–86. https://doi.org/10.1016/j.archoralbio.2018.08.020.

Stebegg, Marisa, Saumya D Kumar, Alyssa Silva-Cayetano, Valter R Fonseca, Michelle A Linterman, and Luis Graca. 2018. "Regulation of the Germinal Center Response." *Frontiers in Immunology* 9: 2469. https://doi.org/10.3389/fimmu.2018.02469.

Stein, M E, D Spencer, P Ruff, R Lakier, P MacPhail, and W R Bezwoda. 1994. "Endemic African Kaposi's Sarcoma: Clinical and Therapeutic Implications. 10-Year Experience in the Johannesburg Hospital (1980-1990)." *Oncology* 51 (1): 63–69. https://doi.org/10.1159/000227312.

Steiner, Israel, Peter G E Kennedy, and Andrew R Pachner. 2007. "The Neurotropic Herpes Viruses: Herpes Simplex and Varicella-Zoster." *The Lancet. Neurology* 6 (11): 1015–28. https://doi.org/10.1016/S1474-4422(07)70267-3.

Stewart, J P, N J Janjua, S D Pepper, G Bennion, M Mackett, T Allen, A A Nash, and J R Arrand. 1996. "Identification and Characterization of Murine Gammaherpesvirus 68 Gp150: A Virion Membrane Glycoprotein." *Journal of Virology* 70 (6): 3528–35. https://doi.org/10.1128/JVI.70.6.3528-3535.1996.

Su, Chao, Lili Wu, Yan Chai, Jianxun Qi, Shuguang Tan, George F Gao, Hao Song, and Jinghua Yan. 2020. "Molecular Basis of EphA2 Recognition by GHgL from Gammaherpesviruses." *Nature Communications* 11 (1): 5964. https://doi.org/10.1038/s41467-020-19617-9.

Sun, Chuankai, Yizhen Guo, Wei Zhou, Chuan Xia, Xiwen Xing, Jun Chen, Xin Li, Hua Zhu, and Jie Lu. 2020. "P300 Promotes Cell Proliferation through Suppressing Kaposi's Sarcoma-Associated Herpesvirus (KSHV) Reactivation in the Infected B-Lymphoma Cells." Virus Research 286 (September): 198066. https://doi.org/10.1016/j.virusres.2020.198066.

Taylor, Graham S, Heather M Long, Jill M Brooks, Alan B Rickinson, and Andrew D Hislop. 2015. "The Immunology of Epstein-Barr Virus-Induced Disease." *Annual Review of Immunology* 33: 787–821. https://doi.org/10.1146/annurev-immunol-032414-112326.

Taylor, J F, A C Templeton, C L Vogel, J L Ziegler, and S K Kyalwazi. 1971. "Kaposi's Sarcoma in Uganda: A Clinico-Pathological Study." *International Journal of Cancer* 8 (1): 122–35. https://doi.org/10.1002/ijc.2910080116.

Tedeschi, R, J Dillner, and P De Paoli. 2002. "Laboratory Diagnosis of Human Herpesvirus 8 Infection in Humans." *European Journal of Clinical Microbiology & Infectious Diseases : Official Publication of the European Society of Clinical Microbiology* 21 (12): 831–44. https://doi.org/10.1007/s10096-002-0836-8.

Temple, Rachel M, Craig Meyers, and Clare E Sample. 2017. "Generation and Infection of Organotypic Cultures with Epstein-Barr Virus." Methods in Molecular Biology (Clifton, N.J.) 1532: 65–78. https://doi.org/10.1007/978-1-4939-6655-4_4.

Temple, Rachel M, Junjia Zhu, Lynn Budgeon, Neil David Christensen, Craig Meyers, and Clare E Sample. 2014. "Efficient Replication of Epstein-Barr Virus in Stratified Epithelium in Vitro." Proceedings of the National Academy of Sciences of the United States of America 111 (46): 16544–49. https://doi.org/10.1073/pnas.1400818111.

Thakker, Suhani, and Subhash C Verma. 2016. "Co-Infections and Pathogenesis of KSHV-Associated Malignancies." *Frontiers in Microbiology* 7: 151. https://doi.org/10.3389/fmicb.2016.00151.

Thorley-Lawson, David A, Jared B Hawkins, Sean I Tracy, and Michael Shapiro. 2013. "The Pathogenesis of Epstein-Barr Virus Persistent Infection." *Current Opinion in Virology* 3 (3): 227–32. https://doi.org/10.1016/j.coviro.2013.04.005.

Tognarelli, Eduardo I, Tomás F Palomino, Nicolás Corrales, Susan M Bueno, Alexis M Kalergis, and Pablo A González. 2019. "Herpes Simplex Virus Evasion of Early Host Antiviral Responses." *Frontiers in Cellular and Infection Microbiology* 9: 127. https://doi.org/10.3389/fcimb.2019.00127.

Totonchy, Jennifer, Jessica M Osborn, Amy Chadburn, Ramina Nabiee, Lissenya Argueta, Geoffrey Mikita, and Ethel Cesarman. 2018. "KSHV Induces Immunoglobulin Rearrangements in Mature B Lymphocytes." *PLoS Pathogens* 14 (4): e1006967. https://doi.org/10.1371/journal.ppat.1006967.

Tyler, Kenneth L. 2003. "Human Herpesvirus 6 and Multiple Sclerosis: The Continuing Conundrum." *The Journal of Infectious Diseases*. United States. https://doi.org/10.1086/374674.

Ueda, Keiji. 2018. "KSHV Genome Replication and Maintenance in Latency." Advances in Experimental Medicine and Biology 1045: 299–320. https://doi.org/10.1007/978-981-10-7230-7_14.

Uldrick, Thomas S, and Denise Whitby. 2011. "Update on KSHV Epidemiology, Kaposi Sarcoma Pathogenesis, and Treatment of Kaposi Sarcoma." *Cancer Letters* 305 (2): 150–62. https://doi.org/10.1016/j.canlet.2011.02.006.

Uldrick, Thomas S, Victoria Wang, Deirdre O'Mahony, Karen Aleman, Kathleen M Wyvill, Vickie Marshall, Seth M Steinberg, et al. 2010. "An Interleukin-6-Related Systemic Inflammatory Syndrome in Patients Co-Infected with Kaposi Sarcoma-Associated Herpesvirus and HIV but without Multicentric Castleman Disease." *Clinical Infectious Diseases : An Official Publication of the Infectious Diseases Society of America* 51 (3): 350–58. https://doi.org/10.1086/654798.

Uppal, Timsy, Sagarika Banerjee, Zhiguo Sun, Subhash C Verma, and Erle S Robertson. 2014. "KSHV LANA--the Master Regulator of KSHV Latency." *Viruses* 6 (12): 4961–98. https://doi.org/10.3390/v6124961.

Van der, Meulen, Emma Meg Anderton, Melissa J Blumenthal, and Georgia Schäfer. 2021. "Cellular Receptors Involved in KSHV Infection." *Viruses* 13 (1). https://doi.org/10.3390/v13010118.

Veettil, Mohanan Valiya, Chirosree Bandyopadhyay, Dipanjan Dutta, and Bala Chandran. 2014. "Interaction of KSHV with Host Cell Surface Receptors and Cell Entry." *Viruses* 6 (10): 4024–46. https://doi.org/10.3390/v6104024.

Veettil, Mohanan Valiya, Sathish Sadagopan, Neelam Sharma-Walia, Fu-Zhang Wang, Hari Raghu, Laszlo Varga, and Bala Chandran. 2008. "Kaposi's Sarcoma-Associated Herpesvirus Forms a Multimolecular Complex of Integrins (AlphaVbeta5, AlphaVbeta3, and

Alpha3beta1) and CD98-XCT during Infection of Human Dermal Microvascular Endothelial Cells, and CD98-XCT Is Essential for the Postentry Sta." Journal of Virology 82 (24): 12126–44. https://doi.org/10.1128/JVI.01146-08.

Vieira, J, M L Huang, D M Koelle, and L Corey. 1997. "Transmissible Kaposi's Sarcoma-Associated Herpesvirus (Human Herpesvirus 8) in Saliva of Men with a History of Kaposi's Sarcoma." Journal of Virology 71 (9): 7083–87. https://doi.org/10.1128/JVI.71.9.7083-7087.1997.

Wakeham, Katie, Emily L Webb, Ismail Sebina, Angela Nalwoga, Lawrence Muhangi, Wendell Miley, W Thomas Johnston, et al. 2013. "Risk Factors for Seropositivity to Kaposi Sarcoma-Associated Herpesvirus among Children in Uganda." *Journal of Acquired Immune Deficiency Syndromes (1999)* 63 (2): 228–33. https://doi.org/10.1097/QAI.0b013e31828a7056.

Wang, F Z, S M Akula, N P Pramod, L Zeng, and B Chandran. 2001. "Human Herpesvirus 8 Envelope Glycoprotein K8.1A Interaction with the Target Cells Involves Heparan Sulfate." Journal of Virology 75 (16): 7517–27. https://doi.org/10.1128/JVI.75.16.7517-7527.2001.

Wang, Q J, F J Jenkins, L P Jacobson, L A Kingsley, R D Day, Z W Zhang, Y X Meng, et al. 2001. "Primary Human Herpesvirus 8 Infection Generates a Broadly Specific CD8(+) T-Cell Response to Viral Lytic Cycle Proteins." *Blood* 97 (8): 2366–73. https://doi.org/10.1182/blood.v97.8.2366.

Webster-Cyriaque, J, K Duus, C Cooper, and M Duncan. 2006. "Oral EBV and KSHV Infection in HIV." Advances in Dental Research 19 (1): 91–95. https://doi.org/10.1177/154407370601900118.

Wei, Xiaoqin, Lei Bai, Lianghui Dong, Huimei Liu, Peidong Xing, Zhiyao Zhou, Shuwen Wu, and Ke Lan. 2019. "NCOA2 Promotes Lytic Reactivation of Kaposi's Sarcoma-Associated Herpesvirus by Enhancing the Expression of the Master Switch Protein RTA." PLoS Pathogens 15 (11): e1008160. https://doi.org/10.1371/journal.ppat.1008160.

Wickham, Hadley, Mara Averick, Jennifer Bryan, Winston Chang, Lucy D'Agostino McGowan, Romain François, Garrett Grolemund, et al. 2019. "Welcome to the Tidyverse." Journal of Open Source Software 4 (43): 1686. https://doi.org/10.21105/joss.01686.

Wies, Effi, Yasuko Mori, Alexander Hahn, Elisabeth Kremmer, Michael Stürzl, Bernhard Fleckenstein, and Frank Neipel. 2008. "The Viral Interferon-Regulatory Factor-3 Is Required for the Survival of KSHV-Infected Primary Effusion Lymphoma Cells." Blood 111 (1): 320–27. https://doi.org/10.1182/blood-2007-05-092288.

Wu, Frederick Y, Qi-Qun Tang, Honglin Chen, Colette ApRhys, Christopher Farrell, Jianmeng Chen, Masahiro Fujimuro, M Daniel Lane, and Gary S Hayward. 2002. "Lytic Replication-Associated Protein (RAP) Encoded by Kaposi Sarcoma-Associated Herpesvirus Causes P21CIP-1-Mediated G1 Cell Cycle Arrest through CCAAT/Enhancer-Binding Protein-Alpha." Proceedings of the National Academy of Sciences of the United States of America 99 (16): 10683–88. https://doi.org/10.1073/pnas.162352299.

Yam-Puc, Juan Carlos, Lingling Zhang, Yang Zhang, and Kai-Michael Toellner. 2018. "Role of B-Cell Receptors for B-Cell Development and Antigen-Induced Differentiation." *F1000Research* 7: 429. https://doi.org/10.12688/f1000research.13567.1.

Yan, Lijun, Vladimir Majerciak, Zhi-Ming Zheng, and Ke Lan. 2019. "Towards Better Understanding of KSHV Life Cycle: From Transcription and Posttranscriptional Regulations to Pathogenesis." *Virologica Sinica* 34 (2): 135–61. https://doi.org/10.1007/s12250-019-00114-3.

Ye, Fengchun, Fuchun Zhou, Roble G Bedolla, Tiffany Jones, Xiufen Lei, Tao Kang, Moraima Guadalupe, and Shou-Jiang Gao. 2011. "Reactive Oxygen Species Hydrogen Peroxide Mediates Kaposi's Sarcoma-Associated Herpesvirus Reactivation from Latency." *PLoS Pathogens* 7 (5): e1002054. https://doi.org/10.1371/journal.ppat.1002054.

Yu, Xiaolan, Abdel-Malek Shahir, Jingfeng Sha, Zhimin Feng, Betty Eapen, Stanley Nithianantham, Biswajit Das, et al. 2014. "Short-Chain Fatty Acids from Periodontal Pathogens Suppress Histone Deacetylases, EZH2, and SUV39H1 to Promote Kaposi's Sarcoma-Associated Herpesvirus Replication." *Journal of Virology* 88 (8): 4466–79. https://doi.org/10.1128/JVI.03326-13.

Zelm, Menno C van, Tomasz Szczepanski, Mirjam van der Burg, and Jacques J M van Dongen. 2007. "Replication History of B Lymphocytes Reveals Homeostatic Proliferation and Extensive Antigen-Induced B Cell Expansion." *The Journal of Experimental Medicine* 204 (3): 645–55. https://doi.org/10.1084/jem.20060964.

Zhang, Hua, Yan Li, Hong-Bo Wang, Ao Zhang, Mei-Ling Chen, Zhi-Xin Fang, Xiao-Dong Dong, et al. 2018. "Ephrin Receptor A2 Is an Epithelial Cell Receptor for Epstein-Barr Virus Entry." *Nature Microbiology* 3 (2): 1–8. https://doi.org/10.1038/s41564-017-0080-8.

Zhang, Zhongheng. 2016. "Reshaping and Aggregating Data: An Introduction to Reshape Package." Annals of Translational Medicine 4 (4): 78. https://doi.org/10.3978/j.issn.2305-5839.2016.01.33.

Zhao, Yang, Xiang Ye, Myriam Shehata, William Dunker, Zhihang Xie, and John Karijolich. 2020. "The RNA Quality Control Pathway Nonsense-Mediated MRNA Decay Targets Cellular and Viral RNAs to Restrict KSHV." Nature Communications 11 (1): 3345. https://doi.org/10.1038/s41467-020-17151-2.

Zhu, Fan Xiu, Jae Min Chong, Lijun Wu, and Yan Yuan. 2005. "Virion Proteins of Kaposi's Sarcoma-Associated Herpesvirus." *Journal of Virology* 79 (2): 800–811. https://doi.org/10.1128/JVI.79.2.800-811.2005.

Appendix A. Supplementary data of Chapter II

A.1   Gating schemes for tonsil lymphocyte lineages

Flow cytometry data for a baseline uninfected sample from a 2-year-old male donor showing representative gating and lineage definitions used in the study for (A) B cell lineages based on vanZelm et. al. 2007 (van Zelm MC, 2007) and (B) T cell lineages based on Mahnke et. al. 2013 (Mahnke YD, 2013).
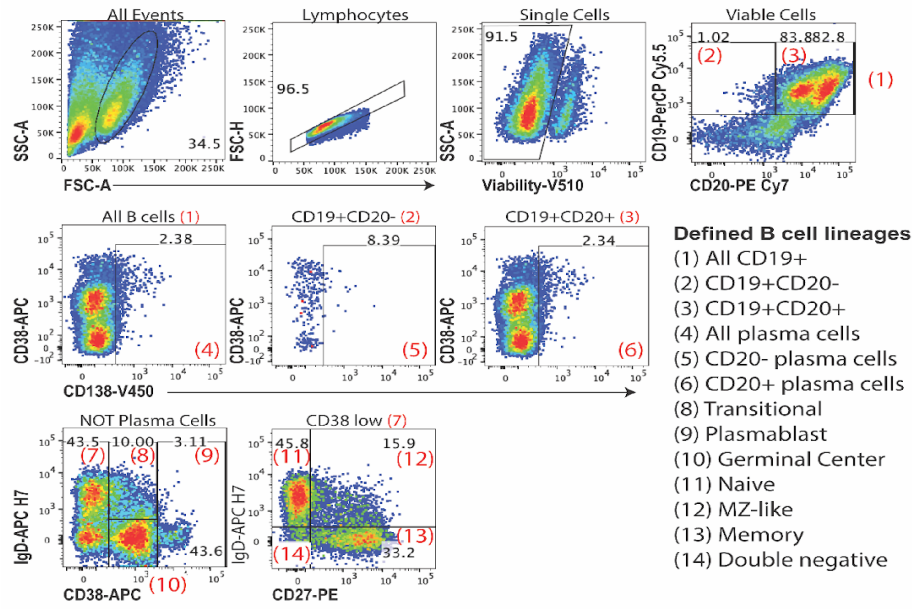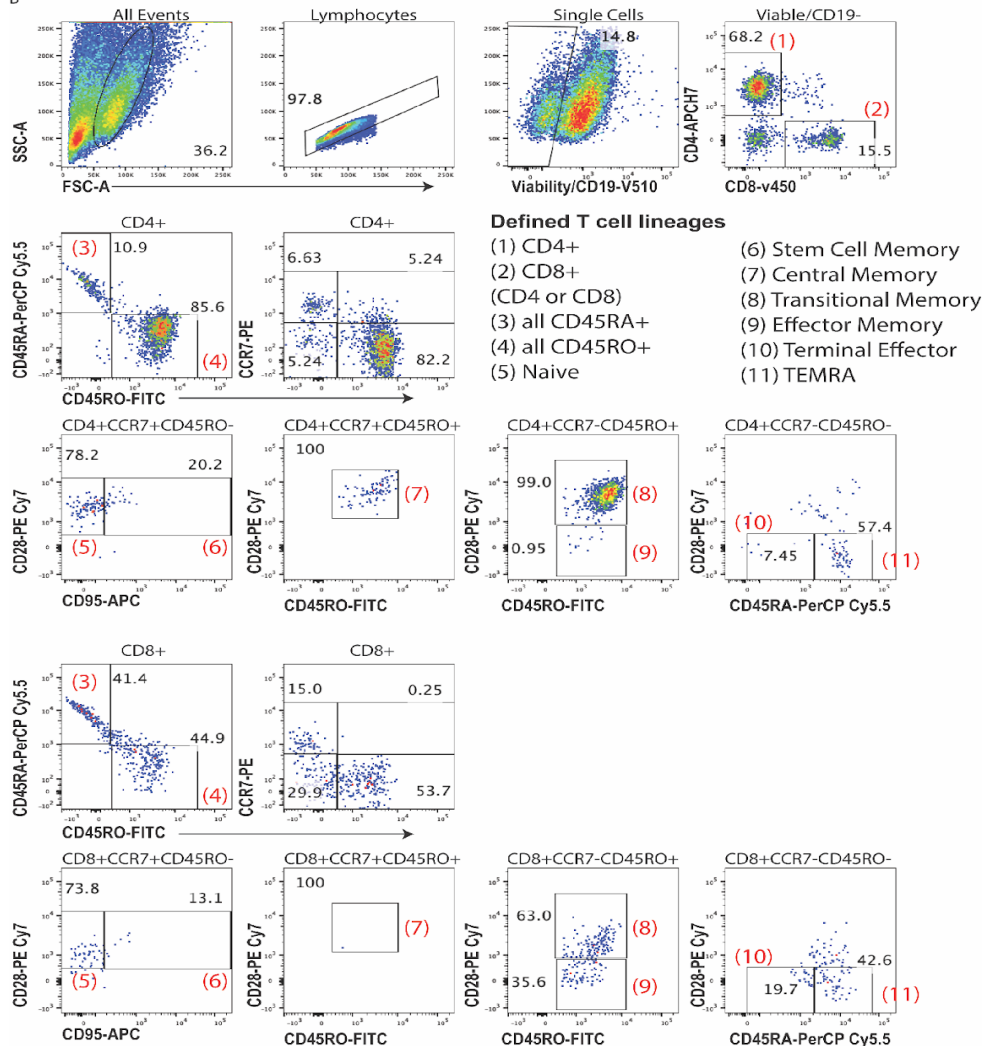
Supplemental Figure 1: Gating schemes tonsil lymphocyte lineages. Flow cytometry data for a baseline uninfected sample from a 2-year-old male donor showing representative gating and lineage definitions used in the study for (A) B cell lineages based on 31 and (B) T cell lineages based on 32.

A.2 Analyzed flow cytometry data

Values derived from flow cytometry analysis for baseline B cell and T cell lineage frequencies, overall infection frequency at 3dpi and lineagespecific infection frequencies for B cells. Comments associated with column headers contain detailed definitions for each subset. (XLSX)

A.3   Analyzed flow cytometry data for B cell lineages at 3 days post infection.

Values derived from flow cytometry analysis for overall B cell lineage frequencies in Mock and

KSHV infected cultures at 3 days post-infection. Abbreviations and lineage definitions are as in

S1 Table comments. https://doi.org/10.1371/journal.ppat.1008968.s003 (XLSX)

| CD19 B	CD19_PC	All B	All_PC	DN	Mem	Na	NE	GC	PB	Trans	DP	DPPC	Sample	Cond
1.74	4.64	49.6	0.55	5.88	7.95	2.4	2.7	42.6	13.7	23.8	47.6	0.82	ND11	Mock
1.2	2.02	59.7	0.45	4.61	5.96	2.39	2.48	33.3	22.4	28.5	52.4	0.42	ND11	Mock
1.45	5.51	49.6	1.95	4.96	8.45	1.52	2.73	45	15.1	20.4	48.1	1.82	ND11	KSHV
0.93	6.98	59	1.31	4.15	6.13	2.23	3.51	34.8	20.9	26.5	55.9	1.73	ND11	KSHV
1.11	0.35	84.1	0.37	10.5	40.9	20.1	28.5	19.8	7.11	64	83	0.37	ND12	Mock
1.23	0.37	85.8	0.39	10.2	41.2	21.2	27.3	19.6	5.76	65	84.6	0.39	ND12	Mock
1.14	3.23	86.5	0.36	9.86	43.1	20.7	26.4	20.5	5.99	63.5	85.3	0.32	ND12	KSHV
1.39	2.35	85.4	0.43	9.88	44	22.6	23.5	21.8	5.92	62.8	84	0.39	ND12	KSHV
1.38	0	55	0.25	4.27	5.65	2.89	2.26	47.8	8.41	28.6	58.4	0.26	ND14	Mock
0.76	0	57.2	0.56	3.67	7.13	1.67	3.23	48.4	8.3	26.5	56.3	0.57	ND14	KSHV
2.58	0	87.7	0.16	1.61	57.4	8.73	32.3	19.2	0.7	62.8	8.52	0.16	ND15	KSHV
2.33	1.02	85.7	0.28	1.94	58	9.39	30.2	13.3	0.86	60.4	33.3	0.25	ND15	KSHV
1.63	0	80.7	0.21	3.77	32.1	2.58	33.4	31.5	1.78	56.8	79.1	0.21	ND18	Mock
1.05	1.23	82.8	0.28	10.3	35	21.6	33.1	33.6	2.82	55.7	81.8	0.27	ND18	KSHV
0.47	1.67	88.2	0.12	5.2	23	39	32.8	16.1	0.8	74.9	87.7	0.12	ND19	Mock
0.61	16.7	36	0.3	4.13	29.4	31.3	35.1	16.3	0.99	71.7	8.53	0.18	ND19	Mock
0.27	3.12	84	0.21	6.94	30.8	24	33.2	16.4	0.76	74	83.7	0.2	ND20	Mock
0.43	3.64	83.5	0.39	6.14	33.9	21.6	33.4	16.9	0.8	72.2	83.1	0.33	ND20	KSHV
3.15	0.32	85.4	1.13	1.84	9.28	1.08	53	33.4	6.01	37.1	76.5	1.13	ND21	Mock
5.55	0	82.9	1.39	1.76	9.73	1.29	4.74	37.5	6.43	36.5	77	2.08	ND21	KSHV
0.91	0	84.4	0.36	1.56	8.36	3.4	2.2	34.1	13.5	41.5	58.3	0.37	ND23	Mock
1.02	1.41	57.3	0.4	1.4	2.96	2.93	2.13	32.7	18.2	39.2	56.1	0.38	ND23	Mock
0.58	3.12	41.8	0.79	1.7	4.28	2.31	2.27	38.6	16.5	33.4	41.1	0.75	ND23	KSHV
0.77	2.44	48.3	0.39	3.85	2.6	2.58	36.5	17.2	35.5	47.5	0.36	ND23	Mock
0.69	2.74	59.2	1.19	4.11	4.52	3.94	2.27	43.9	16.2	23.8	52.5	1.17	ND25	Mock
0.74	0	55	0.23	4.58	2.94	7.31	1.73	40.5	11.3	31.4	55.2	0.23	ND25	KSHV
0.23	0	54.1	1.09	1.2	1.33	1.11	0.6	24.7	27.5	42.6	58.9	1.09	ND26	Mock
0.14	0	56.3	0.65	0.76	0.97	1.58	0.76	20.8	30.1	44.3	56.1	0.65	ND26	Mock
0.2	0	57.8	0.7	1.13	1.48	1.3	1	34	20.7	39.8	57.6	0.7	ND26	KSHV
0.33	0	48.5	1.25	1.63	1.64	1.73	1.06	31.4	24.1	37.2	48.1	1.26	ND26	KSHV
1.76	0.37	80.5	0.28	1.5	1.69	2.73	1.04	36.6	9.3	46.9	78.6	0.29	ND27	Mock
2.14	0	70.4	0.49	2.47	2.61	2.13	1.5	58.7	6.61	30.4	68	0.51	ND27	KSHV
2.73	0	85.8	0.56	4.09	26	8.8	7.68	10.6	0	41.3	84	0.57	ND81	KSHV
3.92	0	85.6	0.84	3.74	24.2	8.97	5.33	12.8	0	43.8	82.3	0.87	ND81	KSHV
2.57	1.36	83.3	0.36	3.25	7.43	4.33	0.62	16.6	0.54	66	80.4	0.33	ND82	Mock
2.25	1.6	83.5	0.47	2.73	7.14	4.35	1.08	15.8	0.73	67	80.9	0.44	ND82	Mock
1.9	1.5	83.2	0.22	2.99	6.98	4.12	1.02	16.5	0.79	66.6	86	0.19	ND82	KSHV
1.63	1.25	87.9	0.31	2.72	7.28	4.01	1.21	16.8	0.82	66.1	86	0.28	ND82	KSHV
3.56	0.24	91.2	0.39	2.56	6.73	4	1.96	19.7	1.27	62.8	87.5	0.39	ND83	Mock
3.65	0.16	94.1	0.36	2.21	5.25	4.5	1.92	16.5	1.09	67.5	90.5	0.37	ND83	Mock
1.15	0.72	93.1	0.24	1.93	6.65	16.6	7.18	11.9	0.99	54.8	91.9	0.24	ND89	Mock
1.06	0.6	94.2	0.32	1.89	6.41	13.7	6.89	12.7	1.07	57.2	93.2	0.32	ND89	Mock
1.23	1.05	93.1	0.58	1.79	6.33	13	6.9	14.1	1.16	55.9	91.9	0.52	ND89	KSHV
1.15	1.98	92.9	0.35	2.38	6.36	12.3	7.18	14	1.47	56.2	91.7	0.33	ND89	KSHV
0.37	3.51	69.9	0.62	5.6	54	10.8	29.5	25.3	3.02	51.5	69.5	0.61	ND4	Mock
0.44	5.38	67.4	0.33	4.42	54.9	10.1	30.6	26.2	3.19	49.2	66.9	0.3	ND4	Mock
0.54	7.45	70.4	1.15	4.02	57.3	11.8	31.8	23.1	1.91	49.9	69.8	1.1	ND4	KSHV
0.72	8.26	69.8	0.84	3.96	55.2	9.92	31.5	25.5	2.33	43.1	68.5	0.87	ND4	KSHV
7.34	0	82.1	0.14	1.61	9.52	12.8	6.76	9.84	0.45	58	74.7	0.16	ND40	Mock
9.29	0	78.5	0.17	1.49	11.7	14	5.85	11.8	0.36	54.8	69.2	0.19	ND40	Mock
6.11	0.84	80.4	0.84	3.07	10.1	11	4.87	14.3	0.54	55.6	74.2	0.29	ND40	KSHV
6.76	2.42	84.1	0.39	1.93	9.42	15.7	7.57	8.14	0.097	56.9	77.3	0.16	ND40	KSHV
3.68	0.42	83.4	0.2	1.68	22.8	12.4	8.5	17.3	0.39	36.2	79.5	0.19	ND41	Mock
5.12	0.18	81.6	0.39	2.9	24.1	8.92	8.29	24.7	0.62	29.6	76.2	0.4	ND41	Mock
5.98	0.092	85.1	0.35	2.8	21.2	12	7.92	23.3	0.57	31.3	78.8	0.36	ND41	KSHV
6.63	0.5	83	0.82	2.3	22.1	11.8	7.31	25.8	1.02	28.1	81	0.35	ND41	KSHV
1.18	3.66	69.8	0.39	1.43	11.2	5.49	3.95	23.6	3	50.4	68.1	0.34	ND42	Mock
0.84	1.39	70.1	0.65	1.86	10.6	5.89	5.44	21.2	1.48	52.7	69.3	0.64	ND42	Mock
1.13	8.86	71.2	1.43	1.57	10.9	5.68	5.32	22.2	3.04	49.8	70.1	1.31	ND42	KSHV
1.06	9.48	66.3	1	1.13	10.8	4.48	4.66	22.4	3.72	52	65.2	0.83	ND42	KSHV
0.72	0	89.2	0.45	1.74	9.42	26.3	17.3	8.43	0.18	35.8	88.5	0.46	ND43	Mock
1.13	3.57	93.4	0.4	1.65	3.18	25	16	10.5	0.22	37.5	92.1	0.36	ND43	KSHV
6.24	0.86	52.2	0.78	3.97	23.2	7.31	7.54	31.1	1.83	23.8	45.7	0.76	ND44	Mock
6.96	1.37	54.3	0.84	2.33	23	6.61	5.52	36.3	2.11	21.6	46.9	0.69	ND44	Mock
2.07	0.31	50.3	1.47	6.23	20.7	5.63	5.33	3.56	1.54	22	43.1	1.51	ND45	Mock
1.22	4.35	44.4	2.06	5.6	19	4.09	4.8	42.3	1.94	19.5	43.2	2	ND45	KSHV
1.73	1.96	90.7	0.84	2.1	10.5	27.7	10.9	5.92	0.09	42.8	89	0.82	ND46	Mock
2.33	1.28	90.4	0.95	1.93	10.8	27	11.4	5.51	0.13	42.6	88	0.94	ND46	Mock
2.39	2.14	91.4	0.88	1.94	10.5	28.5	11.7	5.27	0.15	41.2	88.5	0.84	ND46	KSHV
2.34	2.79	89.6	1.56	2.37	11.4	23.4	11	7.24	0.16	43.1	86.7	1.51	ND46	KSHV
5.69	0.63	83.4	1.51	2.11	30	3.38	8.82	21	1.51	21.5	77.7	1.57	ND47	Mock
5.1	1.62	89.1	2.32	3.25	26.1	4.68	7.4	28.3	1.48	26.5	84	2.36	ND47	KSHV
2.9	0.62	84.3	1.48	2.63	15	3.62	6	37.3	2.09	31.3	81.4	1.52	ND48	Mock
3.13	1.11	84.4	1.47	2.72	14.3	3.28	5.3	36.8	1.9	33.1	81.2	1.48	ND48	Mock
2.04	4.82	84.6	1.64	2.31	14.1	2.63	5.63	37.2	3.54	32.3	82.5	1.15	ND48	KSHV
1.66	1.7	79.7	1.36	2.43	13	2.33	4.8	40.4	3.99	31.6	78.1	1.35	ND48	KSHV
4.98	1.56	41.6	1.69	5.62	44.9	2.53	12.9	3.56	0.19	5.62	36.4	1.71	ND49	Mock
4.89	14.1	68.3	2.66	4.22	33.2	27.6	14.3	3.77	0	13.7	63.7	1.8	ND49	KSHV
3.28	0.57	92	0.3	2.72	21.5	17.2	13.1	13.7	0.21	25.4	88.6	0.31	ND50	Mock
3.19	1.39	92.2	1.11	2.89	22.6	20	19.4	11.4	0.14	22.8	88.8	1.1	ND50	KSHV
3.3	1.43	92	1.72	3.19	22.7	17.7	17	13.5	0.25	23.7	88.4	1.73	ND50	KSHV
2.13	1.05	91.7	1.47	2.88	20.9	14.8	14.9	13	0.33	26.4	89.5	1.47	ND50	KSHV
3.16	0.24	94.6	0.35	1.27	3.93	8.4	5.04	21.9	1.15	52	86	0.36	ND51	Mock
10.1	0.048	94.2	0.31	1.22	9.73	9.32	5.29	23.2	1.09	49	83.6	0.35	ND51	Mock
6.54	0.37	96.2	0.3	0.99	8.34	7.2	52	22	2.02	52.1	88.1	0.33	ND51	KSHV
8.36	0.045	96.6	0.54	1.16	9.5	9.5	5.82	21.8	1.33	50.6	87.8	0.58	ND51	KSHV
1.15	3.77	60.6	2.14	2	21	3.75	12.5	21.3	4.21	33	58.5	2.11	ND52	Mock
1.64	1.68	80.5	1.5	2.39	15.2	2.92	6.66	33	7.58	30.5	78.9	1.48	ND52	KSHV
1.38	0.88	94.8	0.31	1.38	6.05	15.5	13	8.21	1.13	49.4	93.4	0.3	ND53	Mock
1.15	4.52	93.9	0.62	1.38	6.34	12.4	17.1	9.6	1.51	51.1	92.8	0.57	ND53	KSHV
3.48	0.39	92.7	0.14	0.82	7.01	9.33	4.85	7	0.38	70.1	89.2	0.13	ND54	Mock
3.77	0.74	91.8	0.75	1	3.56	15.4	5.33	7.19	0.28	61.6	83	0.74	ND54	KSHV
7.05	0.52	90.7	0.76	1.85	11.3	9.35	6.08	17.1	3.17	56.6	83.6	0.78	ND55	Mock
6.23	0.91	92.2	1.58	1.91	9.72	3.35	5.12	17.5	2.45	58.3	86	1.63	ND55	KSHV
1.7	3.06	58	2.29	3.86	28.7	4.58	7.96	21.6	1.11	29.8	51.3	2.27	ND56	Mock
1.88	4.35	58.1	2.26	3.74	28.3	4.31	8.28	23.2	1.38	27.2	51.2	2.18	ND56	KSHV
2.58	0	82.2	0.78	2.58	17.3	14.4	13.3	8.69	0.14	42.3	79.6	0.81	ND57	Mock
3.22	3.6	82.6	1.86	2.42	19.7	14	13.7	10.7	0.07	37.4	79.4	1.79	ND57	KSHV
0.74	2.27	82.4	0.87	1.07	7.13	2.57	1.12	14.2	1.21	71.7	81.6	0.96	ND58	Mock
1.23	0.89	82.3	0.62	1.14	7.35	2.81	1.11	13.4	1.09	72.5	81.6	0.61	ND58	Mock
0.21	8.39	67	1.23	2.67	3.33	1.07	0.7	19.3	3.13	67.9	66.3	1.21	ND58	KSHV
0.35	4.65	70.9	0.78	2	4.36	1.04	0.6	13.9	3.7	68.6	70.6	0.76	ND58	KSHV
0.13	10.7	72.2	0.71	0.93	4.47	1.58	0.76	13.4	1.79	70.4	72.1	0.68	ND60	KSHV
0.23	2.04	74.3	0.52	0.92	4.34	1.73	0.95	13.1	1.45	72	74.6	0.52	ND60	KSHV
0.2	11.7	69	1.3	0.76	53	0.76	0.88	28.2	4.61	58.2	68.8	1.27	ND61	KSHV
0.17	15.4	67.4	0.85	5.27	0.71	0.73	27.2	4.88	58.6	67.8	0.77	ND61	KSHV
0.089	12.1	68.4	1.58	4.52	10.5	4.17	3.46	30.3	3.35	42.1	68.3	1.58	ND62	KSHV
0.084	0	74.7	0.63	4.45	10.7	4.58	3.94	25.9	3	46.4	74.6	0.63	ND62	KSHV
0.23	11	86.6	0.79	1.13	5.92	1.1	0.22	10.9	6.9	73	86.3	0.76	ND63	KSHV
0.39	6.42	84.7	0.55	1.31	6.72	0.99	0.24	11.4	9	69.8	84.5	0.59	ND63	KSHV
0.41	8.32	81.8	1.26	0.95	9.4	0.95	1.08	33.2	2.48	50.7	81.4	1.22	ND64	KSHV
0.58	3.33	79.7	0.54	0.94	9.87	1.05	1.02	30.4	1.95	54.2	79.2	0.52	ND64	KSHV
0.22	37.5	91.5	0.44	0.41	7.24	2.47	3.26	12.9	0.29	72.9	91.3	0.35	ND65	KSHV
0.13	0	89	0.52	0.24	8.56	1.36	3.13	11.1	0.28	70.7	88.8	0.52	ND65	Mock
0.51	2.6	74.3	1.13	2.85	6.35	1.05	0.89	14.4	3.63	67.6	74.3	1.17	ND66	Mock
1.11	1.54	77.6	0.63	3.13	56	1.45	0.79	14.4	2.58	71.4	76.5	0.63	ND66	Mock

Appendix B. Supplementary data of Chapter III

B.1 Percent of GFP+ cells within each subset for each condition.

Data normalized to the sample and virus specific GFP value.
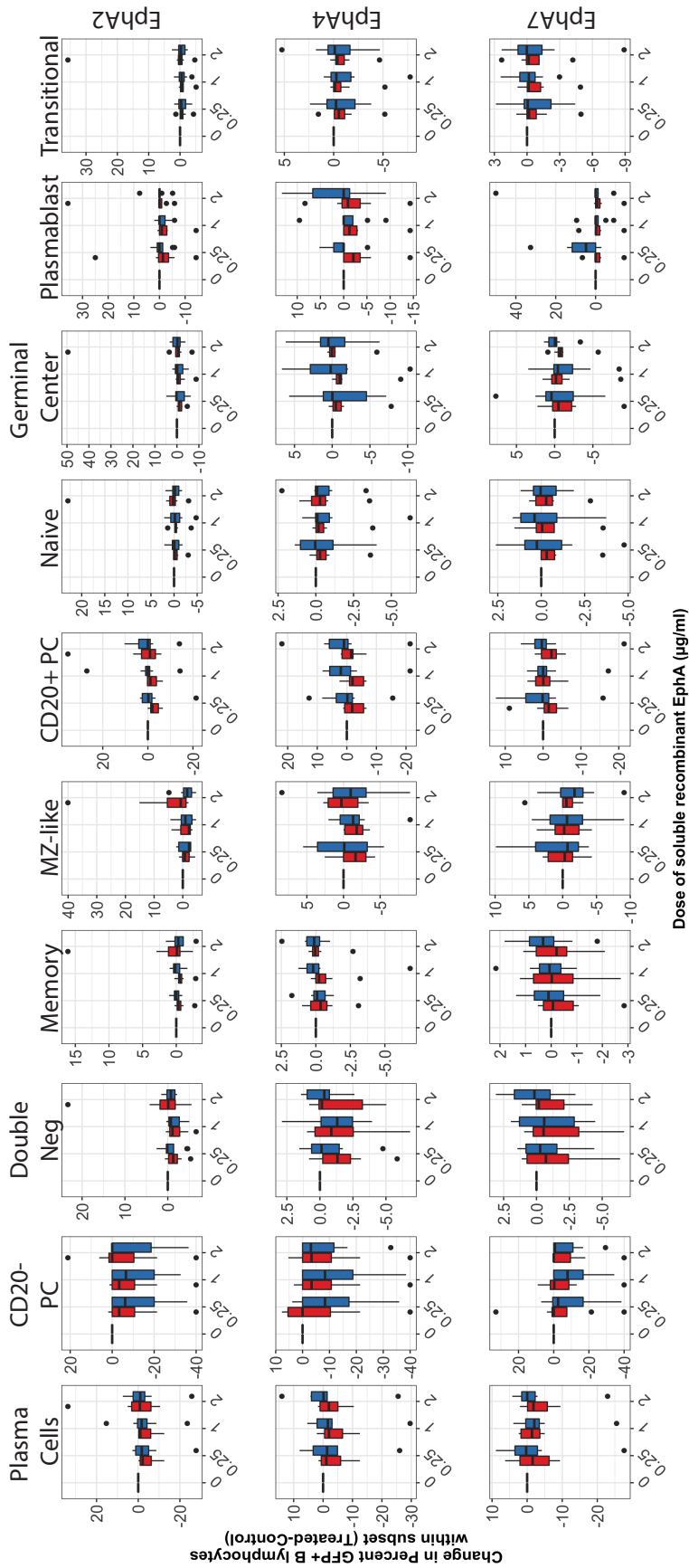
B.2 Three way repeated measures ANOVA analysis of KSHV infection in B cell subsets for soluble EphA neutralization data.

Target B cell subset	Effect	DFn	DFd	F	p	p<.05	ges
Plasma cells	Eph	1.17	8.17	0.066	0.84		0.000447
Plasma cells	Cond	1	7	1.178	0.314		0.022
Plasma cells	Dose	1.36	9.53	2.134	0.176		0.065
Plasma cells	Eph:Cond	2	14	1.315	0.3		0.006
Plasma cells	Eph:Dose	1.96	13.71	1.379	0.284		0.02
Plasma cells	Cond:Dose	1.3	9.11	0.028	0.921		0.001
Plasma cells	Eph:Cond:Dose	1.85	12.96	1.945	0.184		0.023
CD20- Plasma Cells	Eph	1.1	7.67	1.957	0.203		0.008
CD20- Plasma Cells	Cond	1	7	0.202	0.666		0.005
CD20- Plasma Cells	Dose	1.28	8.97	6.55	0.026	*	0.166
CD20- Plasma Cells	Eph:Cond	2	14	0.063	0.939		0.000244
CD20- Plasma Cells	Eph:Dose	2.32	16.23	1.612	0.229		0.01
CD20- Plasma Cells	Cond:Dose	1.26	8.83	0.22	0.706		0.01
CD20- Plasma Cells	Eph:Cond:Dose	1.95	13.62	1.113	0.355		0.007
Double Negative	Eph	1.13	7.92	0.296	0.629		0.003

Double Negative	Cond	1	7	1.08	0.333		0.012
Double Negative	Dose	3	21	2.543	0.084		0.078
Double Negative	Eph:Cond	1.07	7.47	1.68	0.236		0.015
Double Negative	Eph:Dose	1.37	9.58	1.208	0.319		0.028
Double Negative	Cond:Dose	1.25	8.75	0.441	0.567		0.008
Double Negative	Eph:Cond:Dose	1.24	8.65	1.486	0.264		0.038
Memory	Eph	1.13	7.88	0.385	0.577		0.002
Memory	Cond	1	7	0.884	0.378		0.034
Memory	Dose	3	21	1.379	0.277		0.018
Memory	Eph:Cond	2	14	0.979	0.4		0.006
Memory	Eph:Dose	1.33	9.3	0.588	0.509		0.011
Memory	Cond:Dose	3	21	1.087	0.376		0.01
Memory	Eph:Cond:Dose	1.61	11.29	1.866	0.201		0.03
MZ-like	Eph	1.16	8.1	0.971	0.368		0.009
MZ-like	Cond	1	7	0.807	0.399		0.01
MZ-like	Dose	3	21	1.144	0.354		0.022
MZ-like	Eph:Cond	1.07	7.47	1.476	0.265		0.015
MZ-like	Eph:Dose	1.39	9.76	2.034	0.186		0.046
MZ-like	Cond:Dose	3	21	2.529	0.085		0.044
MZ-like	Eph:Cond:Dose	1.26	8.79	1.268	0.304		0.031

CD20+ Plasma Cells	Eph	2	14	0.33	0.725		0.002
CD20+ Plasma Cells	Cond	1	7	0.778	0.407		0.015
CD20+ Plasma Cells	Dose	3	21	0.658	0.587		0.016
CD20+ Plasma Cells	Eph:Cond	2	14	1.136	0.349		0.008
CD20+ Plasma Cells	Eph:Dose	2.32	16.27	1.53	0.246		0.031
CD20+ Plasma Cells	Cond:Dose	3	21	0.249	0.861		0.007
CD20+ Plasma Cells	Eph:Cond:Dose	2.28	15.96	1.177	0.339		0.023
Naive	Eph	1.05	7.33	1.622	0.243		0.012
Naive	Cond	1	7	0.753	0.414		0.017
Naive	Dose	2.03	14.2	1.15	0.345		0.023
Naive	Eph:Cond	1.05	7.35	0.938	0.369		0.008
Naive	Eph:Dose	1.11	7.8	1.21	0.312		0.029
Naive	Cond:Dose	1.62	11.37	0.716	0.482		0.013
Naive	Eph:Cond:Dose	1.12	7.82	1.019	0.354		0.025
Centroblasts	Eph	1.13	7.92	0.233	0.672		0.001
Centroblasts	Cond	1	7	1.232	0.304		0.031
Centroblasts	Dose	3	21	1.357	0.283		0.029
Centroblasts	Eph:Cond	2	14	0.956	0.408		0.008
Centroblasts	Eph:Dose	1.67	11.72	0.649	0.514		0.012
Centroblasts	Cond:Dose	3	21	0.593	0.626		0.012

Centroblasts	Eph:Cond:Dose	1.27	8.9	0.482	0.55		0.011
Centrocytes	Eph	1.04	7.28	1.17	0.317		0.014
Centrocytes	Cond	1	7	0.022	0.886		0.000174
Centrocytes	Dose	2	14.01	0.694	0.516		0.015
Centrocytes	Eph:Cond	1.06	7.43	0.652	0.454		0.003
Centrocytes	Eph:Dose	1.16	8.14	1.363	0.285		0.03
Centrocytes	Cond:Dose	1.32	9.27	1.072	0.35		0.016
Centrocytes	Eph:Cond:Dose	1.09	7.62	0.745	0.426		0.029
Germinal Center	Eph	1.15	8.04	0.746	0.431		0.005
Germinal Center	Cond	1	7	0.753	0.414		0.011
Germinal Center	Dose	1.86	13.05	1.133	0.348		0.028
Germinal Center	Eph:Cond	1.2	8.39	0.905	0.388		0.008
Germinal Center	Eph:Dose	1.2	8.42	1.163	0.325		0.024
Germinal Center	Cond:Dose	3	21	0.58	0.635		0.009
Germinal Center	Eph:Cond:Dose	1.12	7.84	0.781	0.418		0.024
Plasmablast	Eph	2	14	0.852	0.447		0.011
Plasmablast	Cond	1	7	0.622	0.456		0.008
Plasmablast	Dose	3	21	1.455	0.255		0.02
Plasmablast	Eph:Cond	2	14	3.341	0.065		0.023
Plasmablast	Eph:Dose	2.25	15.74	0.444	0.671		0.016

Plasmablast	Cond:Dose	3	21	0.779	0.519		0.014
Plasmablast	Eph:Cond:Dose	2.19	15.35	1.084	0.368		0.027
Transitional	Eph	1	7.03	0.953	0.362		0.009
Transitional	Cond	1	7	0.479	0.511		0.01
Transitional	Dose	1.8	12.61	1.084	0.361		0.022
Transitional	Eph:Cond	1.03	7.18	0.772	0.412		0.007
Transitional	Eph:Dose	1.16	8.09	1.088	0.34		0.028
Transitional	Cond:Dose	1.23	8.61	0.625	0.483		0.01
Transitional	Eph:Cond:Dose	1.12	7.83	0.891	0.386		0.025

Appendix C.

IL-21 signaling promotes early dissemination of KSHV infection in B lymphocytes

Nedaa Alomari[1], Farizeh Aalam[1], Romina Nabiee[1], Jesus Ramirez Castano[1] and Jennifer Totonchy‡

[1]Biomedical and Pharmaceutical Sciences, Chapman University, Irvine, CA USA

‡Corresponding Author

Jennifer Totonchy

Chapman University School of Pharmacy

9410 Jeronimo Road

Irvine, CA

Phone: 714-516-5438

Email: totonchy@chapman.edu

Short Title: IL-21 and KSHV infection of B cells

Abstract

Kaposi's sarcoma-associated herpesvirus (KSHV) extensively manipulates the host immune system and the cytokine milieu, and cytokines are known to influence the progression of KSHV-associated diseases. However, the precise role of cytokines in the early stages of KSHV infection remains undefined. Here, using our unique model of KSHV infection in tonsil lymphocytes, we investigate the influence of host cytokines on the establishment of KSHV infection in B cells. Our data demonstrate that KSHV manipulates the host cytokine microenvironment during early infection and susceptibility generally associated with downregulation of multiple cytokines. However, we show that IL-21 signaling promotes KSHV infection by promoting both plasma cell numbers and increasing KSHV infection in plasma cells. Our data reveal that IL-21 producing T cells, particularly Th17/Tc17 and central memory CD8+ T cells may represent immunological factors that modulate host-level susceptibility to KSHV infection. These results suggest that IL-21 plays a significant role in the early stages of KSHV infection in the human immune system and may represent a novel mechanism to be further explored in the context of preventing KSHV transmission.

Author Summary

Very little is known about how KSHV is transmitted and how it initially establishes infection in a new human host and this lack of information limits our ability to prevent KSHV-associated cancers by limiting its person-to-person transmission. Saliva is thought to be the primary route of person-to-person transmission for KSHV, making the tonsil a likely first site for KSHV replication in a new human host. In particular, the tonsil is likely to be the first place KSHV is able to enter B cells, which are thought to be a major site of persistent infection. Our previous work identified

185

plasma cells as a highly targeted cell type in early KSHV infection in cultured cells from human tonsil. In this study, we show that the human cytokine IL-21 promotes both overall KSHV infection and the establishment of infection in plasma cells. We also investigate the immunological mechanisms underlying this effect. Our results demonstrate that IL-21 and IL-21-producing cells are a novel factor that influences the initial establishment of KSHV infection in humans.

Introduction

Kaposi's Sarcoma Herpesvirus (KSHV) is a lymphotropic gamma-herpesvirus, originally discovered as the causative agent of Kaposi Sarcoma (KS) [1]. KS is a highly proliferative tumor derived from lymphatic endothelial cells [2]. KSHV is also associated with the B cell lymphoproliferative diseases, Primary Effusion Lymphoma (PEL) and Multicentric Castleman's Disease (MCD) [3, 4], as well as the inflammatory disorder KSHV inflammatory cytokine syndrome (KICS) [5]. KSHV is linked to 1% of all human tumors, and the World Health Organization (WHO) has classified it as class I carcinogen [6, 7]. KSHV infection is asymptomatic in most healthy individuals, and KSHV-associated malignancies arise primarily in immunocompromised patients. Indeed, KS remains one of the most common cancers in people living with HIV/AIDS [8].

The geographical distribution of KSHV is not ubiquitous. KSHV infection is endemic in sub-Saharan Africa and in the Mediterranean basin. KSHV prevalence is also high in subpopulations in other parts of the world such as men who have sex with men (MSM). Saliva is the only secretion where KSHV DNA is commonly detected [9], and, based on this, person-to-person transmission of KSHV is thought to occur via saliva. The oral lymphoid tissues are rich in KSHV target cell types including lymphatic endothelial cells and B cells, and are therefore a likely site for the initial

establishment of KSHV infection in a new human host. However, the exact mechanisms for KSHV transmission and how environmental, behavioral and host factors influence transmission and early infection events remain to be established. This gap in our understanding dramatically affects our ability to find efficient strategies to decrease the transmission or influence host-level susceptibility to KSHV infection. One of the main factors that has been linked to KSHV-associated lymphoproliferations is cytokine dysregulation [10]. However, their contribution to the early stages of KSHV infection and whether the cytokine milieu in the oral cavity contributes to host-level susceptibility to KSHV infection is unclear. KSHV-infected cells in KSHV-associated lymphoproliferative diseases generally display plasma cell or plasmablast features [11], and our recent work showed that KSHV targets plasma cells in early infection in tonsil B lymphocytes [12]. Whether the KSHV-infected plasma cells we observe arise from direct infection or differentiation from a precursor B cell subset remains to be established. In either case, it is likely that cytokines play a role in supporting the survival and/or differentiation of KSHV-infected plasma cells.

IL-21 is a pleiotropic cytokine that has diverse effects on B cell, T cell, macrophage, monocyte, and dendritic cell biology. It is produced mainly by natural killer T (NKT) cells and CD4+ T cells, including follicular helper (TFH) cells [13]. The IL-21 receptor is expressed by several immune cells, including B and T cells and is comprised of a unique IL-21R subunit and the common cytokine receptor γ chain (CD132), which is also part of the receptor for IL-2, IL-4, IL-7, IL-9, and IL-15 [14]. IL-21 plays a critical role in B cell activation and expansion [15], and plays a critical role in B cell differentiation to immunoglobulin (Ig)-secreting plasma cells. The regulation of maturation of B cells into plasma cell is driven by the several transcription factors including

187

Blimp1 and Bcl6 [16], which can both be induced by IL-21 signaling, indicating that IL-21 is an important regulator of plasma cell differentiation [17, 18].

There are few studies to date examining the contribution of IL-21 to KSHV infection and KSHV-associated disease. However, IL-21 is detected in interfollicular areas in MCD patients [19]. Moreover, IL-21 induces differentiation of B-lymphoblastoid cell lines (BCLs) into late plasmablasts/early plasma cells and regulates the expression of many latent proteins in EBV[+] Burkitt lymphoma cell lines [20, 21]. Importantly, IL-21 signaling is required for the establishment of MHV-68 infection and the generation for MHV-68 infected long-lived plasma cells in mice [22].

In this study, we use our well-established tonsil lymphocyte infection model to explore whether KSHV alters cytokine secretion early in infection and whether cytokine levels have an effect on the establishment of KSHV infection. We identify IL-21 as a factor that specifically influences KSHV infection in plasma cells, which we previously characterized as a highly targeted cell type in early infection [12]. We demonstrate that IL-21 signaling increases plasma cell levels in our *ex vivo* model system and that this effect promotes overall KSHV infection. We explore the mechanisms of IL-21 signaling by establishing which B cell types are responding IL-21 and what T cell subsets are producing IL-21 in our model.

We determine that expression of IL-21 receptor (IL-21R) on naïve and classical memory T cells is correlated with increased KSHV infection in IL-21 treated cultures, and we demonstrate that both KSHV infection and IL-21 treatment modulates IL-21R expression on B cells. We examine IL-21 secretion by T cell subsets in our tonsil lymphocyte cultures and demonstrate that the magnitude and distribution of IL-21 secretion varies considerably based on tonsil donor, but is not significantly modulated by KSHV infection. Interestingly, RoRγT+ T cells (both CD4+ and CD8+)

188

contributed substantially to IL-21 secretion and were positively correlated with KSHV infection of plasma cells at 3 dpi. Moreover, IL-21 secretion by CD8+ central memory T cells was positively correlated with both overall KSHV infection and plasma cell targeting.

These results identify IL-21 signaling as a factor that influences the establishment of KSHV infection in B lymphocytes and, together with our previous work, underscores the importance of plasma cell biology in the initial establishment of KSHV infection in the oral lymphoid tissues. Based upon this work, we conclude that specific IL-21 secreting T cell subsets represent an important susceptibility factor for KSHV transmission.

Results

Host cytokines influence the establishment of KSHV infection B lymphocytes

Despite the critical interplay between KSHV and host cytokine signaling, little is known about whether cytokines influence host susceptibility to KSHV infection. In fact, the roles of proinflammatory cytokines during KSHV infection have been studied mostly in naturally-infected human B cell lines derived from PEL [23, 24]. In order to examine whether cytokines alter the early stages of KSHV infection in the tonsil, we quantitated the levels of 13 cytokines in the supernatants of Mock and KSHV-infected tonsil lymphocyte cultures at 3 days post-infection using a bead-based multiplex immunoassay. This dataset includes 33 independent infections using 24 unique tonsil specimens. IL-6, IFNg, TNFa and IL-22 were the most prevalent cytokines in our cultures based on the median values overall (Fig 1A, panel order). IL-6 was the only cytokine significantly induced in KSHV-infected cultures compared to Mock cultures (Fig 1A) and the magnitude of IL-6 induction by KSHV infection is far greater than the effect of infection on any

189

other cytokine (Fig 1B). This result is consistent with our previous results in cultures containing only naïve B lymphocytes [25]. Our data also reveals statistically significant reductions in IL-5 and IL-4 concentrations in KSHV-infected cultures compared to Mock cultures (Fig 1A), but these changes are very small compared to those seen with IL-6 (Fig 1B). Interestingly, IFNg concentrations were highly affected by KSHV infection, but there were sample-specific differences in whether this effect was positive or negative (Fig 1B).

In order to determine whether cytokines affect the establishment of KSHV infection, we examined whether the concentration of cytokines in the supernatants of KSHV-infected cultures is correlated with the level of infection in B lymphocytes (based on GFP reporter expression) in the same culture by flow cytometry analysis (Fig 1C & D). On a per-sample level, many individual cytokines (notably IL-6 and IFNg) were induced or repressed independent of susceptibility. However, there is a cluster of highly susceptible samples (ND19, ND40, ND41, ND32, ND4) in which multiple cytokines are repressed in the KSHV-infected cultures (Fig 1C). Pairwise comparisons between overall GFP level in B lymphocytes and the level of each cytokine in the KSHV-infected cultures revealed universally negative correlations between overall KSHV infection and cytokine levels with lower cytokine levels observed in more susceptible samples. These negative correlations were statistically significant for IL-2, IL-9, IL-10, TNFa, IL-4 and IL-22 (Fig 1D). Since plasma cells were identified as a highly targeted cell type in our previous study [12], we examined the correlations between cytokine levels in KSHV-infected cultures and infection in the CD138+ plasma cell subset. This analysis revealed negative correlations similar to those seen with overall infection with IL-13, IL-9, IFNg, TNFa and IL-22 levels showing statistically significant negative correlations with plasma cell infection. However, in this analysis IL-21 levels showed a significant positive correlation with plasma cell infection (Fig 1E). Taken together, these data

190

demonstrate that (1) KSHV infection influences the production of multiple cytokines in our *ex vivo* infection model, (2) lower cytokine levels and/or repression of cytokines during infection are generally associated with higher susceptibility to KSHV infection, (3) several individual cytokines show significant negative associations with susceptibility to KSHV infection and (4) IL-21 is positively correlated with KSHV infection of plasma cells. Overall, these data suggest that distinct inflammatory responses in each tonsil specimen contribute to variable susceptibility to KSHV infection.

IL-21 supplementation increases KSHV infection in tonsil B lymphocytes

Because IL-21 production was positively correlated with plasma cell infection in our initial dataset (Fig 1E), we wanted to examine the impact of manipulating IL-21 levels on the establishment of KSHV infection. To do this, we performed Mock infection or KSHV infection in 12 unique tonsil samples and supplemented the resulting cultures with varying concentrations of recombinant IL-21. At 3 dpi, we analyzed these cultures for GFP+ B lymphocytes by flow cytometry to assess the magnitude of KSHV infection (Fig 2A & B). Although the specimens included in this data set had high variability in their baseline susceptibility, we can see increased infection in response to IL-21 treatment, and the effect seems to be particularly strong in the more susceptible samples (Fig 2A). Normalization of the data to each specimen's untreated control reveals that at 10/12 samples show increased infection upon treatment with 100pg/ml of IL-21. Importantly, most of these concentrations were higher than what was observed in our initial dataset quantitating native cytokine secretion in our culture system (Fig 1A), which may explain why we didn't observe an association of IL-21 secretion with overall infection in that data (Fig 1D). We then repeated these supplementation experiments with only the 100pg/ml dose of recombinant IL-21 in an additional

12 tonsil specimens and examined both overall infection and subset-specific responses in these cultures at 3 dpi using our B cell immunophenotyping panel. Similar to the initial dataset, this analysis shows increased infection in response to recombinant IL-21 in the majority of tonsils, and the difference in GFP+ B lymphocytes was statistically significant in IL-21 treatment compared to control (p=0.02, F=6.4) (Fig 2C).

IL-21 increases plasma cell frequency and susceptibility in primary human tonsil B lymphocytes

In order to determine whether IL-21 signaling influences the overall distribution of B cell subsets in both Mock and KSHV infected cultures, we performed B cell immunophenotyping. Analysis of overall subset frequencies, with all subsets represented as a fraction of viable CD19+ B cells, at 3 dpi revealed that most subsets did not change with either KSHV infection or IL-21 treatment. We did observe a statistically significant increase in CD20+ B cells and plasmablasts in the KSHV-infected conditions independent of IL-21 treatment. Naïve B cells showed significant main effects for both infection and treatment, with both KSHV infection and IL-21 treatment reducing naïve B cells in the culture, but the interaction was not significant. Importantly, this analysis revealed a highly significant increase in total plasma cell frequency associated with both IL-21 treatment and KSHV infection with a significant interaction of the two variables. This effect seems to be restricted to CD20+ plasma cells in the mock conditions and distributed between both CD20+ and CD20- plasma cells in the KSHV-infected cultures. However, both CD20+ and CD20- plasma cells showed statistically significant interactions between infection and treatment (Fig 2D, Table 2). Post hoc paired T tests revealed significant differences with IL-21 treatment on total plasma cells (p=0.0002) and CD20+ plasma cells (p=0.002) for the KSHV-infected conditions only. The

IL-21 effect on naïve B cell frequencies was significant for both Mock (p=0.01) and KSHV infected conditions (p=0.003). Moreover, in IL-21 treated conditions there was a significant difference between Mock and KSHV cultures for total plasma cells (p=0.0003), CD20+ plasma cells (p=0.02) and naïve B cells (p=0.006). One interpretation of this data is that IL-21 can independently drive plasma cell differentiation of B cells in our culture system resulting in decreased naïve cells and increased plasmablast and plasma cells, and KSHV infection acts synergistically with IL-21 to potentiate the same effect. We next wanted to determine whether IL-21 treatment altered the B cell subset-specific distribution of KSHV infection. For this analysis, we quantitated the percent of each B cell subset that was GFP+ to determine the within-subsets distribution of KSHV infection in control or IL-21 treated cultures (Fig 2E). In this analysis, we observed a significant increase in plasma cell targeting with IL-21 treatment (p=0.02, F=6.6). We next examined whether increased frequency of plasma cells or increased plasma cell targeting was directly correlated with the observed increase in overall KSHV infection in the IL-21 treated conditions (Fig 2F). These results reveal a significant linear correlation between total GFP and plasma cell frequency (r=0.7, p=0.007) and a weaker correlation between total GFP and the frequency of GFP+ cells within the plasma cell subset (r=0.56, p=0.04).

Taken together this data shows that IL-21 treatment promotes the establishment of KSHV infection in human tonsil lymphocytes and that this increased infection is correlated with both increased plasma cell frequencies and increased plasma cell infection. Thus, our results suggest that IL-21 signaling facilitates the establishment of KSHV infection by driving the proliferation, survival or differentiation of plasma cells in our tonsil lymphocyte cultures. The observation that naïve B cell frequencies are significantly decreased in KSHV-infected, IL-21-treated cultures (Fig 2D)

supports the latter conclusion that increased plasma cell frequencies are a result of B cell differentiation in response to IL-21 signaling.

Table 2: Statistically significant effects from two-way repeated measures ANOVA analysis in Fig 2D

Variable	Effect	DFn	DFd	F	p	ges
GFP	Treatment	1	13	6.425	0.025	0.081
GFP	Infection	1	13	102.896	1.52e-07	0.708
GFP	Tx:Inf	1	13	7.635	0.016	0.084
Plasma cells	Treatment	1	13	18.596	0.000844	0.163
Plasma cells	Infection	1	13	18.575	0.000848	0.166
Plasma cells (PC)	Tx:Inf	1	13	22.779	0.000364	0.09
Naive	Treatment	1	13	13.643	0.003	0.099
Naive	Infection	1	13	8.462	0.012	0.069
Plasmablast	Infection	1	13	6.023	0.029	0.02
CD20- PC	Tx:Inf	1	13	12.645	0.004	0.043
All CD20+CD19+	Infection	1	13	6.234	0.027	0.016
CD20+ PC	Treatment	1	13	4.858	0.046	0.028

CD20+ PC	Tx:Inf	1	13	7.798	0.015	0.012

Neutralization of IL-21 inhibits KSHV infection in primary tonsil B lymphocytes

We next wanted to determine whether neutralization of the natively-secreted IL-21 in our tonsil lymphocyte cultures would affect the establishment of KSHV infection. To do this we performed infections with Mock or KSHV-infection in 11 unique tonsil specimens, included varying concentrations of an IL-21 neutralizing antibody in the resulting cultures, and assessed the magnitude and distribution of KSHV infection at 3 dpi by flow cytometry. These results revealed decreased KSHV infection in the presence of IL-21 neutralizing antibodies (Fig 3A). One-way repeated measures ANOVA revealed a significant effect of IL-21 neutralization on GFP in KSHV infected cultures (p=0.00001, F=9.4) and post-hoc Dunnett test revealed significance at the 100µg/ml dose (p=0.03). When each sample was normalized to its untreated control, we observed that 9/11 samples had decreased infection in the presence of 100µg/ml IL-21 neutralizing antibody and this increased to 10/11 samples at higher antibody doses (Fig 3B).

When we examined the overall frequency of B cell subsets at 3dpi in these experiments, we observed statistically significant effects of IL-21 neutralization on a number of B cell subsets, but there were no significant interaction effects with IL-21 neutralization and KSHV infection using two-way repeated measures ANOVA (Fig 3C). Specifically, IL-21 neutralization increased IgG+ (p=0.04, F=5.0), memory (p=0.03, F=3.4), and double negative (p=0.02, F=3.8) B cells and decreased IgM+ (p=0.0003, F=8.6) and transitional (p=0.01, F=4.1) subsets. Post-hoc paired T-tests showed a statistically significant decrease of on both overall (p=0.02) and CD20+ (p=0.005)

195

plasma cell frequencies at the 200μg/ml dose in the mock infected cultures only. The observation that the effect of IL-21 neutralization on plasma cell frequencies is restricted to mock infected cultures is interesting in the context of our IL-21 supplementation data where we observed significant main effects of both IL-21 and KSHV infection on plasma cell frequencies as well as a significant interaction between the two factors (Fig 2D & Table 1). The two data sets taken together support several interesting conclusions: (1) IL-21 affects plasma cell frequencies independent of KSHV infection; evidenced by opposite significant effects of IL-21 supplementation and neutralization in mock cultures, (2) KSHV infection affects plasma cell frequencies independent of IL-21 signaling; evidenced by significant main effect of infection in supplemented cultures and a lack of inhibition in KSHV-infected neutralized cultures, and (3) IL-21 and KSHV can synergistically affect plasma cell frequencies; evidenced by the significant interaction effect and the significant increase in plasma cell frequencies in KSHV-infected cultures that are supplemented with IL-21.

We next wanted to determine whether neutralization of IL-21 influences the frequency of KSHV infection within B cell subsets. One-way repeated measures ANOVA revealed a significant effect of neutralization on infection of transitional B cells (p=0.01, F=4.0) but paired T tests were not significant for any individual dose. When we plotted this data normalized to the per-sample, per-subset infection rate of the untreated control cultures, we observed that neutralization was associated with lower levels of infection in transitional, plasmablast, and CD20+ PC populations (Fig 3D). We hypothesized that if IL-21 signaling is affecting overall infection by contributing substantially to differentiation of KSHV-infected cells, we might observe a correlation between overall infection and the contribution of specific subsets to infection within neutralized cultures compared to control cultures. If this hypothesis is correct, subsets whose differentiation is

196

important to the establishment of infection would accumulate with IL-21 neutralization and this accumulation would correlate with decreased overall levels of infection in the same cultures. To examine this, we calculated the change in IL-21 neutralized cultures compared to control cultures (neutralized-control) for both overall infection and the contribution of each subset to infection (between subsets frequency of GFP), and performed correlation analysis using Pearson's method. This analysis reveals that decreased overall infection with IL-21 neutralization was significantly correlated with a decreased contribution of plasma cells (r=0.6, p=0.0002), CD20+ plasma cells (r=0.6, p=0.0002), and transitional B cells (r=0.5, p=0.003) and an increased proportion of infected germinal center cells (r=-0.4, p=0.02) (Fig 3E). Interestingly, these correlations were driven more by sample-specific differences (indicated by point color) compared to dose response of neutralization (indicated by point shape). This data could indicate that IL-21 signaling increases the overall establishment of KSHV infection in tonsil lymphocytes by driving differentiation of KSHV-infected germinal center cells into transitional and CD20+ plasma cells. Our previous studies demonstrated that plasma cells display a mixture of lytic and latent KSHV infection [12]. Therefore, we wanted to determine whether the increase in overall KSHV infection with IL-21 treatment and decrease in infection with IL-21 neutralization is due to IL-21-mediated alterations in KSHV lytic reactivation. To examine this, we performed RT-PCR for LANA (latent) and K8.1 (lytic) on total RNA from untreated, IL-21 supplemented or IL-21 neutralizing antibody treated, KSHV-infected cultures from 8 unique tonsil specimens. GAPDH was used as a housekeeping gene and normalizing factor for the viral gene expression data. This data is consistent with our previous data showing a mix of lytic and latent transcripts in infected lymphocytes [12]. These data reveal no significant influence of either supplementation or neutralization on lytic gene

197

expression (Fig 3F). In the majority of samples K8.1 expression remained unchanged or changes were also reflected in LANA transcripts (Fig 3G).

IL21 receptor distribution in primary human tonsil B lymphocytes affects the magnitude and distribution of KSHV infection

Our data presented thus far demonstrates that IL-21 signaling has a positive effect on the overall establishment of KSHV infection (Fig 2C and 3B) and this increase in overall infection is related to both the absolute number of plasma cells (Fig 2D&F and 3C), and the establishment of infection in plasma cells (Fig 2E&F and 3E). Moreover, our data suggests that the increase in plasma cell numbers and targeting may be due to differentiation of new plasma cells via a process that requires IL-21 signaling to germinal center B cells (Fig 3E). To further address the early stages of the IL-21 response during infection, we examined expression of the IL21 receptor in primary human tonsil B lymphocytes at baseline (day 0) in each tonsil specimen. We observed that IL-21 receptor expression is rare on B cells in tonsil at less than 3% of total viable B cells in most samples (Fig 4A). The distribution of IL-21 receptor positive cells among B cell sub-populations is broad, but IL-21 receptor-expressing B cells are most likely to have an MZ-like or plasmablast immunophenotype (Fig 4B) and on a per-sample basis, either plasmablast or MZ-like subsets dominated the IL-21R positive cells in most tonsil samples (Fig 4C)

In order to determine whether IL-21 receptor expression at baseline influenced the establishment of KSHV infection, we aggregated the untreated conditions from both the supplementation and the neutralization experiments and examined correlations between baseline IL21R distribution and KSHV infection based on overall GFP. This analysis revealed that the proportion of plasmablasts within IL21R+ B cells is significantly correlated with overall susceptibility to KSHV infection

(r=0.81, p=0.0007) (Fig 4D). In experiments where we supplemented cultures with IL-21, the positive effect of IL-21 treatment on overall KSHV infection at 3 dpi (Fig 2C) is correlated with the baseline frequency of IL-21 receptor expression on naïve B cells (r=0.82, p=0.01) and classical memory B cells (r=0.7, p=0.05) (Fig 4E). The significant correlation between the IL-21 response and baseline IL-21 receptor expression is particularly interesting and consistent with our hypothesis that differentiation of naïve B cells into plasma cells contributes to the increase in overall infection we see with IL-21 treatment (Fig 2D).

When we correlated baseline IL21R expression with the positive effect of IL-21 treatment on total plasma cell numbers in KSHV-infected cultures (Fig 2D), no significant positive correlations were found (Fig 4F). This lack of correlation suggests that the plasma cell response to IL-21 at 3 dpi in KSHV infected cultures may be a product of IL-21 receptor up-regulation in response to infection instead of intrinsic baseline levels of IL-21 on plasma cells or plasma cell precursors in our tonsil lymphocyte cultures. Indeed, modulation of IL-21 receptor expression by KSHV infection could be one mechanism for the synergistic promotion of plasma cell numbers we observe with both IL-21 treatment and infection (Fig 2D).

In order to examine this hypothesis, we analyzed IL-21R expression on B cell subsets at 3 dpi in our culture system with or without IL-21 supplementation to determine whether KSHV and/or IL-21 can modulate the response to IL-21 during infection. These results reveal that the majority of effects on IL-21R at 3 dpi are present in both Mock and KSHV-infected cultures, indicating they are a product of the culture system and not driven by KSHV. However, the proportion of plasmablasts within IL21R+ cells was significantly different comparing Mock to KSHV-infected cultures without IL-21 treatment (p=0.03) and this difference was increased with the combination

of KSHV infection and IL-21 treatment (Fig 4G). This result may indicate that infection is affecting IL21R expression on plasmablasts or that KSHV is infecting a precursor B cell and driving differentiation of these cells into IL21R+ plasmablasts. Taken together with the fact that IL-21R expression on plasmablasts at day 0 is highly correlated with overall infection (Fig 4D), these data strongly suggest that plasmablasts play a role in the response of KSHV infection to IL-21 treatment. Although not statistically significant, a similar trend can be observed for IL21R+ plasma cells while the converse trend is seen for IL21R positive germinal center cells (Fig 4G), these observations are consistent with the data from our IL21 neutralization studies that suggests germinal center cells may be differentiating into plasma cells in response to IL-21 signaling (Fig 3E), potentially via a plasmablast intermediate phenotype.

Characterization of T cell subsets producing IL-21 in primary human tonsil B lymphocytes

We next wanted to determine the source of native IL-21 secretion in our culture system, and determine whether the production of IL-21 is affected by KSHV infection. To accomplish this, we utilized an additional immunophenotyping panel for T cell subsets (Table 1 and Supplemental Fig 1) and performed intracellular cytokine staining (ICCS) to identify IL-21 producing T cells at 3 dpi in Mock and KHSV-infected cultures from 14 unique tonsil samples. This data reveals that IL-21 secretion in T cells is highly variable between tonsil lymphocyte cultures, but is not significantly affected by KSHV infection (Fig 5A). More of the IL-21+ cells were CD4+ T cells vs. CD8+ T cells and this distribution was also not affected by KSHV infection (Fig 5B). When we examined the subset-level distribution of IL-21 secretion within T cells, we observed that within CD4+ cells CD45RO+, central memory, TFH and RoRγT+ cells were contributing most to IL-21 secretion.

Among CD8+ T cells, CD45RA+, stem cell memory, central memory and RoRγT+ cells were the highest contributors to IL-21 secretion (Fig 5C). When we examined whether KSHV infection altered the contribution of T cell subsets to IL-21 secretion in these cultures, we found that the contribution of CD4+ CD45RA+, CD4+ RoRγT+ and CD8+ central memory subsets was significantly decreased in KSHV-infected cultures vs. Mock cultures (Fig 5D). However, KSHV infection did not significantly change the overall levels and subset distribution of T cells within these cultures, indicating these are biological changes within T cell subsets and not due to changes in the T cell population during infection (Supplemental Fig 2).

IL-21 secretion by CD8+ central memory T cells influences both overall KSHV infection and plasma cell targeting

We wanted to determine whether IL-21 secretion by any particular T cell subset was correlated with susceptibility to KSHV infection in our experiments. To do this, we performed B cell immunophenotyping analysis to determine the extent and distribution of KSHV infection in the same cultures where ICCS was performed on T cell subsets. When we examined correlations between IL-21 secretion by T cell subsets and overall KSHV infection in B cells we found that only IL-21+ CD8+ central memory cells were significantly correlated (r=0.57, p=0.03) (Fig 6A). Interestingly, when we examined correlations between IL-21+ T cell subsets and the B cell subset-specific distribution of KSHV infection at 3dpi, we found that the positive correlation between IL-21+ CD8+ central memory T cells is coupled with a highly significant positive correlation to the

targeting of plasma cells (r=0.82, p=0.0003) (Fig 6B & 6C). In addition, both CD4+ and CD8+ IL-21+ T cells that express RoRγT+ (the Th17/Tc17-defining transcription factor) were significantly correlated with plasma cell targeting by KSHV (Fig 6B & 6D). These correlations were stronger for CD4+ cells and were coupled with a negative correlation with KSHV-infection of naïve T cells (Fig 6B). When we examined whether baseline (day 0) frequencies of T cell subsets influenced the magnitude and distribution of KSHV infection at 3dpi we found several interesting correlations (1) frequencies of CD8+ central memory cells significantly correlated with KSHV targeting of plasma cell subsets (Fig 6E and 6F), (2) baseline frequencies of CD4+ RoRγT+ cells significantly correlated with infection of CD20+ plasma cells (Fig 6D) and (3) both CD4+ and CD8+ RoRγT+ were negatively correlated with KSHV infection of naïve B cells at 3dpi (Fig 6D). Taken together, these results support a hypothetical model in which CD8+ central memory T cells secrete IL-21, which supports the differentiation, survival or targeting of plasma cells, resulting in higher plasma cell infection frequencies and also an overall increase in dissemination of KSHV within B lymphocytes. Our data also support the conclusion that RoRγT+ T cells are participating in KSHV targeting of plasma cells via IL-21 signaling, possibly by mediating differentiation of naïve B cells, but this effect does not have a significant influence on overall infection in this data set.

Discussion

Our results presented in this study indicate that KSHV can influence cytokine production in tonsil-derived lymphocytes and that the host inflammatory state contributes to the dramatic variation in susceptibility we observe among our tonsil lymphocyte specimens [12]. This result is not surprising considering dysregulation of the inflammatory environment is a hallmark of all KSHV-

associated malignancies [24, 26, 27]. However, the role of the baseline inflammatory environment in the oral cavity as a potentially modifiable susceptibility factor for the acquisition of KSHV infection in humans is an interesting consideration stemming from these results that deserves further study.

Our previous work demonstrated that plasma cells are highly targeted during early KSHV infection, and subsequent results from our group have shown that manipulations which increase plasma cell numbers also increase overall KSHV infection in B cells [28]. This latter observation suggested that, in addition to being a highly targeted cell type, plasma cells are playing an active role in early infection events that ultimately influences the success of initial dissemination for KSHV within the B cell compartment. The results presented herein are consistent with that conclusion, and mechanistically extend our understanding of how the immune microenvironment influences the establishment of infection in plasma cells. Specifically, we uncovered a critical role for IL-21 signaling in this process.

While the precise role of IL-21 and IL-21R in human KSHV disease is poorly characterized, IL-21 has been studied in the pathogenesis of chronic lymphocytic choriomeningitis virus (LCMV) infection, influenza virus, and, perhaps most relevant to this study, murine gammaherpesvirus 68 (MHV68) [22, 29, 30]. Collins and Speck recently used IL-21R knockout mice to demonstrate that IL-21 signaling is critical for the establishment of MHV68 latency specifically in B cells. Interestingly, this study showed that the mechanisms of decreased infection were related to decreases in both germinal center and plasma cell frequencies as well as decreased infection in both the germinal center and plasma cell compartment at later timepoints post-infection [22], suggesting a critical mechanism for IL-21 in MHV68 transit of the germinal center and

differentiation of follicular-derived plasma cells. These results are generally consistent with our current findings showing that IL-21 signaling promotes KSHV infection and dissemination in tonsil via promotion of both plasma cell frequencies and plasma cell targeting (Fig 2&3), potentially via differentiation through a germinal center intermediate (Fig 3E). Despite this, our data presented herein do not adequately address the question of whether plasma cells are differentiating in response to KSHV infection and IL-21 signaling, or whether the effect we see is increased survival or expansion of existing plasma cells. Studies are currently ongoing to address this question more directly, and to examine the influence of viral and cellular factors on B cell differentiation in our model system.

Moreover, both IL-21 and IL-6, which is highly induced in our KSHV-infected cultures (Fig 1), are involved in the generation of RoRγT+ T cells via STAT3 signaling. The resulting Th17 cells produce IL-17A which is another cytokine that promotes the establishment of chronic MHV68 infection via promotion of the MHV68-mediated germinal center response [31] and is mechanistically linked to suppression of T cell-intrinsic IRF-1 [32]. These results are particularly interesting in light of our current findings showing that IL-21 secretion from, and baseline levels of, RoRγT+ T cells correlate with the early targeting of plasma cells during KSHV infection (Fig 6B and 6D), suggesting that the Th17/Tc17 environment in the tonsil may be a critical factor influencing donor-specific susceptibility to KSHV infection. Indeed, as an important site for mucosal immunity in the oral cavity, the Th17/Tc17 environment in tonsil is highly dynamic and physiologically important. In fact, Th17 cells play a major role in host defenses against several pathogens and immunopathogenesis [33, 34]. Many studies have shown that certain parasites modulate the immune response by inducing Th17 [35, 36]. Previous finding suggest that parasite

infection is linked with KSHV infection in Uganda [37]. Thus, the parasite burden in sub-Saharan Africa may modulate susceptibility to KSHV infection via manipulating Th17/Tc17 frequencies.

Consistent with the MHV68 literature, our current results mechanistically implicate germinal center cells in these observations. However, although our *ex vivo* model of KSHV infection in primary lymphocytes is a powerful tool, it certainly does not recapitulate the complex interactions that are needed for a functional germinal center reaction, so further examination of these particular mechanisms will require the utilization of an alternative model system, such as a humanized mouse. Interestingly, neither IL-21 secretion from, nor baseline levels of, CXCR5+, PD1+ TFH cells correlated with increased KSHV infection or increased plasma cell targeting in our study. This was surprising given that TFH are generally considered the canonical IL-21 producing cells in secondary lymphoid organs [38]. This observation may indicate that IL-21 acts support plasma cell numbers during infection via an extrafollicular pathway, which is consistent with literature implicating extrafollicular maturation of KSHV-infected B cells in the pathogenesis of MCD [39].

We observed that IL-21 secretion by CD8+ T cells with a central memory immunophenotype (CCR7+CD45RO+CD28+) was significantly correlated with both overall KSHV infection and plasma cell targeting, and baseline levels of CD8+ central memory T cells were also correlated with plasma cell targeting at 3 dpi (Fig 6). Interestingly, recent studies have shown that IL-6 regulates IL-21 production in CD8+ T cells in a STAT3-dependent manner, and that CD8+ T cells induced in this way can effectively provide help to B cells [40]. Thus, the induction of human IL-6 during KSHV infection may modulate the function of CD8+ T cells in a way that favors the establishment and dissemination of KSHV infection within the lymphocyte compartment independent of traditional CD4+ helper T cells, which would be an interesting dynamic in the

context of CD4+ T cell immunosuppression associated with HIV infection where KSHV-mediated malignancies are common.

Material and Methods

Ethics Statement. Human specimens used in this research were de-identified prior to receipt, and thus were not subject to IRB review as human subjects research.

Reagents and Cell Lines. CDw32 L cells (CRL-10680) were obtained from ATCC and were cultured in DMEM supplemented with 20% FBS (Sigma Aldrich) and Penicililin/Streptomycin/L-glutamine (PSG/Corning). For preparation of feeder cells CDw32 L cells were trypsinized and resuspended in 15 ml of media in a petri dish and irradiated with 45 Gy of X-ray radiation using a Rad-Source (RS200) irradiator. Irradiated cells were then counted and cyropreserved until needed for experiments. Cell-free KSHV.219 virus derived from iSLK cells [39] was a gift from Javier G. Ogembo (City of Hope). Human tonsil specimens were obtained from the National Disease Research Interchange (NDRI; ndriresource.org). Human fibroblasts for viral titering were derived from primary human tonsil tissue and immortalized using HPV E6/E7 lentivirus derived from PA317 LXSN 16E6E7 cells (ATCC CRL-2203). Antibodies for flow cytometry were from BD Biosciences and Biolegend and are detailed below. Recombinant human IL-21 was from Preprotech (200-21) and IL-21 neutralizing antibody was from R&D Systems (991-R2).

Isolation of primary lymphocytes from human tonsils. De-identified human tonsil specimens were obtained after routine tonsillectomy by NDRI and shipped overnight on wet ice in DMEM+PSG. All specimens were received in the laboratory less than 24 hours post-surgery and were kept at 4˚C throughout the collection and transportation process. Lymphocytes were extracted by dissection and maceration of the tissue in RPMI media. Lymphocyte-containing

media was passed through a 40µm filter and pelleted at 1500rpm for 5 minutes. RBC were lysed for 5 minutes in sterile RBC lysing solution (0.15M ammonium chloride, 10mM potassium bicarbonate, 0.1M EDTA). After dilution to 50ml with PBS, lymphocytes were counted, and pelleted. Aliquots of $5(10)7$ to $1(10)8$ cells were resuspended in 1ml of freezing media containing 90% FBS and 10% DMSO and cryopreserved until needed for experiments.

Infection of primary lymphocytes with KSHV. Lymphocytes were thawed rapidly at 37˚C, diluted dropwise to 5ml with RPMI and pelleted. Pellets were resuspended in 1ml RPMI+20%FBS+100µg/ml DNaseI+ Primocin 100µg/ml and allowed to recover in a low-binding 24 well plate for 2 hours at 37˚C, 5% CO2. After recovery, total lymphocytes were counted and naïve B cells were isolated using Mojosort Naïve B cell isolation beads (Biolegend 480068) or Naïve B cell Isolation Kit II (Miltenyi 130-091-150) according to manufacturer instructions. Bound cells (non-naïve B and other lymphocytes) were retained and kept at 37˚C in RPMI+20% FBS+ Primocin 100µg/ml during the initial infection process. $1(10)^6$ Isolated naïve B cells were infected with iSLK-derived KSHV.219 (dose equivalent to the ID20 at 3dpi on human fibroblasts) or Mock infected in 400ul of total of virus + serum free RPMI in 12x75mm round bottom tubes via spinoculation at 1000rpm for 30 minutes at 4˚C followed by incubation at 37˚C for an additional 30 minutes. Following infection, cells were plated on irradiated CDW32 feeder cells in a 48 well plate, reserved bound cell fractions were added back to the infected cell cultures, and FBS and Primocin (Invivogen) were added to final concentrations of 20% and 100µg/ml, respectively and recombinant cytokines or neutralizing antibodies were also added at this stage, depending upon the specific experiment. Cultures were incubated at 37˚C, 5% CO2 for the duration of the experiment. At 3 days post-infection, cells were harvested for analysis by flow

cytometry and supernatants were harvested, clarified by centrifugation for 15 minutes at 15,000 rpm to remove cellular debris, and stored at -80˚C for analysis.

Bead-based immunoassay for supernatant cytokines. Clarified supernatants were thawed on ice and 25µl of each was added to a 13-plex LEGENDplex (Biolegend) bead-based immunoassay containing capture beads for the following analytes: IL-5, IL-13, IL-2, IL-9, IL-10, IL17A, IL-17F, IL-6, IL-21, IL-22, IL-4, TNF-α, and IFN-γ. These assays were performed according to the manufacturer's instructions, data was acquired for 5000 beads per sample (based on approximately 300 beads per analyte recommended by the manufacturer) using a BD FACS VERSE flow cytometry analyzer and cytokine concentrations in the experimental supernatants was calculated from standard curves using the LEGENDPlex software.

Flow cytometry analysis of baseline lymphocyte subsets and KSHV infection. Approximately $5(10)^6$ lymphocytes per condition were harvested into a 96- well round bottom plate at day 0 (baseline) or at 3 days post-infection at 1500 rpm for 5 minutes. Cells were resuspended in 100µl PBS containing zombie violet fixable viability stain (BL Cat# 423113) and incubated on ice for 15 minutes. After incubation, cells were pelleted and resuspended in 100ul PBS, containing the following: 2% FBS and 0.5% BSA (FACS Block) was added to the wells. Cells were pelleted at 1500rpm 5 minutes and resuspended in 200ul FACS Block for 10 minutes on ice. Cells were pelleted at 1500rpm for 5 minutes and resuspended in 50µl of PBS with 0.5% BSA and 0.1% Sodium Azide (FACS Wash), **For B cell frequencies** 10µl BD Brilliant Stain Buffer Plus and antibodies as follows: IgD-BUV395 (2.5µl/test BD 563823), CD77-BV510 (2.0 µl/ test BD 563630), CD138- BV650 (2µl/test BD 555462), CD27-BV750 (2µ/test BD 563328), CD19-PerCPCy5.5 (2.0µl/test BD 561295), CD38-APC (10µl/test BD 560158), CD20-APCH7 (2ul/test

BL 302313), IgM (2μl/test BL 314524), IgG (2μl/test BD 561298), IgE (2μl/test BD 744319) and IL-21 receptor (2μl/test BD 330114). **For baseline T cell frequencies**. For baseline T cell frequencies $0.5(10)^6$ cells from baseline uninfected total lymphocyte samples were stained and analyzed as above with phenotype antibody panel as follows: CD95-APC (2μl, Biolegend 305611), CCR7-PE (2μl, BD 566742), CD28-PE Cy7 (2μl, Biolegend 302925), CD45RO-FITC (3μl, Biolegend 304204), CD45RA-PerCP Cy5.5 (2μl, 304121), CD4-APC H7 (2μl, BD 560158), CD19-V510 (3μl, BD 562953), CD8-V450 (2.5μl, BD 561426). and incubated on ice for 15 minutes. After incubation, 150μl FACS Wash was added. Cells were pelleted at 1500rpm for 5 minutes followed by two washes with FACS Wash. Cells were collected in 200μl FACS Wash for flow cytometry analysis. Cells were analyzed using an LSR Fortessa X-20 cell analyzer (BD Biosciences). BD CompBeads (51-90-9001229) were used to calculate compensation for all antibody stains and methanol-fixed Namalwa cells (ATCC CRL1432) +/- KSHV were used to calculate compensation for GFP and the fixable viability stain. Flow cytometry data was analyzed using FlowJo software and exported for quantitative analysis in R as described below.

ICCS for IL-21 secretion. At 3dpi, cultures were treated for 6 hours with [4 ul for every 6ml of cel culture] monensin to block cytokine secretion. Following incubation, approximately 1 million cells were harvested and viability and surface staining for T cell lineage markers was performed as described above. After the final wash, cells were fixed for 10 minutes in BD cytofix/cytoperm (51-2090KZ), pelleted and further treated for 10 minutes with cytofix/cytoperm+10% DMSO (superperm) to more effectively get intracellular antibodies into the nucleus. Intracellular antibodies, as follows, were diluted in 1x BD Permwash (51-2091KZ) and left on fixed cells overnight at 4˚C. RoR-γT-BV421 (563282, 5μl/test), FoxP3-BB700 (566527, 5 μl/test), IL-21-

APC (513007, 5 μl/test), BLC6-BV711 (561080, 5μl/test). Cells were then washed twice with 1x permwash and analyzed as described above.

RT-PCR. At 3 days post infection, $1(10)^6$ lymphocytes were harvested into an equal volume of Trizol and DNA/RNA shield (Zymo Research R110-250). Total RNA was extracted using using Zymo Directzol Microprep (Zymo Research R2060) according to manufacturer instructions. RNA was eluted in 10μl H2O containing 2U RNase inhibitors and a second DNase step was performed for 30 minutes using the Turbo DNA-Free kit (Invitrogen AM1907M) according to manufacturer instructions. One-step RT-PCR cDNA synthesis and preamplification of GAPDH, LANA and K8.1 transcripts was performed on 15ng of total RNA using the Superscript III One-step RT-PCR kit (ThermoFisher 12574026).

Duplicate no RT (NRT) control reactions were assembled for each sample containing only Platinum Taq DNA polymerase (Thermofisher 15966005) instead of the Superscript III RT/Taq DNA polymerase mix. After cDNA synthesis and 20 cycles of target pre-amplification, 2μl of pre-amplified cDNA or NRT control reaction was used as template for multiplexed real-time PCR reactions using TaqProbe 5x qPCR MasterMix -Multiplex (ABM MasterMix-5PM), 5% DMSO, primers at 900nM and probes at 250nM against target genes. All primer and probe sequences used in these assays have been previously published [12]. Real time PCR was performed using a 40-cycle program on a Biorad real time thermocycler. Data is represented as quantitation cycle (Cq) and assays in which there was no detectable Cq value were set numerically as Cq = 41 for analysis and data visualization. The expression of each gene was normalized to that of a housekeeping gene *GAPDH*.

Statistical Analysis. The indicated data sets and statistical analysis were performed in Rstudio software using ggplot2 [41], ggcorrplo [42] , and tidyverse [43] packages. Statistical analysis was performed using rstatix [44] package. Specific methods of statistical analysis including Anova, independent t-test and Pearson correlations and resulting values for significance and correlation are detailed in the corresponding figure legends.
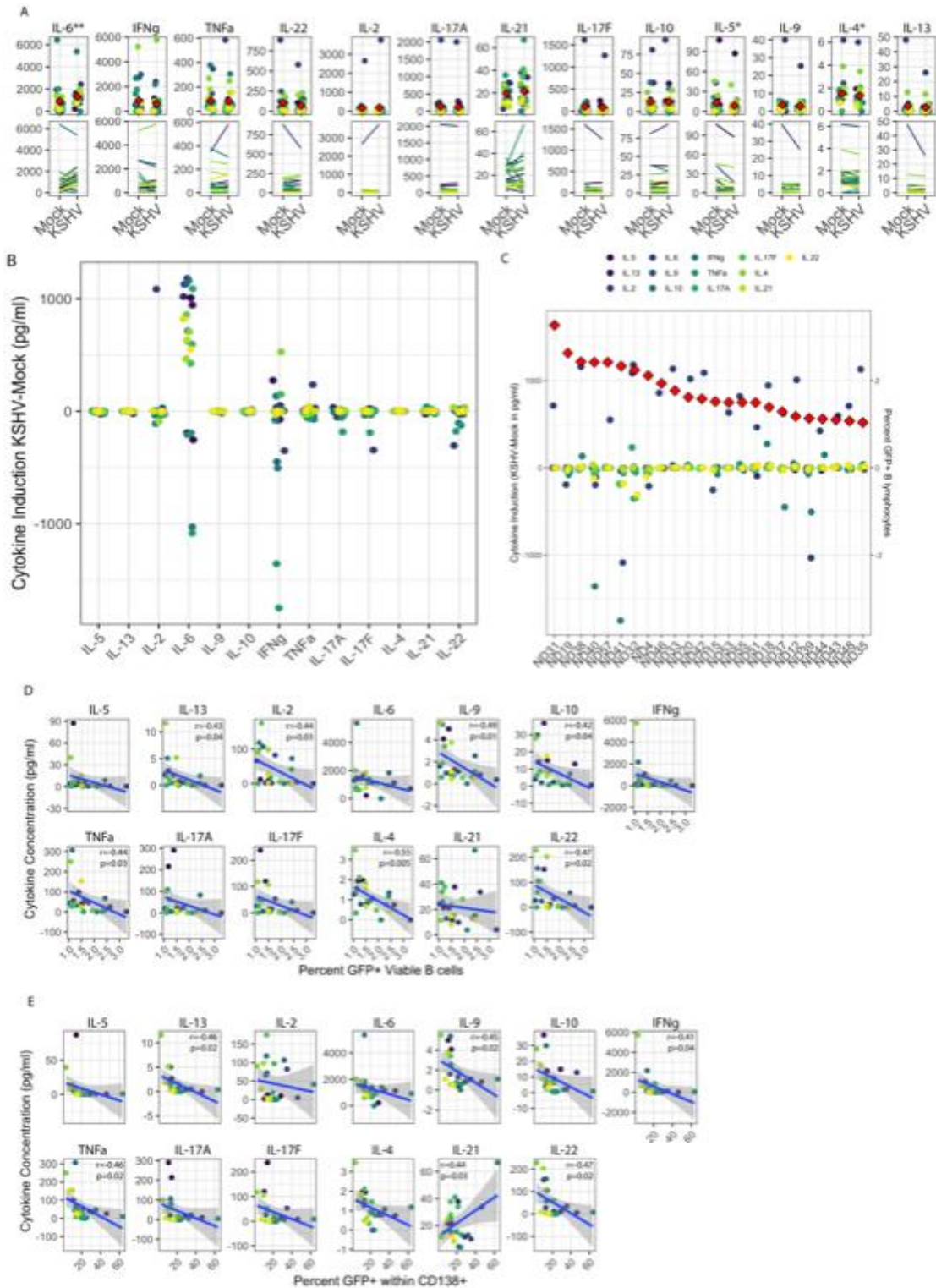
Figure 1: KSHV alters cytokine secretion and cytokines affect the establishment of infection.
33 replicate infections using 24 unique tonsil specimens were performed using KSHV.219 infection of naïve B lymphocytes followed by reconstitution of the total lymphocyte environment and culture on CDW32 feeder cells. At 3 dpi, cells were collected for flow cytometry analysis for infection (GFP) and B cell subsets using our previously-characterized immunophenotyping panel and supernatants were collected for analysis of cytokines by multiplex immunoassay (Biolegend Legendplex) **(A)** cytokine production in Mock and KSHV-infected cultures showing individual sample quantities and means (red diamonds, top panels) and matched Mock and KSHV samples to show trends of induction/repression (bottom panels) Statistical analysis was performed by one-way repeated measures ANOVA. p=0.01 F=7.06 for IL-5, p=0.0001 F=14 for IL-6, p=0.5 F=4.3 for IL-4 **(B)** Data as in (A) showing the level of induction or repression of each cytokine comparing KSHV to matched Mock cultures **(C)** Induction or repression of all cytokines (left y-axis) on a per-sample basis ordered based on overall susceptibility based on percentage of GFP+ B lymphocytes in the same culture (right y-axis, red diamonds) **(D)** Pairwise correlations using Pearson method between cytokine concentration (y-axis) and overall infection (x-axis) in KSHV-infected lymphocyte cultures **(E)** Pairwise correlations using Pearson method between cytokine concentration (y-axis) and Percent GFP+ within CD138+ (x-axis) in KSHV-infected lymphocyte cultures. For panels A, B, D and E colors indicate individual tonsil specimens and can be compared between panels.
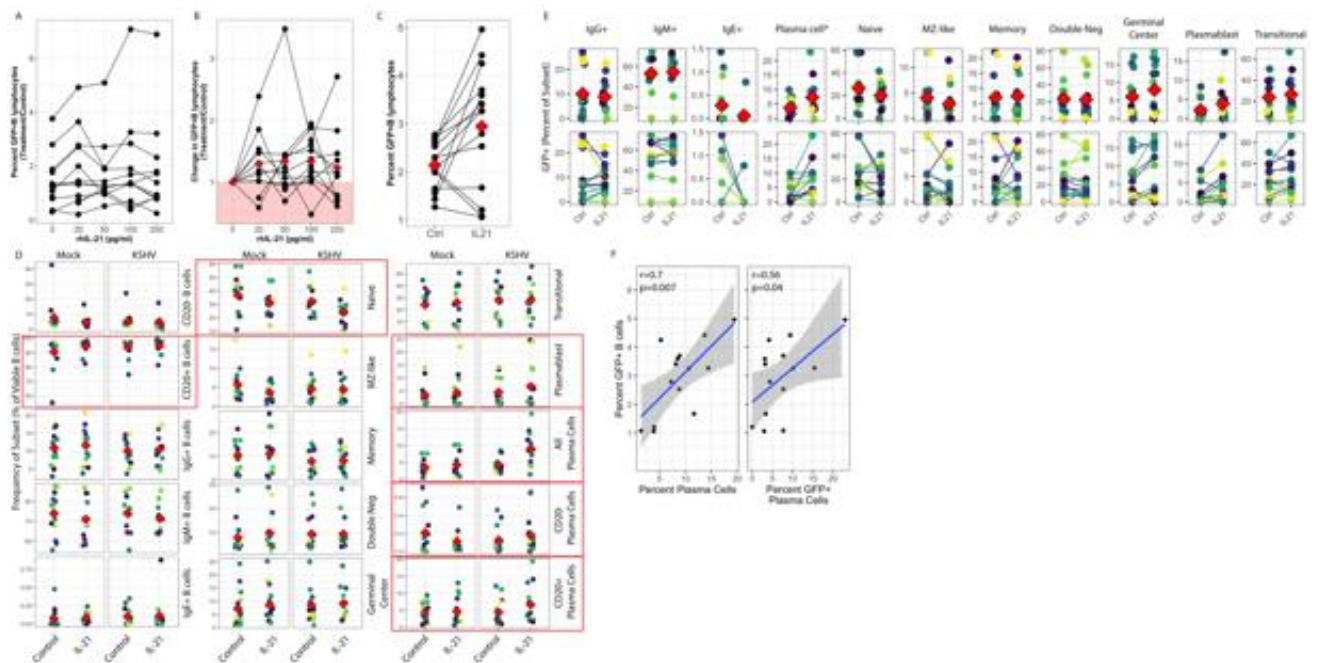
Figure 2: IL-21 supplementation increases overall KSHV infection and plasma cell frequencies. Lymphocytes from 12 tonsil donors were infected with KSHV.219 and cultured with indicated doses of recombinant human IL-21 and analyzed at 3dpi by flow cytometry (A) the dose effect of IL-21 supplementation on GFP+ viable B lymphocytes. (B) data as in (A) normalized to the untreated control for each specimen. (C) 14 additional tonsil donors analyzed as in (A) with only 100pg/ml IL-21 treatment. Red diamonds indicate group means. p=0.02, F=6.4 via one-way repeated measures ANOVA. (D) tonsil lymphocyte specimens from (C) were stained for B cell immunophenotypes and analyzed by flow cytometry. Red boxes indicate subsets with significant main effects of, and/or interactions between, KSHV infection and IL-21 treatment by two-way repeated measures ANOVA analysis. See Table 1 for p-values and F statistics from this analysis. (E) immunophenotyping data was used to determine the within-subset frequency of GFP+ cells in the KSHV-infected conditions with or without IL-21 treatment. Top panels show individual sample quantities and means (red diamonds) and bottom panels show trends of

214

increased/decreased subset targeting on a per-sample basis. Colored points denote unique tonsil specimens and can be compared between panels D and E. (F) Pearson correlation between overall GFP+ B cells in KSHV-infected, IL-21 treated cultures as in (C) and the level of plasma cells (right) and infection of plasma cells (left). Blue line is linear model regression and grey shading indicates 95% confidence interval.
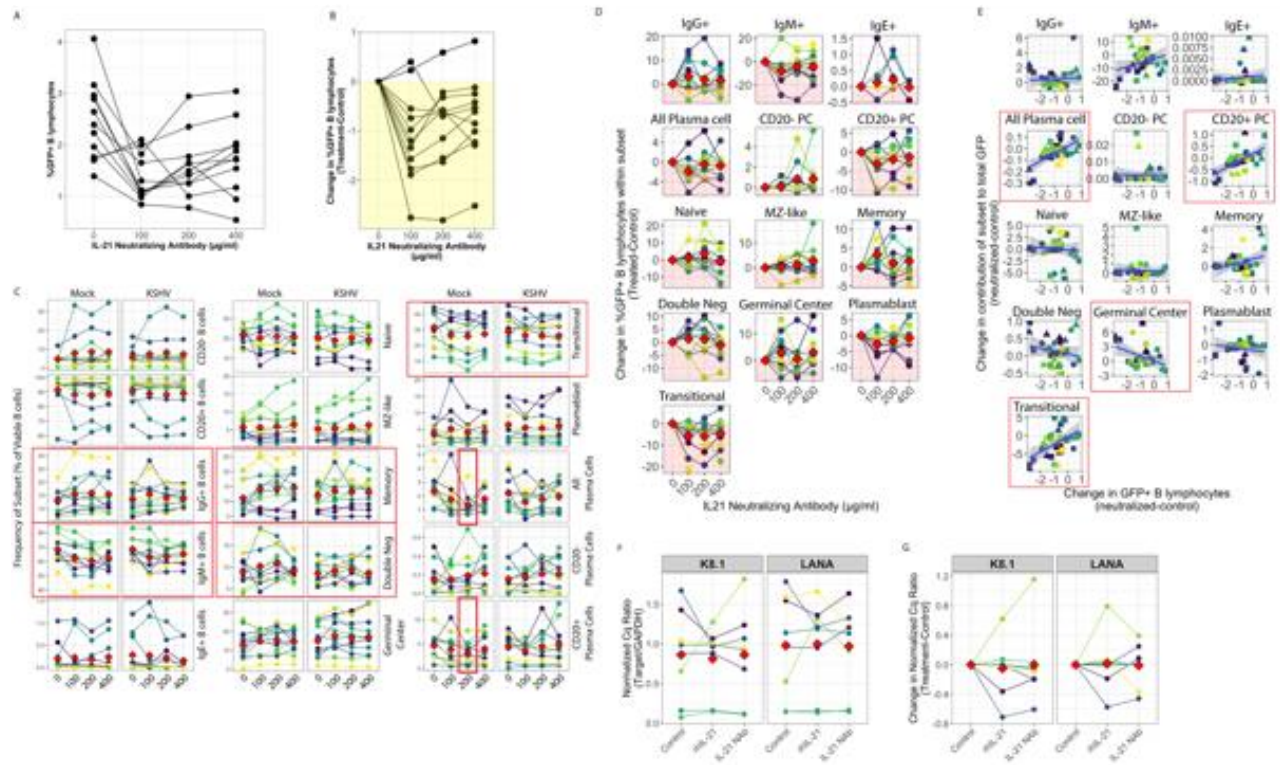
Figure 3: IL-21 neutralization inhibits the establishment of KSHV infection. Naïve B cells from 11 unique tonsil specimens were Mock or KSHV-infected and indicated concentrations of IL-21 neutralizing antibody was added to the resulting total lymphocyte cultures. Cultures were analyzed at 3 dpi for B lymphocyte immunophenotypes and the distribution of KSHV infection via GFP expression. Total GFP+ viable B lymphocytes represented as (A) raw percentages or (B) normalized to the untreated control for each tonsil sample. For (A) one-way repeated measures ANOVA shows p=0.00001, F=9.4 for the main effect of IL-21 neutralization and Dunnett's test reveals p=0.03 at the 100µg/ml dose. (C) frequencies of B cell subsets in the cultures. Red boxes indicate significant results as follows: Two-way repeated measures ANOVA on the raw data showed significant effects of IL-21 treatment on B subset frequencies; IgG+ (p=0.04, F=5.0),

memory (p=0.03, F=3.4), and double negative (p=0.02, F=3.8), IgM+ (p=0.0003, F=8.6), transitional (p=0.01, F=4.1). Post-hoc paired T-tests showed significant effect of 200μg/ml neutralizing antibody on total plasma cells (p=0.02) and CD20+ plasma cells (p=0.005) in Mock cultures only. (D) Effect of indicated doses of IL-21 neutralizing antibody on KSHV infection of B cell subsets. Data is normalized to each sample's untreated control level for each B cell subset. One-way repeated measures ANOVA on the raw data reveals a significant effect on infection of transitional B cells (p=0.01, F=4.0). (E) Correlation between the effect of IL-21 neutralization on overall infection (x-axis) and the contribution of each subset to KSHV infection in the same condition (y-axis). Shapes indicate doses in this panel (circle=100μg/ml, triangle=200μg/ml, square=400μg/ml). Subsets with statistically significant correlations are indicated by red boxes with statistics from Pearson's linear correlation as follows: CD20+ plasma cells (r=0.6, p=0.0002), plasma cells (r=0.6, p=0.0003), transitional (r=0.5, p=0.004), germinal center (r=-0.4, p=0.02). For panels C-E colors indicate unique tonsil specimens and can be compared between these panels and red diamonds indicate the mean value for all tonsil specimens. RT-PCR analysis of KSHV transcripts at 3 dpi in 8 unique tonsil specimens with either IL-21 supplementation at 100 pg/ml (Fig 2) or IL-21 neutralizing antibody at 100μg/ml with LANA (latent) and K8.1 (lytic) transcript targets. No RT controls were used to determine that RT-PCR signal is not due to DNA contamination (F) Cq values for viral targets normalized to the within-sample Cq for GAPDH (G) GAPDH-normalized values further normalized to the within-sample value for the untreated control.
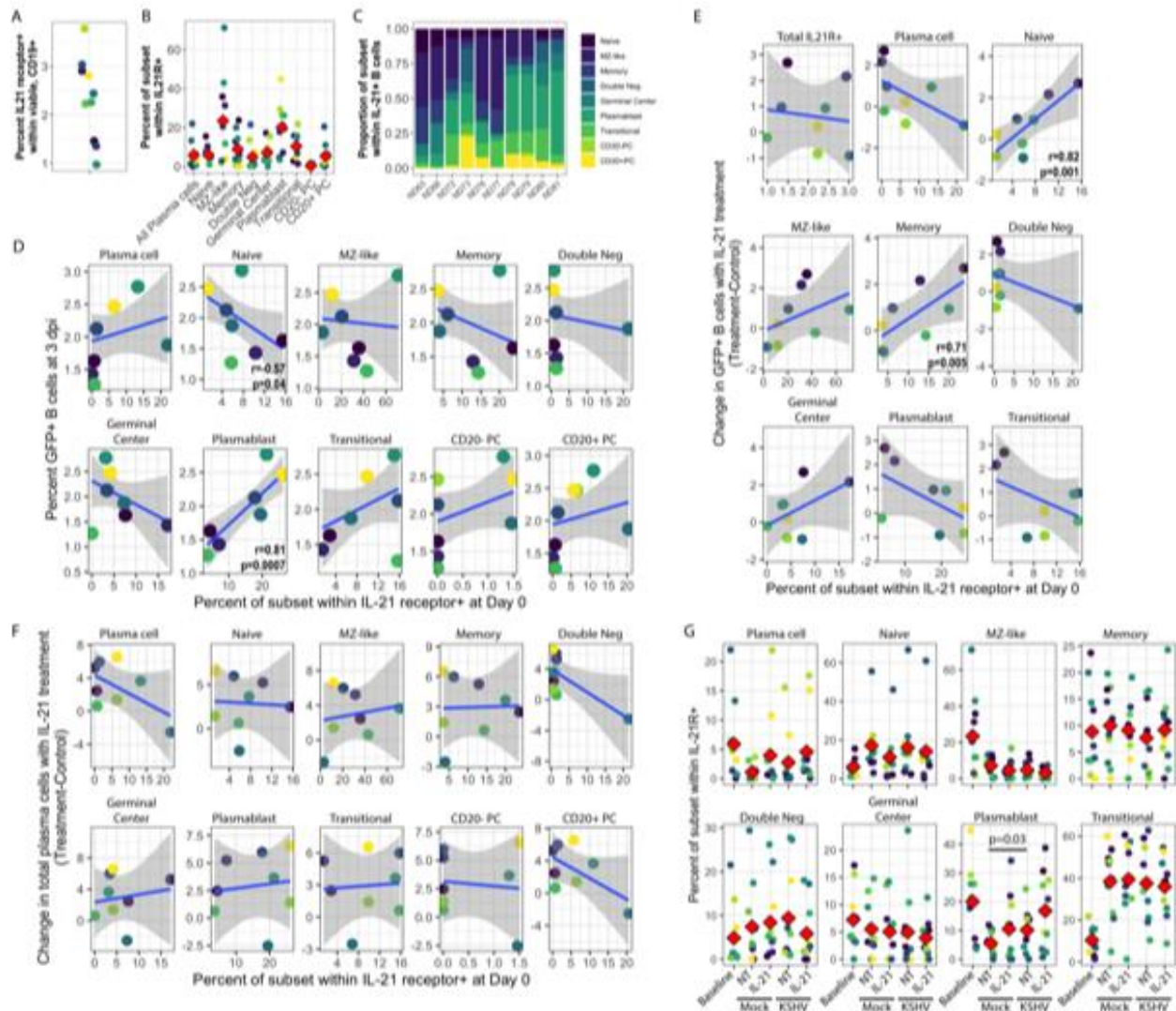
Figure 4: IL21 receptor distribution in primary human tonsil B lymphocytes affects the magnitude and distribution of KSHV infection. B cell immunophenotyping analysis including IL-21R was performed at baseline (Day 0) for 10 unique tonsil specimens. (A) total percentage of IL-21R+ within viable CD19+ B cells. (B) Percent of individual B cell subsets within IL-21+ B cells. Red diamonds indicate the mean value for all tonsil specimens and (C) distribution of B cell subsets within IL-21+ on a per-tonsil basis. (D) correlation analysis of baseline IL-21 receptor distribution within subsets and the overall susceptibility of the same tonsil specimen to KSHV infection at 3 dpi. Pearson correlation coefficients and p-values are denoted on panels where the

218

result is statistically significant. (E) correlation analysis of baseline IL-21 receptor distribution with the effect of IL-21 supplementation on overall KSHV infection in the same tonsil specimens. Pearson correlation coefficients and p-values are denoted on panels where the result is statistically significant. (F) correlation analysis of baseline IL-21 receptor distribution with the IL-21 mediated increase in total plasma cell numbers at 3dpi in KSHV-infected cultures in the same tonsil specimens. (G) Distribution of IL-21 receptor at day 0 (baseline) or 3dpi within Mock, Mock+100ng/ml IL-21, KSHV or KSHV+ 100ng/ml IL-21 conditions. Red diamonds indicate the mean values for each condition and significant differences were assessed via paired T-test.
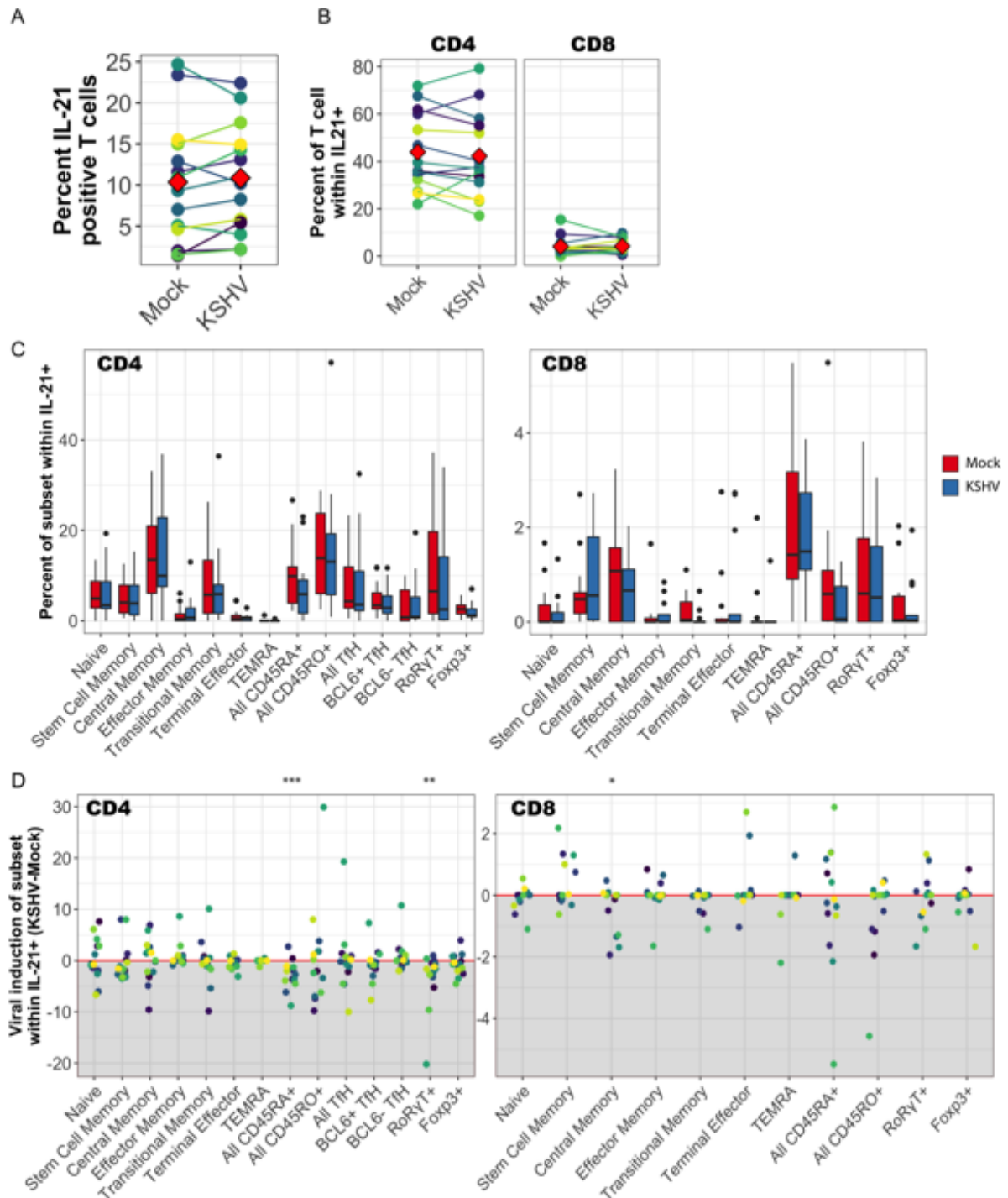
Figure 5: Characterization of T cell subsets producing IL-21 in primary human tonsil B lymphocytes. T cells were analyzed by surface immunophenotyping, intracellular transcription

factor staining and ICCS for IL-21 secretion in Mock and KSHV-infected total lymphocyte cultures at 3 dpi in 14 unique tonsil specimens. (A) Total IL-21+ viable non-B cells (B) percent of CD4+ or CD8+ T cells within IL-21+. For (A) and (B) red diamonds indicate the mean value for the condition and colors indicate specific tonsil specimens and can be compared between the panels. (C) Immunophenotypic analysis of T cell subsets (Table 1) within IL-21+ in Mock (red) and KSHV (blue) cultures. (D) Data as in (C) but normalized to show the induction or repression of the T cell subset within IL-21+ cells (KSHV-Mock). *p=0.05; **p=0.04; ***p=0.003 comparing Mock and KSHV-infected via paired T test pre-normalization.
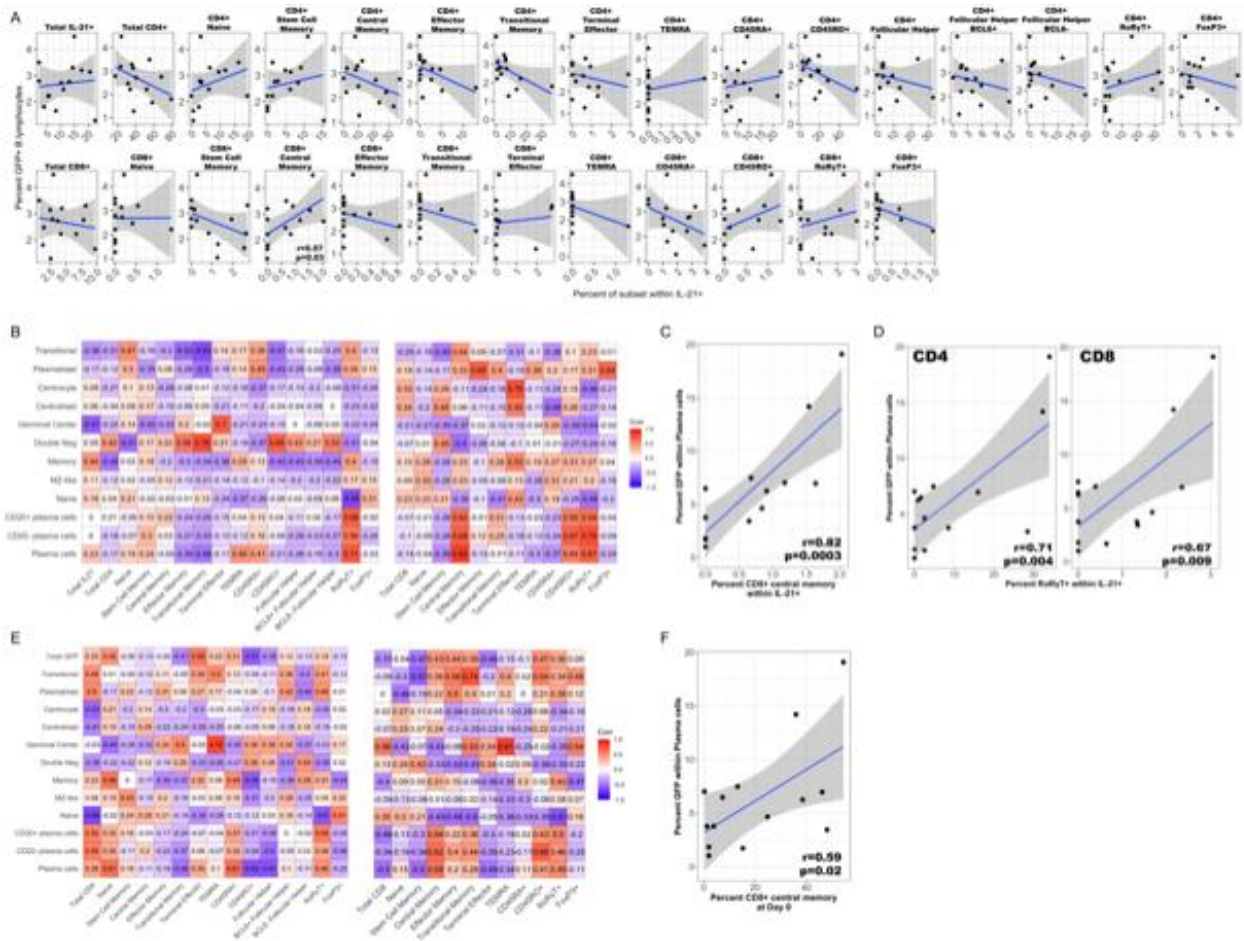
Figure 6: IL-21 secretion by CD8+ central memory T cells influences both overall KSHV infection and plasma cell targeting. Lymphocyte cultures from the experiments shown in Fig 5 were further analyzed for B cell subsets and the magnitude and distribution of KSHV infection. (A) correlation analysis of total GFP+ within viable, CD19+ B lymphocytes at 3 dpi with total IL-21 secretion in non-B cells or the contribution of individual T cell subsets to IL-21 secretion. Pearson's correlation coefficient and p-value is shown on panels that have statistically significant correlations. (B) correlogram of Pearson correlations between the distribution of KSHV infection within B cell subsets (y-axis) and total IL-21 or the contribution of individual T cell subsets to IL-21 secretion (x-axis). Pearson's r values with an absolute value greater than or equal to 0.53 are

222

statistically significant for this dataset. (C) scatterplot and linear model fit for the correlation between GFP+ plasma cells and IL-21 secretion by CD8+ central memory T cells (D) Scatterplots and linear model fits for the correlations between GFP+ plasma cells and secretion of IL-21 by RoRγT+ CD4+ (left) or CD8+ (right) T cells. (E) correlogram of Pearson correlations between the distribution of KSHV infection within B cell subsets (y-axis) and baseline (Day 0) levels of T cell subsets. Pearson's r values with an absolute value greater than or equal to 0.53 are statistically significant for this dataset. (F) scatterplot and linear model fit for the correlation between GFP+ plasma cells and baseline frequency of CD8+ central memory T cells. For A, C, D and F grey shading indicates 95% confidence intervals.
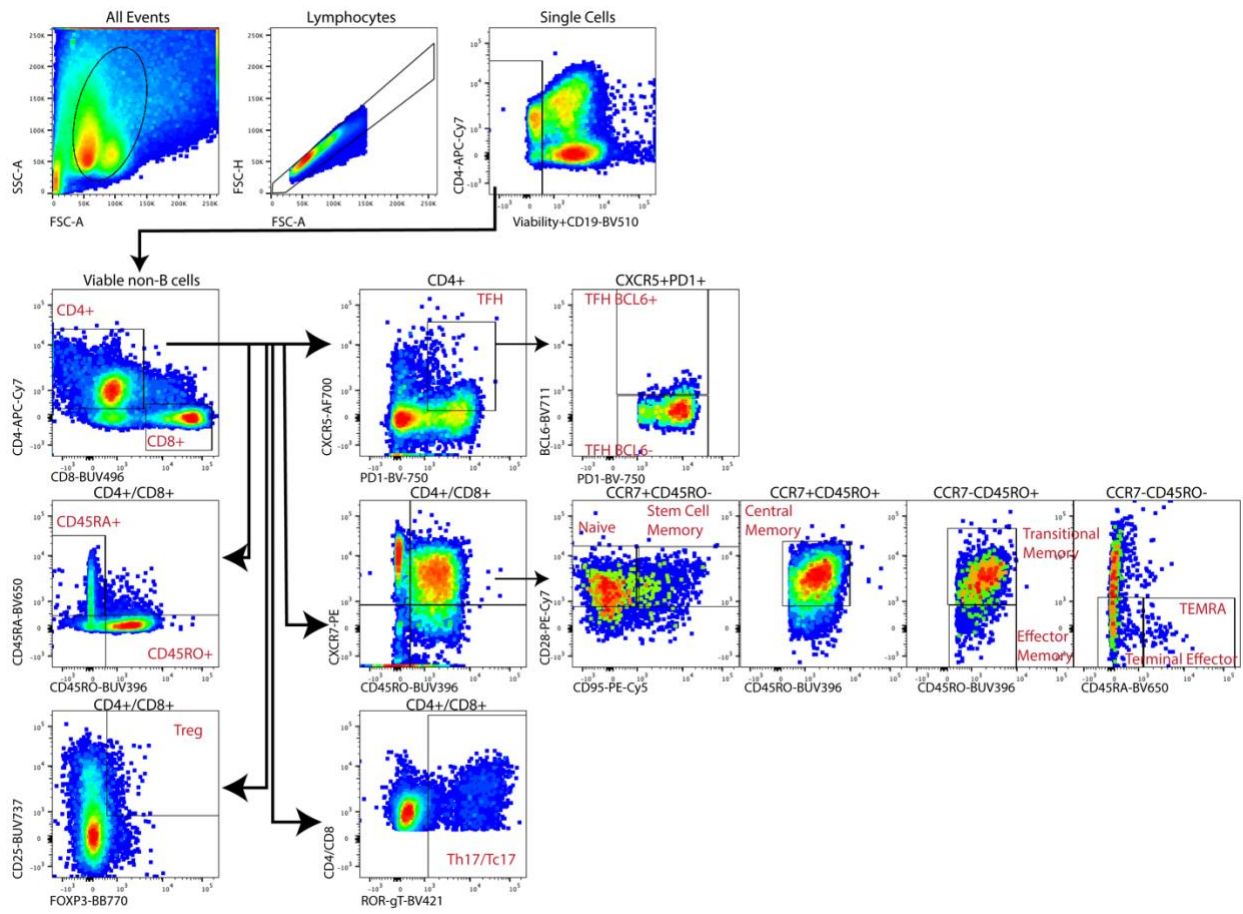
Supplemental Figure 1: Representative gating scheme for T cell immunophenotyping using lineage definitions as detailed in Table 1.
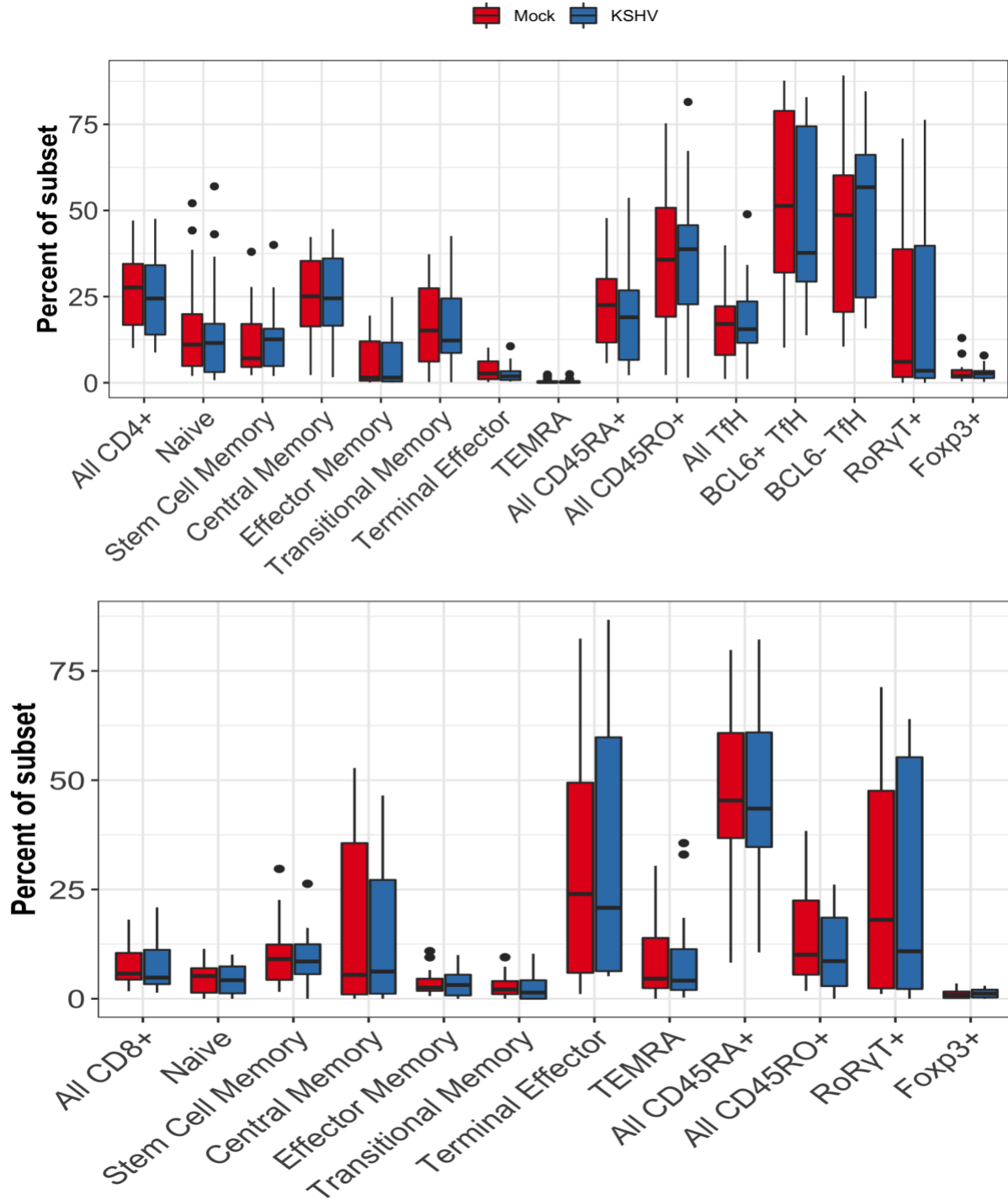
Supplemental Figure 2: Total T cell subset frequencies in Mock and KSHV-infected cultures as in Figure 5.

References

1. Chang, Y., et al., *Identification of herpesvirus-like DNA sequences in AIDS-associated Kaposi's sarcoma.* Science, 1994. **266**(5192): p. 1865-1869.
2. Ablashi, D.V., et al., *Spectrum of Kaposi's sarcoma-associated herpesvirus, or human herpesvirus 8, diseases.* Clinical microbiology reviews, 2002. **15**(3): p. 439-464.
3. Cesarman, E., et al., *Kaposi's sarcoma–associated herpesvirus-like DNA sequences in AIDS-related body-cavity–based lymphomas.* New England Journal of Medicine, 1995. **332**(18): p. 1186-1191.
4. Soulier, J., et al., *Kaposi's sarcoma-associated herpesvirus-like DNA sequences in multicentric Castleman's disease [see comments].* Blood, 1995. **86**(4): p. 1276-1280.
5. Uldrick, T.S., et al., *An interleukin-6-related systemic inflammatory syndrome in patients co-infected with Kaposi sarcoma-associated herpesvirus and HIV but without Multicentric Castleman disease.* Clinical Infectious Diseases, 2010. **51**(3): p. 350-358.
6. Bouvard, V., et al., *A review of human carcinogens--Part B: biological agents.* The Lancet. Oncology, 2009. **10**(4): p. 321-322.
7. Parkin, D.M., *The global health burden of infection-associated cancers in the year 2002.* International journal of cancer, 2006. **118**(12): p. 3030-3044.
8. Ganem, D., *KSHV and the pathogenesis of Kaposi sarcoma: listening to human biology and medicine.* The Journal of clinical investigation, 2010. **120**(4): p. 939-949.
9. Casper, C., et al., *Frequent and asymptomatic oropharyngeal shedding of human herpesvirus 8 among immunocompetent men.* The Journal of infectious diseases, 2007. **195**(1): p. 30-36.
10. Alomari, N. and J. Totonchy, *Cytokine-Targeted Therapeutics for KSHV-Associated Disease.* Viruses, 2020. **12**(10): p. 1097.
11. Carbone, A., et al., *Understanding pathogenetic aspects and clinical presentation of primary effusion lymphoma (PEL) through its derived cell lines.* AIDS (London, England), 2010. **24**(4): p. 479.
12. Aalam, F., et al., *Analysis of KSHV B lymphocyte lineage tropism in human tonsil reveals efficient infection of CD138+ plasma cells.* PLoS pathogens, 2020. **16**(10): p. e1008968.
13. Parrish-Novak, J., et al., *Interleukin-21 and the IL-21 receptor: novel effectors of NK and T cell responses.* Journal of leukocyte biology, 2002. **72**(5): p. 856-863.
14. Parrish-Novak, J., et al., *Interleukin 21 and its receptor are involved in NK cell expansion and regulation of lymphocyte function.* Nature, 2000. **408**(6808): p. 57-63.
15. Kuchen, S., et al., *Essential role of IL-21 in B cell activation, expansion, and plasma cell generation during CD4+ T cell-B cell collaboration.* The journal of immunology, 2007. **179**(9): p. 5886-5896.
16. Konforte, D., N. Simard, and C.J. Paige, *IL-21: an executor of B cell fate.* The Journal of Immunology, 2009. **182**(4): p. 1781-1787.
17. Ozaki, K., et al., *Regulation of B cell differentiation and plasma cell generation by IL-21, a novel inducer of Blimp-1 and Bcl-6.* The Journal of Immunology, 2004. **173**(9): p. 5361-5371.
18. Calame, K.L., K.-I. Lin, and C. Tunyaplin, *Regulatory mechanisms that determine the development and function of plasma cells.* Annual review of immunology, 2003. **21**(1): p. 205-230.

19. Yajima, H., et al., *Loss of interleukin-21 leads to atrophic germinal centers in multicentric Castleman's disease.* Annals of hematology, 2016. **95**(1): p. 35-40.

20. Konforte, D. and C.J. Paige, *Identification of cellular intermediates and molecular pathways induced by IL-21 in human B cells.* The Journal of Immunology, 2006. **177**(12): p. 8381-8392.

21. Konforte, D., N. Simard, and C.J. Paige, *Interleukin-21 regulates expression of key Epstein–Barr virus oncoproteins, EBNA2 and LMP1, in infected human B cells.* Virology, 2008. **374**(1): p. 100-113.

22. Collins, C.M. and S.H. Speck, *Interleukin 21 signaling in B cells is required for efficient establishment of murine gammaherpesvirus latency.* PLoS pathogens, 2015. **11**(4): p. e1004831.

23. Gasperini, P. and G. Tosato, *Targeting the mammalian target of Rapamycin to inhibit VEGF and cytokines for the treatment of primary effusion lymphoma.* Leukemia, 2009. **23**(10): p. 1867-1874.

24. Gasperini, P., S. Sakakibara, and G. Tosato, *Contribution of viral and cellular cytokines to Kaposi's sarcoma-associated herpesvirus pathogenesis.* Journal of leukocyte biology, 2008. **84**(4): p. 994-1000.

25. Totonchy, J., et al., *KSHV induces immunoglobulin rearrangements in mature B lymphocytes.* PLoS pathogens, 2018. **14**(4): p. e1006967.

26. Chang, J., et al., *Induction of Kaposi's sarcoma-associated herpesvirus from latency by inflammatory cytokines.* Virology, 2000. **266**: p. 17-25.

27. Chang, J., et al., *Inflammatory cytokines and the reactivation of Kaposi's sarcoma-associated herpesvirus lytic replication.* Virology, 2000. **266**(1): p. 17-25.

28. Palmerin, N., et al., *Suppression of DC-SIGN and gH Reveals Complex, Subset-Specific Mechanisms for KSHV Entry in Primary B Lymphocytes. Viruses 2021, 13, 1512.* 2021, s Note: MDPI stays neutral with regard to jurisdictional claims in published ….

29. Schmitz, I., et al., *IL-21 restricts virus-driven Treg cell expansion in chronic LCMV infection.* PLoS pathogens, 2013. **9**(5): p. e1003362.

30. Pallikkuth, S., et al., *Upregulation of IL-21 receptor on B cells and IL-21 secretion distinguishes novel 2009 H1N1 vaccine responders from nonresponders among HIV-infected persons on combination antiretroviral therapy.* The Journal of Immunology, 2011. **186**(11): p. 6173-6181.

31. Jondle, C., et al., *Gammaherpesvirus Usurps Host IL-17 Signaling To Support the Establishment of Chronic Infection.* Mbio, 2021. **12**(2): p. e00566-21.

32. Jondle, C., et al., *T Cell-Intrinsic Interferon Regulatory Factor 1 Expression Suppresses Differentiation of CD4+ T Cell Populations That Support Chronic Gammaherpesvirus Infection.* Journal of Virology, 2021. **95**(20): p. e00726-21.

33. Gaddi, P.J. and G.S. Yap, *Cytokine regulation of immunopathology in toxoplasmosis.* Immunology and cell biology, 2007. **85**(2): p. 155-159.

34. Kelly, M.N., et al., *Interleukin-17/interleukin-17 receptor-mediated signaling is important for generation of an optimal polymorphonuclear response against Toxoplasma gondii infection.* Infection and immunity, 2005. **73**(1): p. 617-621.

35. Shainheit, M.G., et al., *The pathogenic Th17 cell response to major schistosome egg antigen is sequentially dependent on IL-23 and IL-1β.* The Journal of Immunology, 2011. **187**(10): p. 5328-5335.

36. Wen, X., et al., *Dynamics of Th17 cells and their role in Schistosoma japonicum infection in C57BL/6 mice.* PLoS neglected tropical diseases, 2011. **5**(11): p. e1399.

37. Wakeham, K., et al., *Parasite infection is associated with Kaposi's sarcoma associated herpesvirus (KSHV) in Ugandan women.* Infectious agents and cancer, 2011. **6**(1): p. 1-7.

38. Song, W. and J. Craft, *T follicular helper cell heterogeneity: time, space, and function.* Immunological reviews, 2019. **288**(1): p. 85-96.

39. Totonchy, J., *Extrafollicular activities: perspectives on HIV infection, germinal center-independent maturation pathways, and KSHV-mediated lymphoproliferation.* Current opinion in virology, 2017. **26**: p. 69-73.

40. Yang, R., et al., *IL-6 promotes the differentiation of a subset of naive CD8+ T cells into IL-21–producing B helper CD8+ T cells.* Journal of Experimental Medicine, 2016. **213**(11): p. 2281-2291.

41. Wickham, H., *Ggplot2 : elegant graphics for data analysis.* Use R! 2009, New York: Springer. viii, 212 p.

42. Kassambara, A., *ggcorrplot: Visualization of a Correlation Matrix using 'ggplot2'.* 2019.

43. Lander, J.P., *R for everyone : advanced analytics and graphics.* Second edition ed. The Addison Wesley data and anlytics series. 2017, Boston: Addison-Wesley. xxiv, 528 pages.

44. Kassambara, A., *rstatix: Pipe-Friendly Framework for Basic Statistical Tests.* 2020.